Université de Montréal

Regulation of inflammation in choroidal neovascularization in age related macular degeneration

par Elisabeth MMA Andriessen

Département de Sciences Biomédicales
Faculté de Médecine

Thèse présentée en vue de l'obtention du grade de Philosophiae Doctor (Ph. D.)
en Sciences Biomédicales Option Médecine Experimentale

Octobre 2020

Université de Montréal
Sciences Biomédicales, Faculté de Médecine

Cette thèse intitulée :

Regulation of Inflammation in Choroidal Neovascularization in Age Related Macular Degeneration

Présentée par :

Elisabeth MMA Andriessen

A été évaluée par un jury composé des personnes suivantes :

Dr Jean-Francois Bouchard
président-rapporteur

Dr Przemyslaw (Mike) Sapieha
directeur de recherche

Dr Alexandre Dubrac
membre du jury

Dre Stéphanie Lehoux
examinateur externe

Dr Michel Cayouette
représentant du doyen de la FES

Résumé

La dégénérescence maculaire liée à l'âge (DMLA) est la cause la plus fréquente de déficience visuelle centrale irréversible chez les personnes de plus de 50 ans dans les pays industrialisés, avec des impacts sociétaux et financiers majeurs. La DMLA est une maladie à multiples facettes provoquée par des interactions entre les facteurs de risque et les antécédents génétiques et l'inflammation joue un rôle important. Les effets pro-inflammatoires provoquent une perturbation de l'environnement sous-rétinien physiologiquement immunosuppresseur. L'accumulation de phagocytes mononucléaires (PM) dans l'espace sous-rétinien qui s'ensuit est au cœur de l'étiologie des formes atrophiques et humides de la DMLA.

Après l'usage de tabac, l'obésité est l'un des facteurs de risque modifiables les plus importants. Nous avons démontré que les régimes riches en graisses exacerbent la néovascularisation choroïdienne (NVC) en modifiant le microbiote intestinal. La dysbiose intestinale entraîne une perméabilité intestinale accrue, une inflammation chronique de bas grade, une augmentation des PM sur le site de l'angiogenèse pathologique dans l'œil et exacerbe finalement la NVC. La modification du microbiote peut réduire l'inflammation et atténuer la NVC et peut ainsi fournir des traitements peu intrusifs et rentables pour prévenir ou retarder la DMLA exsudative.

Une autre option thérapeutique qui pourrait réduire la NVC par modulation inflammatoire consiste à piéger localement les ligands de NRP1 avec un piège dérivé de NRP1. Les ligands de NRP1 sont élevés dans le vitré des patients atteints de DMLA. Nous avons constaté que les PM exprimant NRP1 favorisaient la NVC en atténuant la production de facteurs inflammatoires et en favorisant l'activation alternative, donnant aux PM un caractère pro-angiogénique. Les PM moins inflammatoires et plus de type M2 qui sont enrichis avec l'âge et exacerbent la NVC peuvent être modulés et devenir moins nuisibles en empêchant l'activation de NRP1.

Cette thèse explore deux angles dans lesquels la régulation de l'inflammation peut influencer la formation de NVC et jette les bases du développement futur de nouveaux traitements préventifs primaires et secondaires efficaces dans le contexte de la DMLA.

Mots clés: Dégénérescence maculaire liée à l'âge, néovascularisation choroïdienne, obésité, microbiote intestinal, angiogenèse, inflammation, rétine, Neuropiline-1, phagocytes mononucléaires, polarisation des macrophages.

Abstract

Age related macular degeneration (AMD) is the most common cause of irreversible central vision impairment in people over 50 in industrialized countries, with major societal and financial impacts. AMD is a multifaceted disease provoked by interactions among environmental risk factors and genetic backgrounds in which inflammation plays an important role. Proinflammatory effects cause a disruption of the physiologically immunosuppressive subretinal environment. The ensuing accumulation of mononuclear phagocytes in the subretinal space is central to the etiology of both atrophic and wet forms of AMD.

After smoking, obesity is one of the most important modifiable risk factors. We demonstrate that high-fat diets exacerbate choroidal neovascularisation (CNV) by altering gut microbiota. Gut dysbiosis leads to heightened intestinal permeability and chronic low-grade inflammation, increases recruitment of microglia and macrophages to the site of pathological angiogenesis in the eye and ultimately exacerbates CNV. Modifying microbiota can reduce systemic and local choroidal inflammation and attenuate pathological neovascularization and may thus provide minimally intrusive and cost-effective paradigms to prevent or delay exudative AMD.

Another therapeutic option that could reduce CNV through inflammatory modulation is locally trapping ligands of NRP1 with a NRP1-derived trap. Ligands for NRP1 are elevated in the vitreous of patients with AMD at times of active CNV. We found that NRP1-expressing MPs promote CNV by mitigating production of inflammatory factors and promoting alternative activation, giving the MPs a pro-angiogenic character. The less inflammatory and more M2-like MPs that are enriched with age and exacerbate CNV can be rendered less detrimental by hindering NRP1 activation.

This thesis explores two angles wherein regulation of inflammation can influence the formation of CNV and lays the groundwork for future development of novel effective primary and secondary preventive treatments for AMD.

Keywords: Age Related Macular Degeneration, Choroidal Neovascularization, Obesity, Gut Microbiota, Angiogenesis, Inflammation, Retina, Neuropilin-1, Mononuclear Phagocytes, Macrophage polarization.

Table of Contents

List of figures

List of tables

List of abbreviations

AB	Antibiotic
ALK	Activin receptor-like kinase
AMD	Age-related macular degeneration
ANOVA	Analysis of variance
AP1	Activator protein 1
APO-1	Apoptosis antigen 1
AREDS	Age-Related Eye Disease Studies
Arg1	Arginase 1
ARM	Age-related maculopathy
ARVO	Association for Research in Visions and Ophthalmology
AZ	Atrophic zone
BlinD	Basal linear deposits
BM	Bruch's membrane
BMDM	Bone marrow derived macrophages
BMI	Body mass index
BMP	Bone morphogenetic protein
BRB	Blood-retinal-barrier
c/EBP	CCAAT-enhancer-binding proteins
C2/CFB	Complement component 2 and factor B gene
C5a	Complement component 5a
cAMP	Cyclic adenosine monophosphate
CCL	C-C-chemokine ligand
CCR	C-C-chemokine receptor
CD	Cluster of differentiation
CD	Crohn's disease
cDNA	Complementary deoxyribonucleic acid
CFH	Complement factor H
cfhr	Complement factor H related factors

CI	Confidence interval
CLR	C-type lectin receptor
CNS	Central nervous system
CNV	Choroidal neovascularization
CREB	Cyclic adenosine monophosphate response element-binding protein
CRP	C-reactive protein
CX3CL1	CX3C chemokine ligand 1
CX3CR1	CX3C chemokine receptor 1
CXCL	C-X-C motif chemokine ligand
CXCR	C-X-C motif chemokine receptor
DAMP	Danger-associated molecular pattern
DC	Dendritic cell
Dll4	Delta-like 4
DMEM	Dulbecco's Modified Eagle Medium
DMLA	Dégénérescence maculaire liée à l'âge
DNA	Deoxyribonucleic acid
EDC	1-Ethyl-3-(3-dimethylaminopropyl)carbodiimide
ERM	Epiretinal membrane
EV	Expanded view
FACS	Fluorescence-activated cell sorting
FADD	Fas-associated death domain
FasL	Fas ligand
FBS	Fetal bovine serum
FDA	Food and Drug Administration
FGF	Fibroblast growth factor
FITC	Fluorescein isothiocyanate
GA	Geographic atrophy
GI	Gastrointestinal
GO	Gene ontology

GSEA	Gene set enrichment analysis
HCL	Hydrogen chloride
HFD	High fat diet
HGD	High glycemia diet
HIF	Hypoxia-inducible factor
HLA-DR	Human Leukocyte Antigen – DR isotype
IB4	Isolectin B4
IBA1	Allograft inflammatory factor 1
IBD	Inflammatory bowel disease
IFNγ	Interferon gamma
Ig	Immunoglobulin
IL	Interleukin
IL6R	Interleukin 6 receptor
iNOS	Inducible nitric oxide synthases
IRF	Interferon regulatory factors
JAK	Janus kinase
JNK	c-Jun N-terminal kinases
LGD	Low glycemia diet
LPS	Lipopolysaccharide
M-CSF	Macrophage colony-stimulating factor
MAM	meprin/antigen 5/receptor tyrosine phosphatase m
MAPK	mitogen-activated protein kinase
MDSC	myeloid-derived suppressor cell
MH	Macular hole
MHC	major histocompatibility complex
MMP	Matrix metalloproteinase
MP	Mononuclear phagocyte
mRNA	Messenger ribosomal ribonucleic acid
NFkB	Nuclear factor kappa-light-chain-enhancer of activated B cells

NHS	N-hydroxysuccinimide
NLR	Nod-like receptor
NRP	Neuropilin
NV	Neovascular
NVC	Néovascularisation choroïdienne
OCT	Optical coherence tomography
OIR	Oxygen-induced retinopathy
OTX	Orthodenticle homebox
PAMP	Pathogen-associated molecular pattern
PBS	Phosphate-buffered saline
PCR	Polymerase chain reaction
PDGF	Platelet derived growth factor
PDR	Proliferative diabetic retinopathy
PDT	Photodynamic therapy
PEDF	Pigment epithelial-derived factor
PFA	Paraformaldehyde
PGF	Placental growth factor
PGN	Peptidoglycans
PI3K	Phosphoinisitide-3 kinase
POS	Photoreceptor outer segment
PRR	Pattern recognition receptor
QIIME	Quantitative insights into microbial ecology
RAS	Rat sarcoma virus
RBC	Red blood cell
rCDI	Recurrent Clostridium difficile infection
RD	Regular-chow diet
RNA	Ribonucleic acid
RNA-seq	Ribosomal ribonucleic acid sequencing
ROP	Retinopathy of prematurity

ROS	Reactive oxygen species
RPE	Retinal pigment epithelium
rRNA	Ribosomal ribonucleic acid
RT	Real-time
RT-qPCR	Real-time quantitative polymerase chain reaction
SEM	Standard error of the mean
SEMA	Semaphorin
sIL6R	Soluble interleukin 6 receptor
SNP	Single-nucleotide polymorphism
sNRP	Soluble Neurpolin
SPR	Surface plasmon resonance
STAT	Signal transducer and activator of transcription
T2D	Type 2 Diabetes Mellitus
TAM	Tumor associated macrophage
TGFβ	Transforming growth factor beta
TGFβR	Transforming growth factor beta receptor
TLR	Toll-like receptor
TM	Transmembrane
TNF	Tumor necrosis factor
Treg	Regulatory T cell
UC	Ulcerative colitis
US	United States
VEGF	Vascular endothelial growth factor
VEGFR	Vascular endothelial growth factor receptor

Acknowledgements

I would like to thank my research director and mentor Przemyslaw Sapieha for his support, stimulation and guidance. With his continuous encouragement to give my best he has helped me develop both academically and personally. I would also like to thank the members of the thesis committee, Jean-Francois Bouchard, Alexandre Dubrac, Stéphanie Lehoux and Michel Cayouette as well as all the members of the Sapieha lab for their valuable contributions.

A very special thank you to my (extended) family Teuntje Andriessen, Jaap Andriessen, Dirk Andriessen, Quinta Andriessen, Maarten Andriessen, Rini Teunissen, Lucie Tétreault, Gilles Tétreault, Jan Bijman and Maaike Gudde, who believed in me and who supported me during all these years.

Finally I want to thank my best friend and spouse Nicolas Tétreault and our lovely kids Olivier and Ada for making every day of this journey a happy one.

Introduction

1. Introduction on Age-related macular degeneration

1.1 Prevalence

With and estimated 196 million people affected in 2020, age related macular degeneration (AMD) is a leading cause of central vision loss worldwide(1). While responsible for 5.8% of blind individuals in 2015, AMD is the fourth most common cause of blindness globally (2). In Canada and other industrialized nations AMD is the primary cause of blindness(3). The prevalence of early and late AMD lie around 8.0% and 0.4% within the age range of 45-85 years, with a steep increase after the age of 75(2). Where in the United States (US) ~2% of the population at age 40 suffers from a form of AMD, approximately one in four people aged 80 and over is afflicted with AMD(3, 4). Due to increased life expectancy and the general ageing of populations the number of individuals with AMD is expected to increase to 288 million by 2040(1, 5). Based on analysis of existing literature and recent meta-analyses, Wong et al determined that early AMD is most common in individuals of European ancestry (11.2%), followed by Asians (6.8%) and least common in individuals of African ancestry. These findings are in line with previous studies, such as the Baltimore Eye Study and other large studies on multiethnic populations(3, 6, 7). In contrast to the finding in two previous meta-analyses(8, 9), where the female sex was found to be a weak risk factor for AMD, Wong et al found that sex was not significantly associated with the development of AMD, which is in line with several other important studies (1, 2, 10-14). Even though the scope of AMD, with an estimated 10 million patients in the US alone, is comparable to the one of cancer (12 million(15)) or Alzheimer's disease (5 million(16)), the exact mechanisms mediating disease progression remains unknown(3, 4).

1.2 Impact on quality of life

In AMD related vision loss central vision is most severely impacted, while peripheral vision remains relatively unaffected. Central vision is not only essential for everyday activities like driving, reading, watching TV, shopping, cooking and cleaning, but also for more basic needs like autonomous mobility, perception of scenes, face recognition and self-care(17). The (progressive)

loss of central vision therefore has a major impact on everyday life of the patients and the people surrounding them(18). Despite intensive research into the pathogenesis, environmental and genetic risk factors, preventive measures and new treatments, treatment options for AMD patients remain very limited, and the impact of vision impairment remains substantial. Both the community and clinicians often underestimate the broad impact of AMD on the quality of life(19). Not only is vision loss linked to an increased morbidity caused by accidents and falls(20, 21), it also impairs the cherished independence of patients and can lead to social isolation and depression(22). The incidence of depression is doubled in AMD patients when compared to other elderly living in the same community, while their significant psychological distress is comparable to the one found in patients with other serious chronic illnesses(19, 23, 24). The trauma of being diagnosed with an incurable and progressive eye disease is often coupled with a perceived lack of information and an unmet need for support by AMD patients, while an early diagnosis, combined with education on prognosis and continuing support can improve functional and psychological health(22). Awareness of the impact of AMD on quality of life is vital for patient wellbeing and should be promoted in parallel to continuing research for a cure to this blinding disease.

1.3 Risk factors

An increasing amount of evidence identifies age and genetic make-up as the most important risk factors for AMD. The strong correlation between family history and AMD, with one study showing a nearly 4-fold increase in risk for AMD for those with a positive family history for AMD(25) is illustrative for the genetic component of the pathogenesis. However, with AMD being a complex multifactorial disease, not one mutation can be judged causative of the pathogenesis. A multitude of genes, including genes with retinal-specific function (e.g. *ABCA4*), genes related to neovascularization (e.g. vascular endothelial growth factor (VEGF)), immune system related genes (e.g. complement factor H (CFH)) and lipoprotein related genes (e.g. ApoE) have been shown to be implicated in the development of AMD(26). For an exhaustive list with approximately 40 genes that may be associated with the development of AMD see 'Risk Factors and Biomarkers of Age-Related Macular Degeneration' from Lambert et al, published in 2016.

Current evidence concerning the female sex as a risk factor is conflicting, but leaning towards exclusion of sex as a risk factor(1, 2, 10-14, 27, 28). Race on the other hand is considered a significant risk factor, with Caucasians being significantly more likely to develop AMD compared to people of African descendance(28-31). And also iris colour has been linked to AMD with a 2-fold higher incidence in people with light coloured eyes than in people with dark eyes showing a protective effect of brown irises(8, 32-34).

All previously mentioned risk factors are non-modifiable and can not be altered by life-style changes. But an increasing number of modifiable risk factors are being identified. Whether sunlight exposure(35), hypertension(36), diet(37), obesity(38, 39), vitamin and mineral supplementation(40), alcohol consumption(41) and oestrogen replacement(42, 43) increase the risk of AMD is more controversial, but there is increasing data available to support a possible role for several of them, especially hypertension and diet(9, 44). Evidence concerning smoking as a risk factor is quite consistent and shows a two to three times higher risk of AMD in smokers than in non-smokers, with a strong correlation between the intensity of smoking and the increasing risk of AMD(45). Education of the general population on ocular health by optometrists, with a focus on modifiable risk factors for AMD, could play a significant role in the public awareness of the risk factors of AMD. Eye protection from sunlight, dietary changes, supplement intake, quitting smoking, exercise and weight loss should all be promoted to reduce the lifetime risk of AMD(44).

1.4 Human eye

The human eye can be subdivided in an anterior and a posterior segment, as indicated in the schematic diagram of Figure 1, inspired by 'Anatomy of the Eyeball' from Frank H. Netter MD. The anterior segment is the part that people see, and the posterior part is the part with which you see. The eye consists of three layers and in the anterior segment these are represented by the cornea, iris and lens. The cornea is the transparent outer layer of the anterior segment and is connected to the sclera together forming the exterior layer of the eye. The iris is the coloured circular disk that lies around the pupil, the black dilatable center of the anterior segment, through which light can enter the eye, and travel via the lens to the posterior segment of the eye. The

space between the cornea and the lens is filled with aqueous humor, a clear fluid that fills the anterior and posterior chamber. The posterior part of the eye is composed of the sclera, choroid and retina. Light entering the eye through the pupil, travels through the vitreous humour, the jelly-like substance that fills the posterior segment of the eye, and reaches the retina, a highly refined multi-layered cell complex that captures the visual information and transmits it to the brain, via the optic nerve. Near the center of the retina lies the macula, an oval-shaped pigmented area responsible for central, high-resolution, colour vision. The macula, and in particular the fovea, the depression at the center of the macula that provides the greatest visual acuity, has a unique structure that constitutes in majority of cone cells and is devoid of blood vessels, relying on the choroidal circulation for nutrient and oxygen supply.

Since AMD is considered a pathology of the back of the eye, with pathologies restricted to the retina-choroid interface of the macula, the next paragraph will review the structural features of the posterior segment in more detail, before moving on to the pathogenesis.

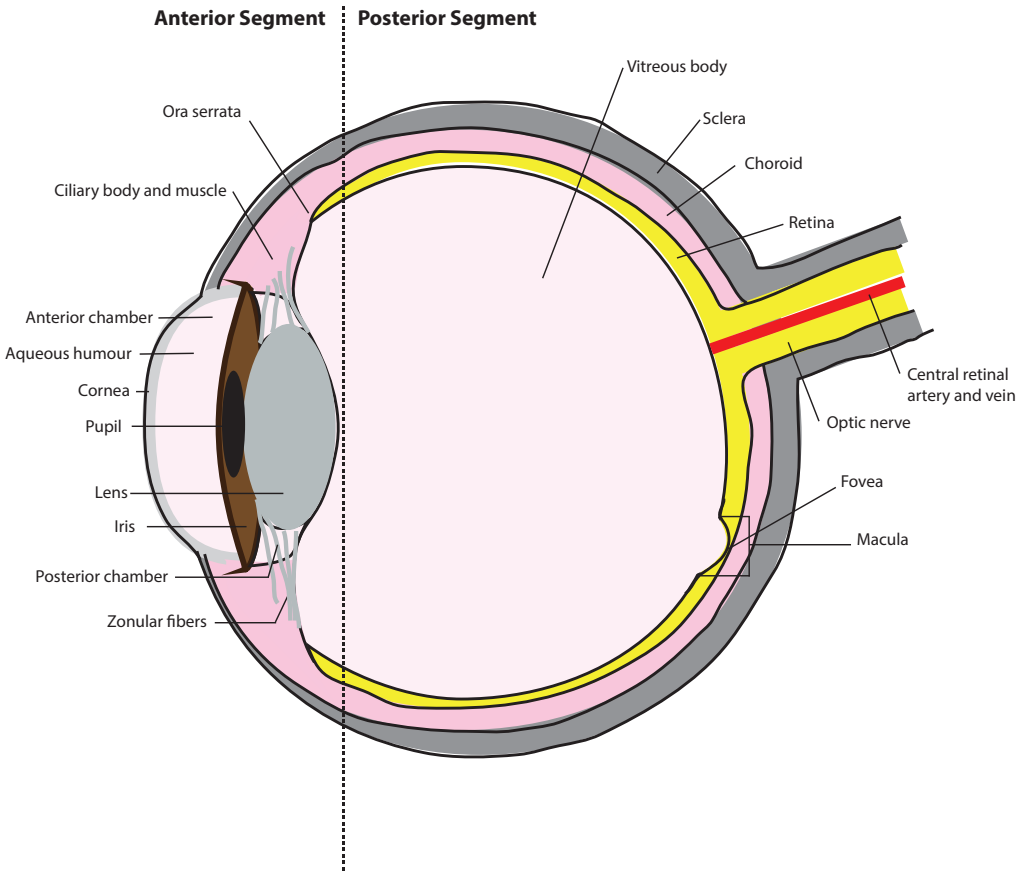

Figure 1 The human eye

Schematic diagram of the human eye subdivided in the anterior and posterior segment inspired by 'Anatomy of the Eyeball' from Frank H. Netter MD(46). The retina is the innermost part of the three layers that make up the back of the eye. Through the optic nerve the retina communicates with the visual cortex of the brain. Age related macular degeneration is an eye disease that affects the back of the eye, with pathologies of the choroid and retina leading to blindness.

1.5 Posterior segments

1.5.1 Retina

The human retina is approximately 200μm thick and consists of 8 different layers, shown in Figure 2, inspired by figure 13-7 of Medical Physiology from Walter F. Boron and Emile L. Boulpaep 2005(47). The retina is a part of the central nervous system (CNS) that converts light into neural signals and passes it on to the brain. Upon entry in the eye, light has to pass through the vitreous

humour and 5 layers of the retina before it reaches the photoreceptors, the light-sensitive cells that capture photons and in collaboration with four additional types of neurons transport the signal to the brain. Photoreceptors can be classified into rod cells, highly sensitive to light, necessary for night vision, and cone cells, adept in detecting a wide spectrum of light, responsible for colour vision. The human eye contains almost 100 times more photoreceptors than ganglion cells, necessitating a convergence of information as it flows from the distal to the proximal part of the retina towards the axons of the ganglion cells that form the nerve fiber layer. Some of the convergence of information is commanded by the bipolar cells, which connect the photoreceptors to the ganglion cells. Horizontal and Amacrine cells are interneurons that spread horizontally and converge information by interconnecting photoreceptors, bipolar cells or ganglion cells, mediating interaction over a wide area of the retina(47).

1.5.2 Retinal pigment epithelium and Bruch's membrane

The retinal pigment epithelium (RPE), a monolayer of pigmented cells located between the vessels of the choriocapillaris and the photoreceptors, closely interacts with the photoreceptor outer segments (POSs) in order to maintain visual function. With its long apical microvilli the RPE surrounds the POSs while facing the Bruch's membrane (BM) with its basolateral membrane(48). The BM, a highly intricate complex of collagen and elastic fibers that lies between the RPE and the choroid, separates the RPE from the fenestrated endothelium of the choriocapillaris(49). All nutrients, ions, water and metabolic end products that are exchanged between the POSs and the choriocapillaris pass through the RPE cell layer and BM, which form an important part of the blood-retinal-barrier (BRB)(50).The photoreceptors in the retina are routinely exposed to photo-oxidative-stress and cope with the damage by continuously shedding and renewing their POSs. The RPE fulfils an important role in the maintenance of photoreceptor functionality through phagocytosis of up to 30,000 POSs per day in order to locally recycle and conserve essential membrane lipids and maintain tissue homeostasis(51-54). The non-recyclable degraded material is discharged into the Bruch's membrane (BM) and cleared by the choriocapillaris.

Besides its phagocytic activities the RPE also secretes a variety of growth- and immunosuppressive factors that are indispensable for the maintenance of structural integrity

and ocular immune privilege(55, 56). Secretion of pigment epithelial-derived factor (PEDF) on the apical side of the RPE has both neuroprotective and antiangiogenic properties(48). It protects neurons against apoptosis while inhibiting endothelial cell proliferation, maintaining retinal structure(57, 58). The PEDF secretion is opposed by low concentrations of VEGF which are secreted on the basal side of the RPE to stabilize the endothelium of the choriocapillaris by suppressing endothelial cell apoptosis(59) and help keep it fenestrated(58, 60-62). Growth factor secretion changes in response to damage or injury can have substantial consequences and play a major role in the pathogenesis of retinal diseases(63-65).

1.5.3 Choriocapillaris

The choriocapillaris, the vascular bed of the choroid, has relatively wide and flat capillaries, fenestrated capillary walls and an enormous blood flow. The highly vascularised choroid is essential in the energy supply to the exceptionally metabolically active retina. With a rate of 1,4L/min/100g tissue the choriocapillaris has a higher perfusion than the kidney(48, 66, 67). Besides regulating the temperature of the back of the eye the choriocapillaris sustains the photoreceptors by supplying nutrients and eliminating waste products(68-70).

It's the choriocapillaris, together with the photoreceptor cells, the RPE and the BM that are particularly involved in the pathogenesis of AMD(71). With age there is an increase in inadequate processing and removal of metabolic waste caused by: a) a declining density of the choriocapillaris(72, 73), b) a decrease in RPE function(74, 75) and c) an increase in thickness of the BM, reducing permeability(73). The accumulation of metabolic waste materials results in extracellular subretinal drusenoid deposits of metabolites and deficient clearing of these deposits can cause a pathologic reaction that causes tissue injury(52). The pursuing degeneration of the macula and central retina, responsible for the high-acuity central vision, is the fundament of vision loss in AMD. In general RPE dysfunction precedes all other phases in AMD progression and can therefore be considered to be at the core of AMD pathogenesis(4).

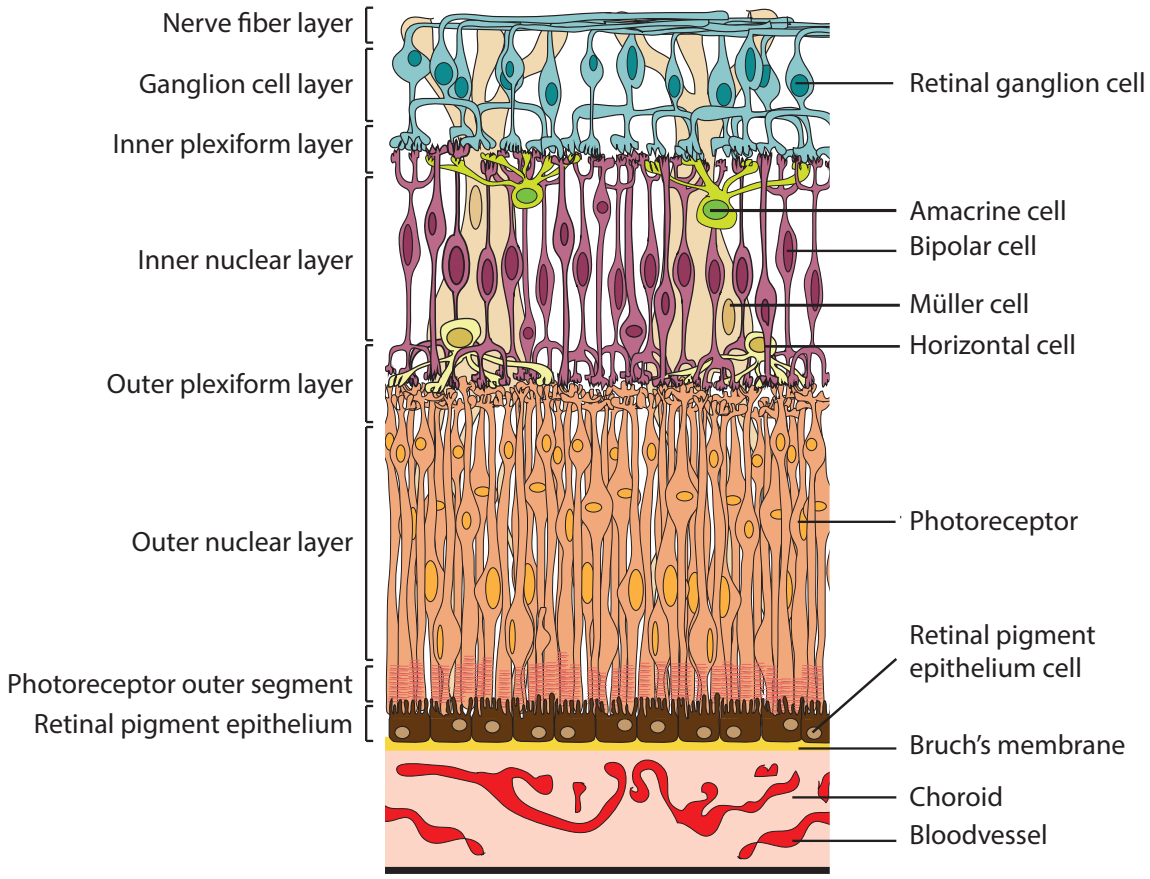

Figure 2 The human retina

Schematic diagram of the human retina inspired by figure 13-7 of Medical Physiology from Walter F. Boron and Emile L. Boulpaep 2005(47). The human retina is composed of 8 different layers made up by a range of different highly specialized cells. All these cells work together to insure proper functioning of this highly metabolically active organ.

1.6 Pathogenesis

AMD is a progressive condition that is untreatable in most patients and is the leading cause of blindness in the elderly worldwide. The precise etiology remains unknown, but an increased

understanding of the mechanisms underlying the AMD pathogenesis has led to various important insights. AMD is a disease with a gradual onset that generally evolves over several years before symptoms appear. A schematic representation of disease progression is presented in Figure 3

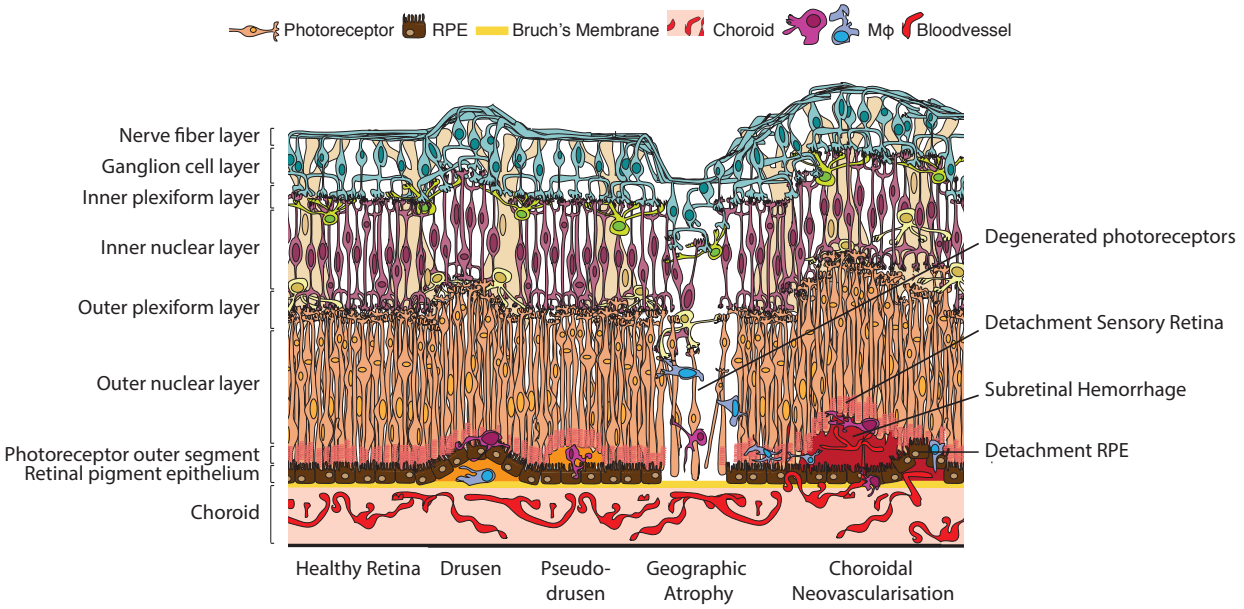

Figure 3 Disease progression in age related macular degeneration.

Age related changes in the eye can cause the insufficient clearing of cell debris in the inner retina, leading to the formation of yellow-white deposits called drusen. Decreased function of the RPE in concert with imbalances in immune reactions cause damage to the neurosensory retina. Excretions of vascular growth attracting molecules by the stressed RPE, photoreceptors and immune cells prompt choroidal vessels to invade the subretinal region. Leaking of these pathological choroidal neovessels can lead to retinal detachment and vision loss. Figure inspired by Guillonneau et al(76) and Walter F. Boron and Emile L. Boulpaep(47).

1.6.1 Drusen

In the early asymptomatic stage of AMD, which is also called age-related maculopathy (ARM), insoluble extracellular lipid-, carbohydrate and protein rich aggregates accumulate between the

basal lamina of the RPE and the inner collagenous layer of the BM(76, 77). It is not clear whether these deposits are derived from the RPE only or also from the choroidal vasculature (76). Based on their size they are classified as basal linear deposits (BlinD) or drusen (>125μm)(78). Additionally, reticular pseudodrusen, subretinal drusenoid deposits located between the RPE and the photoreceptors are strongly associated with AMD(79). The term "Drusen" is derived from the word "Druse" which means geode in German, a rock cavity filled with crystals, and was first used by Heinrich Müller around 1850. He probably chose this name because some large drusen have a crystalline core(80). Disturbance of the nutrient exchange between the RPE and the choriocapillaris caused by the accumulation of BlinD and drusen contributes to the deterioration of the RPE(81). Besides that, drusen can cause deformations and protrusions of the basal lamina of the RPE which leads to local loss of sensitivity and thinning of the photoreceptor layer(82, 83), as shown in Figure 4.

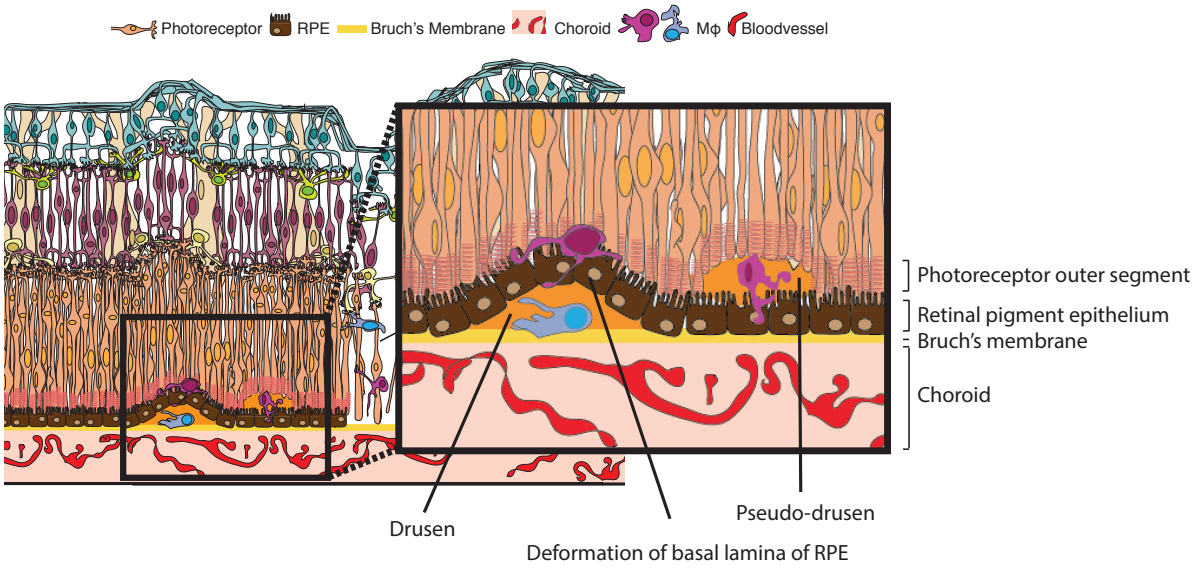

Figure 4 Close-up of drusen and Pseuso-drusen formation in the inner retina

Formation of drusen and pseudodrusen, extracellular aggregates that accumulate near the RPE, causes deformations and protrusions of the retina and complicate the critical photoreceptor support by the RPE. Mononuclear phagocytes, derived from circulating monocytes, resident

macrophages and microglial cells, infiltrate the subretinal space and phagocyte cell debris and pigment from dying retinal pigment epithelium and photoreceptors and excrete proinflammatory factors. Figure inspired by Guillonneau et al(76) and Walter F. Boron and Emile L. Boulpaep(47).

1.6.2 Geographic atrophy and dry age related macular degeneration

Although the cause-effect relationship of drusen and RPE cell death are not fully understood, there seems to be an autostimulatory loop where drusen formation, RPE damage and inflammatory responses reinforce each other(4, 84, 85). Upon progression of AMD, drusen can lead to geographic atrophy (GA), where the continuous loss of RPE cells and the degeneration of the photoreceptor cell layer which relies on the RPE for support, results in an atrophic zone (AZ). Residual photoreceptors in the AZ often lack their POS and are not capable of sensing light(86), causing loss of retinal sensitivity and central (scintillating) scotomas. GA often commences in the periphery, but can progress towards the central retina and the macula, severely affecting visual acuity(87, 88). For a visual demonstration of a scintillating scotoma, visit https://en.wikipedia.org/wiki/Scotoma.

GA is an advanced form of AMD and is also called “dry” AMD, distinguishing it from the other form of advanced AMD which is called “wet” AMD. While vision loss caused by the dry form of AMD is typically gradual, wet AMD can cause rapid decrease in vision when neovascular tufts originating from the choriocapillaris emerge(89).

1.6.3 Choroidal neovascularization and wet age related macular degeneration

“Wet”, “exudative” and “neovascular” (NV) are all terms that are used to describe the second form of advanced AMD, where subretinal neovascularization develops below (occult) or above (classic) the RPE. Choroidal neovascularization (CNV) is a prevalent and serious complication in diseases that affect the posterior segment of the eye and is a hallmark of wet AMD(90). CNV is more than just a vascular pathological condition and is better defined as an aberrant tissue invasion of endothelial and inflammatory cells in which both angiogenesis and inflammation play a key role(91). CNV is often of low quality and is in consequence inclined to hemorrhage or leak. The subretinal exudative deposits of blood and lipids can cause retinal edema,

photoreceptor cell death, fibrovascular scarring and retinal detachment(76). Since the adherence of the RPE to the BM is weakened by drusen and increased inflammation, and the retina is only loosely attached to the RPE, serous exudate and blood can cause detachments over area's much larger than the region of vascular invasion(81). Consequently, vision loss by NV AMD can be rapid and is often more severe than by GA in dry AMD.

Even though previous GA is not required for progression to NV AMD, since NV AMD can develop without any GA present, and patients suffering from GA do not necessarily progress to NV AMD, there is a high concurrence between GA and CNV formation. Typically patients develop dry AMD before progressing to wet AMD and as such, dry AMD can be considered a risk factor or even precursor for wet AMD(4).

1.6.4 Vascular endothelial growth factor

Why choroidal vessels decide to grow into the subretinal space is not well known, but it's widely accepted to be a complex multifactorial process that does not necessarily follow a rigid pathogenic process. Experimental and clinical evidences show that VEGF is a pivotal cue for promoting angiogenesis in AMD(92). VEGF production has a number of potential sources including RPE, photoreceptors, pericytes, glial cells, Müllers cells and ganglion cells(91, 93-95). Especially excretion of vascular growth attracting molecules by stressed RPE and photoreceptor cells combined with an influx of mononuclear phagocytes (MPs) play a main role in the course of CNV formation(76, 81).

VEGF-A, generally simply called VEGF, is the best known member of a gene family that also includes placental growth factor (PGF), VEGF-B, VEGF-C, VEGF-D, and orf-virus-encoded VEGF-E(96, 97). VEGF production is mainly elicited by hypoxic stimuli and triggers the growth of the vascular endothelium of arteries, veins and lymphatics whilst acting as a survival factor for endothelium, enhancing microvascular permeability and promoting monocyte chemotaxis(91, 98, 99).

Alternative splicing of the mRNA from the 8-exon VEGFA gene results in the generation of multiple VEGF isoforms that are named based on the number of amino acids after the signal sequence of slicing: VEGF-121, VEGF-165, VEGF-189 and VEGF-206(98). VEGF-165 is freely

diffusible but a significant fraction remains bound to the cell surface and in the extracellular matrix(100). Based on these optimal characteristics of bioavailability and biological potency VEGF-165 is the most important isoform(98).

VEGF binds VEGF receptor (VEGFR)-1 and VEGFR-2, two highly analogous receptor tyrosine kinases that consist of seven Immunoglobulin (Ig)-like extracellular domains, a single transmembrane region and a consensus tyrosine kinase sequence that is interrupted by a kinase-insert domain(98, 101-103). In addition to VEGFR-1 and VEGFR-2, VEGF interacts with a family of coreceptors, the Neuropilins (NRP) (98), which will be discussed in detail in paragraph 6. VEGFR-1 and VEGFR-2 are both expressed on the cell surface of vascular endothelial cells, but the major mediator of cell mitogenesis, survival and microvascular permeability is VEGFR-2(98).

To this day, there are not any approved treatments available for dry AMD. The development of anti-angiogenic therapies with anti-VEGF, that decreases permeability and inhibit formation of neovessels, has been an important breakthrough in the treatment of exudative AMD(104). However, most exudative lesions continue to show some signs of activity and a significant number of patients proceed to lose 3 lines or more of visual acuity, while thromboembolic events, neuronal toxicity and a higher incidence of GA are cause of concern(105). With anti-VEGF's adverse effects increasing with the duration of the treatment, developing both alternative and adjunct therapies is necessary(106).

1.7 Treatments

The growth of blood vessels inward from the choroid is for an important part caused by an imbalance of VEGF, the most critical regulator of ocular angiogenesis, and PEDF, a potent antiangiogenic factor. RPE cells are capable of excreting both factors, and in physiological circumstances, they release VEGF on the laminar side, towards the choroid and PEDF on the apical side towards the retina. NV AMD patients have been shown to express increased VEGF and reduced PEDF levels(71). Most of the currently available therapies for NV AMD are aiming to diminish VEGF expression in the eye and currently there are three main drugs available. Ranibizumab, approved by the Food and Drug Administration (FDA) in 2006 for the treatment of

NV AMD is a recombinant humanized IgG1 kappa isotype monoclonal antigen-binding fragment that targets and binds VEGF with high affinity. Aflibercept, approved by the FDA in 2011, is a fusion protein that combines a fragment crystallizable region of a human IgG1 and two key binding domains of human VEGF receptors 1 and 2. Finally bevacizumab, an off-label drug for the treatment of AMD sold under the trade name Avastin, is a full-length humanized antibody that binds and blocks all VEGF isoforms. Being the most used ocular antiangiogenic and the 7th best-selling drug in the world, it revenued over 6.5 billion US dollars in 2016(107, 108).

Where bevacizumab and ranizumab are Ig antibodies that bind to all isoforms of VEGF and aflibercept is a recombinant fusion protein that forms a trap for VEGF, VEGF-B and PGF, conbercept is a full human DNA sequence that binds VEGF, VEGF-B, VEGF-C and PGF(109). Approved for treatment of NV AMD in 2014 in China, it's currently seeking global approval and is expected to bring a new treatment option in 2023(110).

All the before mentioned therapies for ocular angiogenesis are anti-VEGF ligands. However, some patients show worsening eye disease, even upon aggressive treatment with anti-VEGF agents, suggesting other vascular mediators contribute to the pathogenesis of NV AMD(111, 112).

Before the FDA approval of ranibizumab in 2011, NV AMD treatment was largely dependent on laser photocoagulation therapy based on a study from the 1970's and a photodynamic therapy (PDT) developed in the 1990's(113). These therapies showed a high recurrence rate, risk of producing vision loss and limited potential to improve vision and their use in practice has dramatically decreased in recent years. Currently PDT is only used in combination with an anti-VEGF agent and/or steroid administration in patients that do not respond to monotherapy(113).

Despite the significant advances in treatment in recent years, AMD remains an incurable and progressive disease. Antiangiogenic treatment does not prevent AMD neither does it alter the course of the disease, it merely delays its progression, and has no beneficial effect on GA in dry AMD(108). In addition, long-term VEGF inhibition is not without risks since it is associated with thromboembolic events, neuronal toxicity and a higher incidence of GA (105, 114). Developing alternative or adjunct therapies is therefore necessary.

1.8 Animal models for age related macular degeneration

The most used animal model for CNV in NV AMD is the laser-induced CNV model, as represented in Figure 5. The model is in fact a wound-healing model and does not have any of the phenotypic aging characteristics of AMD, but it's highly reproducible and results in CNV in almost 80% of the lesions. In addition, it can be performed in transgenic mice, opening up various options to study the contribution of inflammation, angiogenic factors and proteolysis(115, 116). The compromise of the BM is instigated by the laser, other conditions of NV AMD can be simulated by for example injectables, diets, mouse age and knock-outs.

For a complete overview of animal models of age related macular degeneration, including non-rodents, one should consult "Animal Models of Choroidal and Retinal Neovascularization" from Grossniklaus et al, published in 2010 (115).

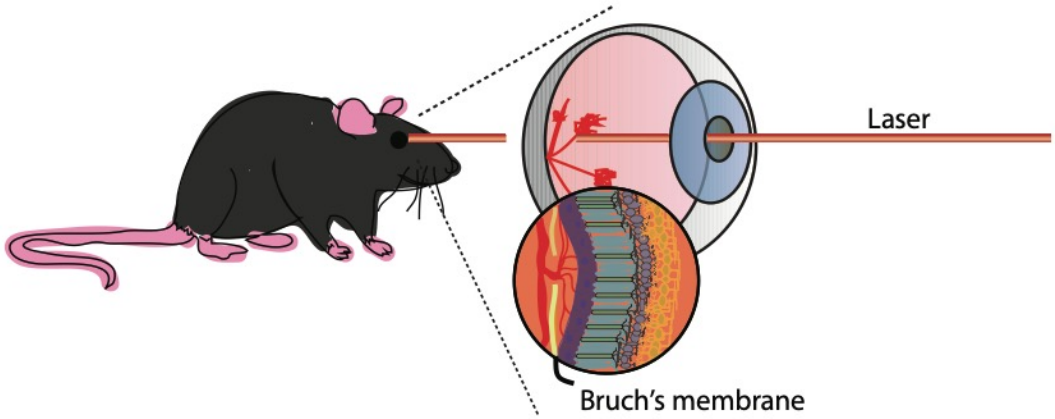

Figure 5 Laser induced choroidal neovascularization model

Using the impact of an argon-laser that enters the eye through the dilated pupil of the anesthetized mouse, the Bruch's membrane is ruptured. The compromise of the membrane that lies between the retina and the choroid collectively with the proangiogenic signalling of the immune cells that are attracted to the site of injury prompt choroidal neovessels to grow into the (sub)retinal space, mimicking the hallmark of wet AMD; choroidal neovascularization.

2. Inflammation

2.1 Inflammatory pathways

The role of the inflammatory response, with its five cardinal signs of inflammation as described in De Medicina by the Roman encyclopedist Aulus Cornelius Celsus; rubor (redness), calor (heat), dolor (pain), tumor (swelling) and functio laesa (loss of function), is to combat infection and tissue injury(117). The innate immune cells such as macrophages, fibroblasts, mast cells, dendritic cells (DC), circulating leukocytes including monocytes and neutrophils work together to orchestrate a proper inflammatory immune response and coordinate the start of long-term adaptive immunity toward specific pathogens(118). Regulatory mechanisms that prevent uncontrolled and chronic inflammation are of vital importance since excessive immune responses can cause severe tissue damage. Multiple layers of regulatory mechanisms have evolved in order to fine-tune the initiation, progression and resolution of inflammation(117).

Innate immune cells recognize pathogens and cell damage by detection of pathogen-associated molecular patterns (PAMPs) and damage-associated molecular patterns (DAMPs) with intracellular or surface-expressed pattern recognition receptors (PRRs). Activated PRRs, such as Toll-like receptors (TLRs) initiate signaling cascades that trigger the release of leukocyte recruiting and activating factors(118). Triggering the activation of transcription factors like nuclear factor kappa-light-chain-enhancer of activated B cells (NFκB), Activator protein 1 (AP1), cyclic adenosine monophosphate (cAMP) response element-binding protein (CREB), CCAAT-enhancer-binding proteins (c/EBP) and Interferon regulatory factors (IRF), induces genes encoding enzymes, cytokines, chemokines, adhesion molecules and regulators of the extracellular matrix.

A major alarm signal in the body in response to infection and inflammation is interleukin (IL) 6 (119, 120). IL6 is produced together with IL1β and tumor necrosis factor (TNF) by myeloid cells after TLR signalling, and, if not inhibited, embarks on a feed-forward loop, leading to a significant amplification of IL6(121). During inflammatory states circulating IL6 levels can rise up to a 1,000-fold when compared to homeostatic conditions, while it can go up to 6 orders of magnitude under septic conditions(122). IL6 signalling can be induced by classic signalling and by trans-signalling. In classic signalling IL6 binds to a membrane-bound IL6 receptor (IL6R) and consequently

associates with glycoprotein 130 kDa (gp130), a second receptor protein. Dimerization of the receptor complex initiates intracellular signalling via the Janus kinase (JAK)/signal transducer and activator of transcription (STAT) and rat sarcoma virus(ras)/mitogen-activated protein kinase (MAPK) and phosphoinisitide-3 kinase (PI3K) pathways. Both gp130 and IL6R need to be expressed in order to signal after stimulation with IL6 and whereas gp130 is expressed by all cells, only hepatocytes and some leukocytes express IL6R(123, 124). Circulating soluble IL6R (sIL6R) can induce signalling by binding IL6 and then associate with gp130(125). This is called IL6 trans-signalling and through this paradigm IL6 can stimulate any cell in the body(120, 126).

IL6 plays an important role in homeostasis with roles in body weight regulation(127), liver physiology(128) and bone metabolism(120, 129). The role of IL6 becomes even more extensive in pathophysiological conditions. Dysregulated continual synthesis of IL6 plays a pathological effect on chronic inflammation and autoimmunity. Rheumatoid arthritis(130), multiple sclerosis(131), various types of cancer(132, 133), atherosclerosis(134), depression(135) and Alzheimer's Disease(136) are only a few examples of pathologies wherein IL6 plays a critical role. Extensive epidemiological evidence underlines a role for IL6 in age-related pathologies, where a state of mild inflammation is associated and predictive of many aging phenotypes(137).

2.2 Aging and inflammaging

Around 500 years before Christ, Heraklitus stated that everything flows, "Pantha rhei", and "No man ever steps in the same river twice". He's philosophising about the change that is constantly happening in and around us. With our current knowledge of cell renewal we know that he was right. Most cells have a shorter life than the organism and are continuously replaced after a lifespan ranging from serval days to several decades(138). Aging, the process of becoming older, can refer to psychological changes, relating to wisdom and maturity as well as to physical changes like getting grey hair. Both are the result of an accumulation of changes in an organism over time(139). In 2004 Bowen et al. stated that the rate of aging is synonymous with the rate of change, with rapid aging associated with growth and development during fetal development to a slower rate of change associated with loss of function (139). Nine hallmarks that represent common denominators of aging are: genomic instability, telomere attrition, epigenetic

alterations, loss of proteostasis, deregulated nutrient sensing, mitochondrial dysfunction, cellular senescence, stem cell exhaustion and altered intercellular communication(140). The progressive loss of physiological integrity and impaired functioning increases the risk for pathologies like cancer, diabetes, cardiovascular disorders and neurodegenerative diseases(140). Aging is the most significant risk factor associated with chronic disease in humans and is strongly associated with inflammation(141). Inflammaging, the chronic, sterile, low-grade inflammation that develops during aging and is a prominent risk factor for morbidity and mortality in elderly. Most, if not all, age-related diseases have an inflammatory component in their pathogenesis, but its causal role in adverse health outcomes remains largely unknown(137). As a response to harmful conditions such as invading pathogens and trauma, acute and transient inflammation is a crucial defense mechanism. Chronic inflammation however is usually low-grade and persistent and can result in tissue degeneration, doing more harm than good. Possible mechanisms of chronic inflammation include: a) persistent production of reactive molecules by infiltrating leukocytes, b) altered immune modulation through damaged nonimmune and activated immune cells and c) interference of anabolic signalling(137). Possible sources of inflammaging are: a) accumulation of damaged macromolecules and cells (self-debris) with age due to increased production and/or inadequate elimination, b) increased presence of harmful products produced by microbial constituents of the human body, such as gut microbiota, c) age-associated mitochondrial activation of Nlrp3 inflammasome, d) cellular senescence, e) age-related increase in coagulation system activation, f) immunosenescence and g) inappropriate regulation of the complement system(137). Even though chronic inflammation generally leads to tissue degeneration, it can also have a protective function, playing a part in normal tissue remodelling. This is demonstrated by the fact that inflammaging and a hypercoagulable state are compatible with health and longevity, as seen in centenarians(142).

Overall, the notion of inflammaging is very similar to para-inflammation, as seen in the aging retina. The dysregulation of a reparative inflammatory mechanism, resulting in a detrimental, chronic low grade inflammation resulting in tissue damage. In the context of AMD one could speak of a local inflammaging process.

2.3 Local inflammation in age related macular degeneration

The multifactorial pathogenesis of AMD includes aging, oxidative stress, genetic and environmental factors and importantly; the immune system and inflammation. The detection of a) inflammatory molecules such as vitronectin, amyloid A/P, Factor X, prothrombin, Ig, Human Leukocyte Antigen – DR isotype (HLA-DR) and complement proteins (C3, C5, C5b-9, CFH and c-reactive protein (CRP) (143), b) immune cells, including MPs, lymphocytes and mast cells (76, 144, 145) and c) genetic polymorphisms in immune related genes like CFH, complement component 2 and factor B gene (C2/CFB), C3, CX3C chemokine receptor 1 (CX3CR1), TLR3/4 (146) all bear testimony to an inflammatory component in the AMD pathogenesis(72). The inflammation observed in AMD primarily involves the innate immune system, is gradual and subtle and is characterized by the absence of acute inflammation (147). The innate immune system is a highly conserved defense system, indispensable for the initial response to injury or infection, initiating inflammatory responses, clearing debris, remodeling tissue and recovering homeostasis. Why this protective system becomes detrimental in chronic age-related diseases like AMD is not well understood.

The eye is an immune-privileged site with unique anatomical features like the BRB, a lack of direct lymphatic drainage and a microenvironment rich with immunosuppressive molecules that influence the activity of immune cells(148). A mixture of growth factors, cytokines, neuropeptides and soluble receptors is continuously working to establish a down-regulatory immune environment within the eye(148, 149). The retina expresses several immunosuppressive signals such as neuronal CX3C chemokine ligand 1 (CX3CL1) and Fas ligand (FasL) by the RPE. CX3CL1 is a transmembrane protein and is the only ligand of CX3CR1. CX3CR1/CX3CL1 signaling mediates an inhibitory signal on microglial cells and Cx3cr1-deficient mice show increased neuroinflammation and degeneration(150). CX3CR1 is expressed on microglia and its deletion stimulates the expression of inflammatory cytokines, leading to recruitment of inflammatory macrophages, resistance to subretinal MP clearing and photoreceptor toxicity(76, 151). A possible direct role for CX3CR1/CX3CL1 signaling is suggested by the fact that CX3CL1 expression decreases with age and Cx3cr1(152) polymorphisms have been associated with AMD(153-157). Fas (apoptosis antigen 1 (APO-1) or CD-95), the receptor for FasL, is a membrane protein and a

member of the TNF receptor family, ubiquitously expressed in various tissues, with abundant expression on immune cells(158). FasL is predominantly expressed on activated T lymphocytes and Natural Killer cells and constitutively in the tissues of immune privileged sites such as the eye(158). RPE cells express FasL on their cell membrane and can cause apoptotic cell death of Fas expressing (immune)cells through the Fas-associated death domain (FADD)(159). Activation of the FADD triggers a sequential signalling cascade that recruits and activates several caspases and DNAses, resulting in apoptotic cell death(160-162). IL6 represses RPE FasL expression and upon defective FasL/Fas signalling subretinal MP can accumulate as a result of their deficient elimination(76, 163).

2.4 Parainflammation

On a scale of inflammatory states, from basal homeostatic conditions to true inflammation, para-inflammation lies in the middle(164). Para-inflammation aims to maintain homeostasis and restore tissue functionality in a setting of low levels of tissue stress and can be both beneficial and detrimental, depending on whether it is well-controlled or dysregulated(164). During aging the retina is subjected to a chronic low grade oxidative insult, activating the retinal immune system commencing a para-inflammatory response(72). In AMD the dysregulation of this reparative para-inflammatory mechanism leads to chronic low grade inflammation, damaging the macula and the BRB, compromising retinal immune privilege and causing the development of retinal lesions(72, 149). Genetic predisposition, environmental risk factors and old age all contribute to the dysregulation of age related retinal para-inflammation(72).

3. Mononuclear Phagocytes in age related macular degeneration

3.1 Mononuclear phagocytes and macrophages

MPs are prevalent immune cells that persist in many tissues, originating in the yolk sac and fetal liver during development. Thereafter monocytes are derived from the bone marrow and can exit

the circulation to migrate into tissue and become resident macrophages, DCs and osteoclasts (165). MPs play a crucial role in development, immunity, inflammation and tissue homeostasis(166). The ubiquitous presence of macrophages in normal and inflamed tissue combined with their potential to become activated in response to relevant stimuli and secrete a great repertoire of cell products allows them to play a key role in both beneficial and pathological processes, with an especially important role for maintaining chronic inflammation(167). Based on their location and origin macrophages are typically divided into three groups: recruited/infiltrating macrophages, tissue-resident macrophages and perivascular macrophages(168).

In non-pathological circumstances recruited macrophages infiltrate a tissue during inflammation and only briefly remain in place before they undergo apoptosis or emigrate(169).

Despite its extremely versatile and omnipotent character though, the primary role of macrophages is not to function as an elite immune effector cell but as a common 'janitorial' cell whose main function is to clear extraneous cellular material and cellular debris(170). These processes take place independently of immune-cell signalling through phagocytosis mediating receptors that do not actively induce transcription or production of cytokines.

3.2 Macrophage polarization

The function a macrophage carries out is dependent on the (patho)physiological situation it finds itself in. Environmental cues can prompt macrophages to activate and change their physiology while the remarkable plasticity that macrophages display gives rise to different populations with different functions(170). Macrophage polarization refers to how macrophages have been activated at a given point in space and time and is routinely viewed as a linear scale, with M1, or classically activated, macrophages on one extreme and M2, alternatively activated macrophages, on the other(170-172). These two activation states are in analogy to the adaptive immune system where T helper cells can be subdivided in Th1 and Th2.

A schematic of macrophage polarization is shown in Figure 6. In the presence of IL4 or IL13, through STAT6, and indirectly by IL10, through STAT3, macrophages become alternatively activated and are polarized to an anti-inflammatory, pro-tissue repair and proangiogenic

phenotype, characterized by low levels of IL12 and IL23 and high levels of IL10, TGFβ and Arg1(173, 174). Macrophages in the presence of IFNγ, through the interferon receptor, TNF, through TNF receptor, PAMPs such as LPS and DAMPS through TLR activation, are classically activated and adopt a pro-inflammatory, anti-angiogenic profile with a high production of cytokines such as IL6, IL12, IL23, TNF and iNOS(173, 174). This is an oversimplified presentation that doesn't take into account that there is a large range of intermediate phenotypes that exist between the extremes of M1 and M2. The polarization state of macrophages can affect the profile of excreted growth factors and affect different stages of angiogenesis(175).

Several techniques can be applied in order to get an idea of the activation of the cells. Morphology can give a first impression of the character(176), with M1 macrophages adopting an enlarged amoeboid cell shape with roundish cell bodies and numerous delicate cytoplasmic extensions on the cellular surface and M2 macrophages demonstrating a bigger heterogeneity with large ramified macrophages with an elongated cell body and cytoplasmic extensions on the apical ends of the cell bodies(177). Secondly, several surface receptors that are indicative of polarization can be detected by immunohistochemistry(178) or fluorescence-activated cell sorting (FACS)(179), with major histocompatibility complex (MHC) II, CD80 and CD86 as M1 markers and CD64, CD163, CD206 and CD209 as M2 markers(180, 181). Then there's still the option of looking at the secretome of macrophages. TNF, IL1β, IL6, IL12, IL23, inducible nitric oxide synthases (iNOS) and a plethora of chemokines from the C-X-C motif chemokine ligand (CXCL-1,3,5,8,9,10,11,13,16) and CC chemokine ligands (CCL-2,3,4,5,8,15,11,19,20) family and C-X3-C motif ligand 1 (CX3CL1) being indicative of M1 polarization(180, 182). A secretome with IL1R, IL10, transforming growth factor beta (TGFβ), arginase 1 (ARG1) and several CCLs (CCL-1,2,13,14,17,18,22,23,24,26) is indicative of M2 polarization(180, 183, 184). Lastly, macrophages can be analyzed based on their gene expression and the transcriptomic characterization of macrophages. Inflammatory and anti-inflammatory gene expression patterns, changes in mitochondrial metabolism and several novel marker genes can help classify the polarization of these enormously plastic cells(185, 186).

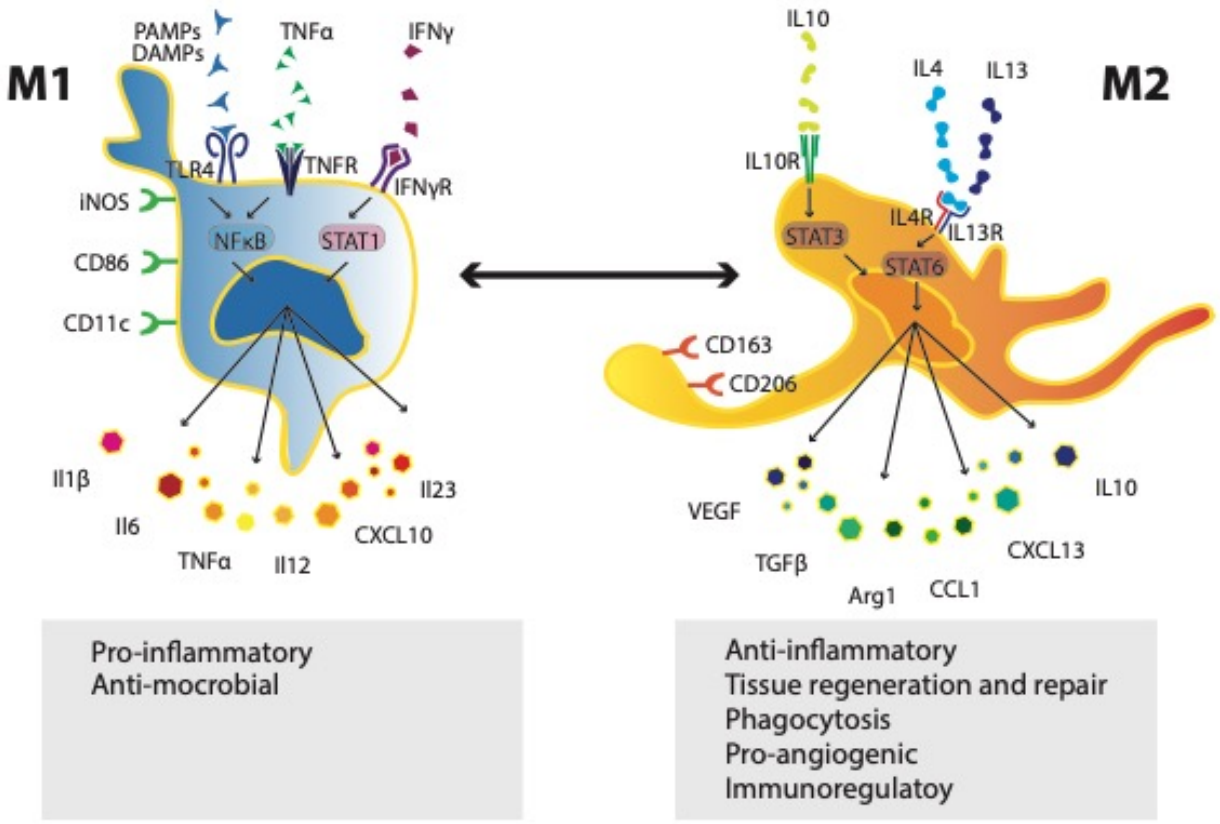

Figure 6 Macrophage polarization

PAMPs, DAMPS, TNF and IFNγ classically activate macrophages that adopt a pro-inflammatory, anti-angiogenic profile with a high production of cytokines such as IL6, IL12, IL23 and TNF. In the presence of IL4, IL10 and IL13 macrophages become alternatively activated and are polarized to an anti-inflammatory, pro-tissue repair and proangiogenic phenotype, characterized by low levels of IL12 and IL23 and high levels of IL10, TGFβ and Arg1. Figure inspired by Biswas et al(187), Tugal et al(188) and Atri et al(181).

3.3 Mononuclear phagocytes in the posterior segment of the eye

The healthy choroid houses numerous resident myeloid cells which remain in close association with the choroidal vessel cultivating important immune-vascular interactions(189). The immune

privileged retina contains several types of MPs, including blood monocytes, tissue-resident macrophages, DCs and microglia(190). Microglia are highly specialized central nervous system resident immune cells that exert significant influence during retinal development and in pathological situations, forming the first barrier against pathogens and environmental insults(191). Fate mapping analysis revealed that adult microglia stem from primitive yolk sac macrophages that have migrated into the retina before the BRB was established(192). Microglia are crucial for retinal growth and neurogenesis during development and are implicated in the clearance of apoptotic neurons and the maintenance of synaptic structure in the adult retina(193).

In adulthood microglia are solely dependent on local expansion and are maintained without recruitment of circulating monocytes(194, 195). By way of self-renewal the retinal population is maintained throughout life(196), forming a highly intricate network with their long protrusions(197) in the inner and outer plexiform layers of the retina(198), leaving the photoreceptor cell layer and the subretinal space devoid of MPs during physiological conditions(76, 199). Besides their very important role as housekeepers, the microglia are imperative as a watchdog for retinal homeostasis(200) and immune response(201, 202). The retina houses a highly sensitive immune system(201) and upon perception of danger signals, like PAMPs or DAMPs, microglia migrate to the site of damage, start proliferating and release pro-inflammatory cytokines and reactive oxygen species (ROS) (197, 203). In addition they greatly increase their phagocytic activity in order to clear debris and prevent accumulation of waste products(204), rapidly de-escalating the insult, repairing damaged tissue and reinstating homeostasis(76, 201). Macrophages that have been attracted from the choroid rapidly disappear from the retina through apoptosis after resolution(205). Tight control of these immune actions is vital for maintenance of retinal health, and is imposed by cross-talk with Müller cells and retinal neurons and by means of regulatory molecules like complement factors, chemokines and neurotrophic factors(206-208). The healthy mammalian retina is devoid of MPs other than microglia and a key feature of macular degeneration is the infiltration of circulating MPs into the subretinal space. Microglia can play a role in immune homeostasis like a double edged sword, with an “adaptive” and a “maladaptive” response(209). In the “adaptive” response reactive

microglia migrate into the subretinal space and restrict disease progression, opposed to the "maladaptive" response, where microglial activation results in a surge of pathogenic monocyte derived cells in the subretinal space(209, 210). Under continuous pathological stimuli, microglial inflammatory response can become dysregulated and worsen pathology.

3.4 Mononuclear phagocytes in age related macular degeneration

Macrophage and microglial dysfunction play an important role in the pathogenesis of AMD and several other retinal diseases(76, 207). A schematic overview of some of the most important pathogenic roles of MP's is shown in Figure 7. When, for a number of possible reasons, including genetic predispositions, high glucose levels, persistent insult or chronic systemic low-grade inflammation and "inflammaging", inflammation does not subside, microglia can cause irreparable damage to the retina(72, 137, 211-213). Chronic retinal inflammation is linked to a decline in RPE function, BRB compromise, formation of neovessels and a protracted recruitment of choroidal macrophages(214-216). Further attraction of MPs from the choroid and circulation through CCL2 and the secretion of pro-inflammatory IL1β, ROS, TNF, iNOS and C1q are the result of inflammatory escalation caused by over-reactive microglia(199, 201, 217, 218). Within this setting microglia are no longer able to distinguish stressed cells from apoptotic cells and proceed to the phagocytosis of viable neurons contributing to retinal decline(219, 220).

Recognizing that non-resolving retinal inflammation is not the primary cause of AMD, it's role in the pathogenesis is significant. AMD is associated with systemic inflammation and local activation of MPs around large drusen, GA lesions and CNV(76). Whether the persistent inflammation is caused by an unsettled primary problem or the inability to exit a downward spiral remains unclear and might very well differ from case to case(76). Breaking the vicious cycle of inflammation and deterioration with appropriate anti-inflammatory therapies is an, at this time, not sufficiently explored possible treatment avenue(76).

The increase in phagocytes-derived cytokines upon disturbance of chororetinal homeostasis causes direct and indirect damage to the retina. The IL1β protein is transcribed from the Il1β gene after inflammatory stimuli like PAMPs and DAMPs, is a potent survival factor for endothelial cells, induces similar genes than VEGF and exacerbates CNV(76, 221-224). Besides its pro-

angiogenic effect, MP derived IL1β can induce neuronal damage like rod apoptosis and cone segment degeneration(151, 225-227). Excessive IL1β is another cause for photoreceptor degeneration in addition to RPE dysfunction and disappearance(199).

Comparable to IL1β, TNF is an important player in the pathogenesis of AMD(228, 229) and an increased expression of TNF by monocytes correlates with a higher prevalence of CNV(230). Early AMD is associated with an increase in recovery time after exposure to high levels of illumination (bleach) and evidence suggests this might be caused by increased levels of TNF produced by infiltrating MPs associated with large drusen(76, 163, 199, 231). TNF greatly affects RPE homeostasis by repressing orthodenticle homebox (OTX)2, a critical transcription factor of the RPE during retinal development and the retinol visual cycle(76, 232). The visual cycle is a complex system which replenishes the compounds that are needed for biological conversion of a photon into an electrical signal in the retina and a slower visual cycle negatively influences daytime vision.

In concert with IL1β, TNF and VEGF, IL6 is a highly relevant contributor to CNV formation(163, 233). IL6 induces VEGF production which promotes angiogenesis and vascular permeability through gp130 signalling, consequent STAT3 phosphorylation and VEGF promotor binding(234). Macular edema in patients with CNV is significantly associated with intraocular levels of IL6 showing an even better correlation than VEGF levels with macular edema(235, 236). IL6 further has an important influence on the immune privilege in the eye, contributing to MP infiltration. IL6 reduces RPE FasL while protecting retinal neurons(163).

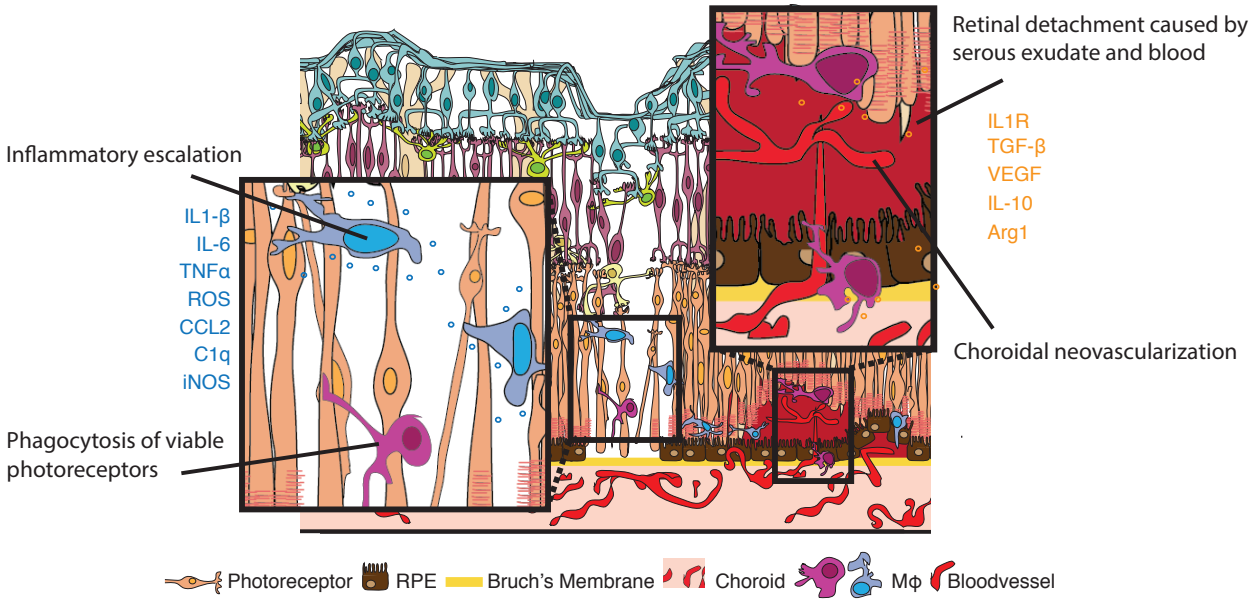

Figure 7 Mononuclear phagocytes in age-related macular degeneration

The secretion of pro-inflammatory IL1β, ROS, TNF, iNOS and C1q are the result of inflammatory escalation caused by over-reactive microglia. Within this setting microglia can proceed to the phagocytosis of viable neurons contributing to retinal decline. IL1β, IL6, TNF and VEGF production promote angiogenesis and vascular permeability. Choroidal neovascularization is often of low quality and are in consequence inclined to hemorrhage or leak. The subretinal exudative deposits of blood and lipids cause retinal edema, photoreceptor cell death, fibrovascular scarring and retinal detachment. Figure partially inspired by Guillonneau et al(76) and Walter F. Boron and Emile L. Boulpaep(47).

4. Obesity

4.1 Prevalence

Over the past two generations the prevalence of obesity, -a complex, multifactorial disease with genetic, behavioral, socioeconomic and environmental origins-, has increased worldwide (237).

Economic growth, industrialization, mechanized transport, urbanization, an increasingly sedentary lifestyle and a nutritional transition to processed foods and high calorie diets have caused an alarming rise in the prevalence of this largely preventable disease(238). According to the World Health Organization obesity has nearly tripled since 1975 and in 2016 more than 1.9 billion adults were overweight, of which 650 million were obese(239). Most of the world's population now lives in a country where overweight kills more people than underweight(239). Obesity is defined as excess of body-fat mass, with a body mass index (BMI)>30 kg/m^2(240). BMI expresses body weight as a function of body height and can be further subcategorized into class 1 (BMI of 30 to <35), class 2 (BMI of 35 to <40), and class 3 (BMI of >40)(241). While representing a major risk factor for diseases such as diabetes mellitus type 2, hypertension, myocardial infarction, stroke, fatty liver disease and several cancers, obesity contributes to a decline in quality of life and life expectancy(237). Unemployment, social disadvantages and reduced socio-economic productivity associated with obesity additionally impact well-being(237). The economic costs of obesity are staggering, with an annual medical spending attributable to an obese individual in 2014 in the US mounting to almost $2000 US, accounting for $149.4 billion nationally(242). With up to one-third of adults in the US affected, obesity is among the most common and costly chronic disorders worldwide(240). Strategies to curb the pandemic of overweight and obesity have not been successful and this disease with its high morbidity and mortality causes a major challenge to chronic disease prevention(238).

4.2 Inflammation in obesity

Despite the failure to slim down the high prevalence of obesity, there is a gain in understanding of its pathophysiology. The search for a mechanism linking obesity to its frequent comorbidities has revealed a connection between nutrient excess and the activation of the innate immune system(243-246). Early on in the onset of obesity the activation of an inflammatory program shifts the immune system to a proinflammatory phenotype. Several different mechanisms have been investigated in rodents and obese individuals(247). In a review from Kanakadurga Singer and Carey Lumeng different early events in obesity-induced inflammation during human development, of which many are sustained into adulthood, have been described(248). For

example, a raised circulation of different lipid species contributes to inflammation through binding to TLR4 and TLR2, resulting in NFκB and c-Jun N-terminal kinases (JNK)1 activation(249-251). Another potential mechanism underlying inflammation acts through hypoxia that develops in the adipose tissue due to inadequate perfusion and increased oxygen consumption(252). Cellular hypoxia initiates inflammation through the induction of the Hypoxia-inducible factor (HIF)1 gene program(253). Not only hypoxia but also mechanical stress caused by the expansion of adipocytes can strain the cells with subsequent proinflammatory responses(254). One last example of an inflammatory cascade initiating causatum is the increase in intestinal permeability caused by obesity(255). Higher circulating levels of lipopolysaccharide (LPS), derived from the Gram-positive bacterial species present in the intestinal lumen, activate PRRs such as TLR4 and cause a systemic chronic low grade inflammation(256). The chronic activation of the innate immune system that is seen in obesity-induced inflammation leads to maladaptive responses such as fibrosis and necrosis and can cause significant tissue damage in multiple organs, including adipose, pancreas, liver, skeletal muscle, heart and brain(247).

The involvement of chronic low grade inflammation in de pathogenesis of AMD combined with the proinflammatory state in obesity have prompted the investigation into a relation between obesity and AMD.

4.3 Obesity and age related macular degeneration

Evidence of chronic low grade inflammation in AMD and the proinflammatory character of obesity inspired several studies, including cross-sectional, case-control and longitudinal cohort(27, 38, 79, 257-264) into the relation between obesity and AMD(39). The evidence for an association between obesity and AMD have not been consistent, with several studies finding a positive association between BMI and AMD(28, 258, 262-270) while some others reported no association(271-274).

BMI has several limitations as a measure for obesity since it combines adipose and nonadipose body components without taking of variation attributable to body frame size into account(275). Adams et al conducted a comprehensive study of body composition and AMD to determine the strength of the associations of different forms and stages of AMD with 5 adiposity measures—

body mass index, waist/hip ratio, waist circumference, fat mass, and body fat percentage(39). Using a large Australian cohort with 21,287 participants from the Melbourne Collaborative Cohort Study the authors found that an increase of 0.1 in waist/hip ratio was associated with a 13% increase in the odds of early AMD and a 75% increase in the odds of late AMD in men. These results suggest a stronger relation between waist/hip ratio and AMD than between BMI and AMD, confirming obesity as a risk factor for AMD.

4.4 Intestinal permeability

With a total surface of more than 200-meter square the gastrointestinal (GI) tract forms one of the most important exposures to the outside world, necessitating a strict separation of the external and internal environment(276). The sole structural barrier between the intestinal lumen and the circulation is a contiguous layer of epithelial cells, ranging from the oesophagus to the anus, functions as a barricade that blocks a wide variation of environmental agents from accessing the body. Intestinal permeability is the feature that allows solute and fluid exchange between the intestinal lumen and the intestinal mucosa(277). Most of the epithelial barrier is formed by enterocytes, cells with a lipid bilayer and a brush border, optimizing its dual function as absorptive and barrier cell. With a marked solubility to lipid compounds but a strong restraint to water soluble factors the enterocyte has several transport systems in place for the transport water soluble compounds(278). Besides the transcellular absorption pathway there is the possibility of the paracellular pathway. At the junction of epithelial cells lie tight junctions and adherens junctions, complex structures of lipid and protein structures that allow for alterative permeability of the cell-cell junction(279). Once considered a static parameter, the permeability of these junctions is now recognized to be highly dynamic. A schematic diagram of intestinal permeability is shown in Figure 8.

With the help of members of the occludin and of the claudin family, two types of membrane proteins found in the vicinity of cell junctions that cross the plasma membrane to interact with proteins from the adjoining cell, epithelial tight junctions can open and close in response to a variety of stimuli(280, 281). The relative abundance of different claudin family members is

important for junction functionality and during normal development and during disease, the relative abundance of claudins can change by up to 1000-fold(282, 283).

There are many factors that impact the regulation of intestinal permeability and whereas normal intestinal permeability is associated with health, increased intestinal permeability is associated with several intestinal and extra intestinal diseases(277). Some matters that influence intestinal permeability are the mucus layer, epithelial cell integrity, epithelial junction, immune responses(284, 285), intestinal vasculature, intestinal motility, stress(286, 287), diet(285) and gut microbiota(277, 279, 288, 289). The gut epithelium insures a selective passage of substances and prevents the entry of harmful elements aided by a thick layer of mucus. The mucus is excreted by goblet cells and is enriched by antimicrobial peptides, cytokines and Igs that are secreted by Paneth cells, epithelial cells and plasma cells(279, 290). These antimicrobial products help eliminate potentially pathogenic bacteria, recruit immune cells, such as T helper cells and neutrophils, or mark bacteria for destruction by intestinal lymphocytes(290). Unchecked inflammatory responses can result in damage to the intestinal epithelium, causing an intestinal barrier breach, allowing for the translocation of gut microbes or their secreted products to cross into the extraluminal system. Both Gram-positive and Gram-negative bacteria shed microbial peptides such as peptidoglycans (PGN) which can translocate when the intestinal barrier has a reduced integrity, acting as PAMPS, inducing endotoxemia and activating pro-inflammatory pathways of the host(291).

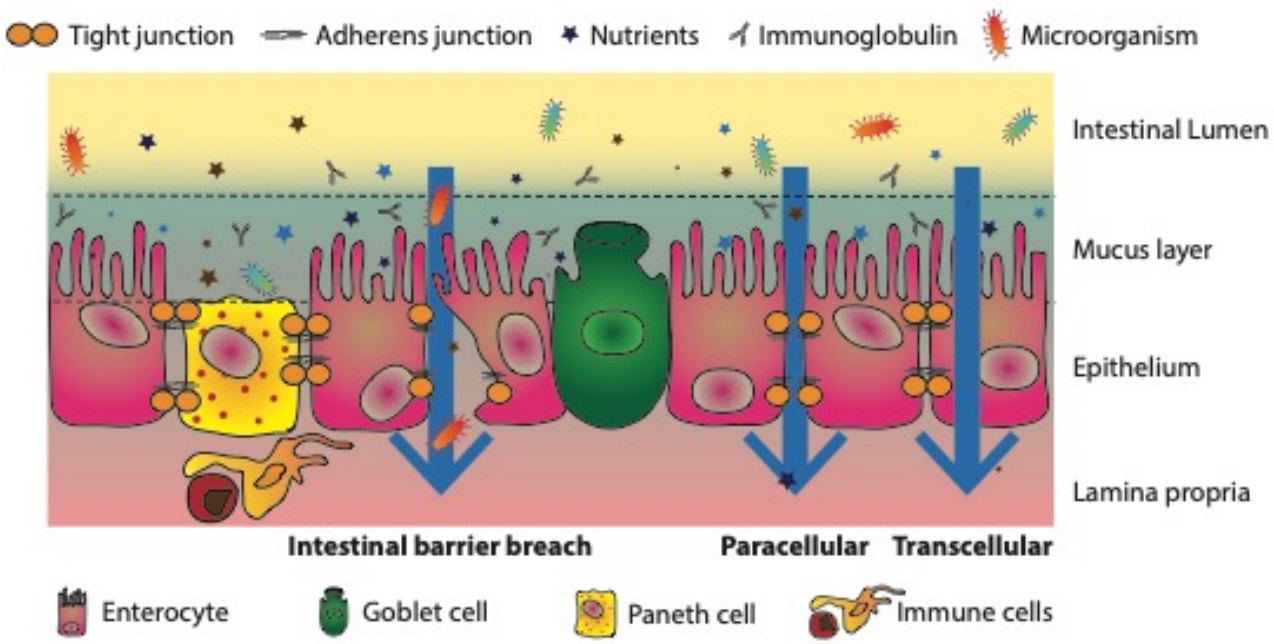

Figure 8 Intestinal permeability

The gut epithelium insures a selective passage of substances through the transcellular or paracellular pathway. At the junction of epithelial cells lie tight junctions and adherens junctions, complex structures of lipid and protein structures that allow for alterative permeability of the cell-cell junction. The epithelium prevents the entry of harmful elements aided by a thick layer of mucus, excreted by goblet cells. Paneth cells enrich the mucus with antimicrobial peptides. Unchecked inflammatory responses can result in damage to the intestinal epithelium, causing an intestinal barrier breach, allowing for the translocation of gut microbes or their secreted products to cross into the extraluminal system. Figure inspired by Natividad et al(292).

4.5 High fat diets and intestinal permeability

The decrease of intestinal barrier functions facilitates the passage of harmful elements such as LPS, PGNs, whole bacteria and other toxins and plays an important role in the pathogenesis of many diseases(293). Gut microbiota, mucus production, intestinal epithelial cells and the mucosal immune system all collaborate in order to preserve a healthy gut barrier. Each of these

players can be significantly influenced by food-derived compounds, either direct or indirect(293-295). The “Western style diet” with its energy-dense, high sugar, high fat and fiber low food increase intestinal permeability(296). One way the fat content of a diet influences intestinal permeability is through the increased production of bile acid. Not only do bile acids function as signalling molecules that can negatively affect the integrity of the intestinal barrier(297), they also exert direct, receptor independent toxicity towards intestinal epithelial cells(298, 299) and induce changes in tight junction proteins(277, 300). The other way high fat diets (HFD) influences intestinal permeability is through inflammation. The HFD induced stimulation of proinflammatory signalling cascades, increase in barrier-disrupting cytokines (TNF(301), IL1β(302), IL6(303) and interferon gamma (IFNγ)(304)) and decrease in barrier-forming cytokines (IL10(305), IL17(306) and IL22(307)) all negatively inflect gut barrier function(308). Finally, a HFD induces gut microbiota changes and dysbiosis with an enrichment of barrier-disrupting species(308-310).

5. Gut microbiota

5.1 We are not alone in our bodies

Inside every person live trillions of microorganisms such as bacteria, viruses, fungi and other life forms(311). The community of microorganisms that reside in an environmental niche is called microbiota. The collective genome of all these microorganisms is called the microbiome. The first one to give a name to the human microbiome was Joshua Lederberg: “microbiome, to signify the ecological community of commensal, symbiotic and pathogenic microorganisms that literally share our body space”(312). Many organs have highly distinct microbiota, as can be seen in Figure 9 that is based on data from The human microbiome, written by Hubert E Blum(313). The group that has attracted the most attention by far is the gut microbiota. The human intestine can be described as an anaerobic bioreactor that is programmed by an enormous population of more than 100 trillion (10^14) microbial cells, almost outnumbering the number of eukaryotic cells of the organism they inhabit(314-317). Our microbiota has coevolved with us and complements and

manipulates our biology in a mutually beneficial way. The microbiota functions in tandem with the host giving the ability to harvest nutrients such as amino acids and short-chain fatty acids from food and acting as a source of essential nutrients and vitamins(318). It also helps maintain stability and protecting us from colonization and invasion by opportunistic pathogens(314, 319). In January of 2020 Nature Research published Nature Outlook, The gut microbiome, a whole issue dedicated to the latest research on the gut microbiome(320). The gut microbiota has attracted tremendous attention in the last few decades in biomedical research and much more research is under way. Gut microbes play a part in health and disease, including cancer(321), autoimmune disorders(322) and autism spectrum disorder(323), while strongly interacting with certain drugs(324). Researchers are investigating what makes a microbiome "good"(325), whether we can influence it with our diet(326) and how fecal microbiota transplantations (FMT) can help cure diseases(327). To this day it is difficult to describe the precise impact of the intestinal microbiota on human health and the involvement in disease and there is still room for plethora or exciting findings related to this "forgotten organ"(328).

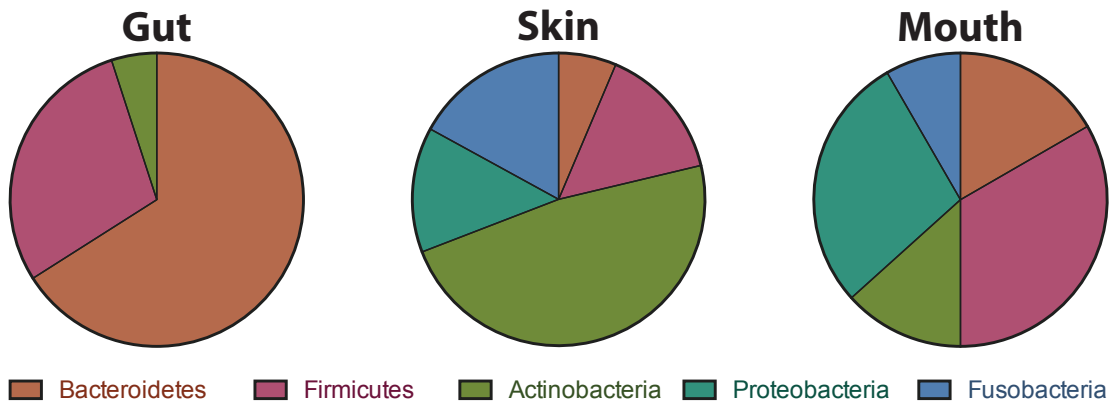

Figure 9 Distinct microbiotal compositions

Different parts of the body – the gut, skin, mouth, etc – all have very different, distinct communities of microbes. While gut microbes have gained a lot of attention, microbes elsewhere are also important. Based on data from The human microbiome, written by Hubert E Blum(313).

5.2 Shaping of the human gut microbiome

The GI tract of a normal fetus is (almost(329)) sterile up until the moment of birth. Rapidly after birth bacteria start to appear in the feces of the newborn(330). Gut microbiota is acquired shortly after birth from the surrounding environment by vertical and horizontal transmission. The delivery mode is one of the first things to affect the colonisation of the gut. Vaginally delivered children are exposed to the high load of lactobacilli and other microbes in the vaginal flora, as opposed to the children delivered by caesarian that come into the world under aseptic conditions before they are placed on their mothers chest(331). As a consequence the pioneering microbes that are the first to colonize the newborn are substantially different. Infants born through caesarian have a lower total microbiota diversity during the first 2 years of life and the abnormal development of the intestinal microbiota may continue even beyond infancy(332). In 2016 Dominguez-Bello et al published a study where they exposed infants delivered by C-section to maternal vaginal fluids at birth. The vaginal microbial transfers were achieved by swabbing the babies, starting with the mouth, then the face and finally the rest of the body with a gauze that had incubated in the mothers vagina during the hour preceding the C-section. Similar to vaginally delivered babies, the gut, oral, and skin microbiome of these newborns during the first 30 days of life was enriched in vaginal bacteria underrepresented in unexposed C-section infants(333).
During the first years of life, microbial diversity increases and the composition of the microbiome matures towards a distinct profile, reaching maturity and the complete functional capacity of an adult microbiota around 2.5 years of age(334-336). Although quite stable in adulthood, the gut microbiome is still prone to disturbance by life events and can shift composition under influence of environmental factors such as diet, exercise and medication(294, 336-338). Imbalances in the gut microbiota are termed “dysbiosis”. Dysbiosis can induce aberrant immune responses and disrupt the local and systemic homeostasis of the host(339).

5.3 16S rRNA analyses

In order to distinguish different microorganisms researchers commonly look at the “16S”. The 16S ribosomal ribonucleic acid (RNA) (rRNA) gene contains highly-conserved hypervariable regions ranging from region V1 to V9 which can be used to determine microbial communities

within samples(340). Initial efforts to determine the number and diversity of microbes were based on culture-based approaches using the 16S rRNA technology(341-344). Yet, 20-60% of the human-associated microbiota is uncultivable, resulting in a gross underestimation of its diversity(344-346). Technological developments of deoxyribonucleic acid (DNA) sequencing have greatly facilitated culture- and cloning-free analyses of the microbiome. Advances in high-throughput sequencing technologies have enabled researchers to explore the microbiome using the hypervariable regions of the 16S rRNA gene in a cost-effective manner(340) including oral(347), vaginal(348, 349), skin(350) and gut microbiota(351). Using the 16S rRNA gene studies have revealed a significant inter-individual diversity of the gut flora(352) and differences between the gut microbiota of obese versus lean donors(353, 354). Inter-individual diversity of gut flora can in part be explained by genetic differences amongst hosts and is also heavily influenced by dietary habits(337, 355).

5.4 Influence of diet on microbiota

With the advances of 16S rRNA sequencing, an increasing number of studies have been able to investigate the impact of diet on microbial composition. Current research shows that diet exercises an extensive effect on the gut microbiotal composition(356). Dietary habits are considered one of the main factors contributing to the richness of human gut microbiota and reduction in microbial diversity is possibly one of the unwanted effects of highly processed, nutrient-rich uncontaminated foods. A decreased exposure to a large array of environmental microbes and a diet low in unabsorbable fibers, promoting a microbe unfriendly habitat in the gut, reduces the richness of the microbiome. Both in the Western world and in developing countries, diets rich in protein, sugar and fat are associated with a rapid increase in the incidence of non-infectious intestinal diseases(357). The probable favourable effects of diets on bowel disorders was already described in the 1970's by Burkitt who noticed a remarkable absence of non-infectious intestinal diseases in Africans(358). De Filippo et al showed in 2010 that the fecal microbiota of European children and that of children from a rural African village of Burkina Faso are compellingly different. In Burkina Faso, where the diet, high in fiber content, is similar to that of early human settlements at the time of the birth of agriculture, children harbor a microbiome

that is significantly richer and more biodiverse than the microbiome of children that grow up in Florence, Italy(357).

But also closer to home, in less dramatic situations, a regime can greatly impact microbiota. Diets composed entirely of animal or plant products rapidly alter the microbial community structure within just 24 hours of initiation, with reversion to baseline within 48 hours of discontinuation(294, 359). This illustrates the volatility if the human microbiome that does not only differ between two individuals living a completely different life-style, but also changes within an individual, depending on his choice of meal.

Not only within humans diets shape the community of microbes living in the gut. A previous study of 59 mammalian species revealed that both host diet and phylogeny influence bacterial diversity and that the gut microbiota of humans consuming a "Western style diet" is typical for omnivorous primates(360). To isolate the effects of phylogeny and diet, Ley et al included multiple samples from many of the mammalian species, as well as species that had unusual diets compared to their close phylogenetic relatives.

5.5 Dysbiosis

Dysbiosis, an imbalance in the gut microbiota, can disrupt local and systemic homeostasis of the host(339). Alterations in the microbiota can be the result of various environmental factors such as diet, drugs, pathogens and toxins(318). Growing evidence shows that dysbiosis is associated with the pathogenesis of both intestinal and extra-intestinal disorders. Examples of intesinal disorders are inflammatory bowel disease, irritable bowel syndrome and coeliac disease. Examples of extra-intestinal disorders associated with gut microbiotal dysbiosis are allergies, asthma, metabolic syndrome, cardiovascular disease and obesity(318).

The hierarchy of biological classification consists of eight major taxonomic ranks, ranging from domain to species, as shown in Figure 10. The kingdom "Bacteria" is constituted of 29 lineages called bacterial phyla. A bacterial phylum is a lineage of bacteria whose 16S rRNA genes share a pairwise sequence of ~25% or more(361). Almost 40% of the microbial genes present in each individual are shared with at least half of the general population, known as the core microbioma(362). The core microbioma is dominated by the phyla *Bacteroidetes* and *Firmicutes*,

as well as *Proteobacteria, Actinobacteria, Fusobacteria, Spirochaetes, Verrucomicrobia* and *Lentisphaerae*(363, 364). Changes in the composition of the intestinal microbiota are often described as changes in relative abundance of beforementioned phyla.

Both in obese mice(353) and humans(354) an increase in the relative abundance of *Firmicutes* and *Bacteroidetes* has been found in addition to a reduction in microbial diversity when compared with lean individuals(355). Antibiotic treatment induced changes in the gut microbiota were accompanied by a decrease in metabolic endotoxemia (an increased plasma concentration of circulating endotoxins such as LPS), and inflammation(365).

Inter-individual and intra-individual variations in addition to age-related changes in the intestinal microbiota make it hard to pinpoint the relation between changes in microbiotal community and health(318). On top of that, it is important to note that it is not always clear whether changes in phylogenetic composition are the cause or a consequence of a given disease(318). Evidence of direct involvement of intestinal microbiota in a pathogenesis can be provided by studies that use germ-free mice. In several disease models, such as those for inflammatory bowel syndrome(366) and autoimmune arthritis(367), severity or incidence of disease are reduced under germ-free conditions.

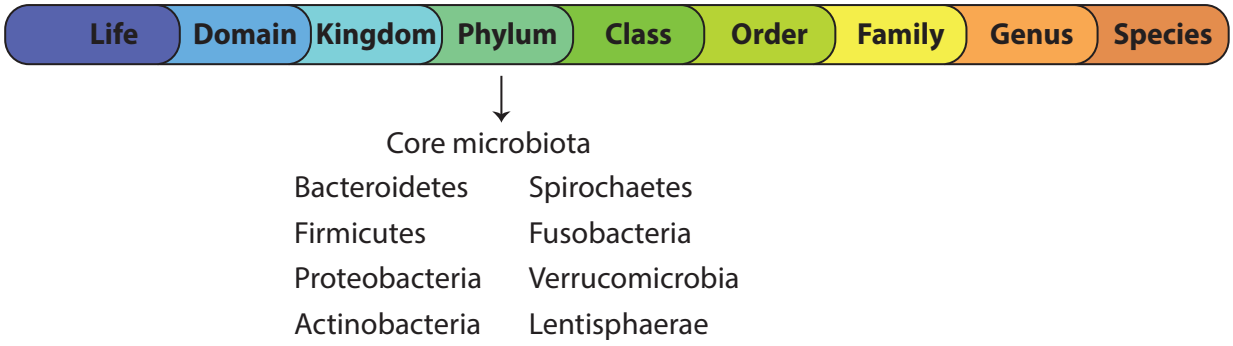

Figure 10 Biological classification in taxonomic ranks

The hierarchy of biological classification consists of eight major taxonomic ranks, ranging from domain to species. The core microbioma is dominated by the phyla Bacteroidetes and Firmicutes, as well as Proteobacteria, Actinobacteria, Spirochaetes, Fusobacteria, Verrucomicrobia and Lentisphaerae. Changes in the composition of the intestinal microbiota are often described as changes in relative abundance of beforementioned phyla.

6. Neuropilin-1

6.1 Structure of Neuropilin-1

NRP1 is a single pass transmembrane glycoprotein that is highly conserved and expressed in all vertebrates(368-370). NRP1 is composed of ~900 amino acids, encoded by 17 exons(368). Originally discovered as an adhesion molecule in the nervous system(371), rediscovered as a semaphorin (SEMA) 3 binding receptor in neurons(372, 373) and subsequently as a VEGF receptor in blood vessels(374), NRP1 has been a topic of interest for several decades now with implications in cardiovascular and neuronal development, angiogenesis, lymphangiogenesis, migration and recruitment(370). More recently NRP1 has attracted attention as an immune response modulator in both physiological and pathological conditions in several distinct immune cells such as DCs(375), T cells(376), B cells(377) and macrophages(368-370, 378, 379). The multipotency of NRP1 can be explained by one's atypical ability to bind several structurally unrelated ligands via distinct sites on its extracellular domain(380-382).

A schematic overview of the NRP1 receptor is shown in Figure 11. NRP1 is comprised of a large extracellular N-terminal containing five domains, a short membrane spanning domain and a small cytoplasmic domain(368). The extracellular part consists of two complement-binding homology domains identified as a1 and a2 followed by two coagulation factor V/VIII homology domains identified as b1 and b2, and a MAM (meprin/antigen 5/receptor tyrosine phosphatase m) domain identified as c(369). The short intracellular (cytoplasmic) domain is catalytically inactive but can bind intracellular proteins containing a PDZ domain with its C-terminal SEA (serine-glutamine-alanine) motif (369). It's through its large and complex extracellular domain that NRP1 interacts with several binding partners and can engage in different signalling pathways(383). The extracellular domains a1 and a2 are essential for binding of SEMA3 family members(372, 373) and the domains b1 and b2 mediate binding to different isoforms of VEGF(374, 375, 380, 384), TGFβ(385), platelet derived growth factor (PDGF)(386, 387) and more(382).

The most described ligands of NRP1 are the SEMA and VEGF families. Semaphorins are axonal chemorepellants that provoke axon growth cone collapse, guiding neurons during the development of the nervous system(388). Eight classes of semaphorins have been described, but

only class 3 semaphorins bind NRP1(389, 390) with SEMA3A being the preferred ligand(368). The VEGF family exists of six proteins(96) of which two (VEGFA and VEGFB) bind NRP1, with VEGFA being the strongest and best characterized ligand(388). The short cytoplasmic and catalytically inactive domain requires NRP1 to form a coreceptor complex in order to transmit intracellular signals. SEMA3A signaling through NRP1 occurs through complexing of NRP1 with a Plexin, a large transmembrane molecule, with NRP1 acting as a bridge between the proteins(388, 391). VEGF signaling also occurs via coreceptor complexes, most commonly between NRP1, VEGFR-2 and the VEGF165 isoform(388). VEGF165 forms a complex binding to VEGFR2 and NRP1, with NRP1 enhancing the binding of VEGF165 and VEGFR2, potentiating VEGFR2 signalling and proangiogenic activities(392).

Several soluble forms of NRP1 (sNRP) have been described, where the absence of the c, transmembrane and intracellular domains keep the receptor from directly interacting with the cell(393-395). By sequestration of available ligands it can however function as a decoy receptor, inhibiting transmembrane NRP1 function(393).

NRP1 has a close homolog identified as NRP2(396). The amino acid sequences of the different domains are ~44% identical to the ones of NRP1, with an identical domain structure(369, 396). There exists a certain overlap in possible ligands, but where NRP1 preferentially binds VEGF165 and SEMA3A, NRP2 prefers VEGF145 and SEMA3F(397). NRP2 plays an important role in neurons but is, unlike NRP1, dispensable for vasculogenesis and angiogenesis.

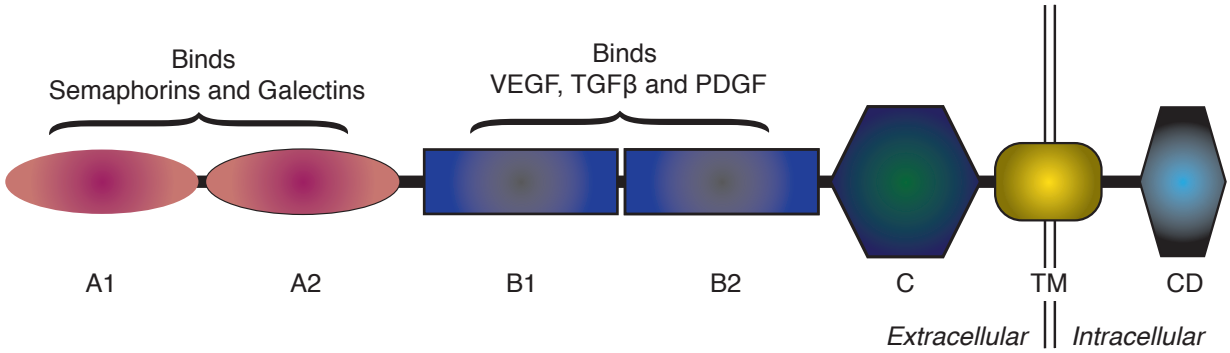

Figure 11 Schematic of the Neuropilin-1 receptor

Neuropilin-1 is comprised of a large extracellular N-terminal containing five domains, a short membrane spanning domain and a small cytoplasmic domain. The extracellular part consists of two complement-binding homology domains identified as a1 and a2 followed by two coagulation factor V/VIII homology domains identified as b1 and b2, and a MAM (meprin/antigen 5/receptor tyrosine phosphatase m) domain identified as c. The short intracellular (cytoplasmic) domain is catalytically inactive but can bind intracellular proteins. The extracellular domains a1 and a2 are essential for binding of SEMA3 family members and the domains b1 and b2 mediate binding to different isoforms of VEGF, TGFβ, PDGF and more. Figure inspired by Raimondi et al(369).

6.2 Functional significance of Neuropilin-1

NRP1 is widely expressed and detected in a majority of human cell types(398). The vascular and neural defects that present in NRP1-null mice are embryonically lethal, demonstrating the essential role of NRP1 in development(368, 399-401). Vascular endothelial NRP1 binds VEGF, a crucial regulator for vasculogenesis and angiogenesis, while NRP1 on the membranes of developing neurons forms part of a receptor complex binding the axon guidance inhibitory class 3 semaphorins, explaining why *Nrp1* inactivation causes vascular defects and disorganization of nerve fiber development(399, 400). Besides an imperative role during embryogenesis, NRP1 has important functions in adult tissues not only in axon guidance and angiogenesis but also in immune responses and tumor progression(402).

NRP1 expression is increased in a variety of cancers (prostate(403), lung(404), colon(405), breast(406), melanoma(402), astrocytoma(407), and glioma(408)) and typically exerts growth-promoting functions(409, 410), positively correlating with tumour progression and poorer outcome. Being implicated in various aspects of tumour vascularization, cell growth, survival, migration and metastasis(388, 405, 411-414), NRP1 is an important target in anti-cancer therapies.

NRP1 acts as a receptor hub on the cell surface forming a complex with one of its many possible co-receptors including but not limited to Plexin(415), VEGFR(416), TGFβ receptor(TGFβR)(417), PDGF receptor(386) and epidermal growth factor receptor(418). In collaboration with these co-receptors NRP1 promotes multiple signaling cascades(419, 420). All ligands of abovementioned co-receptors of NRP1 are growth factors or semaphorins and function as modulators of angiogenesis (410). The extent of eligible ligands combined with its broad presence on vascular endothelial and smooth muscle cells enables NRP1 to play an important role in promoting pathologic angiogenesis. Targeting NRP1 pathways may offer numerous windows for intervention in angiogenesis-dependent diseases, including several eye diseases.

6.3 Neuropilin-1 in sprouting angiogenesis

VEGF and Notch signalling pathways are implicated in the designation of tip and stalk cells in the vascular endothelium during sprouting angiogenesis(421). NRP1 forms a complex with VEGF165 and VEGFR2, enhancing the binding of VEGF165 and VEGFR2, potentiating VEGFR2 signaling.(388). VEGF stimulation incites an upregulation of Delta-like (Dll) 4 expression in tip cells(422). Subsequent activation of Notch signaling by Dll4 ligands in the stalk suppresses the tip cell phenotype while also reducing VEGFR2 expression and increasing VEGFR1 levels(423). Contrary to the stalk cell, the tip cell receives low Notch signaling, favoring high expression of VEGFR2 and NRP1 though low VEGFR1. Opposed to Dll4 in tip cells, Jagged1 ligand is expressed in stalk cells, antagonizing Dll4-Notch signaling in the sprouting front, enhancing differential Notch activity between tip and stalk cells(421-423).

6.4 Neuropilin-1 in immune cells

Studies in recent years have characterized NRP1 expression in different immune cells and shown an important regulating role in immune responses mediated by macrophages, DCs and T cell subset, especially regulatory T cell (Treg) populations(370). Here we will provide a short introduction on the role of NRP1 in different cell types. For a more complete reference we refer the reader to "Multifaceted Role of Neuropilins in the Immune System: Potential Targets for Immunotherapy" by Sohini Roy, published in 2017(370).

In T cells NRP1 has been mainly associated with suppressive functions. NRP1 plays an important role in the formation of the immunological synapse between DCs and T cells(424). DC secreted Sema4A binds to NRP1 and favors Treg survival, stability and quiescence(425). In CD8-positive T cells NRP1 is involved in maintenance of immune homeostasis in absence of danger signals(426).

In order to activate T cells following antigen exposure, DCs need to migrate to lymphoid tissues. NRP1, PlexinA1 and Sema3A regulate cytoskeleton rearrangement in DCs during their transmigration to lymphatics(427). By acting as a receptor for several viruses (including SARS-Cov-2)(428) NRP1 increases the susceptibility to infection of different cells, including DCs and mediates virus transmission to non-infected cells(429, 430).

Resident macrophage NRP1 is involved in vasculogenesis and maintenance in the fetus(431-433) while tumor associated macrophage (TAM) resident NRP1 promotes angiogenesis and immunosuppression(378, 434-438). Adipose tissue macrophages that express NRP1 play an essential role in limiting obesity-associated inflammation(439). In microglia NRP1 is linked to TGF β release and immunosuppression by Tregs(440) and promotes M2 polarization and phagocytosis of cellular debris(441).

Hypothesis and objectives

AMD, the primary cause of blindness in developed countries and the third cause worldwide, is a progressive retinal disease that occurs in elderly(442). Given increasing life expectancy in developed countries, the impact of AMD will only increase in the coming years. Central vision loss from AMD poses a significant burden on health care systems and profoundly impacts well-being and mental health(17). While a clear mechanism of pathogenesis has yet to be elucidated, environmental risk factors for AMD have in common they all induce inflammation. Interestingly, overall abdominal obesity has recently been linked to increased risk for progression to late stage NV AMD, most probably through the low-grade inflammation that is associated with obesity(443).

The human intestinal tract hosts an estimated 100 trillion microorganisms, outnumbering the human cells by 10-fold. This microbiota exercises great influence on human health(444) and several studies have associated dysbiosis of the microbiota with the onset of chronic inflammatory diseases such as obesity, diabetes and metabolic syndrome(444). Inducing changes in gut microbiota composition with diet, antibiotics and pre/pro-biotics influences inflammation. Cani et al defined the LPS from Gram-negative intestinal microbiota as the triggering factor for metabolic endotoxaemia and chronic low-grade inflammation. In mice, a high-fat diet stimulates the growth of LPS-containing bacteria in the gut. The changes in gut-microbiota composition increase the gut-permeability by disruption of the tight-junction proteins Zonula Occludens-1 and Occludin, resulting in increased plasma LPS levels(444).

Given the link between diet, microbiota and inflammation our first hypothesis is that gut microbiota influences development of AMD by modulating chronic low-grade inflammation. We aim to assess the influence of microbiotal dysbiosis induced by HFD on the formation of CNV. And whether microbiota of RD fed mice can influence the formation of CNV of HFD fed mice through fecal transplant and vice versa. This study will provide mechanistic insight on the link between obesity and para-inflammation. In the long term, therapeutic modulation of gut microbiota may yield an easily applicable and cost-effective frontline strategy that could provide an adjunct to current regimes to treat or prevent AMD.

To date, the available treatments such as intra-ocular injections with Anti-VEGF's are invasive and show neuronal toxicity. In addition, approximately 1 out of 10 treated patients does not respond to anti-VEGF therapy(445) with neovascular network complexes persisting despite monthly intravitreal injections. Recent studies have raised the possibility that NRP1 functions that are VEGF – independent and function by other ligands of this receptor, such as Sema3A, may also be possible therapeutic targets. NRP1 is highly expressed on cells of both the innate and adaptive immune system(370) where it plays an important role in homing and modulating myeloid cell function(370, 378, 379, 446). Considering the pro-angiogenic properties of several NRP1 ligands, our second hypothesis is that myeloid-resident NRP1 plays a promoting role in the formation of CNV in NV AMD. Our objective is to elucidate the role of NRP1-positive MPs in CNV in the pathogenesis of AMD, while exploring intravitreal injections with sNRP as a possible therapeutic target in neovascular eye disease.

Publication #1

Title: Gut Microbiota Influences Pathological Angiogenesis in Obesity-driven Choroidal Neovascularization

Authors: Elisabeth MMA Andriessen[1], Ariel M Wilson[2], Gaelle Mawambo[3], Agnieszka Dejda[3,4], Khalil Miloudi[5], Florian Sennlaub[6], Przemyslaw Sapieha[1,3,4,5] *

Affiliations:
[1]Department of Biomedical Sciences, Maisonneuve-Rosemont Hospital Research Centre, University of Montreal, Montreal, Quebec, H1T 2M4, Canada;
[2]Department of Engineering Physics, École Polytechnique de Montréal, Laser Processing and Plasmonics Laboratory, Montreal, Quebec, H3T 1J4, Canada;
[3]Department of Biochemistry, Maisonneuve-Rosemont Hospital Research Centre, University of Montreal, Montreal, Quebec, H1T 2M4, Canada;
[4]Department of Ophthalmology, Maisonneuve-Rosemont Hospital Research Centre, University of Montreal, Montreal, Quebec, H1T 2M4, Canada;
[5]Department of Neurology-Neurosurgery, McGill University, Montreal, Quebec, H3A 2B4 Canada
[6]INSERM, U 968, Paris, F-75012, France, Sorbonne Universités, Université Pierre et Marie Curie Paris 06, Unité Mixte de Recherche S 968, Institut de la Vision, Paris, F-75012, CNRS, Unité Mixte de Recherche 7210, Paris, F-75012, France

* Correspondence to:
Przemyslaw (Mike) Sapieha, PhD
Université de Montréal
Maisonneuve-Rosemont Hospital Research Centre
5415, blvd de L'Assomption
Montréal, Qc H1T 2M4
Phone: (1) 514-252-3400 x7711
Fax: (1) 514-252-3569
Email: mike.sapieha@umontreal.ca

Keywords: Age Related Macular Degeneration, Obesity, Gut Microbiota, Inflammaging, Angiogenesis.

Short Title: Gut Microbiota Influences Pathological Angiogenesis

Abstract

Age-related macular degeneration in its neovascular form (NV AMD) is the first cause of vision loss among adults above the age of 60. Epidemiological data suggests that in men, overall abdominal obesity is the second most important environmental risk factor after smoking for progression to late-stage NV AMD. To date, the mechanisms that underscore this observation remain ill defined. Given the impact of high-fat diets on gut microbiota, we investigated whether commensal microbes influence the evolution of AMD. Using mouse models of NV AMD, microbiotal transplants and other paradigms that modify the gut microbiome, we uncoupled weight gain from confounding factors and demonstrate that high-fat diets exacerbate choroidal neovascularisation (CNV) by altering gut microbiota. Gut dysbiosis leads to heightened intestinal permeability and chronic low-grade inflammation characteristic of inflammaging with elevated production of IL-6, IL-1β, TNF-α and VEGF-A that ultimately aggravate pathological angiogenesis.

Introduction

While AMD is the leading cause of irreversible blindness in the industrialized world(1-3), the cellular and molecular mechanisms that precipitate disease remain incompletely understood despite significant genome-wide association studies identifying susceptibility genotypes and target mechanistic pathways(4-7). Obesity has long been suspected as a risk factor for AMD, but increased body-mass index associations with AMD were inconsistent(8). Using 21,287 participants from the Melbourne Collaborative Cohort Study, it was recently demonstrated that each increase of 0.1 in waist/hip ratio (a measure for abdominal obesity) was associated with a 13% increase in the odds of early AMD and a 75% increase in the odds of late AMD in men, making obesity the second most important environmental risk factor for late AMD after cigarette smoking(9).

Progression of AMD is influenced by single or compounded environmental and genetic risk factors that lead to persistent low-grade inflammation and a largely innate immune response(10-12). Evidence for environmental factors predisposing to AMD is supported by the fact genetically

unrelated individuals with shared long-term environmental exposure develop the disease with a concordance of 70.2%(13). A consequence of cohabitation and common lifestyle habits that prospectively impact disease modifiers such as systemic inflammation is microbial exchange(14). Given that commensal gut microbiota exert profound influence on digestion, dietary metabolism, endotoxemia and immune responses(15-18), they are prime candidates to impact chronic low-grade inflammation(19). Microbiota related low-grade inflammation is characterized by elevated pro-inflammatory gene expression and is a common consequence of an altered host-microbiota relationship caused by instigator bacteria or dietary components, that influence intestinal permeability(20). There is accumulating evidence that assert the importance of intestinal permeability, a barrier aspect closely associated with the intestinal commensal microbiota as well as to the mucosal immune system, in intestinal and systemic health(21-25). Heightened intestinal permeability can allow for an increased translocation of bacterial products like LPS and other pathogen associated molecular pattern molecules (PAMPs)(16, 18, 26). These PAMPs impact pro-inflammatory signaling through pattern recognitions receptors (PRRs) of the innate immune system, especially the toll-like receptors (TLRs) and Nod-like receptors (NLRs), inducing low-grade systemic inflammation(20). Microglia, perivascular macrophages, a small number of dendritic cells and RPE cells express various PRRs, including TLRs and NLRs and may predispose for PAMPs of intestinal origin to impact ocular inflammation(27). In addition, bacterial products or metabolites from gut microbiota can modulate microglia maturation, morphology and function(28) and activate retina-specific T cells that are thought to be involved in autoimmune uveitis(29).

Dysbiosis in gut microbes is particularly important for the aging population given that they modulate aging-related changes in innate immunity, sarcopaenia, cognitive function and frailty in general (30). Here we sought to evaluate the contribution of intestinal flora to progression of NV AMD, particularly in the context of obesity-driven CNV.

Results

High-fat diet modulates gut microbiota and exacerbates CNV.

In light of epidemiologic data linking obesity to CNV(8, 31), we first investigated the propensity of diets with elevated fat content to exacerbate CNV. C57BL/6J mice were raised under sterile barrier conditions and placed on a regular-chow diet (RD; 16% kcal fat) or high-fat diet (HFD; 60% kcal fat), from 6 weeks of age (Fig 1A). As expected, upon sacrifice at 13 weeks, HFD-fed mice gained over 50% more weight than control RD-fed mice (Fig 1B, C). At 11 weeks of life, we subjected mice to a laser-induced photocoagulation model of CNV, where perforation of BM initiates sprouting of subretinal blood vessels from the choroid, thus mimicking NV AMD(32). Quantification of FITC-dextran perfused neovessels over isolectin B4 (IB4)-labeled impact area by confocal imaging 14 days after laser burn revealed a robust 60% increase in CNV in HFD-fed mice when compared to RD controls (Fig 1D, E). These experimental mouse data are in line with previously published results(33) and verify human studies(9, 31).

To tease out the contribution of gut microbes to heightened CNV in mice receiving HFD, mice were administered 0.5g/L of the broad-spectrum, non-gut permeable(16) antibiotic (AB) neomycin trisulfate salt hydrate orally through their drinking water. Remarkably, HFD-fed mice treated with neomycin displayed levels of CNV akin to RD-fed control mice and thus significantly less than HFD-fed mice receiving vehicle control (Fig 1D, E). Treatment with neomycin did not impact weight gain (Fig 1B, C), hence uncoupling mouse weight from extent of CNV and strengthening the link between gut flora and pathological angiogenesis.

To ascertain that HFD and oral neomycin modify intestinal flora, we next profiled gut microbiomes. The ratio of *Bacteroidetes* and *Firmicutes,* the two dominant phyla that make up over 90% of bacterial phylogenetic types in the distal gut(34), is affected by diet(35, 36). Comparison of distal gut microbiota from lean and obese individuals shows that the relative proportion of *Bacteroidetes* is decreased in obese individuals compared to lean individuals(17, 35), which is consistent with mouse studies and underscores that diet impacts intestinal flora(17, 34, 37). We characterized gut microbiome composition by sequencing the hyper-variable regions

V2, V3, V4, V6, V7, V8 and V9 of bacterial 16S rRNA extracted from fecal pellets originating from RD-fed and HFD-fed mice receiving vehicle, as well as HFD-fed and RD-fed mice receiving neomycin (Fig 1F, EV1A). Consistent with clinical data(17, 34, 38), mice on HFD had shifted ratios of commensal gut microbes. *Bacteroidetes*/*Firmicutes* ratios shifted from 66%/33% of total bacteria in RD to 19%/67% in HFD. Importantly, oral neomycin restored the proportion of *Bacteroidetes* to ~65% of total bacteria and reduced *Firmicutes* from ~65% to less than 10%. In addition, relative abundance of *Proteobacteria* (a microbial signature of dysbiosis in gut microbiota(38)) rose with HFD and further with antibiotic treatment reaching 25% of the population (fig 1G). Of note, HFD-fed mice host the most diverse microbiome, with a modest but important presence of *Actinobacteria* and *Spirochaetes* (0.5 and 1.5% of the total). These phyla were undetectable in RD-fed mice or after receiving oral neomycin. RD-mice on neomycin showed consistently higher levels of *Proteobacteria* at the expense of *Firmicutes,* confirming microbial shifts with oral neomycin. Together, these data reconcile that modulation in gut microbiota correlates with severity of CNV.

High-fat diet potentiates recruitment of microglia and macrophages during CNV.

Mononuclear phagocytes (MPs) such as microglia and macrophages contribute to AMD pathogenesis (39-41) and localize to sites of neovascularization following laser-induced CNV(12, 42, 43) (44) (Fig 2A-C). Microglia are CNS-resident macrophages that are derived from primitive macro phages in the yolk sac(45). Upon CNS injury, they move to sites of insult and polarize to an activated state and produce pro-inflammatory cytokines.(46) Depending on the extent of injury, circulating monocytes may also be recruited from the bloodstream.

Analysis by FACS of whole retinas and RPE-choroid- sclera complexes from mice on regular diets revealed a 2-fold rise in MPs ($Ly6G^-$, $F4/80^+$, $CD11b^+$) at 3 (p3) and 7 (p7)) days post laser burn (Fig 2D, E) when compared to non-burned eyes (gating scheme in Fig S2A). At day 14 post-burn (p14), the number of MPs returned to basal levels (Fig 2D, E). A Similar kinetic profile was observed for microglia ($Ly6G^-$, $F4/80^+$, $CD11b^+$, $CX3CR1^{hi}$ $CD45^{lo}$) (Fig 2F, G). Notably, the overall proportion of microglia within the MP population dropped in the first week following laser burn (p3 and p7), suggesting cellular infiltration from circulation (Fig EV2B).

Importantly, a HFD potentiated these effects as the heightened CNV observed in HFD-fed mice (Fig 1D, E) was accompanied by a ~2-fold increase in MPs and microglia at sites of lesion when compared to control RD-fed mice(Fig 2H-K). This increase in subretinal MPs persisted at 14 days post burn as determined by immunofluorescent quantification of IBA-1^{+} cells around the laser-induced lesion (Fig 2L, M). Oral neomycin abrogated this recruitment (Fig 2H-M), which is consistent with the observed reduction in CNV (Fig 1D, E). Hence, the intestinal microbiota of HFD-fed mice augments recruitment of microglia and other MPs that may be central to disease progression.

Heightened CNV in mice with dysbiosis is accompanied by increased intestinal permeability, metabolic endotoxemia and systemic inflammation.

Pattern recognition receptors (PRRs) allow the innate immune system to recognize pathogen associated molecular patterns (PAMPs) and trigger an inflammatory reaction to fight off the microbes that produce them(47). Although PAMPs circulate at low concentrations under physiologic conditions(48), an increase in LPS concentrations, a condition termed “metabolic endotoxemia” may provoke low-grade inflammation(16), insulin resistance(49), augmented cardiovascular risk(23), fatty liver disease(21), white adipose tissue inflammation(50) and retinopathy of prematurity (ROP)(51). In obesity, changes in gut microbiota have been suggested to compromise barrier function of the epithelial layer of the gut, thus increasing entry of PAMPs into systemic circulation (16, 52, 53).

Analysis of intestinal permeability by Evans Blue assay revealed that HFD elevated intestinal permeability by 3-fold when compared to controls (Fig 3A). In our experimental paradigm, antibiotic treatment did not restore intestinal permeability of HFD-fed mice as there was no significant difference between HFD-fed mice and HFD-fed mice that were treated with antibiotics (Fig 3A).

We next determined whether the levels of circulating PAMPS were sufficient to trigger a PRR response. We therefore subjected murine macrophages that express several PRRs with a chromosomal integration of a secreted embryonic alkaline phosphatase reporter construct

inducible by NF-κB and AP-1 (RAW-Blue™ cells) to serum from mice under various feeding paradigms. This reports on activation of PRRs such as toll-like receptors (TLRs), NOD-like receptors (NLRs), RIG-I-like receptors (RLRs) and C-type lectin receptors (CLRs).

Serum from HFD-fed mice activated PPRs significantly more readily than serum from RD-fed mice as had been suggested (16, 22, 54) or HFD-fed mice receiving antibiotic treatment (Fig 3B). The reduction in PRR response in antibiotic-treated mice may occur due to an overall reduction in the absolute number of bacteria present in the intestine.

We next investigated both systemic and local profiles of classic inflammatory mediators that are associated with para-inflammation in AMD(27). Consistent with the heightened activation of PPRs (Fig 3B), serum cytokine concentrations of IL-1β, IL-6, TNF-α IL-17A and IFN-γ were significantly induced with HFD, as was anti-inflammatory IL-10 (Fig 3C, EV3A). Oral intake of neomycin reversed the trend (Fig 3C, EV3A). Moreover, this pattern held in naive choroids (without laser-induced CNV) with transcript levels of *Il-1β*, *Il-6* and *Tnf-α* as well as with the cardinal angiogenic factor *Vegf-a* (Fig 3D). Moreover, neomycin treatment of HFD-fed mice improved their glucose tolerance (Fig EV3B, C) suggesting a general improvement in metabolic health, an important risk factor for AMD(55), and confirming efficient modulation of gut microbes(49). These data suggest that HFD primes choroids for CNV in a gut flora-dependent manner, where dysbiosis of the gut microbial community results in alterations of circulating levels of pro- and anti-inflammatory cytokines and the expression of inflammation associated mRNAs.

Microbiotal transplants confirm that high-fat diet aggravates CNV through gut microbiota.

To ascertain that HFD-associated gut microbial communities drive increased CNV, we transplanted by oral gavage cecal microbiota harvested from the feces of RD-fed mice to HFD-fed mice (HFDxRDT). RD-fed mice transplanted with a fecal suspension of RD microbiota (RDxRDT) and HFD-fed mice transplanted with fecal suspension of HFD microbiota (HFDxHFDT) served as controls (Fig 4A). Prior to microbiotal transplantation, recipient mice were treated with ampicillin and neomycin in drinking water to deplete their original commensal microbiome. Gavage with cecal microbiota was repeated on a weekly basis to maintain a constant composition

of the transplanted flora (Fig 4B). Although mice on HFD were significantly heavier than those on RD, microbiotal transfer from RD-fed mice did not significantly alter weight gain of HFD-fed mice and thus permitted to uncouple the effects of weight gain from those of microbial transfer (Fig 4C, D).

To verify successful transplantation of diet-associated microbial phyla, we characterized fecal microbiota as above (Fig 4E, EV4A). In RDxRDT-mice, *Bacteroidetes* were the most abundant phylum representing 75-80% of the microbiome while accounting for only 35% in HFDxHFDT-mice where *Firmicutes* and *Proteobacteria* filled the balance. Transfer of RD microbiota to HFD-fed mice restored microbial proportions found in RD-fed mice (Fig 4F). In addition, improved glucose tolerance in HFDxRDT-mice compared to HFDxHFDT-mice attests to successful microbiotal transplants (Fig EV4B, C).

While HFDxHFDT showed a ~2-fold increase in CNV when compared to RDxRDT, transfer of RD-microbiota to HFD-fed mice diminished CNV by ~35% supporting a role for gut microbiota in pathological CNV (Fig 4G, H). In addition, our data attest to intestinal permeability being lowered through microbiotal transfer. Whereas, HFDxHFDT mice show 2-fold higher levels of serum Evans Blue compared to RDxRDT, transfer of RD microbiota to HFD-fed mice reduced permeability to levels seen in RDxRDT mice (Fig 4I). Analysis of choroidal levels of *Il-6, Tnf-α* and *Vegf-a*, confirmed that transfer of RD-fed fecal suspensions to HFD-mice reduced overall inflammation (Fig 4J). *Il-1β* transcripts were not affected. In concert, these results provide evidence for the influence of gut microbiota on CNV.

Discussion

With an increasing prevalence of obesity and increasing life expectancy, the societal impact and financial burden of AMD are expected to rise dramatically in the coming years(56, 57). Polymorphisms in genes implicated in inflammation predispose to AMD(58) with strong linkage to single nucleotide polymorphisms in CFH factors, CFHR (CFH related factors), ARMS2, VEGFA, and TGFBR1(59-62), yet by themselves, no single mutation can account for disease development. To date, the contribution of our 'second genome' (the microbiome) has not been investigated. Our study suggests that gut microbiota influence development of neovascular lesions associated

with AMD and this particularly when obesity is a predisposing factor. We show that diets rich in fat alter the gut microbiome and in turn elevate choroidal and systemic inflammation and heighten pathological CNV. This effect could originate from increased intestinal permeability to PAMPs secondary to dysbiosis (**fig. 5**). In this regard, obesity related changes in gut microbiota have been shown to decrease barrier function of the gut, allowing increased entry of PAMPs into systemic circulation and consequently triggering inflammation (16, 52, 53). Both antibiotic treatment and microbiotal transplants from RD-fed mice lower systemic and choroidal inflammation, yet only RD-microbiotal transplants significantly lower intestinal permeability. While the microbial community of HFDxRDT mice resembles the one of RD-fed mice more closely than that of HFD-fed mice treated with antibiotics, the effects of neomycin treatment likely occur through a decrease in the absolute number of bacteria present in the gut.

Modifying microbiota can reduce systemic and local choroidal inflammation and attenuate pathological neovascularization. Of note, one of the most heavily regulated inflammatory cytokines in our experimental paradigms was IL-6. Elevated levels of IL-6 are associated with early(63) and late AMD(64) and are significantly related to smoking, higher body mass index and "inflammaging", the low-grade, chronic, systemic sterile inflammation in aging, in the absence of infection(65). Dysbiosis of gut flora may thus be an additional factor that accounts for the inconsistent responses between individuals subjected to dietary interventions designed to stall progression of AMD such as AREDS formulations(66, 67). In addition, from an experimental perspective, our study strengthens the notion that housing and dietary considerations must be taken into account when designing animal-based studies on angiogenesis and aging. Gut microbiota is acquired shortly after birth from the surrounding environment, forming a relatively stable community that can shift composition under influence of environmental factors such as diet, exercise and medication(35, 36, 68). Modifying gut microbiomes may thus provide minimally intrusive and cost-effective paradigms to prevent or delay exudative AMD.

Materials and methods

Animals

All animal procedures were validated by the Animal Care Committee of the University of Montreal and Hôpital Maisonneuve Rosemont in accordance with the guidelines established by the Canadian Council on Animal Care.

Briefly, 6-week-old male C57BL/6 WT mice, purchased from The Jackson Laboratory, raised under sterile barrier conditions and housed under a 12h light cycle with water and food ad libitum were placed on either a regular-chow diet (RD) (16% kcal fat, 63% kcal carbohydrate, 21% kcal protein) or a high-fat diet (HFD) (60% kcal fat, 26% kcal carbohydrate, 14% kcal protein) for 7 weeks and weighed weekly to register weight gain. At the age of 9 weeks, half of the RD, and half of the HFD mice received antibiotic treatment with 0.5g/L neomycin trisulfate salt hydrate in their drinking water, resulting in 4 different experimental groups: Control (RD), Antibiotics (RD+AB), High-Fat (HFD) and High-Fat + Antibiotics (HFD+AB). Neomycin is not absorbed from the gut(16), therefore the antibiotic treatment was isolated to the GI-tract and had no direct systemic effect.

At the age of 13 weeks, fecal pellets and blood were collected before sedation with Isoflurane gas and cervical dislocation. Eyes were enucleated, dissected and stored at -80°C for mRNA extraction.

Laser induced CNV

At the age of 11 weeks, mice were anesthetized with 10uL/g body weight of a 10% ketamine, 4% xylazine solution, and their BM was ruptured using an argon laser as described previously(32). Two weeks after CNV induction the mice were perfused with 0,5mL of 15mg/mL of Fluorescein Isothiocyanate (FITC)–dextran (average mol wt 20,000) and sacrificed. Eyes were enucleated and processed for analysis by immunohistochemistry. The sclera-choroid-RPE-cell complex was mounted onto a slide and the burns and macrophages were photographed with an Olympus FV1000 microscope. The neovascularization was captured in a Z-Stack, and the lesion caused by the laser impact was captured in a single plane image. The Z-stacks were compressed into one image and the FITC-dextran labeled neovascular area and the area of the lesion were measured per lesion in Image-J.

Immunohistochemistry

Eyes were fixed for 30 minutes in 4% PFA at room temperature, before dissection of the sclera-choroid-RPE-cell complex. After a secondary fixation of 15 minutes in 4% PFA at room temperature, the choroids were stained with Rhodamine labeled Griffonia (Bandeiraea) Simplicifolia Lectin I (Vector Laboratories Inc.) in 1 mM CaCl2 in PBS and IBA1 (rabbit polyclonal; Wako).

Microbiome Sequencing

DNA was extracted from fecal pellets with the Qiagen QIAmp Fast Stool Mini Kit according to manufacturer's instructions with several small modifications, briefly: 2-3 fecal pellets were homogenized in 500uL InhibitEX Buffer using a disposable homogenizing pestle and vortex. The suspension was heated for 5 min at 70°C before stool particles were pelleted by 1 min centrifugation at 20.000g. The supernatant was thoroughly mixed with 20uL Poteinase K before 500uL Buffer AL was added and the mix was incubated at 70°C for 10 min. After the addition of 500uL of 100% ethanol the lysate was applied to the QIAamp spin column and centrifuged for one minute at 20.000g. The filtrate was discarded before 500uL Buffer AW1 was added to the spin column and centrifuged for 1 minute at 20.000g. This step was repeated with 500uL Buffer AW2. The spin column was dried by centrifugation for 3 minutes at 20.000g in a clean 2mL collection tube. The DNA was eluted in 200uL of Buffer ATE, directly pipetted on the QIAamp membrane and collected in a clean eppendorf.

After DNA extraction from the fecal pellets, the Thermo Fisher Ion Ion 16S™ Metagenomics Kit was used to amplify the hyper-variable regions V2, V3, V4, V6, V7, V8 and V9 of bacterial 16S rRNA. The amplified fragments were then barcoded, sequenced on the Ion PGM sequencer system and analyzed with the Ion Reporter Software.

FACS

Retinas and sclera-choroid-RPE-cell complexes of non-burned and burned mice at p3, p7 and p14 were cut into small pieces and homogenized in a solution of 750 U/mL DNaseI (Sigma-Aldrich

Corp., St. Louis, MO, USA) and 0.5 mg/mL of collagenase D (Roche, Basel, Switzerland) for 20 minutes at 37°C. Homogenates were filtered through a 70-µm cell strainer and washed in PBS. After incubation with LEAF purified anti-mouse CD16/32 (101310; BioLegend, San Diego, CA, USA) for 15 minutes at room temperature to block Fc receptors, cells were incubated for 30 minutes at room temperature with the following antibodies: Alexa Fluor 700 anti-mouse CD45.2 (109822; BioLegend), FITC anti-mouse/human CD11b (101206; BioLegend), PE/CY7 anti-mouse Ly-6G/Ly-6C (Gr-1; 108416; BioLegend), Pacific blue anti-mouse F4/80 (123124; BioLegend), 7AAD (51-68981E; BD Biosciences, San Jose, CA, USA), anti-mouse CX3CR1 Phycoerythrin conjugated Goat IgG (FAB5825P; R&D Systems, Inc., Minneapolis, MN, USA). Fluorescence-activated cell sorting (FACS) was performed on a LSRII (BD Biosciences) device and data were analyzed using FlowJo software (version 7.6.5; FlowJo, Ashland, OR, USA).

Intestinal Permeability Assay

Mice were injected by oral gavage with 1mL of 50 mg/mL Evans Blue divided over 5 injections, 30 minutes apart. After 24h, 120ul of blood was collected from the submandibular vein. Serum was analyzed for Evans Blue concentration with a spectrophotometer at an optical density of 620-740nm and quantified with the help of a standard dilution curve.

RAW-Blue Assay

Blood was collected through cardiac puncture and serum was stored at -80°C until use in the Raw-Blue assay. PAMPs were assayed with RAW-Blue™ cells (InvivoGen, San Diego, CA) through detection of NF-κB/AP-1 activation following activation of TLRs (with the exception of TLR5), NOD1/2 and Dectin-1 using a modified version of the manufacturer's protocol. RAW-Blue™ cells were grown in growth medium (DMEM, 4.5 g/L glucose, 2mM L-glutamine, 10% fetal bovine serum (FBS), 100 µg/mL Zeocin™ (InvivoGen, San Diego, CA)). The assay was performed when the cells were in passage 10-15 by plating 10^5 cells in 96-well plates containing basal DMEM. After 6 hours of starvation 30 ul of mouse serum, 30 ul of FBS(- control) or 30 ul of FBS+LPS(+ control) was added per well and cells were incubated for 21 h at 37°C under an atmosphere of 5% CO2/95% air. SEAP levels were determined using a spectrophotometer at 620-655nm after a 1-3

h incubation at 37°C of 20 ul of induced RAW-Blue™ cells supernatant with 180 ul QUANTI-Blue™(InvivoGen, San Diego, CA).

Cytokine Assessment

Serum cytokine assays were performed using a Bio-plex Mouse Cytokine 6-plex panel (1x96-well) (Bio-Rad) according to the manufacturer's instructions. The Bio-Plex cytokine assay is a multiplex bead-based assay involving matrices that is designed to quantitate multiple cytokines as follows. The wells of a 96-well plate were pre-wet with 100uL of Bio-Plex assay buffer. 50uL of vortexed multiplex bead working solution was pipetted into each well and immediately removed. Wells were washed twice with the Bio-Plex wash buffer before 25uL of vortexed Bio-Plex Detention Antibody working solution was added to each well and incubated for 30 min. After a triple wash with the Bio-Plex wash buffer, 50uL of vortexed 1× streptavidin-PE was added to each well and incubated for 30 min. After 3 washes, the beads in each well were resuspended with 125 µl of Bio-Plex assay buffer, shaken at 1100 rpm for 30 s, and the plate was immediately read on the Bio-Plex system. Cytokine concentrations were calculated from the standard curve by use of Bio-Plex manager software. Samples were run in duplicate.

Real-time PCR analysis

After enucleation eyes were dissected to isolate retinas and sclera-choroid-RPE-cell complex. RNA was isolated using Trizol and digested with DNase I to prevent amplification of genomic DNA contaminants. M-MLV reverse transcriptase (Life Technologies) was used for the reversed transcription, and SYBR Green (Bio-Rad) to determine gene expression in an ABI Biosystems Real-Time PCR machine with β-Actin as a reference gene. We used to following primers: Mouse *β-Actin*= F: 5'-GAC GGC CAG GTC ATC ACT ATT G-3', R: 5'-CCA CAG GAT TCC ATA CCC AAG A-3'. Mouse *Il-1β*= F: 5' CTG GTA CAT CAG CAC CTC ACA-3', R: 5'-GAG CTC CTT AAC ATG CCC TG-3'. Mouse *Il-6*= F: 5'AGA CAA AGC CAG AGT CCT TCA GAG A-3', R: 5'-GCC ACT CCT TCT GTG ACT CCA GC-3'. Mouse *Tnf-α*= F:5'-CCC TCA CAC TCA GAT CAT CTT CT-3', R:5'-GCT ACG ACG TGG GCT ACA G-3'. Mouse *Vegf-a*= F: 5'-GCC CTG AGT CAA GAG GAC AG-3', R: 5'-CTC CTA GGC CCC TCA GAA GT-3'.

Microbiota transplant

A litter of 6 C57BL/6 WT mice was divided over 3 cages, representing 3 experimental groups: regular-chow diet-fed mice receiving a transplant from regular-chow diet-fed mice (RD x RDT), high-fat diet-fed mice receiving a transplant from high-fat diet-fed mice (HFD x HFDT) and high-fat fed mice receiving a transplant from regular-chow diet-fed mice (HFDxRDT). At the age of 6 weeks 2 cages were started on HFD while the other cage remained on a regular-chow diet. Mice received anitibiotics (ampicillin 1.0g/L + neomycin 0.5g/L) in their drinking water for 5 days, to deplete the original gut microbiota, as described before(69). Two days after discontinuing the antibiotics they received their first microbiota transplant, either from mice on a regular-chow diet or a high-fat diet.

Feces were collected from 20 different donor mice, either on RD, or HFD for at least 5 weeks. The fecal pallets were collected in 2.5mL of sterile PBS with 0.05% cysteine HCL, homogenized and centrifuged at 600rpm for 5 minutes. 200uL of the supernatant was introduced orally to the mice with the help of flexible gavage needles. This was repeated with fresh fecal samples every 7 days for the duration of the experiment. At the age of 11 weeks mice were subjected to 4 laser burns per eye. Mice were weighed weekly and feces were collected for analysis by 16S sequencing. Mice are coprophagic and hence care is taken to isolate individuals with given gut microbiota modifying protocols.

Glucose Tolerance Test (GTT)

Mice were starved 12 hours overnight. Blood glucose was measured (Accu-Chek; Roche) at baseline, 15, 30, 60, 120 and 240 minutes following intra-peritoneal injection of 2mg/kg of 10% D-glucose.

Statistical analysis

Results are presented as mean ± SEM. GraphPad Prism version 6.00 (GraphPad Software, San Diego, CA; www.graphpad.com) was used to analyze the statistical significance of differences by one-way ANOVA and Tukey's multiple comparisons test or a 2 tailed Student's t-test, where

appropriate. Data with $P < 0.05$ was considered statistically different; *P< 0.05, **P< 0.01, ***P< 0.001.

Acknowledgements

E.A. holds scholarships from the Réseau en Recherche en Santé de la Vision and the Faculté des Études Supérieures de l'UdM. P.S. holds The Wolfe Professorship in Translational Vision Research and the Canada Research Chair in Retinal Cell Biology and the Alcon Research Institute Young Investigator Award. This work was supported by grants to P.S. from The Foundation Fighting Blindness Canada (FFB), the Canadian Institutes of Health Research (324573), the Canadian Diabetes Association (OG-3-11-3329-PS), and The Natural Sciences and Engineering Research Council of Canada (418637) and the Fondation de l'Avenir, Paris, France- Etude n°AP-RMA-2015-010 to FS.

Author Contributions

P.S. and E.A. designed the study. E.A, A.W, G.M, A.D, K.M. performed experiments. FS provided valuable insight and comments on study design and the manuscript. E.A. and P.S. wrote the paper. All authors discussed the results and commented on the manuscript at all stages.

Competing Financial Interests

The authors declare no competing financial interests. Correspondence and requests for materials should be addressed to P.S. (mike.sapieha@umontreal.ca).

The paper explained

Problem

Age-related macular degeneration in its neovascular form (NV AMD) is the first cause of vision loss among adults above the age of 60. Epidemiological data suggests that in men, overall abdominal obesity is the second most important environmental risk factor after smoking for progression to late-stage NV AMD. To date, the mechanisms that underscore this observation remain ill defined. Given the impact of high-fat diets on gut microbiota, we investigated whether commensal microbes influence the evolution of AMD.

Results

Using mouse models of NV AMD, microbiotal transplants and other paradigms that modify the gut microbiome, we uncoupled weight gain from confounding factors and demonstrate that high-fat diets exacerbate choroidal neovascularisation (CNV) by altering gut microbiota. Gut dysbiosis leads to heightened intestinal permeability and chronic low-grade inflammation with elevated production of IL-6, IL-1β, TNF-α and VEGF-A that ultimately exacerbate pathological angiogenesis.

Impact

With an increasing prevalence of obesity and increasing life expectancy, the societal impact and financial burden of AMD are expected to rise dramatically in the coming years. Our study suggests that gut microbiota influence development of neovascular lesions associated with AMD and this particularly when obesity is a predisposing factor. Modifying microbiota can reduce systemic and local choroidal inflammation and attenuate pathological neovascularization and may thus provide minimally intrusive and cost-effective paradigms to prevent or delay exudative AMD.

References

1. Maberley DAL, Hollands H, Chuo J, Tam G, Konkal J, Roesch M, et al. The prevalence of low vision and blindness in Canada. Eye (The Royal College of Ophthalmologists). 2006;20(3):341-6.

2. Klein R, Klein BEK. Do statins prevent age-related macular degeneration? American journal of ophthalmology. 2004;137(4):747-9.

3. Wong WL, Su X, Li X, Cheung CM, Klein R, Cheng CY, et al. Global prevalence of age-related macular degeneration and disease burden projection for 2020 and 2040: a systematic review and meta-analysis. Lancet Glob Health. 2014;2(2):e106-16.

4. Sobrin L, Seddon J. Nature and nurture- genes and environment- predict onset and progression of macular degeneration. Progress in Retinal and Eye Research. 2014;40:1-15.

5. Fritsche L, Chen W, Schu M, Yaspan B, Yu Y, Thorleifsson G, et al. Seven new loci associated with age-related macular degeneration. Nature Genetics. 2013;45(4):433-9, 9e1.

6. Fritsche LG, Igl W, Bailey JN, Grassmann F, Sengupta S, Bragg-Gresham JL, et al. A large genome-wide association study of age-related macular degeneration highlights contributions of rare and common variants. Nat Genet. 2016;48(2):134-43.

7. Black JR, Clark SJ. Age-related macular degeneration: genome-wide association studies to translation. Genet Med. 2016;18(4):283-9.

8. Zhang QY, Tie LJ, Wu SS, Lv PL, Huang HW, Wang WQ, et al. Overweight, Obesity, and Risk of Age-Related Macular Degeneration. Invest Ophthalmol Vis Sci. 2016;57(3):1276-83.

9. Adams MKM, Simpson J, Aung K, Makeyeva G, Giles G, English D, et al. Abdominal obesity and age-related macular degeneration. American journal of epidemiology. 2011;173(11):1246-55.

10. Sennlaub F, Auvynet C, Calippe B, Lavalette S, Poupel L, Hu SJ, et al. CCR2(+) monocytes infiltrate atrophic lesions in age-related macular disease and mediate photoreceptor degeneration in experimental subretinal inflammation in Cx3cr1 deficient mice. EMBO molecular medicine. 2013;5(11):1775-93.

11. Ambati J, Atkinson J, Gelfand B. Immunology of age-related macular degeneration. Nature Reviews Immunology. 2013;13(6):438-51.

12. Combadière C, Feumi C, Raoul W, Keller N, Rodéro M, Pézard A, et al. CX3CR1-dependent subretinal microglia cell accumulation is associated with cardinal features of age-related macular degeneration. Journal of Clinical Investigation. 2007;117(10):2920-8.

13. Gottfredsdottir MS, Sverrisson T, Musch DC, Stefánsson E. Age related macular degeneration in monozygotic twins and their spouses in Iceland. Acta ophthalmologica Scandinavica. 1999;77(4):422-5.

14. Song S, Lauber C, Costello E, Lozupone C, Humphrey G, Berg Lyons D, et al. Cohabiting family members share microbiota with one another and with their dogs. eLife. 2013;2:e00458-e.

15. Backhed F, Ley RE, Sonnenburg JL, Peterson DA, Gordon JI. Host-bacterial mutualism in the human intestine. Science. 2005;307(5717):1915-20.

16. Cani P, Bibiloni R, Knauf C, Waget A, Neyrinck A, Delzenne N, et al. Changes in gut microbiota control metabolic endotoxemia-induced inflammation in high-fat diet-induced obesity and diabetes in mice. Diabetes. 2008;57(6):1470-81.

17. Turnbaugh P, Ley R, Mahowald M, Magrini V, Mardis E, Gordon J. An obesity-associated gut microbiome with increased capacity for energy harvest. Nature. 2006;444(7122):1027-31.

18. Cerf-Bensussan N, Gaboriau-Routhiau V. The immune system and the gut microbiota: friends or foes? Nat Rev Immunol. 2010;10(10):735-44.

19. Tremaroli V, Backhed F. Functional interactions between the gut microbiota and host metabolism. Nature. 2012;489(7415):242-9.

20. Chassaing B, Gewirtz AT. Gut microbiota, low-grade inflammation, and metabolic syndrome. Toxicol Pathol. 2014;42(1):49-53.

21. Brun P, Castagliuolo I, Di Leo V, Buda A, Pinzani M, Palu G, et al. Increased intestinal permeability in obese mice: new evidence in the pathogenesis of nonalcoholic steatohepatitis. Am J Physiol Gastrointest Liver Physiol. 2007;292(2):G518-25.

22. Neves AL, Coelho J, Couto L, Leite-Moreira A, Roncon-Albuquerque R, Jr. Metabolic endotoxemia: a molecular link between obesity and cardiovascular risk. J Mol Endocrinol. 2013;51(2):R51-64.

23. Manco M, Putignani L, Bottazzo GF. Gut microbiota, lipopolysaccharides, and innate immunity in the pathogenesis of obesity and cardiovascular risk. Endocr Rev. 2010;31(6):817-44.

24. Bischoff SC, Barbara G, Buurman W, Ockhuizen T, Schulzke JD, Serino M, et al. Intestinal permeability--a new target for disease prevention and therapy. BMC Gastroenterol. 2014;14:189.

25. Gerova VA, Stoynov SG, Katsarov DS, Svinarov DA. Increased intestinal permeability in inflammatory bowel diseases assessed by iohexol test. World J Gastroenterol. 2011;17(17):2211-5.

26. Mehal WZ. The Gordian Knot of dysbiosis, obesity and NAFLD. Nat Rev Gastroenterol Hepatol. 2013;10(11):637-44.

27. Chen M, Xu H. Parainflammation, chronic inflammation, and age-related macular degeneration. Journal of leukocyte biology. 2015;98(5):713-25.

28. Erny D, Hrabe de Angelis AL, Jaitin D, Wieghofer P, Staszewski O, David E, et al. Host microbiota constantly control maturation and function of microglia in the CNS. Nat Neurosci. 2015;18(7):965-77.

29. Horai R, Zarate-Blades CR, Dillenburg-Pilla P, Chen J, Kielczewski JL, Silver PB, et al. Microbiota-Dependent Activation of an Autoreactive T Cell Receptor Provokes Autoimmunity in an Immunologically Privileged Site. Immunity. 2015;43(2):343-53.

30. O'Toole PW, Jeffery IB. Gut microbiota and aging. Science. 2015;350(6265):1214-5.

31. Seddon J, Cote J, Davis N, Rosner B. Progression of age-related macular degeneration: association with body mass index, waist circumference, and waist-hip ratio. Archives of ophthalmology. 2003;121(6):785-92.

32. Lambert V, Lecomte J, Hansen S, Blacher S, Gonzalez M-L, Struman I, et al. Laser-induced choroidal neovascularization model to study age-related macular degeneration in mice. Nature Protocols. 2013;8(11):2197-211.

33. Sene A, Khan AA, Cox D, Nakamura RE, Santeford A, Kim BM, et al. Impaired cholesterol efflux in senescent macrophages promotes age-related macular degeneration. Cell Metab. 2013;17(4):549-61.

34. Ley R, Turnbaugh P, Klein S, Gordon J. Microbial ecology: human gut microbes associated with obesity. Nature. 2006;444(7122):1022-3.

35. David L, Maurice C, Carmody R, Gootenberg D, Button J, Wolfe B, et al. Diet rapidly and reproducibly alters the human gut microbiome. Nature. 2014;505(7484):559-63.

36. Turnbaugh P, Ridaura V, Faith J, Rey F, Knight R, Gordon J. The effect of diet on the human gut microbiome: a metagenomic analysis in humanized gnotobiotic mice. Science translational medicine. 2009;1(6):6-.

37. Hildebrandt M, Hoffmann C, Sherrill Mix S, Keilbaugh S, Hamady M, Chen Y-Y, et al. High-fat diet determines the composition of the murine gut microbiome independently of obesity. Gastroenterology. 2009;137(5):1716-24.e1.

38. Wu N, Yang X, Zhang R, Li J, Xiao X, Hu Y, et al. Dysbiosis signature of fecal microbiota in colorectal cancer patients. Microbial Ecology. 2013;66(2):462-70.

39. Langmann T. Microglia activation in retinal degeneration. J Leukoc Biol. 2007;81(6):1345-51.

40. Ambati J, Anand A, Fernandez S, Sakurai E, Lynn BC, Kuziel WA, et al. An animal model of age-related macular degeneration in senescent Ccl-2- or Ccr-2-deficient mice. Nat Med. 2003;9(11):1390-7.

41. Combadiere C, Feumi C, Raoul W, Keller N, Rodero M, Pezard A, et al. CX3CR1-dependent subretinal microglia cell accumulation is associated with cardinal features of age-related macular degeneration. J Clin Invest. 2007;117(10):2920-8.

42. Indaram M, Ma W, Zhao L, Fariss R, Rodriguez I, Wong W. 7-Ketocholesterol increases retinal microglial migration, activation, and angiogenicity: a potential pathogenic mechanism underlying age-related macular degeneration. Scientific Reports. 2015;5:9144-.

43. Liu J, Copland D, Horie S, Wu W-K, Chen M, Xu Y, et al. Myeloid cells expressing VEGF and arginase-1 following uptake of damaged retinal pigment epithelium suggests potential mechanism that drives the onset of choroidal angiogenesis in mice. PLoS One. 2013;8(8):e72935-e.

44. Luckoff A, Caramoy A, Scholz R, Prinz M, Kalinke U, Langmann T. Interferon-beta signaling in retinal mononuclear phagocytes attenuates pathological neovascularization. EMBO molecular medicine. 2016;8(6):670-8.

45. Prinz M, Tay TL, Wolf Y, Jung S. Microglia: unique and common features with other tissue macrophages. Acta Neuropathol. 2014;128(3):319-31.

46. Hanisch UK, Kettenmann H. Microglia: active sensor and versatile effector cells in the normal and pathologic brain. Nat Neurosci. 2007;10(11):1387-94.

47. Dorrestein PC, Mazmanian SK, Knight R. Finding the missing links among metabolites, microbes, and the host. Immunity. 2014;40(6):824-32.

48. DiBaise JK, Frank DN, Mathur R. Impact of the Gut Microbiota on the Development of Obesity: Current Concepts. Am J Gastroenterol Suppl. 2012;1(1):22-7.

49. Cani PD, Amar J, Iglesias MA, Poggi M, Knauf C, Bastelica D, et al. Metabolic endotoxemia initiates obesity and insulin resistance. Diabetes. 2007;56(7):1761-72.

50. Caesar R, Tremaroli V, Kovatcheva-Datchary P, Cani PD, Backhed F. Crosstalk between Gut Microbiota and Dietary Lipids Aggravates WAT Inflammation through TLR Signaling. Cell Metab. 2015;22(4):658-68.

51. Tremblay S, Miloudi K, Chaychi S, Favret S, Binet F, Polosa A, et al. Systemic inflammation perturbs developmental retinal angiogenesis and neuroretinal function. Invest Ophthalmol Vis Sci. 2013;54(13):8125-39.

52. Osborn O, Olefsky JM. The cellular and signaling networks linking the immune system and metabolism in disease. Nat Med. 2012;18(3):363-74.

53. Amar J, Burcelin R, Ruidavets JB, Cani PD, Fauvel J, Alessi MC, et al. Energy intake is associated with endotoxemia in apparently healthy men. Am J Clin Nutr. 2008;87(5):1219-23.

54. Membrez M, Blancher F, Jaquet M, Bibiloni R, Cani PD, Burcelin RG, et al. Gut microbiota modulation with norfloxacin and ampicillin enhances glucose tolerance in mice. FASEB J. 2008;22(7):2416-26.

55. Ghaem Maralani H, Tai BC, Wong TY, Tai ES, Li J, Wang JJ, et al. Metabolic syndrome and risk of age-related macular degeneration. Retina. 2015;35(3):459-66.

56. Friedman DS, O'Colmain BJ, Munoz B, Tomany SC, McCarty C, de Jong PT, et al. Prevalence of age-related macular degeneration in the United States. Arch Ophthalmol. 2004;122(4):564-72.

57. Rein D, Zhang P, Wirth K, Lee P, Hoerger T, McCall N, et al. The economic burden of major adult visual disorders in the United States. Archives of ophthalmology. 2006;124(12):1754-60.

58. Hageman G, Anderson D, Johnson L, Hancox L, Taiber A, Hardisty L, et al. A common haplotype in the complement regulatory gene factor H (HF1/CFH) predisposes individuals to age-

related macular degeneration. Proceedings of the National Academy of Sciences of the United States of America. 2005;102(20):7227-32.

59. Ambati J, Ambati B, Yoo S, Ianchulev S, Adamis A. Age-related macular degeneration: etiology, pathogenesis, and therapeutic strategies. Survey of ophthalmology. 2003;48(3):257-93.

60. Yu Y, Bhangale T, Fagerness J, Ripke S, Thorleifsson G, Tan P, et al. Common variants near FRK/COL10A1 and VEGFA are associated with advanced age-related macular degeneration. Human molecular genetics. 2011;20(18):3699-709.

61. Ratnapriya R, Chew EY. Age-related macular degeneration-clinical review and genetics update. Clinical genetics. 2013;84(2):160-6.

62. Klein R, Zeiss C, Chew E, Tsai J-Y, Sackler R, Haynes C, et al. Complement factor H polymorphism in age-related macular degeneration. Science. 2005;308(5720):385-9.

63. Klein R, Myers C, Cruickshanks K, Gangnon R, Danforth L, Sivakumaran T, et al. Markers of inflammation, oxidative stress, and endothelial dysfunction and the 20-year cumulative incidence of early age-related macular degeneration: the Beaver Dam Eye Study. JAMA ophthalmology. 2014;132(4):446-55.

64. Klein R, Knudtson M, Klein BEK, Wong T, Cotch M, Liu K, et al. Inflammation, complement factor h, and age-related macular degeneration: the Multi-ethnic Study of Atherosclerosis. Ophthalmology. 2008;115(10):1742-9.

65. Franceschi C, Campisi J. Chronic inflammation (inflammaging) and its potential contribution to age-associated diseases. J Gerontol A Biol Sci Med Sci. 2014;69 Suppl 1:S4-9.

66. Lutein + zeaxanthin and omega-3 fatty acids for age-related macular degeneration: the Age-Related Eye Disease Study 2 (AREDS2) randomized clinical trial. JAMA: the Journal of the American Medical Association. 2013;309(19):2005-15.

67. A randomized, placebo-controlled, clinical trial of high-dose supplementation with vitamins C and E, beta carotene, and zinc for age-related macular degeneration and vision loss: AREDS report no. 8. Archives of ophthalmology. 2001;119(10):1417-36.

68. Evans C, LePard K, Kwak J, Stancukas M, Laskowski S, Dougherty J, et al. Exercise prevents weight gain and alters the gut microbiota in a mouse model of high fat diet-induced obesity. PLoS One. 2014;9(3):e92193-e.

69. Ellekilde M, Selfjord E, Larsen C, Jakesevic M, Rune I, Tranberg B, et al. Transfer of gut microbiota from lean and obese mice to antibiotic-treated mice. Scientific Reports. 2014;4:5922-
.

Figures and legends

Figure 1

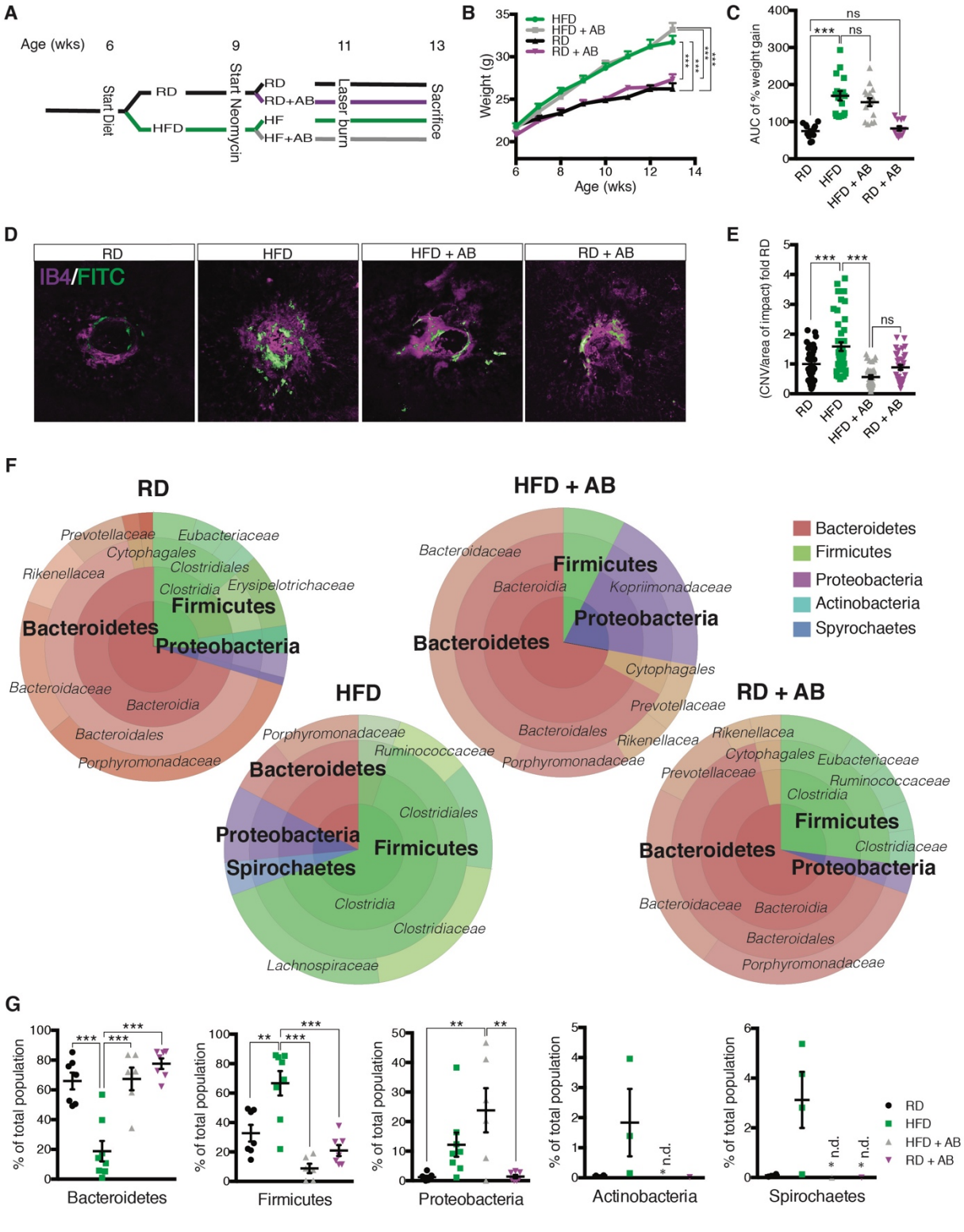

Figure 12 Publication#1 Figure 1. High-fat diet exacerbates CNV and influences gut microbiota.

Figure 1. High-fat diet exacerbates CNV and influences gut microbiota.

(**A**) Schematic representation of experimental timeline where half of the mice start a high-fat diet (HFD) at 6 weeks and later half of these receive neomycin (AB) treatment from the age of 9 weeks until sacrifice at week 13. Control mice were fed a Regular-chow Diet (RD). At the age of 11 weeks, mice are subjected to 4 laser burns per eye to perforate BM and recruit subretinal blood vessels from the choroid. (**B**) Weight gain and (**C**) area under the curve of percentage weight gain of HFD-fed mice compared to RD-fed mice, treated with vehicle or antibiotic; n= 13(RD), 17(HFD), 16(HFD+AB), 12(RD+AB); CI 99.9% (**D**) Compilation of compressed Z-stack confocal image of FITC-dextran-labeled CNV and single-plane confocal image of isolectin B4-stained choroidal flat mounts from RD- and HFD-fed mice, with vehicle or antibiotic treatment. (**E**) Quantification of area of FITC-dextran-labeled CNV over isolectin B4-stained laser impact area fold RD; n= 11(RD), 16(HFD), 11(HFD+AB), 12(RD+AB), with 36(RD), 32(HFD), 33(HFD+AB), 34(RD+AB) burns total; CI 99%. (**F**) Representative circle charts of relative abundance of bacterial phyla, class, order and family (from central to peripheral), in gut microbiota of RD-fed mice with vehicle, HFD-fed mice with, HFD-fed mice with neomycin and RD-fed mice with neomycin and (**G**) relative proportion per group of different phyla; n= 7(RD), 8(HFD), 6(HFD+AB), 7(RD+AB); *Bacteroidetes*; CI 99.9%, *Firmicutes*; CI 99%, *Proteobacteria*; CI 99%, *Actinobacteria* and *Spirochaetes*. All comparisons between groups are analyzed using one-way analysis of variance (ANOVA) and Tukey's multiple comparisons test; *P< 0.05, **P< 0.01, ***P< 0.001; error bars represent mean ± S.E.M. Each "n" represents one mouse per experimental group CI: Confidence interval. Scale bar: 100µm.

Figure 2

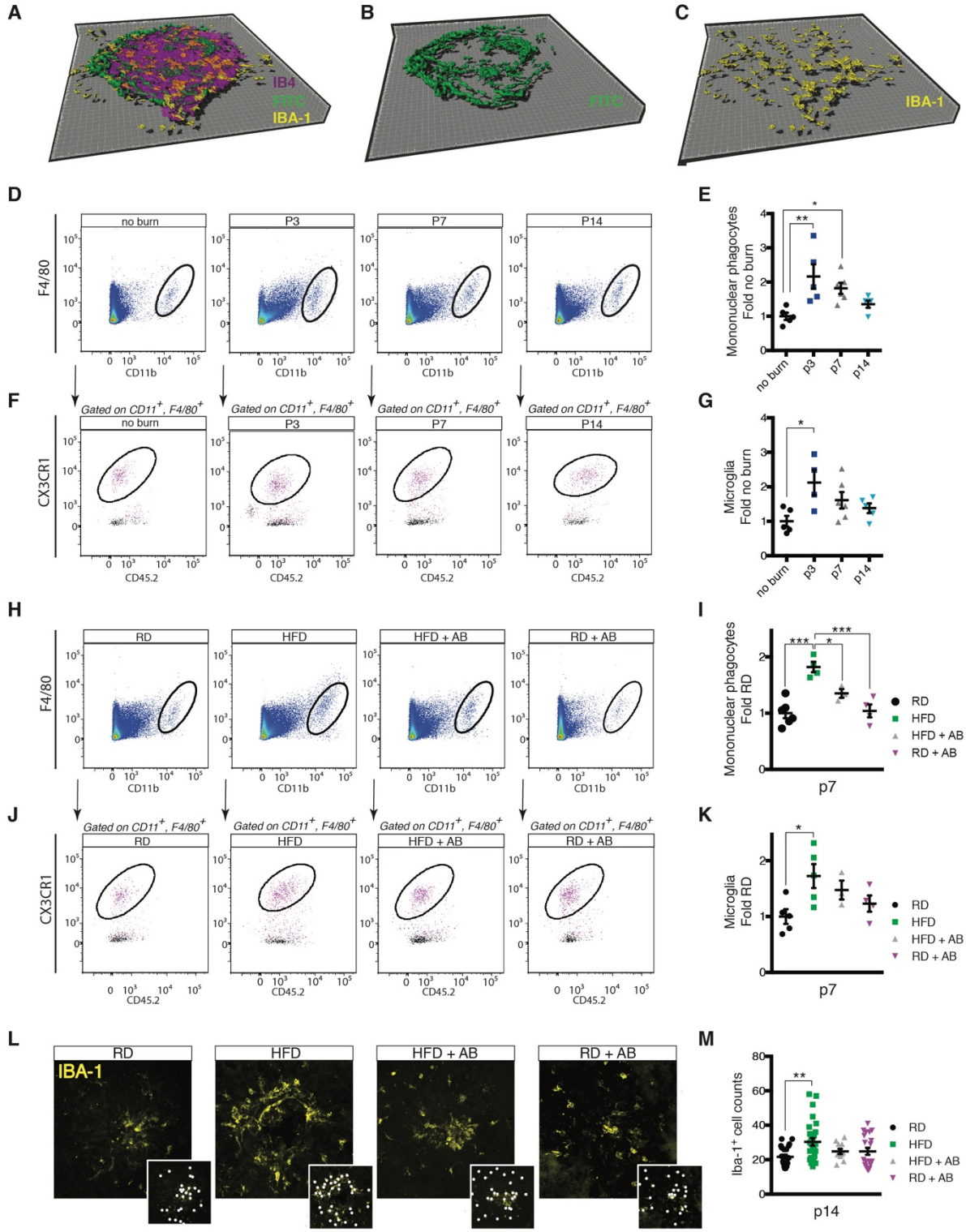

Figure 13 Publication#1 Figure 2. High-fat diet increases recruitment of microglia and macrophages.

Figure 2. High-fat diet increases recruitment of microglia and macrophages.

(**A-C**) 3D rendering of Z-stack confocal image showing Isolectin B4-stained laser-burn with FITC-dextran-labeled CNV and IBA-1-stained MPs. (**D**) Representative FACS plots of retinas and sclera-choroid-RPE-cell complexes from Regular-chow Diet (RD)-fed mice without and 3, 7 and 14 days after laser-burn. (**E**) Quantification of MPs ($Ly6G^-$, $F4/80^+$, $CD11b^+$) at p3, p7 and p14; fold naïve (no burn); n= 5(no burn), 5(p3), 6(p7), 5(p14); CI 95%. (**F**) Representative FACS plots and (**G**) quantification of microglia ($Ly6G^-$, $F4/80^+$, $CD11b^+$, $CX3CR1^{hi}$ $CD45^{lo}$) fold naïve; n= 5(no burn), 4(p3), 6(p7), 5(p14); CI 95%. (**H**) Representative FACS plots of retinas and sclera-choroid-RPE-cell complexes from RD- and HFD-fed mice, with vehicle or antibiotic treatment at p7. (**I**) Quantification of MPs at p7 fold RD; n= 6(RD), 4(HFD), 3(HFD+AB), 4(RD+AB); CI 95%. (**J**) Representative FACS plots and (**K**) quantification of microglia ($Ly6G^-$, $F4/80^+$, $CD11b^+$, $CX3CR1^{hi}$ $CD45^{lo}$) fold RD; n= 5(RD), 5(HFD), 3(HFD+AB), 4(RD+AB); CI 95%. (**L**) Representative confocal images of IBA-1-stained MPs on choroidal flat mounts from RD- and HFD-fed mice, treated with vehicle or with neomycin. Examples of labeled macrophages (white dots) are presented in side-panels. (**M**) Total number of MPs around laser impact area; n= 7(RD), 9(HFD), 4(HFD+AB), 7(RD+AB), with 23(RD), 29(HFD), 13(HFD+AB), 23(RD+AB) burns total; CI 99%. All comparisons between groups are analyzed using one-way analysis of variance (ANOVA) and Tukey's multiple comparisons test; *P< 0.05, **P< 0.01, ***P< 0.001; error bars represent mean ± S.E.M. Each "n" represents one mouse per experimental group; CI: Confidence interval. Scale bar: 100µm.

Figure 3

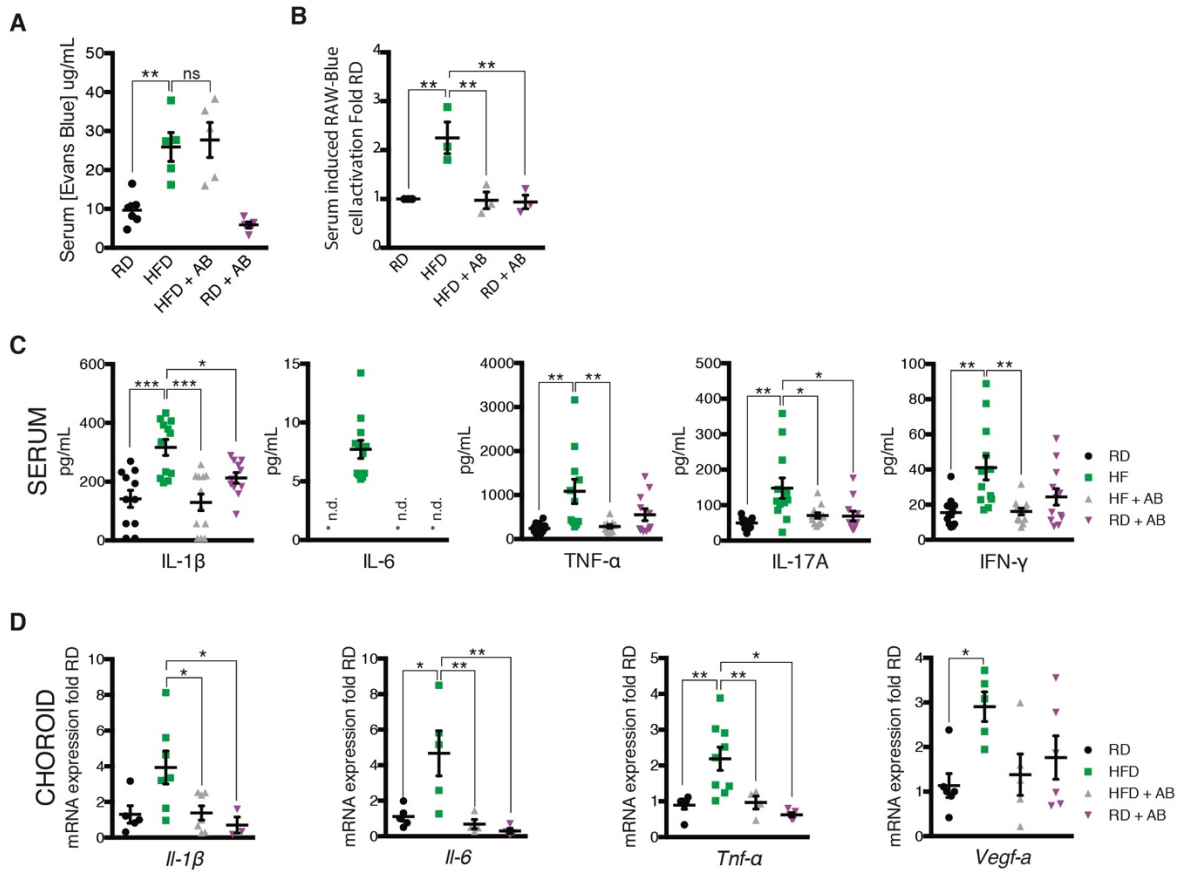

Figure 14 Publication#1 Figure 3. High-fat diet augments gut permeability, metabolic endotoxemia and systemic inflammation.

Figure 3. High-fat diet augments gut permeability, metabolic endotoxemia and systemic inflammation.

(A) Concentration of gut absorbed Evans Blue in serum 24 hours after oral administration in Regular-chow Diet (RD)- and high-fat diet (HFD)-fed mice, treated with vehicle or with antibiotic treatment; n= 6(RD), 5(HFD), 5(HFD+AB), 5(RD+AB); CI 99%. (**B**) Activation of PRRs induced by stimulation with serum isolated from mice fed RD or HFD for 7 weeks and receiving vehicle or neomycin for 3 weeks; fold RD; n=3 for all groups; CI 99%. (**C**) Serum cytokine profiles determined by Bio-Plex assay (Bio-Rad) of IL-1β, n= 11(RD), 12(HFD), 12(HFD+AB), 11(RD+AB); CI 95%; IL-6, n= 11(RD), 12(HFD), 12(HFD+AB), 11(RD+AB), CI 99.9%; TNF-α n=11 for all groups, CI 99%; IL-17A n= 11(RD), 12(HFD), 12(HFD+AB), 11(RD+AB); CI 95%; and IFN-γ; n= 12 for all groups; CI 95%. (**D**) mRNA expression of *Il-1β*; n= 5(RD), 7(HFD), 7(HFD+AB), 3(RD+AB); CI 95%, *Il-6*; n= 5(RD), 5(HFD), 4(HFD+AB), 4(RD+AB); CI 95%, *Tnf-α*; n= 6(RD), 9(HFD), 4(HFD+AB), 5(RD+AB); CI 95% and *Vegf-a*; n= 6(RD), 5(HFD), 5(HFD+AB), 6(RD+AB); CI 95% in choroids. All comparisons between groups are analyzed using one-way analysis of variance (ANOVA) and Tukey's multiple comparisons test; *P< 0.05, **P< 0.01, ***P< 0.001; error bars represent mean ± S.E.M. Each "n" represents one mouse; CI: Confidence interval.

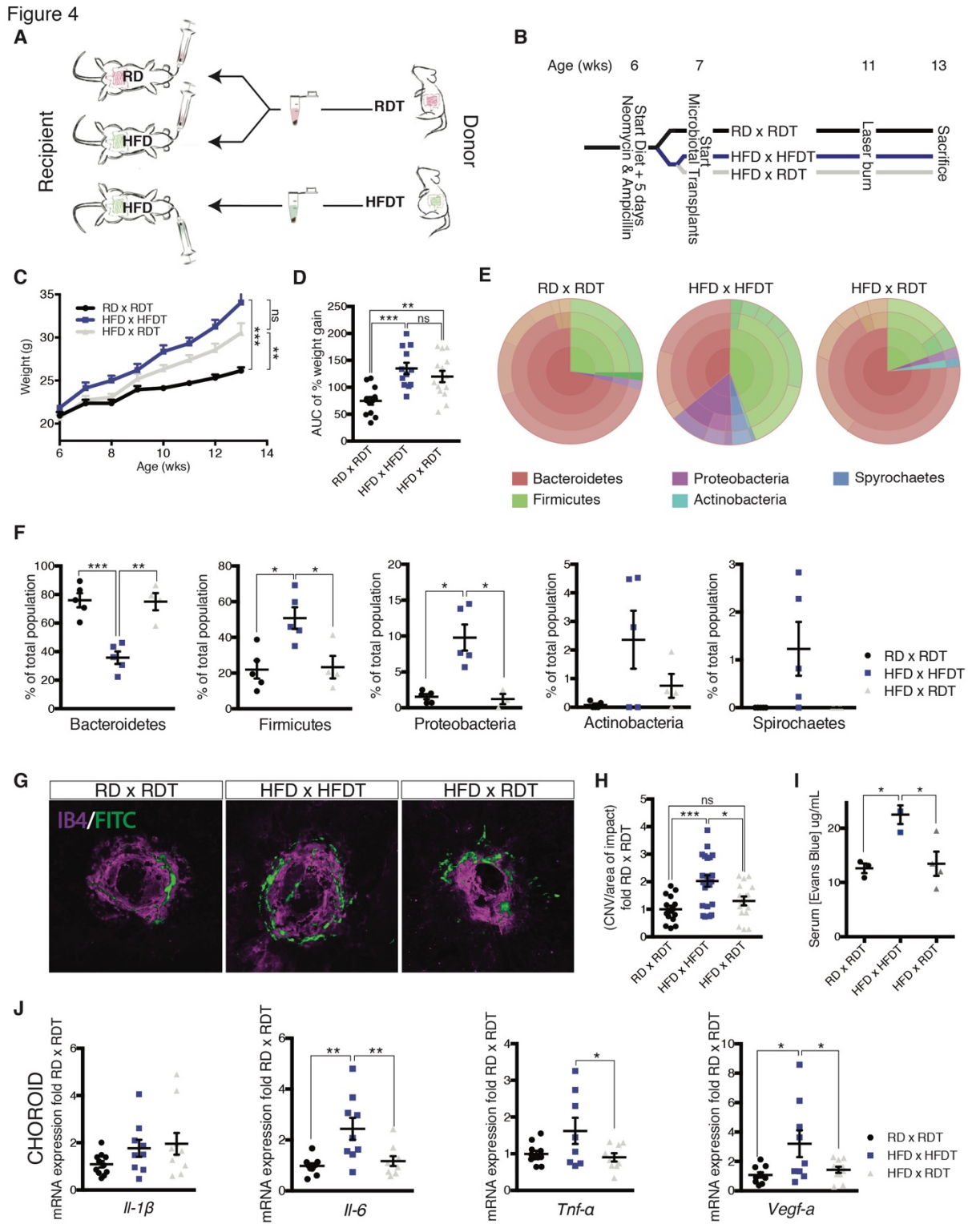

Figure 15 Publication#1 Figure 4. High-fat diet exacerbates CNV through gut microbiota.

Figure 4. High-fat diet exacerbates CNV through gut microbiota.

(**A**) Schematic representation of microbiotal transfer experiments where recipient mice are gavaged with a suspension of fecal pellets in PBS from donor mice that are either fed a Regular-chow Diet (RD) or a high-fat diet (HFD). (**B**) Experimental timeline describing preparation of mice for microbiotal transfers where mice receive 5 days of antibiotics (Neomycin and Ampicillin) at 6 weeks of age. Starting at 7 weeks of life, RD x RDT- and HFD x RDT-mice receive weekly microbiotal transplants from RD donor mice and HFD x HFDT-mice receive weekly microbiotal transplants from HFD donor mice until sacrifice at week 13. At the age of 11 weeks, mice are subjected to 4 laser burns per eye. (**C**) Weight gain and (**D**) area under the curve of percentage weight gain of RD x RDT, HFD x RDT and HFD x HFDT mice; n= 13(RDxRDT), 12(HFDxHFDT), 14(HFDxRDT); CI 99%. (**E**) Representative circle charts of relative abundance of bacterial phyla in gut microbiota of RD-fed mice receiving a RD transfer and HFD-fed mice receiving a HFD or RD transfer (**F**) relative proportion per experimental group of different phyla; n= 5(RDxRDT), 5(HFDxHFDT), 4(HFDxRDT); *Bacteroidetes*; CI 99%, *Firmicutes*; CI 95%, *Proteobacteria*; CI 95%, *Actinobacteria* and *Spirochaetes*. (**G**) Compilation of compressed Z-stack confocal images of FITC-dextran-labeled CNV and single-plane confocal images of isolectin B4-stained choroidal flat mounts from RD x RDT, HFD x RDT and HFD x HFDT mice. (**H**) Quantification of area of FITC-dextran-labeled CNV over area of isolectin B4-stained laser impact area fold RD x RDT; n= 6(RDxRDT), 9(HFDxHFDT), 9(HFDxRDT), with 15(RDxRDT), 21(HFDxHFDT), 16(HFDxRDT) burns total; CI 95%. (**I**) Concentration of gut absorbed Evans Blue in serum 24 hours after oral administration in RD- and HFD-fed mice, after RD or HFD microbiotal transplant; n= 3(RDxRDT), 3(HFDxHFDT), 4(HFDxRDT); CI 95%. (**J**) mRNA expression of *Il-1β*; n= 5(RDxRDT), 4(HFDxHFDT), 5(HFDxRDT), *Il-6*; n= 5(RDxRDT), 4(HFDxHFDT), 4(HFDxRDT); CI 99%, *Tnf-α*; n= 5(RDxRDT), 4(HFDxHFDT), 4(HFDxRDT); CI 95% and *Vegf-a*; n= 5(RDxRDT), 4(HFDxHFDT), 5(HFDxRDT); CI 95% in choroids. All comparisons between groups are analyzed using one-way analysis of variance (ANOVA) and Tukey's multiple comparisons test; *P< 0.05, **P< 0.01, ***P< 0.001; error bars represent mean ± S.E.M. Each "n" represents one mouse, per experimental group, in (**I**) both eyes were used for mRNA extraction, giving two data points per mouse; CI: Confidence interval. Scale bar: 100µm.

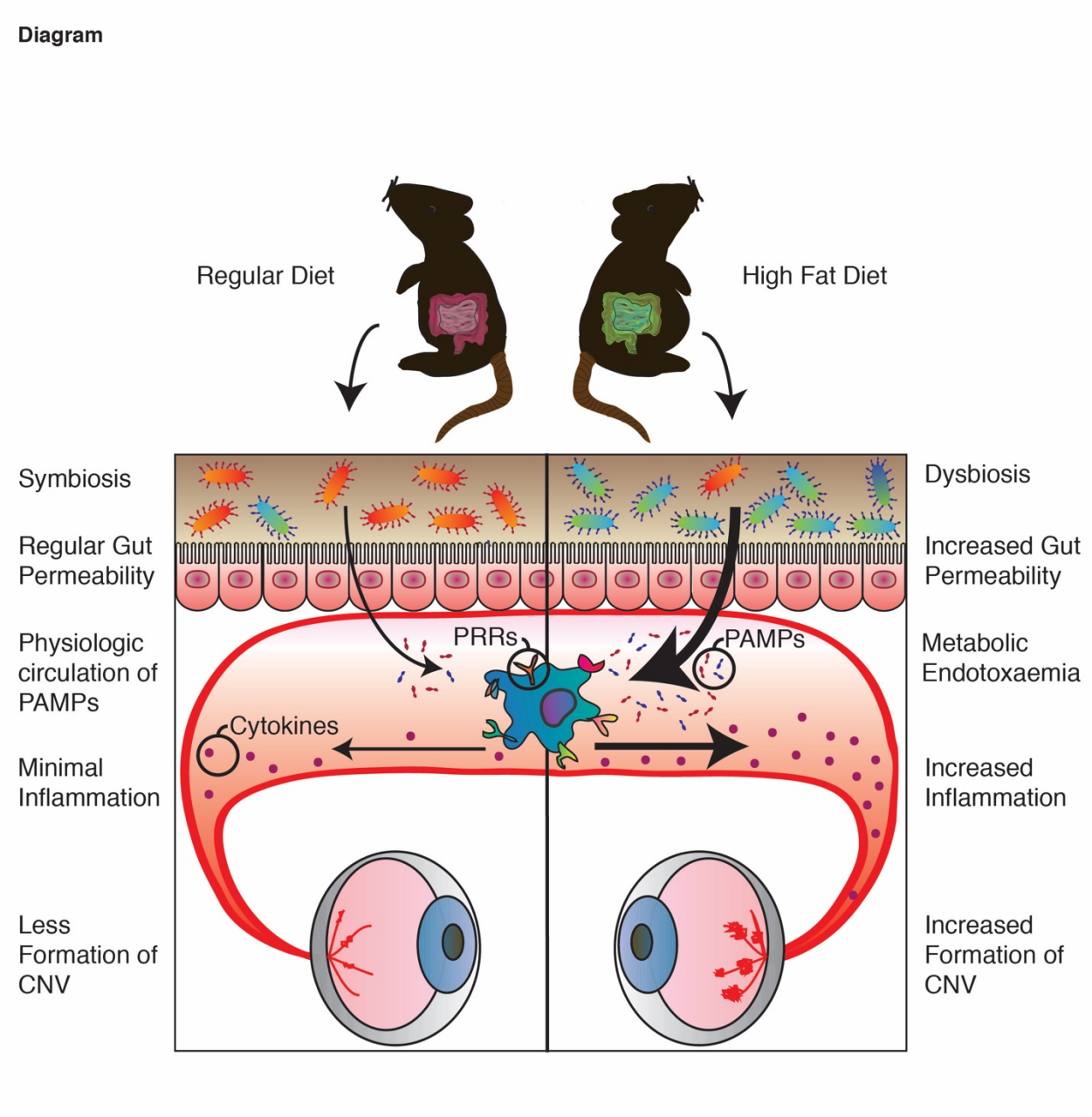

Figure 16 Publication#1 Figure 5. High-fat diet induced dysbiosis increases intestinal permeability, metabolic endotoxemia, systemic and local inflammation and ultimately contributes to CNV.

Figure 5. High-fat diet induced dysbiosis increases intestinal permeability, metabolic endotoxemia, systemic and local inflammation and ultimately contributes to CNV.

The ratio of *Bacteroidetes* and *Firmicutes,* the two dominant phyla in intestinal flora, decreases significantly in high-fat diet (HFD)-fed mice compared to Regular-chow Diet (RD)-fed mice, with a relative increase of *Firmicutes* in HFD-fed mice and decrease of *Bacteroidetes.* This dysbiosis is accompanied by heightened intestinal permeability, which allows increased translocation of pathogen associated molecular patterns (PAMPs) (endotoxemia). Recognition of these microbe-specific molecules by pattern recognitions receptors (PRRs) present on innate immune cells triggers synthesis and excretion of cytokines causing chronic systemic low-grade inflammation. Ultimately, this exacerbates CNV.

Expanded View Figures and Legends

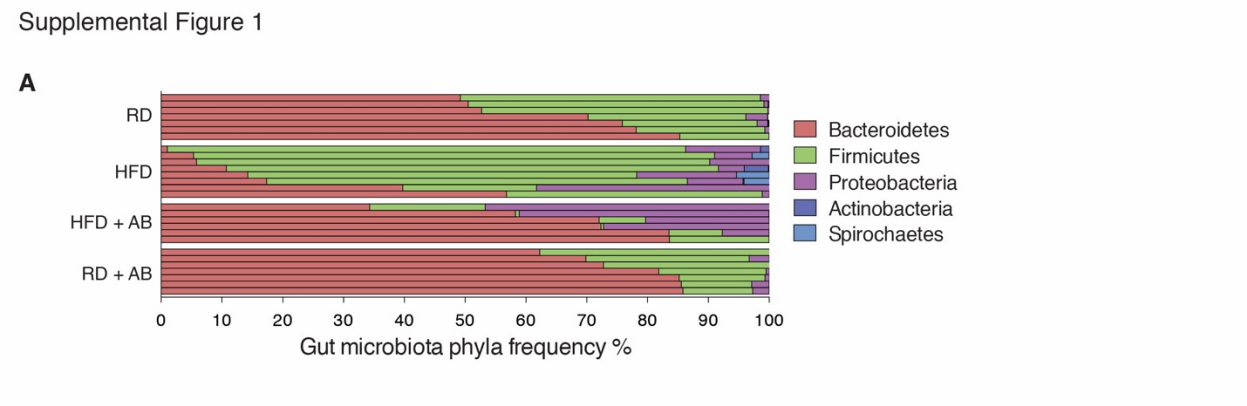

Figure 17 Publication#1 Figure EV1. Mice on HFD have shifted ratios of commensal gut microbes.

Figure EV1. Mice on HFD have shifted ratios of commensal gut microbes.

(A) Relative abundance of bacterial phyla in gut microbiota of RD-fed mice with vehicle, HFD-fed mice with vehicle, HFD-fed mice with neomycin and RD-fed mice with neomycin, shown per sample; n=7(RD), 8(HFD), 6(HFD+AB), 7(RD+AB).

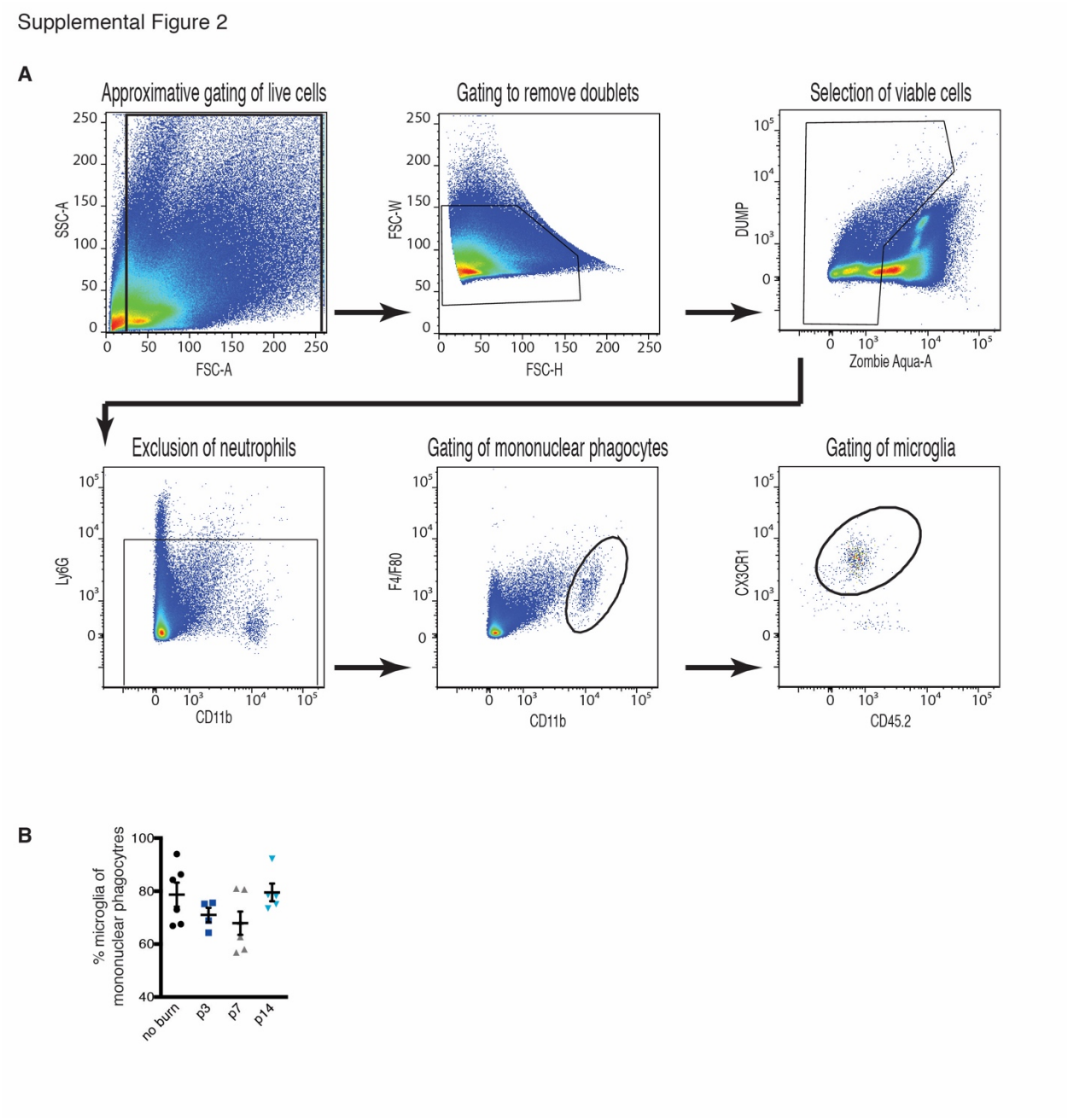

Figure 18 Publication#1 Figure EV2. FACS gating scheme and relative expression of MPs.

Figure EV2. FACS gating scheme and relative expression of MPs.

(**A**) Gating scheme explaining the identification of the Ly6G $^{-}$, F4/80^{+}, CD11b^{+} mononuclear phagocytes and the Ly6G^{-}, F4/80^{+}, CD11b^{+}, CX3CR1^{hi} CD45^{lo} microglia in retinas and sclera-choroid-RPE-cell complexes. 1. gating of live cells, 2. removal of doublets, 3. selection of viable cells, 4. exclusion of neutrophils, 5. gating of mononuclear macrophages, 6. gating of microglia. (**B**) Quantification of overall proportion of microglia within the MP population; n= 6(no burn), 4(p3), 6(p7), 5(p14). Error bars represent mean ± S.E.M. Each "n" represents one mouse.

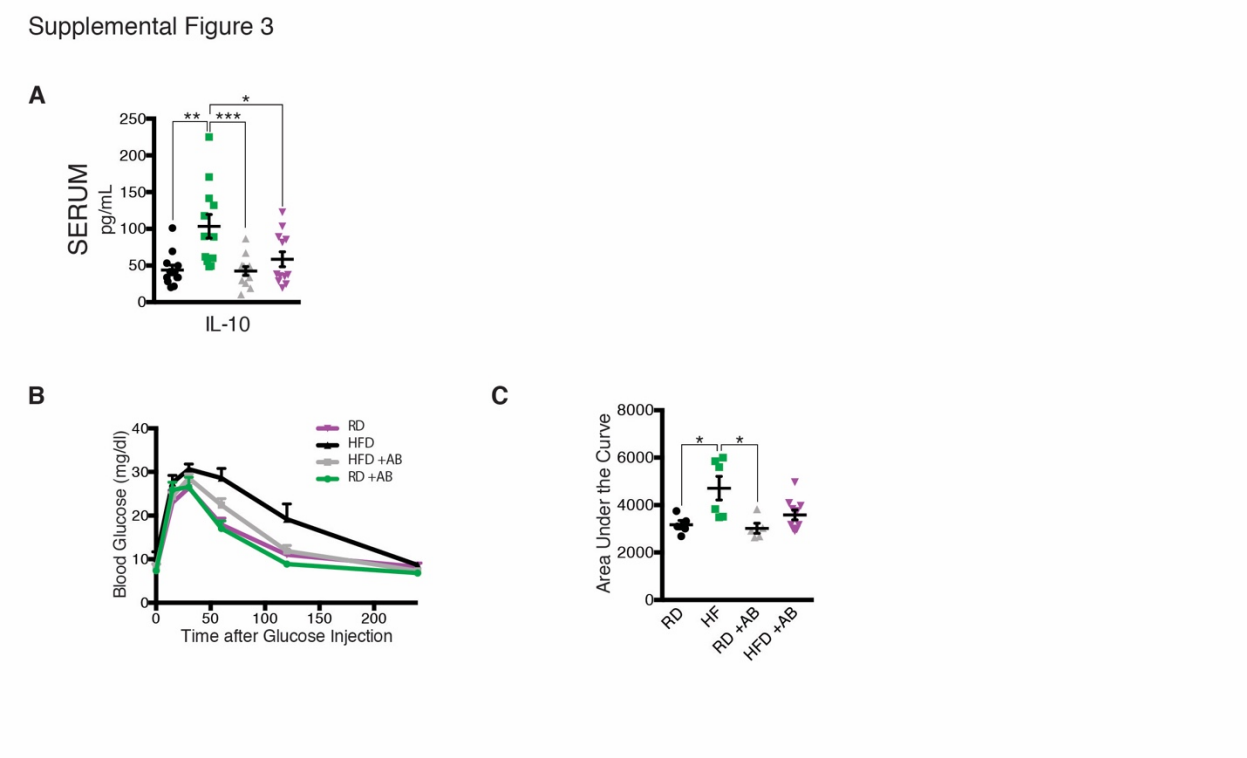

Figure 19 Publication#1 Figure EV3. Serum Il-10 is induced with HFD and neomycin treatment in HFD-mice improves glucose tolerance.

Figure EV3. Serum Il-10 is induced with HFD and neomycin treatment in HFD-mice improves glucose tolerance.

(**A**) Serum Il-10 profile; n=12 for all groups; CI 95%. (**B**) Blood glucose (mg/dl) following intraperitoneal injection of glucose (2mg/kg) in RD, HFD, HFD+AB and RD+AB-mice. (**C**) Area under the curve (AUC) of the same groups; n= 5(RD), 6(HFD), 5(HFD+AB), 10(RD+AB); CI 95%. All comparisons between groups are analyzed using one-way analysis of variance (ANOVA) and Tukey's multiple comparisons test; *P< 0.05, error bars represent mean ± S.E.M. Each "n" represents one mouse; CI: Confidence interval.

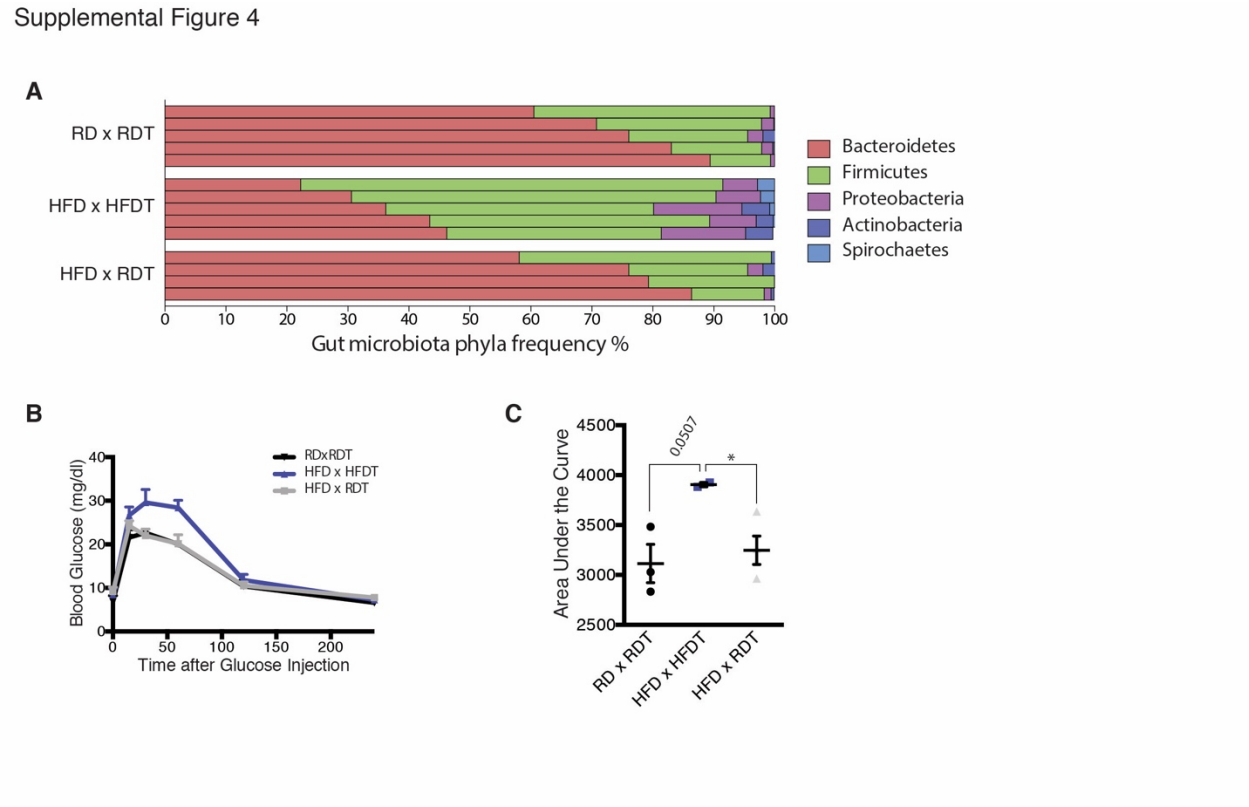

Figure 20 Publication#1 Figure EV4. Transplantation of RD-feces into HFD-mice rebalances gut microbiota and improves glucose tolerance.

Figure EV4. Transplantation of RD-feces into HFD-mice rebalances gut microbiota and improves glucose tolerance.

(A) Relative abundance of bacterial phyla in gut microbiota of RDxRDT, HFDxHFDT and HFDxRDT mice, shown per sample; n= 5(RDxRDT), 5(HFDxHFDT), 4(HFDxRDT). (**B**) Blood glucose (mg/dl) following intraperitoneal injection of glucose (2mg/kg) in RDxRDT, HFDxHFDT, HFDxRDT-mice. (**C**) Area under the curve (AUC) of the same groups; n= 3(RDxRDT), 2(HFDxHFDT), 4(HFDxRDT); CI 95%. All comparisons between groups are analyzed using one-way analysis of variance (ANOVA) and Tukey's multiple comparisons test; *P< 0.05; error bars represent mean ± S.E.M. Each "n" represents one mouse; CI: Confidence interval.

Publication #2

Report

Title: Myeloid-resident Neuropilin-1 promotes Choroidal Neovascularization while Mitigating Inflammation

Running Title: **Targeting Neuropilin-1 for CNV**

Authors:
Elisabeth MMA Andriessen[1#], François Binet[2,3#], Frédérik Fournier[4], Masayuki Hata[4], Agnieszka Dejda[3], Gaëlle Mawambo[4], Sergio Crespo-Garcia[3,4], Frédérique Pilon[3], Manuel Buscarlet[4], Karine Beauchemin[2], Veronique Bougie[2], Garth Cumberlidge[2], Ariel M Wilson[3], Steve Bourgault[6], Flavio A Rezende[3], Normand Beaulieu[2], Jean-Sébastien Delisle[5], Przemyslaw Sapieha[1,2,3,4]*

Affiliations:
Departments of [1]Biomedical Sciences, [3]Ophthalmology, [4]Biochemistry and Molecular Medicine and [5]Medicine, Maisonneuve-Rosemont Hospital Research Centre, University of Montreal, Montreal, Quebec, H1T 2M4, Canada.
[2]SemaThera Inc. 4 Westmount Square, Suite 160, Montreal, Quebec, H3Z 2S6, Canada.
[6]Department of Chemistry, Université du Québec à Montréal, Montreal, Quebec, H2L 2C4, Canada
# These authors contributed equally.

Contact: Przemyslaw (Mike) Sapieha, Ph.D.
Maisonneuve-Rosemont Hospital Research Centre
Research Centre 5415 Assomption Boulevard, Montreal,
QC, H1T 2M4, Canada.
TEL: (514) 252-3400 ext. 7711. FAX: (514) 252-3430
E-mail: mike.sapieha@umontreal.ca

Keywords: **Age Related Macular Degeneration, Angiogenesis, Inflammation, Neuropilin-1, Mononuclear Phagocytes.**

ABSTRACT

Age related macular degeneration (AMD) in its various forms is a leading cause of blindness in industrialized countries. Here we provide evidence that ligands for neuropilin-1 (NRP1), such as Semaphorin 3A and VEGFA, are elevated in the vitreous of patients with AMD at times of active choroidal neovascularization (CNV). We further demonstrate that NRP1-expressing myeloid cells promote and maintain CNV. Expression of NRP1 on cells of myeloid lineage is critical for mitigating production of inflammatory factors such as IL6 and IL1β. Therapeutically trapping ligands of NRP1 with a NRP1-derived trap reduces CNV. Collectively, our findings identify a role for NRP1-expressing myeloid cells in promoting pathological angiogenesis during CNV and introduce a therapeutic approach to counter neovascular AMD.

INTRODUCTION

Age-related macular degeneration (AMD) is a slowly progressing condition of the aging eye and the leading cause of central vision loss in industrialized countries (1, 3, 5, 443). Central vision loss from AMD poses a significant burden on health care systems and profoundly impacts well-being and mental health (17). In the early asymptomatic stages of disease, insoluble extracellular lipid aggregates termed drusen accumulate in the subretinal space. Inadequate clearance of these deposits can trigger a pathologic inflammatory response and ensuing tissue damage (51, 76). Advanced AMD is often classified into 'dry' atrophic AMD or 'wet' neovascular (NV) AMD. Visual impairment in the late stages of atrophic AMD is characterized by areas with progressive degeneration of the retinal pigment epithelium (RPE) and the photoreceptors that rely on RPE for support (4, 88). While vision loss resulting from the dry form of AMD is typically gradual and protracted, wet AMD can rapidly compromise the central visual field. This typically occurs when neovascularization from the choroid (choroidal neovascularization; CNV), sprouts into the subretinal space and neuro-retina, hemorrhages, leaks and ultimately provokes photoreceptor death, fibrovascular scarring and retinal detachment of the macular region (88).

To date, the mechanisms that precipitate NV AMD remain only partially defined, with vascular endothelial growth factor A (VEGF-A) playing a cardinal role in CNV (4). Current standards of care for wet AMD such as Aflibercept, Ranibizumab and off-label Bevacizumab target VEGF-A have revolutionized treatment of NV AMD. Unfortunately, long-term use of anti-VEGF-A therapies may have limited efficacy (444), possible neuronal side-effects (445) and have been shown to cause degeneration of the RPE-choriocapillaris complex in mouse models (446-448). In addition, approximately 1 out of 10 treated patients does not respond to anti-VEGF-A therapy (441) with NV network complexes persisting despite monthly intravitreal injections. Therefore, alternative treatments that block retinal neovascularization in AMD are required. A pharmacogenomic link has been suggested with the variability in treatment response (449, 450) and it has recently been proposed that a single-nucleotide polymorphism (SNP) in Neuropilin-1 (*Nrp1;* rs2070296) is associated with decreased anti-VEGF-A therapy response (451).

NRP1 is a single-pass transmembrane receptor with a large ~860 amino acid extracellular domain subdivided into 3 sub-domains; a large extracellular domain with two CUB motifs (A1, A2), two domains with similarity to coagulation factor V/VIII (B1, B2), a MAM domain (C) and a single transmembrane domain (TM) followed by a short cytoplasmic domain (CD) (452). The A1 and A2 domains bind Semaphorin 3A (SEMA3A) while the B1 and B2 domains bind VEGF-A, transforming growth factor beta (TGF-β), placental growth factor 2 (PGF) (378) and platelet-derived growth factor (PDGF) (365, 383, 453, 454). NRP1 can collaborate with several receptors and their ligands such as VEGFR2 and VEGF-A (370, 388), Plexin A1 and SEMA3A (411), TGF-βR and TGF-β (413) and PDGF-R and PDGF-BB (382) and hence has the potential to modulate multiple receptor signaling pathways (415, 416, 455). Of note, all above ligands are known to regulate angiogenesis, suggesting that NRP1-mediated signaling could be of interest for NV AMD (456-460).

In addition to vessels and neurons, NRP1 is highly expressed on cells of both the innate and adaptive immune system (366) where it plays an important role in homing and modulating myeloid cell function (366, 374, 375, 442) and in T-cell migration (461) and differentiation (373). Here we sought to elucidate the contribution of myeloid-resident NRP1 in NV AMD.

RESULTS

NRP1 ligands are elevated in patients with NV AMD and in a mouse model of CNV

NRP1 has been implicated in diseases characterized by deregulated vasculature such as cancer (384, 405, 416, 462, 463), and in diseases of the retina such as diabetic retinopathy diabetic macular edema (464, 465) and retinopathy of prematurity ((466), (467). We therefore sought to determine whether NRP1 ligands were present in NV AMD. We obtained vitreous from patients diagnosed with active proliferating NV AMD as determined by fundus imaging and optical coherence tomography (OCT) and from age- and sex-matched control patients with non-vascular retinal pathologies such as macular hole or epiretinal membranes. Representative horizontal B-scan and thickness maps of an AMD patient with active CNV lesions and a control patient with a non-vascular retinal pathology (macular hole) are shown in **Figure 1A, B**. Detailed characteristics of patients are included in **Table 1**. We used ELISA-based detection for NRP1 ligands and found a

significant increase in VEGF-A, from 129 ng/mL to 513 ng/mL and SEMA3A, from 0.001 ng/mL to 0.33 ng/mL (**Figure 1C, D**). TGF-β showed a trend towards increase from 1 ng/mL in control patients to 1.3 ng/mL in NV AMD patients (**Figure 1E**), while PDGF-BB and PGF did not change (**Figure 1F, G**) as previously reported (468).

We next modeled NV AMD in mice by subjecting them to the laser-induced photocoagulation model of CNV, where disruption of the Bruch's membrane triggers sprouting of subretinal vessels from the choroid (469) as depicted with fundus photography and fluorescein angiography (**Figure 1H**). Although this model does not mimic chronic aspects of human disease, it is relatively reproducible and widely used to model CNV in NV AMD. Following induction of CNV, we sacrificed mice and collected RPE-choroid-sclera complexes over the 2-week period of active CNV (3, 7, 10 or 14 days after laser-burn). We assessed transcript levels of *Nrp1* ligand by real-time quantitative PCR (RT-qPCR) and *Vegfa* levels were found to rise significantly compared to naïve choroids at day 10 (**Figure 1I**), while *Sema3a* levels rose 2-fold by day 14 (**Figure 1J**). *Tgfb1* transcripts increased as early as 3 days after laser and were elevated throughout the course until day 14 (**Figure 1K**). Consistent with PDGF-BB levels in human vitreous (**Figure 1F**), levels of *Pdgfb* did not significantly vary (**Figure 1L**). *Pgf* expression dropped in the first week after burn and rose slightly around day 10 (**Figure 1M**) as reported by others (470). Collectively, these data obtained in both humans and mice suggest that various ligands of NRP1 are elevated in NV AMD.

NRP1-expressing mononuclear phagocytes rise in the retina upon injury and promote CNV

Under physiological conditions, the subretinal space and photoreceptor cell layer are devoid of mononuclear phagocytes (76). In late AMD, the immunosuppressive subretinal environment is disturbed and mononuclear phagocytes accumulate and contribute to pathogenesis (76, 204, 471, 472). Secondary to laser-induced CNV, mononuclear phagocytes including microglia and circulating monocytes are recruited to sites of neovascularization (206). NRP1 is highly expressed on retinal mononuclear phagocytes (473) and we have previously demonstrated a role for NRP1-expressing myeloid cells in mediating pathological angiogenesis in oxygen-induced retinopathy

(467, 473). Hence we sought to determine the contribution of NRP1-expressing mononuclear phagocytes to CNV.

Analysis by FACS of whole retinas and RPE-choroid-sclera complexes at day 3 (D3) of CNV revealed a rise in $Ly6G^-$, $F4/80^+$,$CD11b^+$ mononuclear phagocytes in laser-burned eyes when compared to controls (**Figure 2A, B)**. Importantly, we observed a proportional 3-fold increase in $NRP1^+$ mononuclear phagocytes at D3 when compared to non-laser eyes (**Figure 2C)** (gating scheme and internal controls in **Expanded View Figure EV1A-C**). In order to establish the role of mononuclear phagocyte-resident NRP1 on CNV, we generated a myeloid specific knockout of *Nrp1* by crossing *Nrp1*-floxed mice with LysM-Cre (LysM-Cre/$Nrp1^{+/+}$) mice, yielding LysM-Cre/$Nrp1^{fl/fl}$ offspring. The resulting mice showed a robust reduction in *Nrp1* transcript (**Figure 2D**) and protein (**Figure 2E, F**) expression in bone marrow-derived macrophages (BMDM) when compared to LysM-Cre/$Nrp1^{+/+}$ littermate controls. FACS analysis revealed a ~30% reduction in $NRP1^+$ microglia in the retina and RPE-choroid-sclera complexes before and 3 days after laser **(Expanded View Figure EV1D, E**). LysM-Cre/$Nrp1^{fl/fl}$ mice on regular diets did not show any difference in body weight, size or open field activity when compared to littermates. Immunofluorescence of lesion sites on flat-mounted RPE-choroid-sclera complexes at D3 post laser-burn reveal that NRP1-positive mononuclear phagocytes (labeled with IBA1) are recruited to sites of injury (**Figure 2G**) while, as expected, LysM-Cre/$Nrp1^{fl/fl}$ mice did not show accretion of NRP1-expressing mononuclear phagocytes.

Throughout the course of CNV, prior to laser-burn until D14 post laser-burn, the number of mononuclear phagocytes present in RPE-choroid-sclera complexes of either LysM-Cre/$Nrp1^{fl/fl}$ or control LysM-Cre/$Nrp1^{+/+}$ mice followed similar trends. Analysis by FACS or immunofluorescence revealed that mononuclear phagocytes in either LysM-Cre/$Nrp1^{fl/fl}$ or control LysM-Cre/$Nrp1^{+/+}$ mice remained similar over time and did not show significant difference either prior to laser-burn or at D3, D7 or D14 (**Figure 2H, I, J & Expanded View Figure EV1F, G**).

Two weeks after laser-burn (D14), quantification of compressed Z-stack confocal images of FITC-dextran-perfused neovessels revealed a ~30%-40% decrease in CNV in LysM-Cre/*Nrp1*$^{fl/fl}$ mice compared to controls (**Figure 2K-N**). The average size of isolectin B4 (IB4)-labeled impact areas did not differ between groups (**Figure 2M)** suggesting that the observed effect is directly on nascent vasculature. Interestingly, the extent of CNV did not vary between groups in the first week post laser-burn (**Expanded View Figure EV1H-K)** implying that NRP1-expressing mononuclear phagocytes partake in later stages of disease. Together, these data suggest that while levels of mononuclear phagocytes are similar between LysM-Cre/*Nrp1*$^{+/+}$ and LysM-Cre/*Nrp1*$^{fl/fl}$ during CNV, NRP1-expressing mononuclear phagocytes promote and maintain neovascularization in the later stages of CNV.

NRP1-expressing mononuclear phagocytes display a pro-angiogenic phenotype

Given that equal numbers of mononuclear phagocytes are present in the back of the eye of LysM-Cre/*Nrp1*$^{+/+}$ and LysM-Cre/*Nrp1*$^{fl/fl}$ mice following laser-burn, yet NRP1^{+} mononuclear phagocytes promote CNV (**Figure 2**), we sought to determine the impact of loss of myeloid-resident NRP1 on choroidal inflammation during CNV. Three days after laser-burn, we observed a significant rise in mRNA transcripts for interleukin 1 β (*Il1b*) and interleukin 6 (*Il6*) (**Figure 3A, B**) in RPE-choroid complexes of LysM-Cre/*Nrp1*$^{fl/fl}$ mice when compared to controls, with a ~2-fold increase in *Il1b* and ~7-fold increase in *Il6.* No significant change was detected in *Vegfa* or tumor necrosis factor (*Tnf*) (**Figure 3C, D**). A similar pattern of expression was observed seven days post laser-burn (**Figure 3 E-H**).

We next investigated immune activation in bone marrow derived macrophages (BMDM) from LysM-Cre/*Nrp1*$^{+/+}$ and LysM-Cre/*Nrp1*$^{fl/fl}$ mice. BMDMs were derived from bone marrow cells using macrophage colony-stimulating factor (M-CSF) which can induce a predominantly anti-inflammatory M2-like cell population (474, 475) However, we observed a significant increase in NF-κB p65 phosphorylation in NRP1-deficient BMDMs (**Figure 3I, J**), accompanied by increased levels of *Il1b* and *Il6* (**Figure 3K, L**) indicative of classical activation of mononuclear phagocytes and suggesting that absence of NRP1 in myeloid cells led to increased levels of these cytokines in

RPE-choroid-sclera complexes (**Figure 3A, B**). In line with these findings, FACS analysis revealed a ~2-fold increase in M1-like (F4/80$^+$, CD11b$^+$, CD11c$^+$, CD206$^-$) BMDMs in LysM-Cre/*Nrp1*$^{fl/fl}$ mice (**Figure 3M, N**) (gating scheme in **Expanded View Figure EV2A),** accompanied by a ~25% decrease in M2-like (F4/80$^+$, CD11b$^+$, CD11c$^-$, CD206$^+$) cells (**Figure 3M, O**).

Moreover, transcriptomic analysis by RNA sequencing (RNA-seq) and gene set enrichment analysis (GSEA) of NRP1-deficient peritoneal macrophages revealed a significant decrease in transcripts from the GO Angiogenesis gene set **(Figure 3P)** in LysM-Cre/*Nrp1*$^{fl/fl}$ macrophages when compared to wildtype controls. These data support the notion that absence of NRP1 on mononuclear phagocytes renders them less pro-angiogenic and more pro-inflammatory. These findings are consistent with the lower levels of CNV observed in LysM-Cre/*Nrp1*$^{fl/f}$ mice (**Figure 2K-N**) and other studies suggesting that heightened inflammation may reduce CNV in the laser-induced mouse model (476).

Therapeutic intravitreal administration of soluble NRP1 reduces CNV in mice

Based on the above data, we sought to determine the therapeutic value of interfering with NRP1 ligands on the outcome of CNV. We generated a recombinant NRP1-derived trap consisting of the extracellular domain of NRP1 (**Figure 4A**). This trap binds and neutralizes NRP1 ligands (464, 467). We initially confirmed the binding of the NRP1 ligands SEMA3A and VEGF-A to the trap by surface plasmon resonance (SPR). The trap was covalently immobilized by standard amine coupling on a carboxymethyl dextran sensor chip with lower charge (CM4) and ligands were injected at various concentrations to evaluate binding kinetics in real-time. Sensorgrams revealed fast association and low dissociation for both ligands, which followed a simple 1:1 stoichiometry model. Equilibrium dissociation constants (K_d) of 0.67 nM and 4.32 nM were respectively extracted for SEMA3A and VEGF-A (**Figure 4B-D**), indicative of high and physiologically relevant binding affinities. Interestingly, while the association rate constants were somewhat similar for both ligands, SEMA3A showed a much slower dissociation to the immobilized Trap compared to VEGF-A, suggesting that the SEMA3A-trap complex is very stable.

Intravitreal injections of NRP1-derived trap in C57BL/6J wildtype mice at D0 led to a robust ~47% decrease in Dextran-FITC-perfused neovessels compared to vehicle controls at day 14 post laser-burn (**Figure 4E, F**). The average size of IB4-labeled impact area was not significantly affected by the treatment (**Figure 4E, G**) and ratios of FITC-labeled neovessels to the size of IB4-labeled post laser-burn scarring were reduced by 41% after trap treatment (**Figure 4E, H**). Transcripts for *Vegfa* and *Tnf* did not vary following treatment with trap while *Il6* rose **(Expanded View Figure EV3A-C)**.

In order to determine if the beneficial effects of NRP1-derived traps on CNV were mediated by influencing $NRP1^{+}$ mononuclear phagocytes, we injected traps into the vitreous of LysM-Cre/$Nrp1^{fl/fl}$ and LysM-Cre/$Nrp1^{+/+}$ mice following laser-burn. Similar to wildtype mice, trap treatment in LysM-Cre/$Nrp1^{+/+}$ led to a significant decrease in FITC-perfused vessels and FITC/IB4-ratios (**Figure 4I, J, L**). Treatment of LysM-Cre/$Nrp1^{fl/fl}$ mice reduced CNV to similar levels as seen in controls, however the magnitude of effect was diminished (**Figure 4I-L**). NRP1 is expressed by several other cells in the retina and sclera-choroid-RPE complex such as endothelial cells and neurons. Intravitreal injection of the NRP1-derived traps will influence ligands that signal in all NRP1-expressing cells. The reduced therapeutic effect of the trap in LysM-Cre/$Nrp1^{fl/fl}$ mice suggests that a portion of the therapeutic effect of the NRP1 trap is mediated through myeloid cells.Together, these data suggest that sequestering NRP1 ligands is an effective strategy to reduce pathological subretinal neovascularization.

DISCUSSION

Here we show that several ligands of NRP1 are induced in the vitreous of patients with active NV AMD and that myeloid-resident NRP1 contributes to pathological angiogenesis in later stages of CNV in mice. Moreover, we demonstrate that while mononuclear phagocyte-resident NRP1 is not essential for cellular recruitment to sites of CNV, it is critical for mitigating myeloid cell inflammation and skews myeloid cells towards a pro-angiogenic phenotype. Absence of NRP1

leads to enhanced production of pro-inflammatory factors as we have previously suggested for dendritic cells (371) and adipose tissue macrophages (375). These data add to the notion that less inflammatory and more M2-like mononuclear phagocytes are enriched with age, and exacerbate CNV in the laser-induced mouse model (476, 477).

Accumulation of mononuclear phagocytes in AMD secondary to the disruption of the physiologically immunosuppressive subretinal environment is central to the etiology of both atrophic and wet forms of disease (76, 196, 472). Our data suggest that NRP1 keeps mononuclear phagocytes in a less inflammatory and more reparative state, towards the M2 portion of the spectrum. This is consistent with findings demonstrating that NRP1-deficient myeloid cells are more pro-inflammatory, classically activated cells in models of obesity (375), tumor growth (366, 374, 453, 478), and sepsis (479). With respect to being pro-angiogenic, NRP1-expressing mononuclear phagocytes have been described as dispensable for physiological angiogenesis in the retina and elsewhere (428, 473), yet important for vessel growth during weight gain (375). They have also been reported to normalize tumor blood vessels (480), and promote pathological angiogenesis in the retina (467) and tumors (Casazza et al., 2013).

Based on the above findings, we sought to determine the therapeutic potential of neutralizing NRP1 ligands. A single intravitreal injection of a recombinant NRP1-derived trap was effective at preventing CNV, highlighting the therapeutic potential of NRP1 for exudative AMD. In addition, others (465) and us (464, 467) have demonstrated efficacy for recombinant NRP1 for retinal vasculopathies characterized by preretinal neovascularization or vasogenic edema. Potentially, non-responders to anti-VEGF therapy could benefit from this treatment paradigm, since a genetic variation of *Nrp1* is an indicator of reduced treatment response to anti-VEGF therapeutics like Ranibizumab in patients with NV AMD (449, 451). NRP1-derived traps have a considerably lower affinity for VEGF-A compared to current anti-VEGF therapeutics such as Ranibizumab, Bevacizumab and Aflibercept (481) and hence may limit toxicity associated with sustained VEGF-A deprivation. Of note, the NRP1-derived trap was less effective in retinas of LysM-Cre/$Nrp1^{fl/fl}$ suggesting a mechanism of action in part redundant with deletion of NRP1 in myeloid cells.

In sum, while a role for endothelial-resident NRP1 has been demonstrated in choroidal and retinal neovascularization (482), we provide evidence that NRP1-expressing immune cells contribute to CNV. Collectively, we provide rationale for therapeutic targeting of NRP1 ligands or NRP1-expressing myeloid cells for exudative AMD.

MATERIALS AND METHODS

Vitrectomy

All patients were previously diagnosed with NV AMD and were followed and treated by a single vitreoretinal surgeon (F.A. Rezende). Control patients underwent surgical treatment for non-vascular pathology (epiretinal membrane or macular hole) by the same surgeon. Patients underwent surgery under local retro/peribulbar anesthesia. Three-port 25-gauge transconjunctival pars plana vitrectomy was performed through 25-gauge valved cannulas (Alcon). Under microscope visualization using a wide-angle viewing system (Resight, Zeiss), undiluted vitreous at the macular area was collected with a 25-gauge vitrector. Vitreous samples were frozen on dry ice immediately after biopsy and stored at -80°C. We obtained approval of human clinical protocols from the Hopital Maisonneuve-Rosemont ethics committee (Ref. CER: 10059). Written informed consent was obtained from all subjects and the experiments conformed to the principles set out in the WMA Declaration of Helsinki and the Department of Health and Human Services Belmont Report.

Quantification of ligands of NRP1 in human vitreous by ELISA

Samples were centrifuged at 15,000g for 5 minutes at 4°C prior to analysis. NRP1 ligands were quantified in supernatants using ELISAs following manufacturer's instructions; VEGF-A (DVE00,. R&D Systems), SEMA3A (LS-F29822, LSBio), TGF-□ (BMS-249-4, Thermo Fisher Scientific Inc.), PGF (EHPGF, Thermo Fisher Scientific Inc.) and PDGF-BB (BMS2071, Thermo Fisher Scientific Inc.)

Animals

All studies were performed in accordance with the Association for Research in Visions and Ophthalmology (ARVO) Statement for the Use of Animals in Ophthalmic and Vision Research. All animal procedures were validated by the Animal Care committee of the University of Montreal and Hôpital Maisonneuve-Rosemont in agreement with the guidelines established by the Canadian Council on Animal Care.

C57BL/6J wild-type (WT), LysM-Cre (Lyz2tm1(cre)Ifo/J; no. 004781), Neuropilin1-floxed (*Nrp1*tm2Ddg/J; no. 005247) mice were purchased from the Jackson Laboratory (Bar Harbor, ME, USA) and bred in house. We generated a line of myeloid-specific transgenic mice by breeding LysM-Cre mice (Cre-recombinase expressed in the myeloid lineage) with NRP1-floxed mice, resulting in a mouse with attenuated *Nrp1* in myeloid cells (LysM-Cre/$Nrp1^{fl/fl}$). Mice were raised under sterile barrier conditions and housed under a 12-h light cycle with water and food ad libitum. Only male mice were used in this study.

In vivo imaging following laser-induced choroidal neovascularization (CNV)

In vivo imaging was performed using a scanning laser ophthalmoscope (Micron IV; Phoenix Laboratories, Pleasanton, CA, USA). Mice of 9 to 11 weeks of age were subjected to pupil dilation (Mydriacyl; Alcon, Mississauga, ON, Canada) and anesthetized with a mix of 10% ketamine and 4% xylazine (10µl/g body weight). Fluorescein (Alcon, 1 unit/g body weight of a 5% fluorescein dilution in 0.9% sodium chloride) was injected subcutaneously and corneas were lubricated with Optixcare ophthalmic gel (Aventix Animal Health, Burlington, ON, Canada). After a fluorescein circulation of 5 minutes, retinas were imaged before and after inducing choroidal neovascularization with 4 distinct laser-burns (50µm, 300mW, 0.05s). Animals were followed-up 3, 7 and 14 days after laser-burn.

Surface plasmon resonance

SPR analyses were performed using a Biacore T200 instrument (GE Healthcare). Purified recombinant trap was immobilized by standard amine-coupling chemistry on a Biacore CM4 carboxymethylated dextran sensor chip, which was pre-activated with 100 mM N-

hydroxysuccinimide (NHS) and 100 mM of 3-(N,Ndimethylamino) propyl-N-ethylcarbondiimide (EDC). Surfaces were blocked by injecting 1 M ethanolamine. An immobilization abundance of 100 to 150 RU of Trap was reached. SEMA3A and VEGFA were respectively injected over the sample and reference flow cells at increasing concentrations (12.5 to 100 nM) at a flow rate of 40 µl/min in PBS buffer supplemented with 0.025% (v/v) Tween-20. Binding sensorgrams were obtained by subtracting the reference flow cell. Response curves were analyzed using BIAevaluation software (GE Healthcare) and data from all concentrations were globally fit to a one-site Langmuir binding model.

Real-time quantitative PCR analysis

Immediately after enucleation eyes were dissected to isolate the sclera–choroid–RPE cell complex. BMDM's were washed 3x in PBS and collected in TRIzol. RNA was isolated using TRIzol and digested with DNase I to prevent amplification of genomic DNA contaminants. All-In-One RT MasterMix (ABM) was used for the reverse transcription, and BrightGreen qPCR MasterMix (ABM) to determine gene expression in an ABI Biosystems Real-Time PCR machine with □-actin (Actb) as a reference gene. We used the following primers: Mouse *Actb* = F: 5'-GAC GGC CAG GTC ATC ACT ATT G-3', R: 5'-CCA CAG GAT TCC ATA CCC AAG A-3'; Mouse *Vegfa* = F: 5'-GCC CTG AGT CAA GAG GAC AG-3', R: 5'-CTC CTA GGC CCC TCA GAA GT-3'; Mouse *Sema3a* = F: 5'-GGG ACT TCG CTA TCT TCA GAA-3', R: 5'-GGC GTG CTT TTA GGA ATG TTG-3'; Mouse *Tgfb1* = F: 5'-ACG CCT GAG TGG CTG TCT TTT GAC-3', R: 5'-GGG CTG ATC CCG TTG ATT TCC ACG-3'; Mouse *Pdgfb*= F: 5'- GAA GTT GGC ATT GGT GCG AT-3', R: 5'- TGG AGT CGA GTC GGA AAG CT-3'; Mouse *Nrp1*=F: 5'- ACC CAC ATT TCG ATT TGG AG-3', R: 5'-TTC ATA GCG GAT GGA AAA CC-3'; Mouse *Il1b* = F: 5'-CTG GTA CAT CAG CAC CTC ACA-3', R: 5'-GAG CTC CTT AAC ATG CCC TG-3'; Mouse *Il6* = F: 5'-AGA CAA AGC CAG AGT CCT TCA GAG A-3', R: 5'-GCC ACT CCT TCT GTG ACT CCA GC-3'; Mouse *Tnf* = F: 5'-CCC TCA CAC TCA GAT CAT CTT CT-3', R: 5'-GCT ACG ACG TGG GCT ACA G-3'; Mouse *iNos* = F: 5'-CGG CAA ACA TGA CTT CAG GC-3', R: 5'-GCA CAT CAA AGC GGC CAT AG-3'; Mouse *Cd163* = F: 5'-ATG CTT CCA TCC AGT GCC TC-3', R: 5'-CAC AAA CCA AGA GTG CCG TG-3'; Mouse *Cd206* = F: 5'-GTT CAC CTG GAG TGA TGG TTC TC-3', R: 5'-AGG ACA TGC CAG GGT CAC CTT T-3'; Mouse *Arg1* = F: 5'-CAF CAC TGA GGA AAG CTG GT-3', R: 5'-CAG ACC GTG GGT TCT TCA CA-3'; Mouse *Pgf* = F: 5'-CAG TTG CTT CTT ACA GGT CC-3', R: 5'-CAC CTC ATC AGG GTA TTC AT-3'.

Laser-induced CNV

At the age of 6 weeks, mice were anesthetized by intraperitoneal injection with 10 μl/g body weight of a 10% ketamine and 4% xylazine solution. Using an argon laser we ruptured their Bruch's membrane, as described previously (469). Mice were sacrificed at 3, 7, 10 or 14 days after we induced 4 burns per eye for the immunohistochemistry analysis and 6 burns per eye for the RT-qPCR and FACS analyses.

Immunohistochemistry

7 or 14 days after CNV induction, mice were sedated with isoflurane gas and cardiacally perfused with 0.5mL of 15mg/mL of fluorescein isothiocyanate (FITC)-dextran (average mol wt 2,000 kDA) and euthanized. Eyes were enucleated and fixed for 30 minutes in 4% PFA at room temperature, before dissection of the sclera-choroid-RPE cell complex. After a secondary fixation of 15 minutes in 4% PFA at room temperature, the choroids were stained with rhodamine-labeled Griffonia (bandeiraea) Simplicifolia Isolectin I (RL-1102-2, Vector Laboratories Inc.) (1:100), NRP1 (AF566, goat polyclonal; R&D Systems) (1:250) and IBA-1 (019-19741, rabbit polyclonal; Wako) (1:350) overnight. After 1 hour incubation with secondary antibodies the sclera-choroid-RPE cell complex was mounted onto a slide, and the burns and macrophages were captured in a Z-stack with an Olympus FV1000 microscope. The Z-stacks were compressed into one image and quantified in ImageJ.

FACS on retina and sclera-choroid-RPE cell complexes

Retinas and sclera-choroid-RPE cell complexes of non-burned (D0) and burned mice at D3 were cut into small pieces and homogenized in a solution of 750U/mL DNAse I (Sigma-Aldrich Corp.) and 0.5mg/mL of collagenase (Roche) for 20 minutes at 37°C. Homogenates were filtered through a 70μm cell strainer and washed in PBS. Viability of the cells was checked by Zombie Aqua (423101: BioLegend) staining for 15 min at room temperature. After incubation with LEAF-purified anti-mouse CD16/32 (101310; BioLegend) for 10 min at 4°C to block Fc receptors, cells were incubated for 25 min at 4°C with the following antibodies: BV711 anti-mouse/human CD11b (101242; BioLegend), PE anti-mouse F4/80 (123110; BioLegend), APC anti-mouse CD64

(139305; BioLegend), FITC anti-mouse CD38 (102705; BioLegend), APC/Cy7 anti-mouse Ly-6G (127624; BioLegend), BV785 anti-mouse CD11c (117335; BioLegend) and PE/Cy7 anti-mouse CD206 (141719; BioLegend). Antibody dilution was determined with titration by lot. Fluorescence-activated cell sorting (FACS) was performed on a BD LSRFortessaTM X-20 cell analyzer, and data were analyzed using FlowJo software (FlowJo version 10.2).

Generation of BMDM

Bone marrow from both femurs and tibiae was harvested through bone flushing with PBS supplemented with 10% FBS. After red blood cell (RBC) lysis, cells were seeded in complete medium (Dulbecco's modified Eagle's medium (DMEM) plus 10% FBS and 1% streptomycin/penicillin) and stimulated with macrophage colony-stimulating factor (M-CSF) (Mouse M-CSF Recombinant Protein, eBioscience™; Invitrogen) 1:5000. After 3 days of incubation at 37°C with 5% CO_2, fresh medium containing M-CSF was added. Cells were allowed to differentiate for a total of 6 days, before their medium was replaced by complete medium without M-CSF. LPS stimulated cells were stimulated for 24 hours with 250ng/mL LPS (*Escherichia coli* O55:B5 lipopolysaccharide; Sigma-Aldrich). The cells were not tested for mycoplasma contamination. As evaluated by flow cytometry, the purity was usually around 99%.

Western blot analysis

For assessment of BMDM protein levels, we collected BMDM by scraping the cells in RIPA1x on ice. Protein concentration was assessed by bicinchoninic acid (BCA) assay (Sigma-Aldrich), and 30μg protein was analyzed for each condition by standard SDS-PAGE technique. Anti-NRP1 antibody (ab81321) (1:2000) and Anti-NF-κB p65 (ab16502) (1:500) antibody were purchased from Abcam.

FACS on BMDM for extracellular staining

BMDM's were collected in PBS through scraping. Viability of the cells was checked by Zombie Aqua (423101: BioLegend) staining for 15 min at room temperature. After incubation with LEAF-purified anti-mouse CD16/32 (101310; BioLegend) for 10 min at 4°C to block Fc receptors, cells

were incubated for 25 min at 4°C with the following antibodies: BV711 anti-mouse/human CD11b (101242; BioLegend), PE anti-mouse F4/80 (123110; BioLegend), APC anti-mouse CD64 (139305; BioLegend), FITC anti-mouse CD38 (102705; BioLegend), APC/Cy7 anti-mouse Ly-6G (127624; BioLegend), BV785 anti-mouse CD11c (117335; BioLegend) and PE/Cy7 anti-mouse CD206 (141719; BioLegend). Antibody dilution was determined with titration by lot. Fluorescence-activated cell sorting (FACS) was performed on a BD LSRFortessaTM X-20 cell analyzer, and data were analyzed using FlowJo software (FlowJo version 10.2).

RNA-seq sample preparation, sequencing and analysis

RNAseq data is available from a previous study (Wilson et al, 2018) in Gene Expression Omnibus (GEO) under the entry GSE110447. RNA-seq was performed as described previously (375). Gene set enrichment analysis GSEA was conducted using GSEA v2.2.1 software provided by Broad Institute of Massachusetts Institute of Technology and Harvard University. We used the gene set contributed by the MSigDB Team, and ANGIOGENESIS contributed by the Gene Ontology Consortium from the Molecular Signature Database of the Broad Institute, Inc.

Intravitreal injections

Wildtype, LysM-Cre/*Nrp1*$^{fl/fl}$ and LysM-Cre/*Nrp1*$^{+/+}$ mice subjected to laser-burn were intravitreally injected with NRP1-derived trap or Vehicle (Saline 0.9%) on the day of the burn and sacrificed at D14.

Statistical Analysis

Data are presented as mean ± SEM Student's T-test was used to compare two different groups or, when indicated, a one-way analysis of variance (ANOVA) and Dunnett's multiple comparisons test. A $P<0.05$ was considered statistically different. N was indicated for each experiment.

Data Availability

This study includes no data deposited in external repositories.

Acknowledgments

P.S. holds the Wolfe Professorship in Translational Research and a Canada Research Chair in Retinal Cell Biology. This work was supported by operating grants to P.S from The Foundation Fighting Blindness Canada and SemaThera Inc. Additional funding was provided by the Canadian Institutes of Health Research (Foundation grant #148460), the Diabetes Canada (DI-3-18-5444-PS) the Canadian the Heart & Stroke Foundation Canada (G-16-00014658), and Natural Sciences and Engineering Research Council of Canada (418637), the Fonds de Recherche en Ophtalmologie de l'Université de Montréal (FROUM) and the Réseau en Recherche en Santé de la Vision. M.H. holds the Banting Fellowship from the CIHR. S.C-G. holds a Fonds de Recherche Santé du Québec (FRQS) scholarship.

Author contributions

E.A. & P.S. designed the research and study. E.A., F.B., F.F., F.P., M.H., A.D., G.M., A.W., N.B., K.B., S.C-G., S.B., carried out experimental work. F.A.R. performed all retinal surgeries. E.A., F.B., A.W. & M.B., analyzed the data. JS.D., G.C. and V.B. provided valuable conceptual insight on research design. E.A., A.W. & P.S. wrote the manuscript with valuable input from authors.

Conflict of interest

P.S. is the founder of and a consultant for SemaThera Inc. G.C. & V.B. are consultants for SemaThera Inc. F.B., N.B., K.B. are employees of SemaThera Inc. The rest of the authors declare no competing interests.

The paper explained:

Problem

Age-related macular degeneration (AMD) is a slowly progressing condition of the aging eye and the leading cause of central vision loss in industrialized countries. Advanced AMD is often classified into 'dry' atrophic AMD or 'wet' neovascular (NV) AMD. Wet AMD typically occurs when neovascularization from the choroid (choroidal neovascularization; CNV), sprouts into the subretinal space and neuro-retina, hemorrhages, leaks and ultimately provokes photoreceptor death, fibrovascular scarring and retinal detachment of the macular region. This can rapidly compromise the central visual field.

Results

In the current study, we show that several ligands of Neuropilin1 (a transmembrane receptor that binds several growth factors and guidance cues and potentiates their signaling) are induced in the vitreous of patients with active NV AMD. We observed that myeloid cells expressing NRP1 contribute to pathological angiogenesis in later stages of CNV in mice. Moreover, we demonstrate that while mononuclear phagocyte-resident NRP1 is not essential for recruitment of immune cells to sites of CNV, it is critical for mitigating myeloid cell inflammation and favors alternative activation. Using a NRP1-derived trap, we significantly reduced CNV.

Impact

Our study ultimately shows that therapeutic targeting of NRP1 ligands or NRP1-expressing myeloid cells hinders CNV.

REFERENCES

Acevedo LM, Barillas S, Weis SM, Gothert JR, Cheresh DA (2008) Semaphorin 3A suppresses VEGF-mediated angiogenesis yet acts as a vascular permeability factor. *Blood* 111: 2674-2680

Ambati J, Atkinson J, Gelfand B (2013) Immunology of age-related macular degeneration. *Nature Reviews Immunology* 13: 438-451

Ambati J, Fowler BJ (2012) Mechanisms of age-related macular degeneration. *Neuron* 75: 26-39

Antipenko A, Himanen JP, van Leyen K, Nardi-Dei V, Lesniak J, Barton WA, Rajashankar KR, Lu M, Hoemme C, Puschel AW *et al* (2003) Structure of the semaphorin-3A receptor binding module. *Neuron* 39: 589-598

Ball SG, Bayley C, Shuttleworth CA, Kielty CM (2010) Neuropilin-1 regulates platelet-derived growth factor receptor signalling in mesenchymal stem cells. *Biochem J* 427: 29-40

Battegay EJ, Rupp J, Iruela-Arispe L, Sage EH, Pech M (1994) PDGF-BB modulates endothelial proliferation and angiogenesis in vitro via PDGF beta-receptors. *J Cell Biol* 125: 917-928

Berber P, Grassmann F, Kiel C, Weber BH (2017) An Eye on Age-Related Macular Degeneration: The Role of MicroRNAs in Disease Pathology. *Mol Diagn Ther* 21: 31-43

Carrer A, Moimas S, Zacchigna S, Pattarini L, Zentilin L, Ruozi G, Mano M, Sinigaglia M, Maione F, Serini G *et al* (2012) Neuropilin-1 identifies a subset of bone marrow Gr1- monocytes that can induce tumor vessel normalization and inhibit tumor growth. *Cancer Res* 72: 6371-6381

Casazza A, Laoui D, Wenes M, Rizzolio S, Bassani N, Mambretti M, Deschoemaeker S, Van Ginderachter JA, Tamagnone L, Mazzone M (2013) Impeding Macrophage Entry into Hypoxic Tumor Areas by Sema3A/Nrp1 Signaling Blockade Inhibits Angiogenesis and Restores Antitumor Immunity. *Cancer Cell* 24: 695-709

Cerani A, Tetreault N, Menard C, Lapalme E, Patel C, Sitaras N, Beaudoin F, Leboeuf D, De Guire V, Binet F *et al* (2013) Neuron-derived semaphorin 3A is an early inducer of vascular permeability in diabetic retinopathy via neuropilin-1. *Cell Metab* 18: 505-518

Chaudhary B, Khaled YS, Ammori BJ, Elkord E (2014) Neuropilin 1: function and therapeutic potential in cancer. *Cancer Immunol Immunother* 63: 81-99

Chen XJ, Wu S, Yan RM, Fan LS, Yu L, Zhang YM, Wei WF, Zhou CF, Wu XG, Zhong M *et al* (2019) The role of the hypoxia-Nrp-1 axis in the activation of M2-like tumor-associated macrophages in the tumor microenvironment of cervical cancer. *Mol Carcinog* 58: 388-397

Comparison of Age-related Macular Degeneration Treatments Trials Research Group, Maguire MG, Martin DF, Ying GS, Jaffe GJ, Daniel E, Grunwald JE, Toth CA, Ferris FL, 3rd, Fine SL (2016) Five-Year Outcomes with Anti-Vascular Endothelial Growth Factor Treatment of Neovascular Age-Related Macular Degeneration: The Comparison of Age-Related Macular Degeneration Treatments Trials. *Ophthalmology* 123: 1751-1761

Crespo-Garcia S, Corkhill C, Roubeix C, Davids AM, Kociok N, Strauss O, Joussen AM, Reichhart N (2017) Inhibition of Placenta Growth Factor Reduces Subretinal Mononuclear Phagocyte Accumulation in Choroidal Neovascularization. *Invest Ophthalmol Vis Sci* 58: 4997-5006

Dai X, Okon I, Liu Z, Wu Y, Zhu H, Song P, Zou MH (2017) A novel role for myeloid cell-specific neuropilin 1 in mitigating sepsis. *FASEB J* 31: 2881-2892

Dejda A, Mawambo G, Cerani A, Miloudi K, Shao Z, Daudelin JF, Boulet S, Oubaha M, Beaudoin F, Akla N *et al* (2014) Neuropilin-1 mediates myeloid cell chemoattraction and influences retinal neuroimmune crosstalk. *J Clin Invest* 124: 4807-4822

Dejda A, Mawambo G, Daudelin JF, Miloudi K, Akla N, Patel C, Andriessen EM, Labrecque N, Sennlaub F, Sapieha P (2016) Neuropilin-1-Expressing Microglia Are Associated With Nascent Retinal Vasculature Yet Dispensable for Developmental Angiogenesis. *Invest Ophthalmol Vis Sci* 57: 1530-1536

Ellis LM (2006) The role of neuropilins in cancer. *Mol Cancer Ther* 5: 1099-1107

Fantin A, Vieira JM, Plein A, Denti L, Fruttiger M, Pollard JW, Ruhrberg C (2013) NRP1 acts cell autonomously in endothelium to promote tip cell function during sprouting angiogenesis. *Blood* 121: 2352-2362

Fernandez-Robredo P, Selvam S, Powner MB, Sim DA, Fruttiger M (2017) Neuropilin 1 Involvement in Choroidal and Retinal Neovascularisation. *PLoS One* 12: e0169865

Fleetwood AJ, Lawrence T, Hamilton JA, Cook AD (2007) Granulocyte-macrophage colony-stimulating factor (CSF) and macrophage CSF-dependent macrophage phenotypes display differences in cytokine profiles and transcription factor activities: implications for CSF blockade in inflammation. *Journal of immunology (Baltimore, Md : 1950)* 178: 5245-5252

Friedman DS, O'Colmain BJ, Munoz B, Tomany SC, McCarty C, de Jong PT, Nemesure B, Mitchell P, Kempen J, Eye Diseases Prevalence Research G (2004) Prevalence of age-related macular degeneration in the United States. *Arch Ophthalmol* 122: 564-572

Funasaka T, Raz A, Nangia-Makker P (2014) Galectin-3 in angiogenesis and metastasis. *Glycobiology* 24: 886-891

García-Quintanilla L, Luaces-Rodríguez A, Gil-Martínez M, Mondelo-García C, Maroñas O, Mangas-Sanjuan V, González-Barcia M, Zarra-Ferro I, Aguiar P, Otero-Espinar FJ *et al* (2019) Pharmacokinetics of Intravitreal Anti-VEGF Drugs in Age-Related Macular Degeneration. *Pharmaceutics* 11

Geretti E, Shimizu A, Klagsbrun M (2008) Neuropilin structure governs VEGF and semaphorin binding and regulates angiogenesis. *Angiogenesis* 11: 31-39

Glinka Y, Stoilova S, Mohammed N, Prud'homme GJ (2011) Neuropilin-1 exerts co-receptor function for TGF-beta-1 on the membrane of cancer cells and enhances responses to both latent and active TGF-beta. *Carcinogenesis* 32: 613-621

Guillonneau X, Eandi CM, Paques M, Sahel JA, Sapieha P, Sennlaub F (2017) On phagocytes and macular degeneration. *Prog Retin Eye Res* 61: 98-128

Handa JT, Cano M, Wang L, Datta S, Liu T (2017) Lipids, oxidized lipids, oxidation-specific epitopes, and Age-related Macular Degeneration. *Biochim Biophys Acta* 1862: 430-440

Hoeben A, Landuyt B, Highley MS, Wildiers H, Van Oosterom AT, De Bruijn EA (2004) Vascular endothelial growth factor and angiogenesis. *Pharmacol Rev* 56: 549-580

Jonas JB, Bourne RR, White RA, Flaxman SR, Keeffe J, Leasher J, Naidoo K, Pesudovs K, Price H, Wong TY *et al* (2014) Visual impairment and blindness due to macular diseases globally: a systematic review and meta-analysis. *Am J Ophthalmol* 158: 808-815

Joyal J-S, Sitaras N, Binet F, Rivera JC, Stahl A, Zaniolo K, Shao Z, Polosa A, Zhu T, Hamel D *et al* (2011) Ischemic neurons prevent vascular regeneration of neural tissue by secreting semaphorin 3A. *Blood* 117: 6024-6035

Jubb AM, Strickland LA, Liu SD, Mak J, Schmidt M, Koeppen H (2012) Neuropilin-1 expression in cancer and development. *J Pathol* 226: 50-60

Krebs I, Glittenberg C, Ansari-Shahrezaei S, Hagen S, Steiner I, Binder S (2013) Non-responders to treatment with antagonists of vascular endothelial growth factor in age-related macular degeneration. *Br J Ophthalmol* 97: 1443-1446

Kurihara T, Westenskow PD, Bravo S, Aguilar E, Friedlander M (2012) Targeted deletion of Vegfa in adult mice induces vision loss. *J Clin Invest* 122: 4213-4217

Lacey DC, Achuthan A, Fleetwood AJ, Dinh H, Roiniotis J, Scholz GM, Chang MW, Beckman SK, Cook AD, Hamilton JA (2012) Defining GM-CSF- and macrophage-CSF-dependent macrophage responses by in vitro models. *Journal of immunology (Baltimore, Md : 1950)* 188: 5752-5765

Lambert V, Lecomte J, Hansen S, Blacher S, Gonzalez M-L, Struman I, Sounni N, Rozet E, de Tullio P, Foidart J *et al* (2013) Laser-induced choroidal neovascularization model to study age-related macular degeneration in mice. *Nature Protocols* 8: 2197-2211

Langmann T (2007) Microglia activation in retinal degeneration. *J Leukoc Biol* 81: 1345-1351

Lazzeri S, Figus M, Orlandi P, Fioravanti A, Di Desidero T, Agosta E, Sartini MS, Posarelli C, Nardi M, Danesi R *et al* (2013) VEGF-A polymorphisms predict short-term functional response to intravitreal ranibizumab in exudative age-related macular degeneration. *Pharmacogenomics* 14: 623-630

Lepelletier Y, Smaniotto S, Hadj-Slimane R, Villa-Verde DM, Nogueira AC, Dardenne M, Hermine O, Savino W (2007) Control of human thymocyte migration by Neuropilin-1/Semaphorin-3A-mediated interactions. *Proc Natl Acad Sci U S A* 104: 5545-5550

Lim LS, Mitchell P, Seddon JM, Holz FG, Wong TY (2012) Age-related macular degeneration. *Lancet* 379: 1728-1738

Lores-Motta L, Riaz M, Grunin M, Corominas J, van Asten F, Pauper M, Leenders M, Richardson AJ, Muether P, Cree AJ *et al* (2018) Association of Genetic Variants With Response to Anti-Vascular Endothelial Growth Factor Therapy in Age-Related Macular Degeneration. *JAMA Ophthalmol* 136: 875-884

Lores-Motta L, van Asten F, Muether PS, Smailhodzic D, Groenewoud JM, Omar A, Chen J, Koenekoop RK, Fauser S, Hoyng CB *et al* (2016) A genetic variant in NRP1 is associated with worse response to ranibizumab treatment in neovascular age-related macular degeneration. *Pharmacogenet Genomics* 26: 20-27

Mamluk R, Gechtman Z, Kutcher ME, Gasiunas N, Gallagher J, Klagsbrun M (2002) Neuropilin-1 binds vascular endothelial growth factor 165, placenta growth factor-2, and heparin via its b1b2 domain. *J Biol Chem* 277: 24818-24825

Massague J, Blain SW, Lo RS (2000) TGFbeta signaling in growth control, cancer, and heritable disorders. *Cell* 103: 295-309

Mimura T, Funatsu H, Noma H, Shimura M, Kamei Y, Yoshida M, Kondo A, Watanabe E, Mizota A (2019) Aqueous Humor Levels of Cytokines in Patients with Age-Related Macular Degeneration. *Ophthalmologica* 241: 81-89

Miyauchi JT, Caponegro MD, Chen D, Choi MK, Li M, Tsirka SE (2018) Deletion of Neuropilin 1 from Microglia or Bone Marrow-Derived Macrophages Slows Glioma Progression. *Cancer Res* 78: 685-694

Muhl L, Folestad EB, Gladh H, Wang Y, Moessinger C, Jakobsson L, Eriksson U (2017) Neuropilin 1 binds PDGF-D and is a co-receptor in PDGF-D-PDGFRbeta signaling. *J Cell Sci* 130: 1365-1378

Nakamura F, Goshima Y (2002) Structural and functional relation of neuropilins. *Adv Exp Med Biol* 515: 55-69

Nakamura R, Sene A, Santeford A, Gdoura A, Kubota S, Zapata N, Apte RS (2015) IL10-driven STAT3 signalling in senescent macrophages promotes pathological eye angiogenesis. *Nat Commun* 6: 7847

Oussa NA, Dahmani A, Gomis M, Richaud M, Andreev E, Navab-Daneshmand AR, Taillefer J, Carli C, Boulet S, Sabbagh L *et al* (2016) VEGF Requires the Receptor NRP-1 To Inhibit Lipopolysaccharide-Dependent Dendritic Cell Maturation. *Journal of immunology (Baltimore, Md : 1950)* 197: 3927-3935

Prud'homme GJ, Glinka Y (2012) Neuropilins are multifunctional coreceptors involved in tumor initiation, growth, metastasis and immunity. *Oncotarget* 3: 921-939

Raimondi C, Brash JT, Fantin A, Ruhrberg C (2016) NRP1 function and targeting in neurovascular development and eye disease. *Prog Retin Eye Res* 52: 64-83

Rashid K, Akhtar-Schaefer I, Langmann T (2019) Microglia in Retinal Degeneration. *Front Immunol* 10: 1975

Rein D, Zhang P, Wirth K, Lee P, Hoerger T, McCall N, Klein R, Tielsch J, Vijan S, Saaddine J (2006) The economic burden of major adult visual disorders in the United States. *Archives of ophthalmology* 124: 1754-1760

Renand A, Milpied P, Rossignol J, Bruneau J, Lemonnier F, Dussiot M, Coulon S, Hermine O (2013) Neuropilin-1 expression characterizes T follicular helper (Tfh) cells activated during B cell differentiation in human secondary lymphoid organs. *PLoS One* 8: e85589

Rizzolio S, Tamagnone L (2011) Multifaceted role of neuropilins in cancer. *Curr Med Chem* 18: 3563-3575

Rizzolio S TL (2017) Neuropilins as signaling hubs, controlling tyrosine kinases and other cell surface receptors. In: *The neuropilins: role and function in health and disease*, Neufeld G. (ed.) pp. 23-39. Springer International Publishing: New York

Robinson GS, Ju M, Shih SC, Xu X, McMahon G, Caldwell RB, Smith LE (2001) Nonvascular role for VEGF: VEGFR-1, 2 activity is critical for neural retinal development. *FASEB J* 15: 1215-1217

Roy S, Bag AK, Singh RK, Talmadge JE, Batra SK, Datta K (2017) Multifaceted Role of Neuropilins in the Immune System: Potential Targets for Immunotherapy. *Front Immunol* 8: 1228

Saint-Geniez M, Maharaj AS, Walshe TE, Tucker BA, Sekiyama E, Kurihara T, Darland DC, Young MJ, D'Amore PA (2008) Endogenous VEGF is required for visual function: evidence for a survival role on müller cells and photoreceptors. *PLoS One* 3: e3554

Sennlaub F, Auvynet C, Calippe B, Lavalette S, Poupel L, Hu SJ, Dominguez E, Camelo S, Levy O, Guyon E *et al* (2013) CCR2(+) monocytes infiltrate atrophic lesions in age-related macular disease and mediate photoreceptor degeneration in experimental subretinal inflammation in Cx3cr1 deficient mice. *EMBO molecular medicine* 5: 1775-1793

Sodhi A, Ma T, Menon D, Deshpande M, Jee K, Dinabandhu A, Vancel J, Lu D, Montaner S (2019) Angiopoietin-like 4 binds neuropilins and cooperates with VEGF to induce diabetic macular edema. *J Clin Invest*

Soker S, Miao HQ, Nomi M, Takashima S, Klagsbrun M (2002) VEGF165 mediates formation of complexes containing VEGFR-2 and neuropilin-1 that enhance VEGF165-receptor binding. *J Cell Biochem* 85: 357-368

Soker S, Takashima S, Miao HQ, Neufeld G, Klagsbrun M (1998) Neuropilin-1 is expressed by endothelial and tumor cells as an isoform-specific receptor for vascular endothelial growth factor. *Cell* 92: 735-745

Takahashi T, Fournier A, Nakamura F, Wang LH, Murakami Y, Kalb RG, Fujisawa H, Strittmatter SM (1999) Plexin-neuropilin-1 complexes form functional semaphorin-3A receptors. *Cell* 99: 59-69

Takamatsu H, Kumanogoh A (2012) Diverse roles for semaphorin-plexin signaling in the immune system. *Trends Immunol* 33: 127-135

Taylor DJ, Hobby AE, Binns AM, Crabb DP (2016) How does age-related macular degeneration affect real-world visual ability and quality of life? A systematic review. *BMJ Open* 6: e011504

Wilson AM, Shao Z, Grenier V, Mawambo G, Daudelin JF, Dejda A, Pilon F, Popovic N, Boulet S, Parinot C *et al* (2018) Neuropilin-1 expression in adipose tissue macrophages protects against obesity and metabolic syndrome. *Sci Immunol* 3

Wong WL, Su X, Li X, Cheung CM, Klein R, Cheng CY, Wong TY (2014) Global prevalence of age-related macular degeneration and disease burden projection for 2020 and 2040: a systematic review and meta-analysis. *Lancet Glob Health* 2: e106-116

Yu C, Roubeix C, Sennlaub F, Saban DR (2020) Microglia versus Monocytes: Distinct Roles in Degenerative Diseases of the Retina. *Trends Neurosci* 43: 433-449

Zandi S, Nakao S, Chun KH, Fiorina P, Sun D, Arita R, Zhao M, Kim E, Schueller O, Campbell S *et al* (2015) ROCK-isoform-specific polarization of macrophages associated with age-related macular degeneration. *Cell reports* 10: 1173-1186

Figures and legends

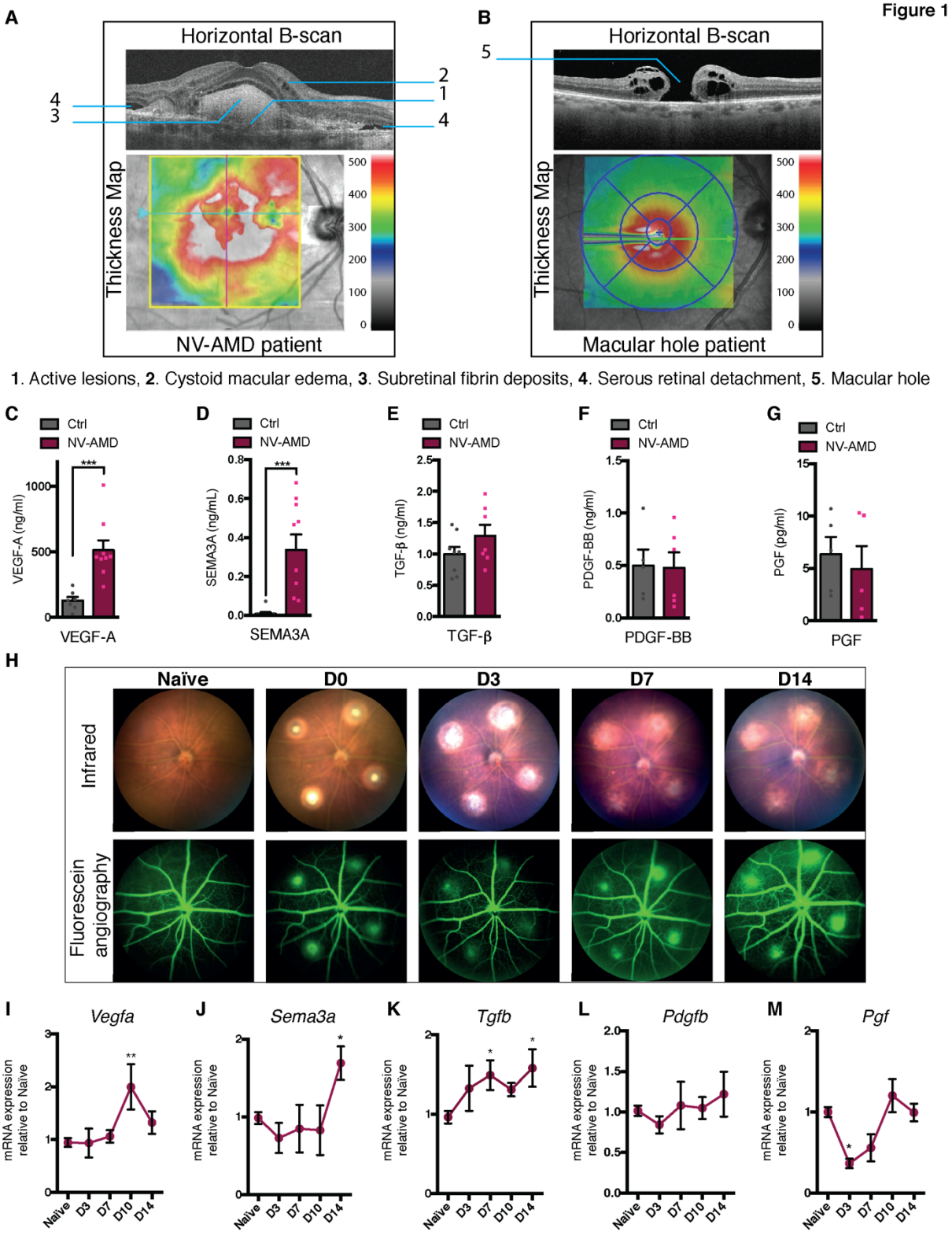

Figure 21 Publication#2 Figure 1. NRP1 ligands are elevated in patients with NV AMD and in a mouse model of CNV.

Figure 1. NRP1 ligands are elevated in patients with NV AMD and in a mouse model of CNV.

A. Optical coherence tomography (OCT) horizontal B-scan and thickness map of neovascular age related macular degeneration (NV AMD) patient with active lesions (1), cystoid macular edema (2), subretinal fibrin deposits (3) and serous retinal detachment (4).

B. Optical coherence tomography (OCT) horizontal B-scan and thickness map of control patient with a medium sized, stage 3, full thickness macular hole (5).

C-G. Vitreous humor analyzed by ELISA for VEGF-A (**C**); n = 7 (Ctrl), 9 (NV AMD), SEMA3A (**D**); n = 10 (Ctrl), 10 (NV AMD), TGFβ (**E**); n = 8 (Ctrl), 7 (NV AMD), PDGF-BB (**F**); n = 5 (Ctrl),6 (NV AMD), PGF (**G**): n = 5 (Ctrl), 5 (NV AMD). Dots represent concentrations of individual patient samples.

H. Micron IV infrared and fluorescein in vivo imaging of naïve mouse fundus and following laser-induced CNV at D0, D3, D7, D14.

I-M. Time course of mRNA expression of NRP1 ligands in mouse RPE-choroid-sclera complexes relative to naïve (no burn), 3 (D3), 7 (D7), 10 (D10), and 14 (D14) days after burn for *Vegfa* (**I**); n = 11 (No burn), 6 (D3) , 7 (D7) , 4 (D10 and D14), *Sema3a* (**J**); n = 17 (No burn), 6 (D3) , 4 (D7) , 3 (D10 and D14), *Tgfb1* (**K**); n = 14 (No burn), 3 (D3) , 7 (D7) , 3 (D10), 6 (D14), *Pdgfb* (**L**); n = 9 (No burn), 5 (D3 and D7), 4 (D10 and D14), *Pgf* (**M**); n = 6 (No burn), 4 (D3) , 3 (D7) , 6 (D10), 3 (D14).

Data information: All comparisons between groups were analyzed using a Student's unpaired t-test (C-G) or a one-way analysis of variance (ANOVA) and Dunnett's multiple comparisons test (I-M); *P < 0.05, **P < 0.01, ***P < 0.001; error bars represent mean ± SEM; exact P values listed in table 2.

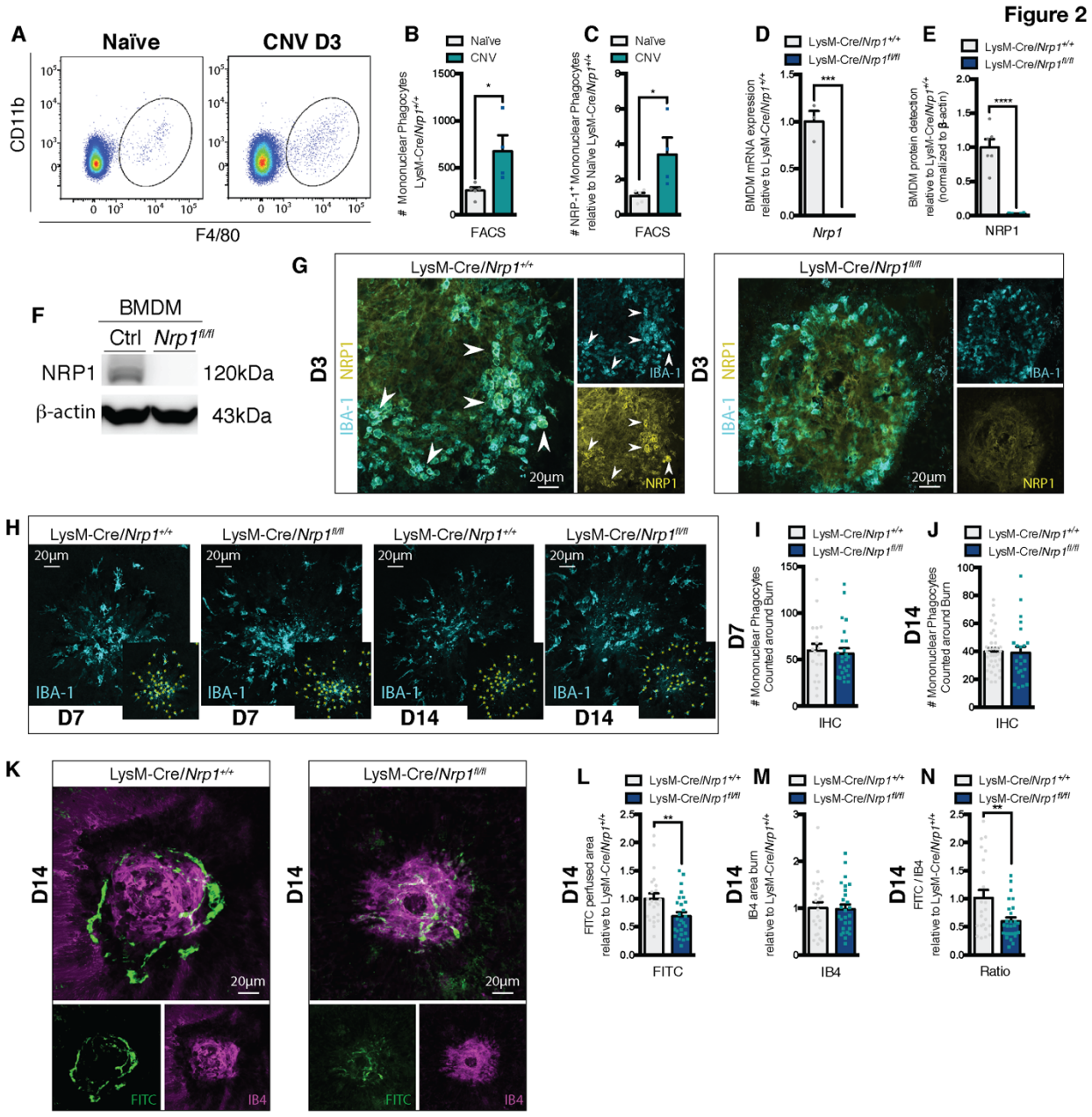

Figure 22 Publication#2 Figure 2. NRP1-expressing mononuclear phagocytes increase in the retina upon injury and promote CNV.

Figure 2. NRP1-expressing mononuclear phagocytes increase in the retina upon injury and promote CNV

A. Representative FACS plots of retinas and sclera-choroid-RPE cell complexes from naïve and burned mice 3 days (D3) after laser-burn.

B. Quantification of mononuclear phagocytes ($Ly6G^-$, $F4/80^+$, $CD11b^+$) in retinas and sclera-choroid-RPE cell complexes at D3 relative to Naïve; n = 5 (Naïve), 4 (CNV).

C. Quantification of $NRP1^+$ mononuclear phagocytes ($Ly6G^-$, $F4/80^+$, $CD11b^+$, $NRP1^+$) in retinas and sclera-choroid-RPE cell complexes at D3 relative to Naïve; n = 5 (Naïve), 4 (CNV).

D. mRNA expression of *Nrp1* in BMDM relative to LysM-Cre/$Nrp1^{+/+}$; n = 3 (LysM-Cre/$Nrp1^{+/+}$), n = 4 (LysM-Cre/$Nrp1^{fl/fl}$).

E. Quantification of NRP1 protein expression in LysM-Cre/$Nrp1^{+/+}$ and LysM-Cre/$Nrp1^{fl/fl}$ BMDM; n= 6.

F. Representative Western Blot showing NRP1 expression in LysM-Cre/$Nrp1^{+/+}$ (Ctrl) and LysM-Cre/$Nrp1^{fl/fl}$ ($Nrp1^{fl/fl}$).

G. Representative confocal images of NRP1 and IBA1-stained mononuclear phagocytes on choroidal flat mounts from LysM-Cre/$Nrp1^{+/+}$ and LysM-Cre/$Nrp1^{fl/fl}$ mice at D3. Arrow heads indicate NRP1-positive mononuclear phagocytes. Scale bar: 20μm.

H. Representative confocal images of IBA-1-stained mononuclear phagocytes on choroidal flat mounts from LysM-Cre/$Nrp1^{+/+}$ and LysM-Cre/$Nrp1^{fl/fl}$ mice at D7 and D14. Examples of macrophage quantification (yellow stars) are presented in side panels. Scale bar: 20μm.

I, J. Total number of IBA-1-positive mononuclear phagocytes counted around laser impact area on confocal images of choroidal flat mounts at D7 (**I**) and D14 (**J**); n = 19 burns (D7 LysM-Cre/$Nrp1^{+/+}$), n = 25 burns (D7 LysM-Cre/$Nrp1^{fl/fl}$) n = 37 burns (D7 LysM-Cre/$Nrp1^{+/+}$), n = 23 burns (D7 LysM-Cre/$Nrp1^{fl/fl}$), 3-5 mice with ~4 burns per eye.

K. Compilation of representative compressed Z-stack confocal images of FITC–dextran-labeled CNV and IB4-stained laser impact area from LysM-Cre/$Nrp1^{+/+}$ and LysM-Cre/$Nrp1^{fl/fl}$ mice at D14. Scale bar: 20μm.

L-N. Quantification of area of FITC–dextran-labeled CNV (**L**), isolectin B4 (IB4)-stained laser impact area (**M**) and the ratio of FITC/IB4 per laser-burn (**N**) relative to LysM-Cre/*Nrp1*$^{+/+}$ at D14; n = 23 burns (LysM-Cre/*Nrp1*$^{+/+}$), n = 27 burns (LysM-Cre/*Nrp1*$^{fl/fl}$).

Data information: All comparisons between groups were analyzed using a Student's unpaired t-test; *P < 0.05, **P < 0.01, ***P < 0.001, ****P< 0.0001; error bars represent mean ± SEM; exact P values listed in table 2.

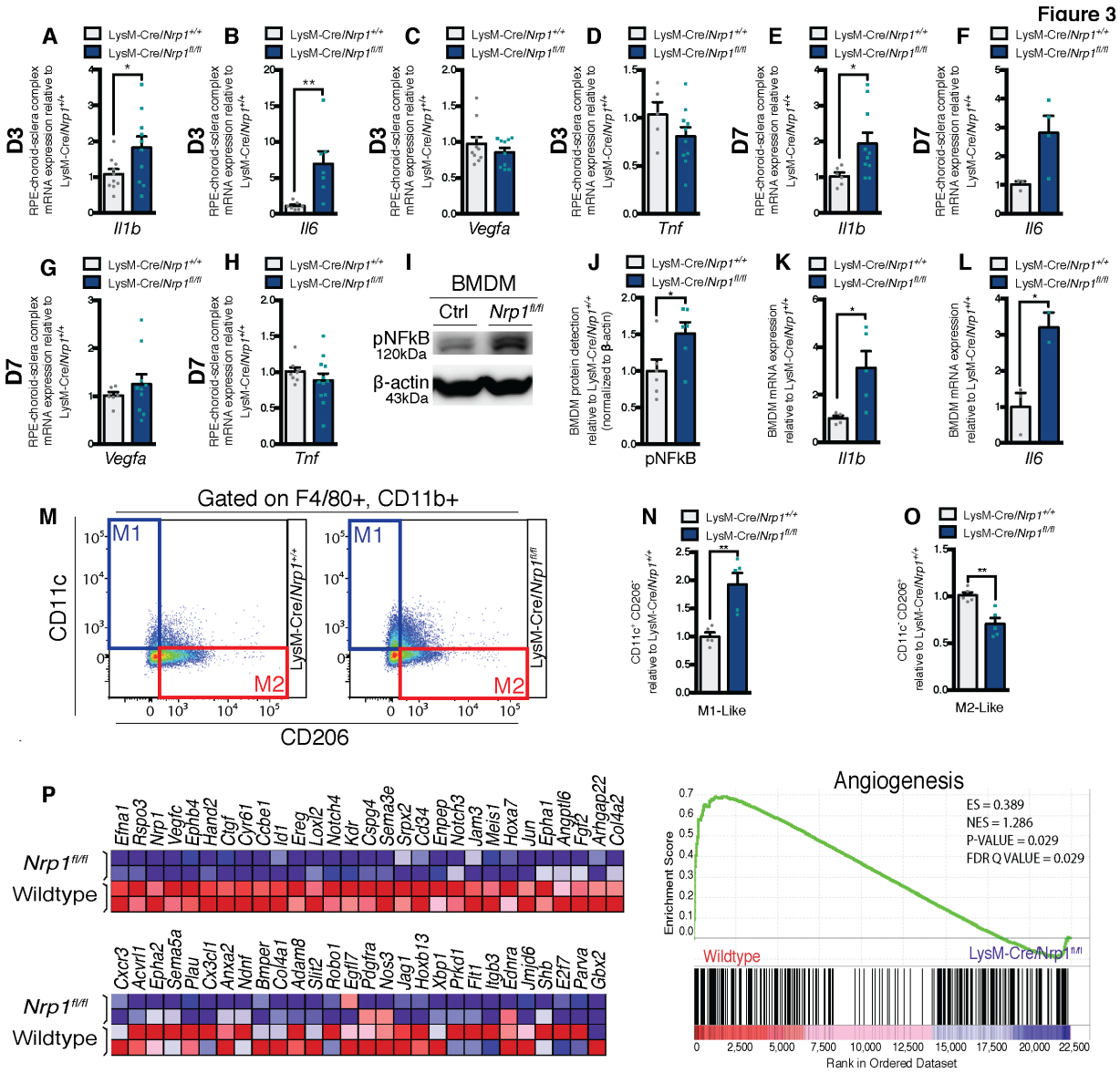

Figure 23 Publication#2 Figure 3. NRP1-expressing mononuclear phagocytes display a pro-angiogenic alternatively activated phenotype.

Figure 3. NRP1-expressing mononuclear phagocytes display a pro-angiogenic alternatively activated phenotype.

A-D. mRNA expression of inflammation markers relative to LysM-Cre/*Nrp1*$^{+/+}$ in mouse RPE-choroid-sclera complexes at D3 for *Il1b* (**A**); n = 10 (LysM-Cre/*Nrp1*$^{+/+}$ and LysM-Cre/*Nrp1*$^{fl/fl}$), *Il6* (**B**); n = 7 (LysM-Cre/*Nrp1*$^{+/+}$ and LysM-Cre/*Nrp1*$^{fl/fl}$), *Vegfa* (**C**); n = 10 (LysM-Cre/*Nrp1*$^{+/+}$ and LysM-Cre/*Nrp1*$^{fl/fl}$), *Tnf* (**D**); n = 5 (LysM-Cre/*Nrp1*$^{+/+}$), n = 10 (LysM-Cre/*Nrp1*$^{fl/fl}$).

E-H. mRNA expression of inflammation markers relative to LysM-Cre/*Nrp1*$^{+/+}$ in mouse RPE-choroid-sclera complexes at D7 for *Il1b* (**E**); n = 6 (LysM-Cre/*Nrp1*$^{+/+}$), n = 10 (LysM-Cre/*Nrp1*$^{fl/fl}$), *Il6* (**F**); n = 3 (LysM-Cre/*Nrp1*$^{+/+}$), n = 4 (LysM-Cre/*Nrp1*$^{fl/fl}$), *Vegfa* (**G**); n = 6 (LysM-Cre/*Nrp1*$^{+/+}$), n = 10 (LysM-Cre/*Nrp1*$^{fl/fl}$), *Tnf* (**H**); n = 8 (LysM-Cre/*Nrp1*$^{+/+}$), n = 12 (LysM-Cre/*Nrp1*$^{fl/fl}$).

I. Representative Western Blot showing pNF-κB expression in LysM-Cre/*Nrp1*$^{+/+}$ (Ctrl) and LysM-Cre/*Nrp1*$^{fl/fl}$ (Nrp1$^{fl/fl}$).

J. Quantification of pNF-κB expression in LysM-Cre/*Nrp1*$^{+/+}$ and LysM-Cre/*Nrp1*$^{fl/fl}$ BMDM; n= 6.

K, L. mRNA expression relative to LysM-Cre/*Nrp1*$^{+/+}$ of inflammation markers in mouse BMDMs for *Il1b* (**K**); n = 4 (LysM-Cre/*Nrp1*$^{+/+}$), n = 5 (LysM-Cre/*Nrp1*$^{fl/fl}$) *and Il6* (**L**); n = 3 (LysM-Cre/*Nrp1*$^{+/+}$), n = 2 (LysM-Cre/*Nrp1*$^{fl/fl}$)

M. Representative FACS plots of M1 and M2-Like macrophages in LysM-Cre/*Nrp1*$^{+/+}$ and LysM-Cre/*Nrp1*$^{fl/fl}$ BMDMs.

N, O. Quantification of M1-Like macrophages (F4/80^{+}, CD11b^{+}, CD11c^{+}, CD206^{-})(**N**), M2-Like macrophages (F4/80^{+}, CD11b^{+}, CD11c^{-}, CD206^{+}) (**O**) in LysM-Cre/*Nrp1*$^{+/+}$ and LysM-Cre/*Nrp1*$^{fl/fl}$ BMDMs relative to LysM-Cre/*Nrp1*$^{+/+}$; n= 5.

P. Heatmap (left) and enrichment plot (right) of GO Angiogenesis gene set enrichment analysis (GSEA) of wildtype and LysM-Cre/*Nrp1*$^{fl/fl}$ peritoneal macrophages; n = 2. NES, normalized enrichment score; FDR, false discovery rate.

Data information: All comparisons between groups were analyzed using a Student's unpaired t-test; *P < 0.05, **P < 0.01; error bars represent mean ± SEM; exact P values listed in table 2.

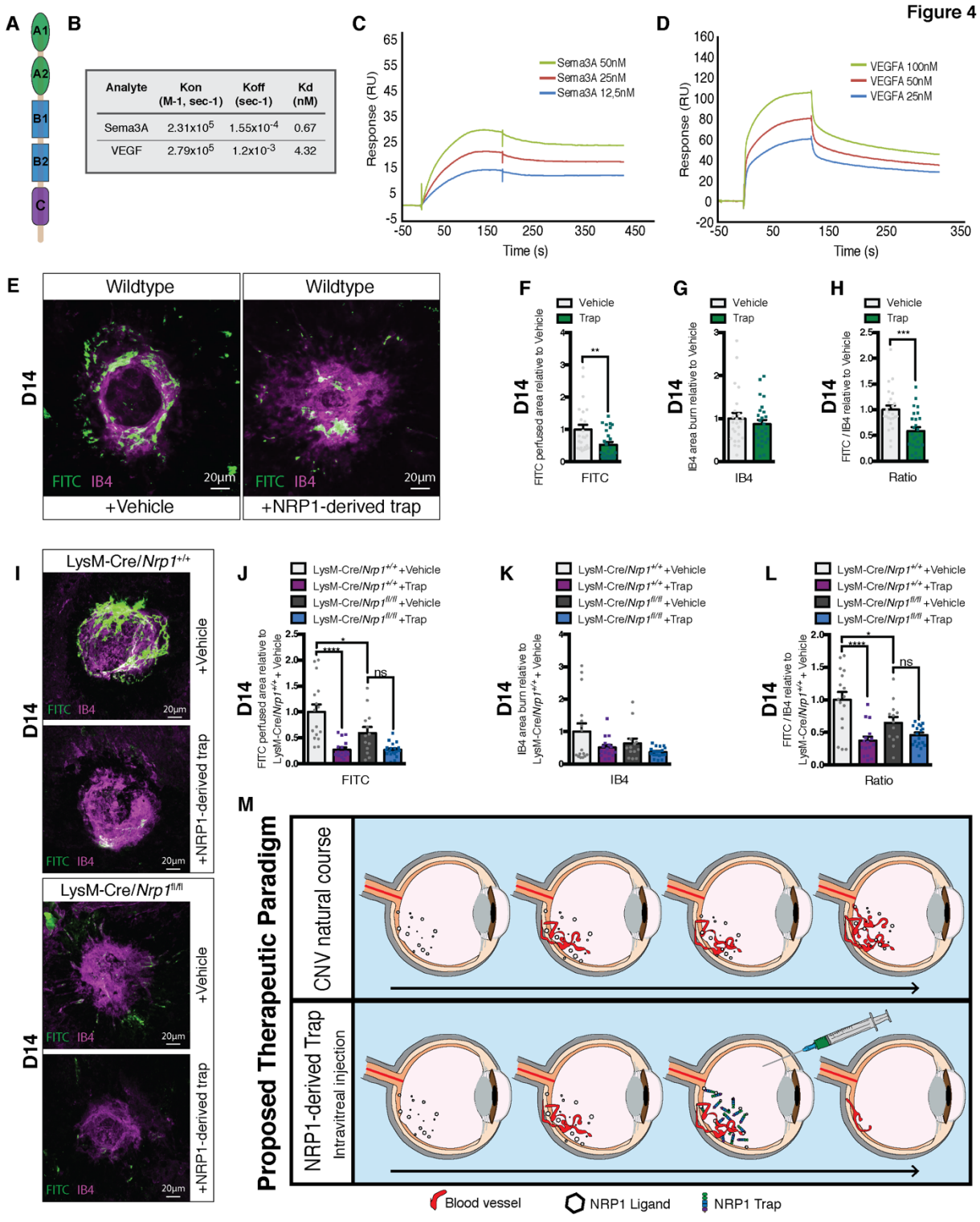

Figure 24 Publication#2 Figure 4. Therapeutic intravitreal administration of soluble NRP1 reduces CNV in mice.

Figure 4. Therapeutic intravitreal administration of soluble NRP1 reduces CNV in mice

A. Schematic representation of a soluble receptor Neuropilin-1, consisting of five domains; two CUB motifs (A1, A2), two coagulation factor domains (B1, B2) and the MAM domain (C).

B. Rate constant and binding affinities of Sema3A and VEGF to immobilized trap obtained using a one-site Langmuir binding model.

C, D. Representative SPR sensorgrams for various concentrations of Sema3A (**C**) and VEGF (**D**) binding to immobilized Trap.

E. Compilation of representative compressed Z-stack confocal images of FITC–dextran-labeled CNV and isolectin B4 (IB4)-stained laser impact area from Vehicle and NRP1-derived trap treated wildtype mice. Scale bar: 20μm.

F-H. Quantification of area of FITC–dextran-labeled CNV (**F**), IB4-stained laser impact area (**G**) and the ratio of FITC/IB4 per laser-burn (**H**) relative to Vehicle at D14; n = 24 burns (Vehicle), n = 26 burns (NRP1-derived trap).

I. Compilation of representative compressed Z-stack confocal images of FITC–dextran-labeled CNV and IB4-stained laser impact area from Vehicle and NRP1-derived trap treated LysM-Cre/$Nrp1^{+/+}$ and LysM-Cre/$Nrp1^{fl/fl}$ mice at D14. Scale bar: 20μm.

J-L. Quantification of area of FITC–dextran-labeled CNV (**J**), isolectin B4 (IB4)-stained laser impact area (**K**) and the ratio of FITC/IB4 per laser-burn (**L**) relative to LysM-Cre/$Nrp1^{+/+}$ + Vehicle in Vehicle and NRP1-derived trap treated LysM-Cre/$Nrp1^{+/+}$ and LysM-Cre/$Nrp1^{fl/fl}$ mice at D14; n = 16 burns (LysM-Cre/$Nrp1^{+/+}$ + Vehicle), n = 16 burns (LysM-Cre/$Nrp1^{+/+}$ + Trap), n = 13 burns (LysM-Cre/$Nrp1^{fl/fl}$ + Vehicle) , n = 19 burns (LysM-Cre/$Nrp1^{fl/fl}$ + Trap).

M. Proposed therapeutic paradigm. From a therapeutic perspective, intravitreal injection of NRP1-derived traps reduces pathological angiogenesis associated with CNV.

Data information: Comparisons between groups were analyzed using a Student's unpaired t-test; (E-G) or one-way ANOVA with Tukey's multiple comparisons test (I-K); *P < 0.05, **P < 0.01, ***P < 0.001, ****P< 0.0001; error bars represent mean ± SEM; exact P values listed in table 2.

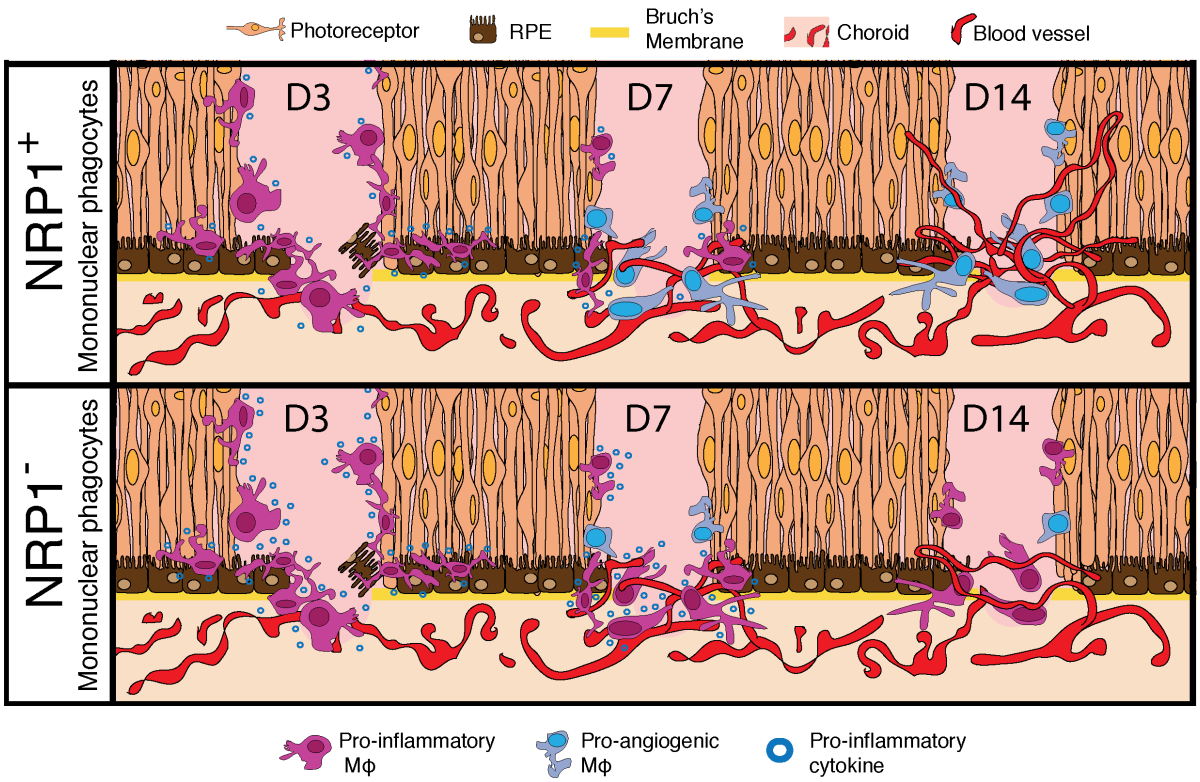

Figure 25 Publication#2 Graphical abstract. Myeloid-resident Neuropilin-1 promotes choroidal neovascularization while mitigating inflammation.

The number of mononuclear phagocytes present in RPE-choroid-sclera complexes of either LysM-Cre/Nrp1$^{fl/fl}$ (NRP1-) or control LysM-Cre/Nrp1$^{+/+}$ (NRP1+) mice after laser-burn follows similar trends. However, the NRP1-mononuclear phagocytes show a more pro-inflammatory character with an increased transcription of pro-inflammatory cytokines. Whereas over time the NRP1+ mononuclear phagocytes adopt a more pro-angiogenic role and promote choroidal neovascularization (CNV), the NRP1- mononuclear phagocytes remain less proangiogenic and more pro-inflammatory. This leads to a significant decrease in CNV formation in LysM-Cre/Nrp1$^{fl/fl}$ mice at D14 compared to controls. While levels of mononuclear phagocytes are similar between LysM-Cre/Nrp1$^{+/+}$ and LysM-Cre/Nrp1$^{fl/fl}$ during CNV, NRP1-expressing mononuclear phagocytes promote and maintain neovascularization in the later stages of CNV.

Tables

Pathology	ELISA	Age
Control Patients		
MH	VEGF, S3A, TGF, PDGF	-
ERM	VEGF, S3A, TGF, PDGF	72
MH	VEGF, S3A, TGF, PGF	82
ERM	VEGF, S3A, TGF	57
ERM	VEGF, S3A, TGF	93
ERM	VEGF, S3A	76
ERM	VEGF, PGF	82
MH	S3A, TGF, PDGF	66
ERM	TGF, PDGF	54
MH	TGF, PDGF	65
MH	S3A	71
ERM	S3A	71
ERM	S3A, PGF	64
ERM	PGF	81
ERM	PGF	80
Age Mean ± SEM: VEGF: 77 ± 4.9; S3A: 72 ± 3.5; TGF: 69 ± 5.2; PDGF: 64 ± 3.7; PGF:78±3.5		
NV AMD Patients		
NV AMD	VEGF, S3A, TGF, PDGF	96
NV AMD	VEGF, S3A, TGF, PDGF	79
NV AMD	VEGF, S3A, TGF, PDGF	86
NV AMD	VEGF, S3A, TGF, PDGF	75
NV AMD	VEGF, S3A, TGF, PDGF	76
NV AMD	VEGF, TGF, PDGF	80
NV AMD	VEGF, S3A	84
NV AMD	VEGF	80
NV AMD	VEGF	74
NV AMD	S3A, TGF, PDGF, PGF	79
NV AMD	S3A, PGF	91
NV AMD	S3A	84
NV AMD	S3A, PGF	80
NV AMD	PGF	71
NV AMD	PGF	85
Age Mean ± SEM: VEGF: 81 ± 2.3; S3A: 83 ± 2.1; TGF: 82 ± 2.7; PDGF: 82 ± 2.7; PGF:81±3.3		

MH: Macular hole **ERM:** Epiretinal membrane **NV AMD:** Neovascular AMD

Table 1 Table of patients ELISA Publication#2 Figure 1

Graph	Data	P-value	Test used	Summary
Figure 1				
C	ELISA	0.0007	T-test	***
D	ELISA	0.0007	T-test	***
I	qPCR	0.0034	ANOVA + Dunnett's	**
J	qPCR	0.0361	ANOVA + Dunnett's	*
K	qPCR	0.0338, 0.0167	ANOVA + Dunnett's	*,*
M	qPCR	0.0189	ANOVA + Dunnett's	*
Figure 2				
B	FACS	0.0303	T-test	*
C	FACS	0.0301	T-test	*
D	qPCR	0.0001	T-test	***
E	WB	< 0.0001	T-test	****
L	CNV	0.0089	T-test	**
N	CNV	0.0069	T-test	**
Figure 3				
A	qPCR	0.0463	T-test	*
B	qPCR	0.0063	T-test	**
E	qPCR	0.0409	T-test	*
J	WB	0.0416	T-test	*
K	qPCR	0.0335	T-test	*
L	qPCR	0.0332	T-test	*
N	FACS	0.0028	T-test	**
O	FACS	0.0025	T-test	**
Figure 4				
F	CNV	0.0074	T-test	**
H	CNV	0.0005	T-test	***
J	CNV	< 0.0001, 0.0197	ANOVA + Tukey's	****,*
L	CNV	< 0.0001, 0.0238	ANOVA + Tukey's	****,*
Expanded View Figure 1				
D	FACS	0.0002	T-test	***
E	FACS	0.0075	T-test	**
Expanded View Figure 3				
A	qPCR	0.041	T-test	*

T-test = Student's unpaired t-test, ANOVA + Dunnett's = Ordinary one-way ANOVA with Dunnett's multiple comparisons test, ANOVA + Tukey's = Ordinary one-way ANOVA with Tukey's multiple comparisons test

Table 2 Table of P-values Publication#2

Expanded View Figures and Legends

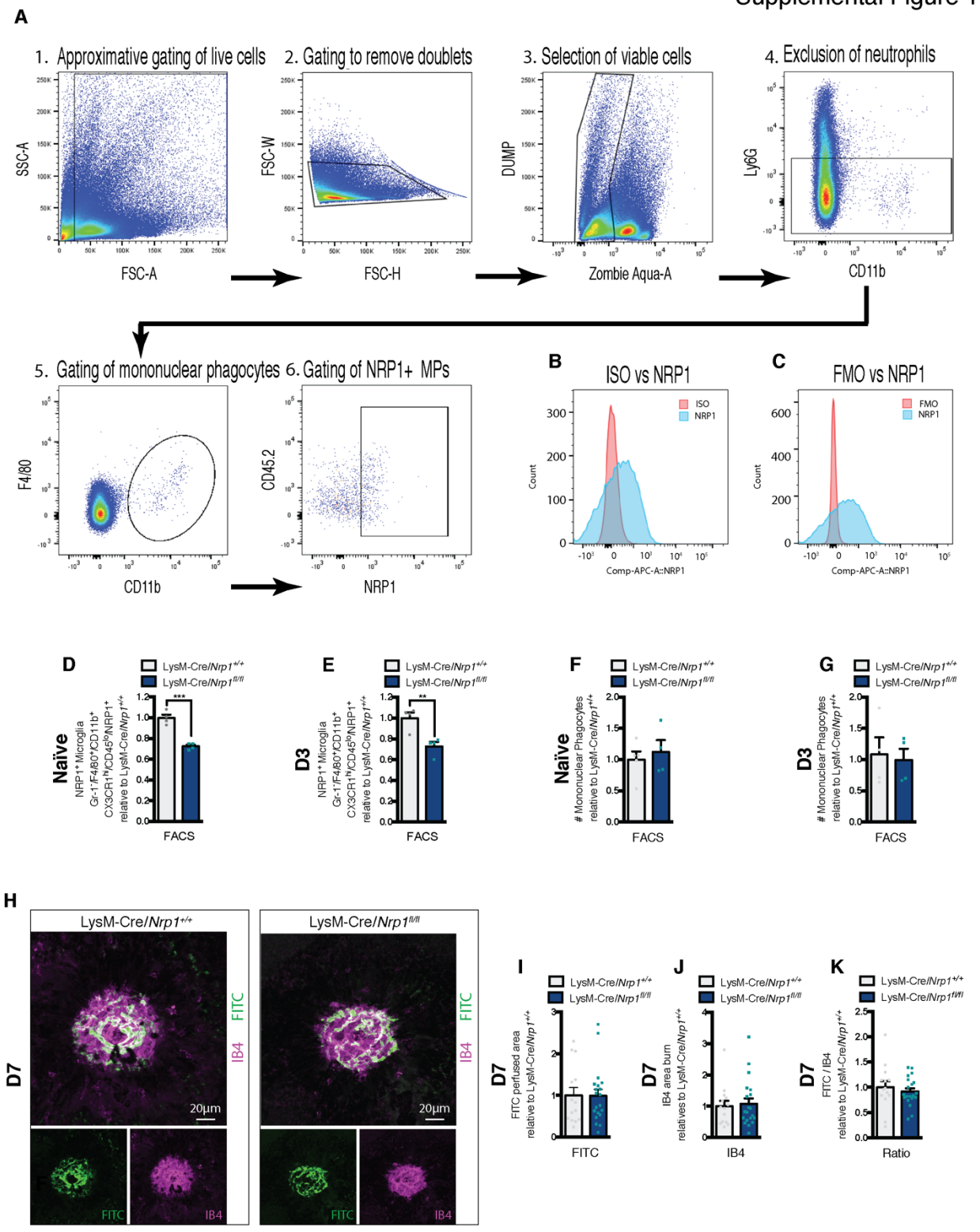

Figure 26 Publication#2 Figure EV1 Mononuclear phagocyte-resident NRP1 expression in LysM-Cre/Nrp1$^{fl/fl}$

Expanded View Figure 1. Mononuclear phagocyte-resident NRP1 expression in LysM-Cre/Nrp1$^{fl/fl}$.

A. Gating scheme explaining the identification of the Ly6G$^-$, F4/80$^+$, CD11b$^+$, NRP1$^+$ mononuclear phagocytes in retinas and sclera-choroid-RPE-cell complexes. 1. Gating of live cells, 2. Removal of doublets, 3. Selection of viable cells, 4. Exclusion of neutrophils, 5. Gating of mononuclear phagocytes, 6. Gating of NRP1$^+$ mononuclear macrophages.

B. FACS histogram of APC-conjugated rat IgG2A isotype control (red) versus anti-mNRP1 APC-conjugated rat IgG2A (R&D systems) (blue).

C. FACS histogram of FMO (fluorescence minus one) versus anti-mNRP1 APC-conjugated rat IgG2A.

D, E. Quantification of NRP1-positive microglia (Ly6G$^-$, F4/80$^+$, CD11b$^+$, CX3CR1^{hi}, CD45^{lo}, NRP1$^+$) in retinas and sclera-choroid-RPE cell complexes in Naïve (non-burned) mice (**D**); n = 4 and at D3 (**E**); n=4.

F, G. Quantification of mononuclear phagocytes (Ly6G$^-$, F4/80$^+$, CD11b$^+$) in retinas and sclera-choroid-RPE cell complexes in Naïve (non-burned) mice (**F**); n = 5 (LysM-Cre/*Nrp1*$^{+/+}$), 4 (LysM-Cre/*Nrp1*$^{fl/fl}$) and at D3 (**G**); n=4.

H. Compilation of representative compressed Z-stack confocal images of FITC–dextran-labeled CNV and IB4-stained laser impact area from LysM-Cre/*Nrp1*$^{+/+}$ and LysM-Cre/*Nrp1*$^{fl/fl}$ mice at D7. Scale bar: 20μm.

I-K. Quantification of area of FITC–dextran-labeled CNV (**I**), isolectin B4 (IB4)-stained laser impact area (**J**) and the ratio of FITC/IB4 per laser-burn (**K**) relative to LysM-Cre/*Nrp1*$^{+/+}$ at D7; n = 14 burns (LysM-Cre/*Nrp1*$^{+/+}$), n = 20 burns (LysM-Cre/*Nrp1*$^{fl/fl}$).

Data information: All comparisons between groups were analyzed using a Student's unpaired t-test; **P < 0.01, ***P < 0.001; error bars represent mean ± SEM; exact P values listed in table 2.

Supplemental Figure 2

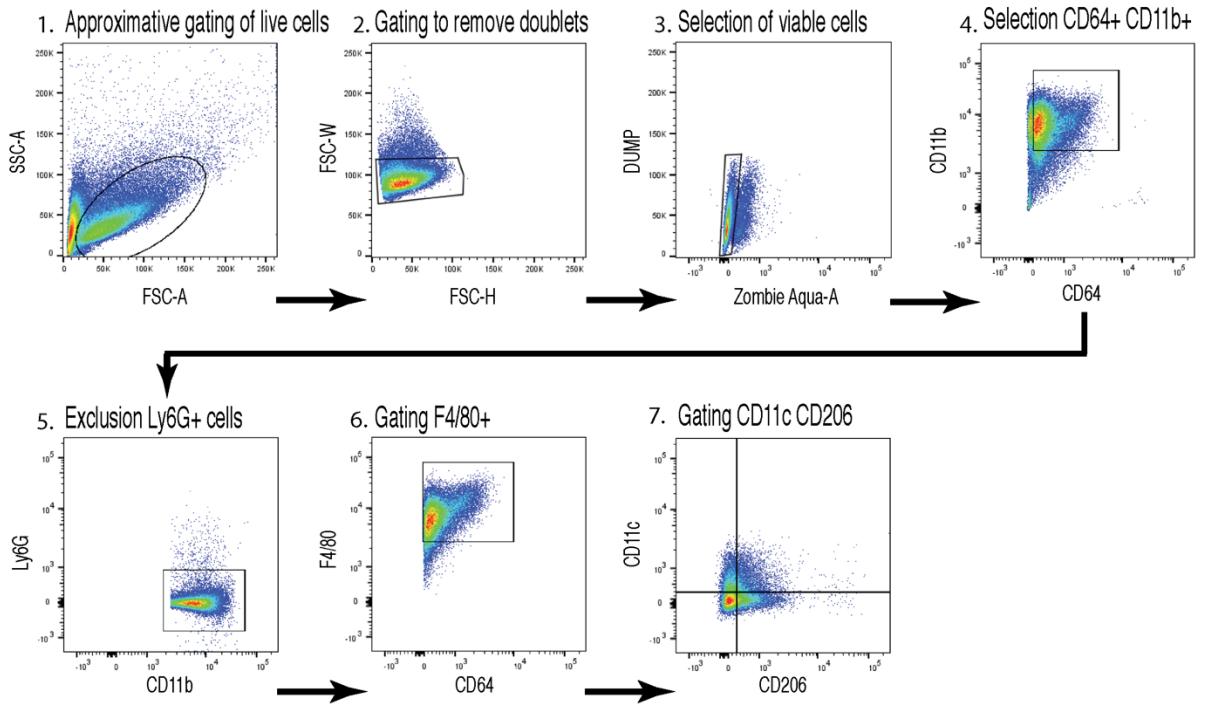

Figure 27 Publication#2 Figure EV2. Gating scheme explaining the identification of the Ly6G$^-$, F4/80$^+$, CD11b$^+$, CD11c$^+$, CD206$^-$ and Ly6G, F4/80$^+$, CD11b$^+$, CD11c$^-$, CD206$^+$ BMDMs

1. gating of live cells, **2**. removal of doublets, **3**. selection of viable cells, **4**. Selection of myeloid cells (CD64+) **5**. exclusion of neutrophils, **6**. gating of mononuclear macrophages, **7**. Gating on CD11c and CD206.

Supplemental Figure 3

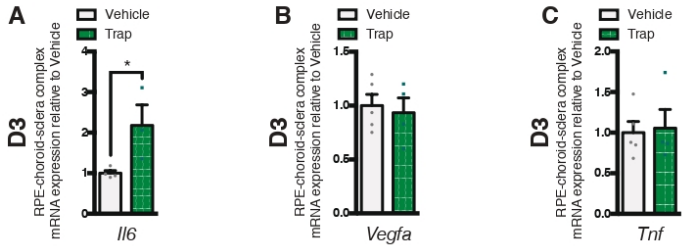

Figure 28 Publication#2 Figure EV3. Inflammatory state of RPE-choroid-sclera complexes following treatment with trap.

A-C. mRNA expression of inflammation markers relative to Vehicle in mouse RPE-choroid-sclera complexes at D3 for *Il6* (**A**); n = 4 (Vehicle), n = 4 (Trap)*, Vegfa* (**B**); n = 5 (Vehicle), n = 4 (Trap)*, Tnf* (**C**); n = 5 (Vehicle), n = 4 (Trap)*.*

Data information: All comparisons between groups were analyzed using a Student's unpaired t-test; *P < 0.05; error bars represent mean ± SEM; exact P values listed in table 2.

Discussion

Even though AMD is the leading cause of irreversible blindness in the industrialized world, the cellular and molecular mechanisms that precipitate disease remain incompletely understood and this despite significant GWAS identifying susceptibility genotypes and target mechanistic pathways. Epidemiological data suggests that in men, overall abdominal obesity is the second most important environmental risk factor after smoking for progression to late-stage neovascular AMD. Until recently, the mechanisms that underscore this observation remained ill defined. Evidence for environmental factors predisposing to AMD is supported by the fact genetically unrelated individuals with shared long-term environmental exposure develop the disease with a high concordance. A consequence of cohabitation and common lifestyle habits that prospectively impact disease modifiers such as systemic inflammation is microbial exchange. With publication #1, Gut Microbiota Influences Pathological Angiogenesis in Obesity-driven Choroidal Neovascularization, we provided the first evidence that gut microbiota are critical regulators of CNV in AMD when obesity is a predisposing factor. Using mouse models of neovascular AMD, fecal transfers and other paradigms that modify the gut microbiome, we uncoupled weight gain from confounding factors and demonstrated that microbiota significantly alter systemic and retinal inflammation and consequently exacerbate CNV. Collectively, these findings provided novel mechanistic insight on AMD and suggest that dysbiosis may be an additional factor that accounts for the inconsistent responses between individuals subjected to dietary interventions designed to stall progression of AMD such as AREDS formulations. In addition, therapeutic modulation of gut microbiomes may thus provide minimally intrusive and cost-effective paradigms to prevent or delay exudative AMD.

In the mechanisms that precipitate NV-AMD, VEGFA and inflammation play cardinal roles. In publication #2 we explored the content of vitreous from patients with active NV-AMD and found elevated levels of ligands for the transmembrane receptor NRP1. We demonstrate that mononuclear phagocytes expressing NRP1 accumulate in retina-choroid complexes during choroidal neovascularization and promote pathological angiogenesis in later stages of disease. Expression of NRP1 on cells of myeloid lineage is critical for mitigating production of inflammatory factors such as IL-6 and IL1β. Ultimately, we show that therapeutically trapping

ligands of NRP1 with a novel NRP1-derived trap, reduces the pertinent features of NV-AMD. Collectively, our data provided significant novel insight into endogenous mechanisms of inflammation associated with NV-AMD and in doing so we also developed a novel therapeutic approach to counter wet AMD.

In order to further the understanding of this complex pathology and enable the advancement of treatments, future research should keep the following points under consideration.

Animal models for AMD

A major challenge faced by researchers in the development of AMD therapies is the lack of good animal models. Besides the absence of a macula or fovea in mouse and rat eyes there are several other limiting factors that complicate the imitation of AMD in vivo. There are three players in the pathophysiology of CNV formation that researchers try to interrelate in the mouse model: inflammation, angiogenesis and proteolysis. The disruption of the BM which is necessary for CNV to develop and to mimic NV AMD, can be induced by laser, mechanically via surgery or in a setting of transgenic mice(115). It is however the chronic-, age-related character of the disease, the basis on which CNV develops, that is so hard to replicate, the main reason there are currently no good animal models for GA. Not only should a good animal model reiterate human CNV as closely as possible, it should also be efficient, reproducible, stable and sustainable over time, be inexpensive to produce and easy to monitor and quantify(115, 447). Simply letting mice age does not reproduce drusen deposition or spontaneously occurring CNV resembling that in patients with AMD, and even transgenic ApoE4 over-expressing mice on a high-fat cholesterol rich diet that were allowed to age 65-127 weeks only develop CNV in 19% of the mice(448). In the mouse model of AMD developed by Ambati et al(449), *Ccr2/Ccl2* (C-C chemokine receptor/ligand-2) deficient mice fail to recruit macrophages to the area of the RPE and BM and consequent accumulation of complement component 5a (C5a) and IgG, both of which induce VEGF production, induced development of CNV in ~25% of the mice. Even though this model is extremely valuable for the understanding of the pathobiology of CNV in regard to macrophage recruitment, it is not an exact replica of the human condition. Overall, future

development of new animal models will be of tremendous experimental value for angiogenesis research in eye studies and beyond.

Molecular weight in intestinal permeability assay

Intestinal permeability is commonly assessed through enteral administration of non-digestible markers, such as mannitol or lactulose, small sugar molecules with a molecular weight of 182 Da and 342 Da respectively(450). In order to determine changes in gut permeability after HFD we used Evans Blue, a highly water soluble dye with a molecular weight of 960 Da. The intestinal permeability to these very small molecules does however not necessarily correlate with epithelial permeability to macromolecules such as bacterial toxins, food antigens and LPS(450, 451). Since small molecules are not antigenic, do not challenge the immune system or lead to immunologically mediated damage, do not correlate with the conditions of barrier dysfunction, do not indicate real damage to tight junctions, and are not an indication of a breakdown in immunological tolerance, the lactulose/mannitol/Evans Blue test can give false negative or false positive results(450, 452). There are various mechanisms and physiological transport pathways that can increase macromolecule uptake and play a key role in the development of various inflammatory and autoimmune disorders(453). For this reason in future studies the intestinal permeability should be measured with large, 12 000- to 15 000- Da polysugars rather than with small molecules(454). The size of these sugars is more suitable to measure intestinal permeability to macromolecules such as bacterial toxins(455).

Gut-eye-axis

Intestinal microbial dysbiosis can exert its influence on ocular pathologies through the gut-eye-axis, which is closely relates to the gut-brain-axis. That the gut-brain-axis can impact the CNS, behaviour and cognitive function(318) is demonstrated by the fact that enteric infections can cause anxiety, depression and cognitive dysfunction through influence on the hypothalamus-pituitary-adrenal axis(456). It is now generally recognized that intestinal microbiota can significantly influence age-related central nervous system diseases such as Alzheimer's

disease(339, 457). The gut-eye-axis has been described for several ocular diseases, including uveitis, diabetic retinopathy, AMD and CNV (290).

Gut microbial alterations through intermittent fasting increased generation of beneficial secondary bile acids in a murine model of type 2 Diabetes Mellitus (T2D) have been reported to provide a neuroprotective effect in the retina and preventing exacerbation of diabetic retinopathy(458). A larger concentration of the phyla *Verrucomicroba* and *Tenericutes*, a decreased concentration of *Bacteroidetes* and *Firmicutes* as well as a decreased abundance of mucus producing goblet cells and increased concentrations of circulating PGN's in T2D mice with ad libitum feeding were associated with exacerbation of diabetic retinopathy(458). The gut microbiota has also been implicated in uveitis. Oral administration of broad-spectrum antibiotics altered gut microbial composition by reducing *Bacteroidetes*, *Firmicutes*, *Alphaproteobacteria* and *Gammaproteobacteria* and reduced uveitis in a model of experimental autoimmune uveitis in mice(459). Pathological inflammation caused by aberrant composition of the gut microbiota can stimulate both the innate and adaptive immune system and cause damage to tissues throughout de body. Inflammation induced disruption of the ocular tissues can exacerbate the progression of DR, AMD, CNV and uveitis. Much work remains to be done to elucidate the mechanisms underlying this process.

Western style diet

Diets have a major impact on human health, either through the gut microbiota resulting in alterations in the host's physiological responses or by directly targeting the host response(460). The complex interactions between the immune system, the microbiota and available nutrients are key players in maintaining homeostasis and barring invading pathogens at mucosal sites. The Westernized diet is defined by a composition of high saturated fats and sucrose combined with low fiber(460). The Western style diet represents a growing health risk because it contributes to the increase in occurrence of metabolic diseases. Within animal models the Western style diet is often imitated by either a HFD or a high glycemia diet (HGD).

Different effects of different high fat diets

Since 1980 the prevalence of obesity has doubled in 73 countries and problems resulting from being overweight or obese now affect more than 2 billion people worldwide(461). In order to identify the main factors that contribute to obesity a great number of studies have been conducted, exploring among other things the role of genetics, environmental factors, exercise and diet(462, 463). Animal models using fat-enriched HFD to generate obese rodents are indispensable for biomedical research on obesity, including research on the effects of diet on metabolism and disease(464). When choosing a HFD for an animal study the type of dietary fat should be considered since the dietary fat composition is of great influence on the phenotype due to the specific roles of some fatty acids on metabolism(465). Diets containing more saturated fat such as lard, beef tallow, or coconut oil are linked to obesity, insulin resistance, impairment of mitochondrial metabolism and reduced leptin secretion, while diets rich in fish oil, containing polyunsaturated fats like omega-3 and omega-6, have been studied for their health effects(465-470). In the eye a high fat diet can have direct and indirect effects on the pathophysiology of several diseases. Directly, the dysregulation of lipid metabolism is closely associated with onset and progression of AMD and diabetic retinopathy while some lipid metabolites exert beneficial effects(53). Indirectly, obesity is an established risk factor for many systemic diseases, including type 2 diabetes mellitus, hypertension, stroke, metabolic syndrome, microbiotal dysbiosis and chronic inflammation, which at their turn are linked with age-related cataract, glaucoma, ARM, and DR(213, 471).

High glycemia diet

Rowan et al investigated the effect HGD on AMD in a wild-type aged-mouse model(472). The consumption of a HGD resulted in many AMD features, including RPE hypopigmentation and atrophy, lipofuscin accumulation, and photoreceptor degeneration. They found that the gut microbiota were responsive to the diet, and identified microbiota in the *Clostridiales* order as being associated with AMD and the HGD, whereas protection from AMD was associated with the *Bacteroidales* order and a low glycemia diet (LGD). These findings are in line with what we showed before(213). Rowan et al describes the dysbiosis that is caused by the HGD on the order

level which is more precise than the phylum level we used in 2016 (213). With an increase in *Clostridiales* which belong to the class of *Clostridia* and the phylum of *Firmicutes* and a decrease in *Bacteroidales* which belong to the class of *Bacteroidia* and the phylum of *Bacteroidetes*, their results are in line with the dysbiosis observed after feeding a HFD. Together these studies confirm that a Western style diet, with a composition high in fat and glucose promotes an increase in intestinal *Firmicutes* which promotes AMD.

Influence of host genetics on microbiota

The relationship between host genetic variation and the diversity of gut microbiomes remains largely unknown. Does the microbiome function as an environmental factor that interacts with the host or is it a genetically determined attribute that is shaped by the host?

Although microbiomes can differ greatly between adults and change composition based on diet, family members are frequently noticed to have more analogous microbiota's than unrelated individuals(355, 362, 473, 474). Familial similarities in microbiotal constitution are usually attributed to shared environmental influences, habits and dietary preferences. And an important consequence of cohabitation is microbial exchange(475). Nonetheless, related individuals show a greater concordance in their microbiotic profile than non-related individuals, raising the question whether shared genetic composition underlies familial microbiome similarities. The distinction between effects of shared genetics and shared environment is frequently investigated by comparing the dissimilarity between groups of monozygotic and dizygotic twins(476). Two studies using twin cohorts (54 and 87 twin pairs) showed that that the degree of similarity in the gut microbiotas of adult monozygotic twin pairs was not greater than that of dizygotic twin pairs, although the difference between monozygotic twins was slightly smaller in both studies.(355, 474). In addition, both monozygotic and dizygotic twins show more similarity in the microbiome than unrelated individuals. A larger study using 416 twin pairs confirmed a heritability of the general composition of the microbiome and also assessed heritability of individual bacteria(477). Several other studies have identified different heritable bacterial taxa but the combined bacterial abundance accounted for by them is low(476-481). Most reported associations between host genetics and gut microbiota prove not the be statistically significant after multiple testing

correction(476). By reanalysing previously published and partially above mentioned data from 2,252 twins from the TwinsUK cohort, Rothschild et al estimate that the average heritability if gut microbiome taxa is only 1.9%(481).

Backing of host genetic effects on the microbiome comes predominantly from studies that take a targeted approach, identifying the increased carriage of specific species or pinpointing specific genetic loci that have shown gene-microbiota interaction(477, 482-485). When Turpin et al recruited a cohort of 1,561 healthy individuals they identified 58 single-nucleotide polymorphisms (SNPs) associated with a relative abundance of 33 taxa. Only four of these loci were replicated in a second cohort of 463 subjects. Perhaps the most interesting gene, encoded in the region of rs62171178, is *UBR3* which is part of a ubiquitin-protein ligase E3. Since ubiquitination is involved in various aspects of the immune response, polymorphisms in *UBR3* might trigger changes in immune responses that possibly resulting in certain bacterial taxa differing in their presence or abundance across individuals(478).

Relative contribution of diet and host genetics

Recently Rothschild et al studied microbial-genetic correlation using the metagenome- and 16S rRNA gene-sequenced gut microbiomes, genotypes, blood and anthropometric measurements, and dietary habits of a cohort of 1,046 healthy Israeli individuals(481). They conclude that the gut microbiome composition is predominantly shaped by environmental factors, is not significantly associated with genetic ancestry or individual SNP and that previously reported associations are not replicated across different studies.

The working hypothesis has been that genetics play a major role in determining microbiome variation among people. This idea has probably been fueled by the fact that all aspects of human health are so profoundly influenced by genetics. But even though microbiome populations are not shaped by host genetics they are complementary for predicting host phenotypes(481). Evaluation of the ability of a linear prediction model to predict human phenotypes from bacterial gene abundances found that phenotype prediction can be substantially improved by using both host genetics and microbiome data.

Next generation sequencing

Since culturing large numbers of microbial taxa in the laboratory is problematic at best, it is very difficult to catalog the individual members comprising a specific microbiome. Understanding how microbial communities function and influence host-pathogen interactions is a complex matter(486). To start, it is critical to map out the healthy human microbiome and its passing variations. In order to accurately identify deviations from normality that could be linked to disease one needs to know what is abnormal(487). Keeping in mind that there are large inter and intrapersonal variations in the microbiotal composition, the human microbiome has to be characterized across lifespans, ethnicities, nationalities, cultures, and geographic locales(487).

The recent advances in sequencing technologies are broad and insights have greatly evolved. The development of technologies like 16S rRNA sequencing allows for high-throughput science, with rapid acquisition of large numbers of distinct variables. The introduction of sample barcoding techniques(488-490) and the decreasing cost of next generation sequencing technologies(491, 492) have encouraged an increasing number of metagenomic studies to be conducted. These studies have allowed researchers to define similarities and differences within human microbiotas. Large online databases (493-495) coupled with an increased accessibility to growing computing power(496, 497) makes it possible to seamlessly perform hundreds and thousands of tests on a given data set. A major barrier in integration of information from thousands of samples used to be the lack of software that could handle the increasingly massive datasets. With the development of QIIME (quantitative insights into microbial ecology), an open-source software pipeline, a wide range of microbial community analyses and visualizations are now available(496). Despite these great advances it is necessary to recognize that there is still a long way to go. The accurate taxonomic identification of 16S rRNA gene data depends on the quality and completeness of the reference databases used(498). The high degree of variability in the microbiota between individuals and within individuals, both between body sites and over time make it extremely difficult to determine what is a healthy microbiome and whether changes in communities are a symptom of disease or a contributing factor(352, 487, 499-501). The sampling of new populations at increasing depth continues to reveal novel species which may be important for determining disease defining differences in communities(487). The currently popular

sequencing technique of partial 16S rRNA gene sequencing often lacks the discriminatory power to differentiate at the species taxonomic level and is generally restricted to genus-level classification due to high sequence conservation(502) (502, 503). Using shotgun metagenomics to obtain genome sequences can ameliorate species-level microorganism discrimination(503). Future studies will have to focus on augmenting their clinically relevant findings within the increasing number of sequences and samples collected in order to advance microbiota research to a level of understanding that allows for effective microbiome-related treatments(487).

Microbiotal Transplants

Fecal microbiotal transplantation is a new therapeutic approach where stool from a healthy donor is infused in the colon or delivered through the upper GI to repopulate the gut with a healthy microbiome(504). Currently microbiotal transplants are used to treat recurrent *Clostridium difficile* infections (rCDI)(505)with success rates approaching 92%(506, 507). The pathogenesis of inflammatory bowel disease (IBD), a term that is used for several disorders that involve chronic inflammation of the GI tract including ulcerative colitis (UC) and Crohn's disease (CD), has an important microbital component(508). Gut dysbiosis with decreased microbiome diversity, fewer *Firmicutes* and more *Proteobacteria* has been associated with UC(509). A meta-analysis of 4 randomized clinical trials in patients with UC demonstrated a 28% remission rate in patients treated with fecal microbiotal transplantation compared to 8% in those who received placebo(510). The success of fecal microbiotal transplants has promoted investigations into its application in other GI disorders and extra-intestinal diseases which have been linked to gut dysbiosis including Parkinson's disease, fibromyalgia, chronic fatigue syndrome, myoclonus dystopia, multiple sclerosis, obesity, insulin resistance, metabolic syndrome, and autism(511). However, the development of microbiotal transplant as a treatment is in a very early state and several important barriers remain. Not only have the characteristics of a healthy microbiome not been fully determined, the safety of the recipient, long-term outcomes, adequate controls and cost-effectiveness need to be further assessed(508).

When applied as a treatment or preventive measure for AMD, a chronic and slowly progressing disease, the relevance of microbiotal transplantation remains in a premature state. With its not

yet fully understood, multifactorial character, researchers are far from pinpointing the preeminent microbiome to slow down AMD pathogenesis. For now, diet changes to "un-Westernize" our diets, diversifying our meals, cutting sugar and fat intake while increasing dietary fiber, in combination with microbiotal diversity stimulating habits such as keeping pets, are our best bet to maintain a healthy gut microbiome, decrease chronic inflammation and curtail AMD(294, 512-514).

M1 and M2 polarization

Macrophage polarization refers to how macrophages have been activated at a given point in space and time and is routinely viewed as a linear scale, with M1, or classically activated, macrophages on one extreme and M2, alternatively activated macrophages, on the other(170-172). These two activation states are in analogy to the adaptive immune system where T helper cells can be subdivided in Th1 and Th2. and gives an oversimplified illustration of the more complex reality(515). Macrophage polarization only gives an estimate of macrophage function and does not describe a fixed state, since macrophages are sufficiently flexible to integrate multiple signals and have been shown to express M1 and M2 markers simultaneously(76). The M1/M2 paradigm provides a useful framework for selected immune responses, but a more comprehensive classification that takes the different gradients of phenotypes into account is required(172). Two alternative versions have been proposed, including a three-category "colour wheel" of macrophage activation that's inspired by the three primary colours representing three basic macrophage populations, classically activated, wound-healing and regulatory macrophages, that can blend into various other "shades" of activation(170). The second alternative renamed M2 to M2a and added the groups M2b, M2c and M2d, where M2a is pro tissue repair, M2b is characterized by immune complex activation, M2c represents deactivated anti-inflammatory macrophages and M2d represents a regulatory macrophage that is often grouped with tumour associated macrophages(516-519).

Some studies use the identification of M1 and M2 markers to indicate whether MPs are "good" or "bad"(76). One must keep in consideration that the two polarization types M1 and M2 are only two activation states out of plenty. The M1/M2 defining proteins such as CD80 and CD86 for

M1 and CD64, CD163, CD206 and CD209 for M2(180, 181) are not regulated by a general transcriptional switch but individually and can be expressed simultaneously(520). Subretinal MPs are often both proinflammatory and neurotoxic as well as angiogenic and fibrotic and can cause damage no matter their polarization state. Therapeutic strategies should aim to restore homeostasis and ebb MP infiltration, re-establishing the balance between beneficial inflammation that is crucial for debris clearance and detrimental chronic inflammation(76).

Macrophages and angiogenesis

Macrophage polarization or activation state are important for angiogenesis promoting capabilities. Vasculogenesis, the generation of blood vessels de novo from mesenchymal blood islands and angiogenesis, the sprouting of new vessels from pre-existing ones, are the two major processes involved in the formation of blood vessels(521, 522). Physiologic angiogenesis occurs during embryonic development, the female reproductive cycle and wound healing and involves the processes of vessel destabilization, endothelial cell migration and proliferation, sprouting and a resolution phase with vessel stabilization(174, 523). During sprouting endothelial cells adopt two distinct cellular phenotypes, known as tip and stalk cells, with unique functions and gene expression patterns(423). By means of sophisticated cross talk between VEGF and Notch signalling, tip cell migration and stalk cell proliferation are regulated. For a more in depth analysis of sprouting angiogenesis please consult “VEGF and Notch in Tip and Stalk Cell Selection” from Raquel Blanco and Holger Gerhardt(423). In a healthy organism angiogenesis is under tight control. The proliferation rate of endothelial cells is very low and it is only for short periods of time, in growth and repair processes, that neovascularization is initiated(524). Abnormal angiogenesis is a cardinal feature in the pathophysiology of several diseases of which cancer, stroke, diabetes, arthritis and CNV associated with AMD are just a few examples(76, 525). Activated macrophages influence each phase of the angiogenic process by releasing proteases, growth factors and monokines.

Polarization of macrophages plays a central role in the adoption of an angiogenic phenotype. The polarization state of macrophages can affect the profile of excreted growth factors and affect different stages of angiogenesis(175). Spiller et al showed that both M1 and M2 macrophages

are required to achieve vascularization. M1 macrophages express genes that are involved in the initiation of angiogenesis, including VEGFA and fibroblast growth factor and M2 macrophages express and secrete high levels of PDGFBB and matrix metalloproteinase (MMP) 9(175).

In response to various chemoattractants such as chemokines, pro-inflammatory signalling molecules and DAMPs, circulating monocytes are attracted to the site of interest and differentiate and mature into macrophages(526). Depending on the areal circumstances the macrophage phenotype is further sculpted to acquire substantial molecular and functional heterogeneity(527). The cytokine milieu to which macrophages are exposed curbs their activation state and determines their proangiogenic capacity(436). In the developmental process of retinal blood vessel remodelling macrophages can acquire anti-angiogenic functions, a rare state of activation that testifies to the broad potential of polarization(528).

The interplay between macrophages and angiogenic factors describes an extensive and complex web of interactions, positive and negative feedback loops. An activated macrophage can produce a wide range of pro- and anti-angiogenic factors, that at their turn can recruit and activate more monocytes, or induce an anti-inflammatory, anti-angiogenic milieu. Beyond this monocyte-monocyte synergy, macrophage produced angiogenic factors like VEGF, PGF, CXCL8 and CXCL12 are major chemoattractants for the recruitment of other myeloid cells like hemangiocytes, myeloid-derived suppressor cells, neutrophils and dendritic cells, that are central in the regulation of angiogenesis(529). The role of these non-monocyte myeloid cells is furthermore multifaceted and includes the production of proangiogenic growth factors and vascular-modulating enzymes, that stimulate the proangiogenic functions of these cells(529).

A multitude of myeloid cell types are implicated in angiogenesis and they cooperate with one and another to ensure adequate vascular development where and when it is needed. Identifying the key elements in such a complex network and translating this knowledge into clinical strategies to prevent abnormal angiogenesis in diseases like cancer, stroke, diabetes, arthritis and CNV associated with age-related macular degeneration will be a major challenge for the future.

Our data suggests that the absence of NRP1 skews MPs to a more pro-inflammatory M1 character, with increased NFκB phosphorylation and production of inflammatory factors,

decreasing pro-angiogenic qualities. This is consistent with findings in models of obesity(379), tumour growth(370, 378, 530, 531), and sepsis(532). With respect to being pro-angiogenic, NRP1-expressing mononuclear phagocytes are important for vessel growth during weight gain(379), normalize tumour vessels(533), and promote pathological angiogenesis in the retina(534) and tumours(378).

Neuropilin-1 as a therapeutic target in neovascular eye disease

The multitude of publications on NRP1 expression in human disease, combined with the evident importance of NRP1 in animal models of vascular pathology have made NRP1 a topic of interest as therapeutic target for several vessel-associated diseases(369). Even though most of the therapeutics are originally developed for the treatment of cancers, many of the findings resulting from these studies are also relevant for ocular diseases(369). NRP1 function may be inhibited in several ways, using monoclonal antibodies, peptides or small molecule inhibitors that target NRP1 and through micro RNA-mediated modulation of *Nrp1* expression(369). Until recently the main focus lay on finding treatments that inhibit NRP1 binding of VEGF but recent studies however have explored other ligands that bind NRP1 as possible targets, such as SEMA3A.

Retinopathy of prematurity and proliferative diabetic retinopathy, leading causes of blindness in children and working-age adults, are examples of proliferative retinopathies that follow an initial microvascular degeneration by a pathologic compensatory hypervascularization of the hypoxic retina(535). Misguidance of the neovessels by the neuronal guidance cue SEMA3A, secreted by hypoxic neurons, mounts to an inability to revascularize the most ischemic regions of the retina, sending the new vessels towards the vitreous instead(536). Using the mouse model of oxygen-induced retinopathy (OIR) to mimic the destructive vasoproliferative phase Joyal and colleagues showed that exogenous SEMA3A may be administered to redirect neovascularization from the vitreous into the retina in retinopathies(535).

In addition to its function as a vascular guidance molecule, SEMA3A also promotes recruitment of myeloid cells to sites of injury and disease in the retina. A subset of NRP1-positive MPs responds to local SEMA3A as a potent chemoattractant and are essential for disease progression in the OIR model(534). The proangiogenic NRP1-positive MPs promote pathological

neovascularization, demonstrating an innate immune cell-mediated function of NRP1 in pathological neovascularization in the eye.

In retinopathy of prematurity and proliferative diabetic retinopathy the pathological neovascularization originates from the retina and grows into the vitreous cavity, whereas in NV AMD the neovascularization originates from the choroid and grows into the subretinal space(537). These three blinding diseases have in common that an unchecked proliferation of neovessels causes damage to the retina. Upon intravitreal administration, sNRP1 provoked a 40% decrease in pathological preretinal angiogenesis when compared with vehicle injected controls in the OIR model(534) and a 47% decrease in CNV in the laser burn model. Together, these data suggest that neutralization of ligands of NRP1 is an effective strategy to reduce destructive neovascularization in eye disease.

Several drugs targeting VEGF are used for the treatment of neovascular AMD. Available treatments such as intraocular injections with anti-VEGF are invasive and show neuronal toxicity. Recent studies have raised the possibility that NRP1 functions that are VEGF–independent and function by other ligands of this receptor, such as Sema3A, may also be possible therapeutic targets and can complement current treatments to treat or prevent AMD. Potentially, non-responders to anti-VEGF therapy could benefit from this treatment paradigm, since a genetic variation of *Nrp1* is an indicator of reduced treatment response to anti-VEGF therapeutics like Ranibizumab in patients with NV AMD(538, 539). A possible set-up for a primary investigation into the efficacy of NRP1 traps in VEGF non-responders, is by studying the effect of an NRP1 trap on angiogenesis in tumors. By selecting several xenograft models known to exhibit varying sensitivity to anti-VEGF therapy, as described by Qi Pan et al in 2007(540), NRP1 trap efficacy could be studied in a simulated non-responder phenotype. Targeting VEGF-independent NRP1 pathways may offer numerous windows for intervention in angiogenesis-dependent diseases, including several eye diseases.

TGFβ/Smad, Neuropilin-1 and Notch in sprouting angiogenesis

Several studies describe a promoting role of TGFβ in NV AMD, either through the induction of VEGF-A secretion by RPE cells(541, 542), through macrophage-mediated inflammation(543) or

through the stimulation of choroidal endothelium proliferation(544). In one pathway that could be of particular interest, described in 2015 by Aspalter et al, NRP1 actively suppresses the TGFβ-induced stalk cell phenotype to allow tip cell formation. The lateral feedback loop of Delta-like (Dll) 4 and Notch uses NRP1 as a pivot that establishes differential responsiveness to TGFβ/ bone morphogenetic protein (BMP)9signalling (545). Activin receptor-like kinase (Alk)1 and Alk5 both belong to a group of seven type I receptors responsible for TGFβ family signal transduction (546). TGFβ and BMP9 belong to a large family of TGF extracellular ligands that exert influence on several cellular compartments, notably epithelial cells, fibroblasts, immune cells and endothelial and perivascular cells(547). TGFβ's effect on blood vessel formation may be both pro- or antiangiogenic and is concentration and context dependent(548). Effects of TGFβ related defects are reflected in the inherited genetic vascular disorder hereditary hemorrhagic telangiectasia and the phenotypes of mice deficient in components of the TGF-b signaling cascade(549-553). Activation of Alk5 and Alk1 in response to TGFβ and BMP9 phosphorylate several members of the Smad-family (Smad1,5,8 and Smad2,3 respectively), the main signal transducers for TGFβRs, which influence stalk cell behavior(554, 555). Alk1/Smad1,5,8 signaling markedly affects tip/stalk cell specification and its inhibition can cause hypersprouting(556). Data from Aspalter et al suggests that NRP1 inhibits phosphorylation of Smad2,3 in tip cells, promoting a tip cell phenotype. VEGF-dependent upregulation of Dll4 in the tip cell leads to Notch activation in the neighboring stalk cell(557). Notch activation decreases NRP1 levels in the stalk cell, lifting NRP1-dependent Smad2/3 inhibition(545). Notch downstream effectors driving stalk cell behavior are interesting targets to prevent pathological angiogenesis in cancer and ocular neovascular disease. This pathway shows that the inhibition of endothelial NRP1, opposed to the previously discussed myeloid NRP1, stimulates TGFβ-induced Smad2/3 activation which inhibits angiogenesis.

TGFβ, a link between NRP1 and gut microbiota in AMD?

TGFβ is a highly pleiotropic cytokine playing a major role in seemingly unrelated phenotypic traits in for example wound healing, angiogenesis, immunoregulation and cancer(558). Underproduction of TGFβ lies at the core of some autoimmune diseases, while overproduction

is linked to many pathological conditions including pulmonary fibrosis, renal interstitial fibrosis, cirrhosis and the IBDs ulcerative colitis and Crohn's disease(420, 559). The chronic intestinal inflammation in these IBDs are characterized by aberrant mucosal immune reactions to intestinal microbes in genetically susceptible hosts(560-562). TGFβ and its dysregulation play a key role in intestinal immunity, suppressing inflammatory responses to luminal bacterial antigens while contributing to immune tolerance(563, 564) with specific intestinal microbes contributing to immune homeostasis by modulating TGFβ production(565). Smad3 is among the loci associated with IBD susceptibility(566) and several TGFβ-related compounds present potential therapeutic strategies for IBD. Hong et al showed that the expression of the Drosophila homolog of TGFβ is elevated under HFD conditions(567), while Biasi et all show that a HFD strongly stimulates the expression and synthesis of TGFβ by cells of the human macrophage lineage(568).

Considering the link between intestinal inflammation and AMD it could be highly interesting to investigate the role NRP1 plays in the differential responsiveness to TGFβ in intestinal homeostasis and dysbiosis and the consequential effects on CNV formation.

Conclusion

AMD is the leading cause of central vision loss in industrialized countries with major societal and financial impacts (1-4). Epidemiological data suggests that in men, overall abdominal obesity is the second most important environmental risk factor after smoking for progression to late-stage NV AMD. Given the impact of high-fat diets on gut microbiota, we investigated whether commensal microbes influence the evolution of AMD. Using mouse models of NV AMD, microbiotal transplants and other paradigms that modify the gut microbiome, we uncoupled weight gain from confounding factors and demonstrate that high-fat diets exacerbate choroidal neovascularisation (CNV) by altering gut microbiota. Gut dysbiosis leads to heightened intestinal permeability and chronic low-grade inflammation with elevated production of IL-6, IL-1β, TNF-α and VEGF. The priming of the immune system increases recruitment of microglia and macrophages to the site of pathological angiogenesis in the eye and ultimately exacerbates pathological angiogenesis.

Our study suggests that gut microbiota influence the development of neovascular lesions associated with AMD and this particularly when obesity is a predisposing factor. Modifying microbiota can reduce systemic and local choroidal inflammation and attenuate pathological neovascularization and may thus provide minimally intrusive and cost-effective paradigms to prevent or delay exudative AMD.

Accumulation of mononuclear phagocytes in AMD secondary to the disruption of the physiologically immunosuppressive subretinal environment is central to the etiology of both atrophic and wet forms of AMD. In addition to microbiotal changes, that can reduce systemic chronic low-grade inflammation and increased MP activity, we show that local treatment with a NRP1-derived trap can lessen CNV. We have provided evidence that ligands for NRP1, such as Semaphorin 3A and VEGFA, are elevated in the vitreous of patients with AMD at times of active CNV. We further demonstrated that NRP1-expressing MPs promote CNV by mitigating production of inflammatory factors such as IL-6 and IL-1β and promoting alternative activation, giving the MPs a pro-angiogenic character. These data add to the notion that less inflammatory and more M2-like MPs are enriched with age and exacerbate CNV in the laser-induced mouse

model(569, 570). Therapeutically trapping ligands of NRP1 with a NRP1-derived trap reduces CNV. Non-responders to anti-VEGF therapy could possibly benefit from this treatment paradigm. During aging the retina is subjected to a chronic low grade oxidative insult, activating the retinal immune system commencing a para-inflammatory response(72). In AMD the dysregulation of this reparative para-inflammatory mechanism leads to chronic low grade inflammation, damaging the macula and the BRB, compromising retinal immune privilege and causing the development of retinal lesions(72, 149). Our results demonstrate that both systemic and local treatments can curtail the detrimental inflammation in AMD.

References

1. Wong WL, Su X, Li X, Cheung CM, Klein R, Cheng CY, et al. Global prevalence of age-related macular degeneration and disease burden projection for 2020 and 2040: a systematic review and meta-analysis. Lancet Glob Health. 2014;2(2):e106-16.
2. Jonas JB, Cheung CMG, Panda-Jonas S. Updates on the Epidemiology of Age-Related Macular Degeneration. Asia Pac J Ophthalmol (Phila). 2017;6(6):493-7.
3. Friedman DS, O'Colmain BJ, Munoz B, Tomany SC, McCarty C, de Jong PT, et al. Prevalence of age-related macular degeneration in the United States. Arch Ophthalmol. 2004;122(4):564-72.
4. Ambati J, Fowler BJ. Mechanisms of age-related macular degeneration. Neuron. 2012;75(1):26-39.
5. Jonas JB, Bourne RR, White RA, Flaxman SR, Keeffe J, Leasher J, et al. Visual impairment and blindness due to macular diseases globally: a systematic review and meta-analysis. Am J Ophthalmol. 2014;158(4):808-15.
6. Klein R, Klein BE, Knudtson MD, Wong TY, Cotch MF, Liu K, et al. Prevalence of age-related macular degeneration in 4 racial/ethnic groups in the multi-ethnic study of atherosclerosis. Ophthalmology. 2006;113(3):373-80.
7. Klein R, Chou CF, Klein BE, Zhang X, Meuer SM, Saaddine JB. Prevalence of age-related macular degeneration in the US population. Arch Ophthalmol. 2011;129(1):75-80.
8. Chakravarthy U, Wong TY, Fletcher A, Piault E, Evans C, Zlateva G, et al. Clinical risk factors for age-related macular degeneration: a systematic review and meta-analysis. BMC Ophthalmol. 2010;10:31.
9. Evans JR. Risk factors for age-related macular degeneration. Prog Retin Eye Res. 2001;20(2):227-53.
10. Smith W, Assink J, Klein R, Mitchell P, Klaver CC, Klein BE, et al. Risk factors for age-related macular degeneration: Pooled findings from three continents. Ophthalmology. 2001;108(4):697-704.
11. Oshima Y, Ishibashi T, Murata T, Tahara Y, Kiyohara Y, Kubota T. Prevalence of age related maculopathy in a representative Japanese population: the Hisayama study. Br J Ophthalmol. 2001;85(10):1153-7.
12. Kawasaki R, Wang JJ, Ji GJ, Taylor B, Oizumi T, Daimon M, et al. Prevalence and risk factors for age-related macular degeneration in an adult Japanese population: the Funagata study. Ophthalmology. 2008;115(8):1376-81, 81 e1-2.
13. Kawasaki R, Wang JJ, Aung T, Tan DT, Mitchell P, Sandar M, et al. Prevalence of age-related macular degeneration in a Malay population: the Singapore Malay Eye Study. Ophthalmology. 2008;115(10):1735-41.
14. Chen SJ, Cheng CY, Peng KL, Li AF, Hsu WM, Liu JH, et al. Prevalence and associated risk factors of age-related macular degeneration in an elderly Chinese population in Taiwan: the Shihpai Eye Study. Invest Ophthalmol Vis Sci. 2008;49(7):3126-33.
15. Hayat MJ, Howlader N, Reichman ME, Edwards BK. Cancer statistics, trends, and multiple primary cancer analyses from the Surveillance, Epidemiology, and End Results (SEER) Program. Oncologist. 2007;12(1):20-37.
16. Brookmeyer R, Johnson E, Ziegler-Graham K, Arrighi HM. Forecasting the global burden of Alzheimer's disease. Alzheimers Dement. 2007;3(3):186-91.
17. Taylor DJ, Hobby AE, Binns AM, Crabb DP. How does age-related macular degeneration affect real-world visual ability and quality of life? A systematic review. BMJ Open. 2016;6(12):e011504.

18. Stevenson MR, Hart PM, Montgomery AM, McCulloch DW, Chakravarthy U. Reduced vision in older adults with age related macular degeneration interferes with ability to care for self and impairs role as carer. Br J Ophthalmol. 2004;88(9):1125-30.
19. Hassell JB, Lamoureux EL, Keeffe JE. Impact of age related macular degeneration on quality of life. Br J Ophthalmol. 2006;90(5):593-6.
20. Ivers RQ, Cumming RG, Mitchell P, Attebo K. Visual impairment and falls in older adults: the Blue Mountains Eye Study. J Am Geriatr Soc. 1998;46(1):58-64.
21. Klein BE, Klein R, Lee KE, Cruickshanks KJ. Performance-based and self-assessed measures of visual function as related to history of falls, hip fractures, and measured gait time. The Beaver Dam Eye Study. Ophthalmology. 1998;105(1):160-4.
22. Mitchell J, Bradley C. Quality of life in age-related macular degeneration: a review of the literature. Health Qual Life Outcomes. 2006;4:97.
23. Rovner BW, Casten RJ, Tasman WS. Effect of depression on vision function in age-related macular degeneration. Arch Ophthalmol. 2002;120(8):1041-4.
24. Williams RA, Brody BL, Thomas RG, Kaplan RM, Brown SI. The psychosocial impact of macular degeneration. Arch Ophthalmol. 1998;116(4):514-20.
25. Priya RR, Chew EY, Swaroop A. Genetic studies of age-related macular degeneration: lessons, challenges, and opportunities for disease management. Ophthalmology. 2012;119(12):2526-36.
26. Lambert NG, ElShelmani H, Singh MK, Mansergh FC, Wride MA, Padilla M, et al. Risk factors and biomarkers of age-related macular degeneration. Prog Retin Eye Res. 2016;54:64-102.
27. Age-Related Eye Disease Study Research G. Risk factors associated with age-related macular degeneration. A case-control study in the age-related eye disease study: Age-Related Eye Disease Study Report Number 3. Ophthalmology. 2000;107(12):2224-32.
28. Risk factors associated with age-related macular degeneration. A case-control study in the age-related eye disease study: Age-Related Eye Disease Study Report Number 3. Ophthalmology. 2000;107(12):2224-32.
29. Friedman DS, Katz J, Bressler NM, Rahmani B, Tielsch JM. Racial differences in the prevalence of age-related macular degeneration: the Baltimore Eye Survey. Ophthalmology. 1999;106(6):1049-55.
30. Rein DB, Wittenborn JS, Zhang X, Honeycutt AA, Lesesne SB, Saaddine J, et al. Forecasting age-related macular degeneration through the year 2050: the potential impact of new treatments. Arch Ophthalmol. 2009;127(4):533-40.
31. Bressler SB, Munoz B, Solomon SD, West SK, Salisbury Eye Evaluation Study T. Racial differences in the prevalence of age-related macular degeneration: the Salisbury Eye Evaluation (SEE) Project. Arch Ophthalmol. 2008;126(2):241-5.
32. Frank RN, Puklin JE, Stock C, Canter LA. Race, iris color, and age-related macular degeneration. Trans Am Ophthalmol Soc. 2000;98:109-15; discussion 15-7.
33. Nicolas CM, Robman LD, Tikellis G, Dimitrov PN, Dowrick A, Guymer RH, et al. Iris colour, ethnic origin and progression of age-related macular degeneration. Clin Exp Ophthalmol. 2003;31(6):465-9.
34. Tomany SC, Klein R, Klein BE, Beaver Dam Eye S. The relationship between iris color, hair color, and skin sun sensitivity and the 10-year incidence of age-related maculopathy: the Beaver Dam Eye Study. Ophthalmology. 2003;110(8):1526-33.
35. Fletcher AE, Bentham GC, Agnew M, Young IS, Augood C, Chakravarthy U, et al. Sunlight exposure, antioxidants, and age-related macular degeneration. Arch Ophthalmol. 2008;126(10):1396-403.
36. Klein R, Klein BE, Tomany SC, Cruickshanks KJ. The association of cardiovascular disease with the long-term incidence of age-related maculopathy: the Beaver Dam eye study. Ophthalmology. 2003;110(4):636-43.

37. Chapman NA, Jacobs RJ, Braakhuis AJ. Role of diet and food intake in age-related macular degeneration: a systematic review. Clin Exp Ophthalmol. 2019;47(1):106-27.
38. Seddon J, Cote J, Davis N, Rosner B. Progression of age-related macular degeneration: association with body mass index, waist circumference, and waist-hip ratio. Archives of ophthalmology. 2003;121(6):785-92.
39. Adams MKM, Simpson J, Aung K, Makeyeva G, Giles G, English D, et al. Abdominal obesity and age-related macular degeneration. American journal of epidemiology. 2011;173(11):1246-55.
40. Evans JR, Lawrenson JG. Antioxidant vitamin and mineral supplements for slowing the progression of age-related macular degeneration. Cochrane Database Syst Rev. 2012;11:CD000254.
41. Adams MK, Chong EW, Williamson E, Aung KZ, Makeyeva GA, Giles GG, et al. 20/20--Alcohol and age-related macular degeneration: the Melbourne Collaborative Cohort Study. Am J Epidemiol. 2012;176(4):289-98.
42. Smith W, Mitchell P, Wang JJ. Gender, oestrogen, hormone replacement and age-related macular degeneration: results from the Blue Mountains Eye Study. Aust N Z J Ophthalmol. 1997;25 Suppl 1:S13-5.
43. Kaarniranta K, Machalinska A, Vereb Z, Salminen A, Petrovski G, Kauppinen A. Estrogen signalling in the pathogenesis of age-related macular degeneration. Curr Eye Res. 2015;40(2):226-33.
44. Armstrong RA, Mousavi M. Overview of Risk Factors for Age-Related Macular Degeneration (AMD). J Stem Cells. 2015;10(3):171-91.
45. Velilla S, Garcia-Medina JJ, Garcia-Layana A, Dolz-Marco R, Pons-Vazquez S, Pinazo-Duran MD, et al. Smoking and age-related macular degeneration: review and update. J Ophthalmol. 2013;2013:895147.
46. Netter FH, Hansen JT, Lambert DR. Netter's clinical anatomy. 1st ed. Carlstadt, N.J.: Icon Learning Systems; 2005. ix, 668 p. p.
47. Boron WF, Boulpaep EL. Medical physiology : a cellular and molecular approach. Updated ed. Philadelphia, Pa.: Elsevier Saunders; 2005. xiii, 1319 p. p.
48. Strauss O. The retinal pigment epithelium in visual function. Physiol Rev. 2005;85(3):845-81.
49. Booij JC, Baas DC, Beisekeeva J, Gorgels TG, Bergen AA. The dynamic nature of Bruch's membrane. Prog Retin Eye Res. 2010;29(1):1-18.
50. Campbell M, Humphries P. The blood-retina barrier: tight junctions and barrier modulation. Adv Exp Med Biol. 2012;763:70-84.
51. Ershov AV, Bazan NG. Photoreceptor phagocytosis selectively activates PPARgamma expression in retinal pigment epithelial cells. J Neurosci Res. 2000;60(3):328-37.
52. Handa JT, Cano M, Wang L, Datta S, Liu T. Lipids, oxidized lipids, oxidation-specific epitopes, and Age-related Macular Degeneration. Biochim Biophys Acta. 2017;1862(4):430-40.
53. Stahl A, Krohne TU, Sapieha P, Chen J, Hellstrom A, Chew E, et al. Lipid metabolites in the pathogenesis and treatment of neovascular eye disease. Br J Ophthalmol. 2011;95(11):1496-501.
54. Inherited and environmentally induced retinal degenerations. Proceedings of the International Symposium on Retinal Degenerations. San Francisco, California, September 2 and 3, 1988. Prog Clin Biol Res. 1989;314:1-727.
55. Ishida K, Panjwani N, Cao Z, Streilein JW. Participation of pigment epithelium in ocular immune privilege. 3. Epithelia cultured from iris, ciliary body, and retina suppress T-cell activation by partially non-overlapping mechanisms. Ocul Immunol Inflamm. 2003;11(2):91-105.
56. Streilein JW, Ma N, Wenkel H, Ng TF, Zamiri P. Immunobiology and privilege of neuronal retina and pigment epithelium transplants. Vision Res. 2002;42(4):487-95.
57. Becerra SP, Fariss RN, Wu YQ, Montuenga LM, Wong P, Pfeffer BA. Pigment epithelium-derived factor in the monkey retinal pigment epithelium and interphotoreceptor matrix: apical secretion and distribution. Exp Eye Res. 2004;78(2):223-34.

58. Dawson DW, Volpert OV, Gillis P, Crawford SE, Xu H, Benedict W, et al. Pigment epithelium-derived factor: a potent inhibitor of angiogenesis. Science. 1999;285(5425):245-8.
59. Burns MS, Hartz MJ. The retinal pigment epithelium induces fenestration of endothelial cells in vivo. Curr Eye Res. 1992;11(9):863-73.
60. Blaauwgeers HG, Holtkamp GM, Rutten H, Witmer AN, Koolwijk P, Partanen TA, et al. Polarized vascular endothelial growth factor secretion by human retinal pigment epithelium and localization of vascular endothelial growth factor receptors on the inner choriocapillaris. Evidence for a trophic paracrine relation. Am J Pathol. 1999;155(2):421-8.
61. Ogata N, Wang L, Jo N, Tombran-Tink J, Takahashi K, Mrazek D, et al. Pigment epithelium derived factor as a neuroprotective agent against ischemic retinal injury. Curr Eye Res. 2001;22(4):245-52.
62. Roberts WG, Palade GE. Increased microvascular permeability and endothelial fenestration induced by vascular endothelial growth factor. J Cell Sci. 1995;108 (Pt 6):2369-79.
63. Campochiaro PA. Retinal and choroidal neovascularization. J Cell Physiol. 2000;184(3):301-10.
64. Frank RN. Growth factors in age-related macular degeneration: pathogenic and therapeutic implications. Ophthalmic Res. 1997;29(5):341-53.
65. Witmer AN, Vrensen GF, Van Noorden CJ, Schlingemann RO. Vascular endothelial growth factors and angiogenesis in eye disease. Prog Retin Eye Res. 2003;22(1):1-29.
66. Alm A, Bill A. Ocular and optic nerve blood flow at normal and increased intraocular pressures in monkeys (Macaca irus): a study with radioactively labelled microspheres including flow determinations in brain and some other tissues. Exp Eye Res. 1973;15(1):15-29.
67. Alm A, Bill A. The oxygen supply to the retina. II. Effects of high intraocular pressure and of increased arterial carbon dioxide tension on uveal and retinal blood flow in cats. A study with radioactively labelled microspheres including flow determinations in brain and some other tissues. Acta Physiol Scand. 1972;84(3):306-19.
68. Bill A, Sperber G, Ujiie K. Physiology of the choroidal vascular bed. Int Ophthalmol. 1983;6(2):101-7.
69. Zouache MA, Eames I, Klettner CA, Luthert PJ. Form, shape and function: segmented blood flow in the choriocapillaris. Sci Rep. 2016;6:35754.
70. Parver LM. Temperature modulating action of choroidal blood flow. Eye (Lond). 1991;5 (Pt 2):181-5.
71. Bird AC. Therapeutic targets in age-related macular disease. J Clin Invest. 2010;120(9):3033-41.
72. Chen M, Xu H. Parainflammation, chronic inflammation, and age-related macular degeneration. Journal of leukocyte biology. 2015;98(5):713-25.
73. Ramrattan RS, van der Schaft TL, Mooy CM, de Bruijn WC, Mulder PG, de Jong PT. Morphometric analysis of Bruch's membrane, the choriocapillaris, and the choroid in aging. Invest Ophthalmol Vis Sci. 1994;35(6):2857-64.
74. Hjelmeland LM, Cristofolo VJ, Funk W, Rakoczy E, Katz ML. Senescence of the retinal pigment epithelium. Mol Vis. 1999;5:33.
75. Boulton M, Dayhaw-Barker P. The role of the retinal pigment epithelium: topographical variation and ageing changes. Eye (Lond). 2001;15(Pt 3):384-9.
76. Guillonneau X, Eandi CM, Paques M, Sahel JA, Sapieha P, Sennlaub F. On phagocytes and macular degeneration. Prog Retin Eye Res. 2017;61:98-128.
77. Hageman GS, Luthert PJ, Victor Chong NH, Johnson LV, Anderson DH, Mullins RF. An integrated hypothesis that considers drusen as biomarkers of immune-mediated processes at the RPE-Bruch's membrane interface in aging and age-related macular degeneration. Prog Retin Eye Res. 2001;20(6):705-32.

78. Curcio CA, Millican CL. Basal linear deposit and large drusen are specific for early age-related maculopathy. Arch Ophthalmol. 1999;117(3):329-39.
79. Klein R, Meuer SM, Knudtson MD, Iyengar SK, Klein BE. The epidemiology of retinal reticular drusen. Am J Ophthalmol. 2008;145(2):317-26.
80. De Jong P. Elusive drusen and changing terminology of AMD. Eye (Lond). 2018;32(5):904-14.
81. Young RW. Pathophysiology of age-related macular degeneration. Surv Ophthalmol. 1987;31(5):291-306.
82. Midena E, Vujosevic S, Convento E, Manfre A, Cavarzeran F, Pilotto E. Microperimetry and fundus autofluorescence in patients with early age-related macular degeneration. Br J Ophthalmol. 2007;91(11):1499-503.
83. Schuman SG, Koreishi AF, Farsiu S, Jung SH, Izatt JA, Toth CA. Photoreceptor layer thinning over drusen in eyes with age-related macular degeneration imaged in vivo with spectral-domain optical coherence tomography. Ophthalmology. 2009;116(3):488-96 e2.
84. Zarbin MA. Current concepts in the pathogenesis of age-related macular degeneration. Arch Ophthalmol. 2004;122(4):598-614.
85. Johnson PT, Brown MN, Pulliam BC, Anderson DH, Johnson LV. Synaptic pathology, altered gene expression, and degeneration in photoreceptors impacted by drusen. Invest Ophthalmol Vis Sci. 2005;46(12):4788-95.
86. Bird AC, Phillips RL, Hageman GS. Geographic atrophy: a histopathological assessment. JAMA Ophthalmol. 2014;132(3):338-45.
87. Sarks JP, Sarks SH, Killingsworth MC. Evolution of geographic atrophy of the retinal pigment epithelium. Eye (Lond). 1988;2 (Pt 5):552-77.
88. Meleth AD, Mettu P, Agron E, Chew EY, Sadda SR, Ferris FL, et al. Changes in retinal sensitivity in geographic atrophy progression as measured by microperimetry. Invest Ophthalmol Vis Sci. 2011;52(2):1119-26.
89. Lim LS, Mitchell P, Seddon JM, Holz FG, Wong TY. Age-related macular degeneration. Lancet. 2012;379(9827):1728-38.
90. Klein R, Peto T, Bird A, Vannewkirk MR. The epidemiology of age-related macular degeneration. Am J Ophthalmol. 2004;137(3):486-95.
91. Campa C, Costagliola C, Incorvaia C, Sheridan C, Semeraro F, De Nadai K, et al. Inflammatory mediators and angiogenic factors in choroidal neovascularization: pathogenetic interactions and therapeutic implications. Mediators Inflamm. 2010;2010.
92. Campochiaro PA, Aiello LP, Rosenfeld PJ. Anti-Vascular Endothelial Growth Factor Agents in the Treatment of Retinal Disease: From Bench to Bedside. Ophthalmology. 2016;123(10s):S78-s88.
93. Lopez PF, Sippy BD, Lambert HM, Thach AB, Hinton DR. Transdifferentiated retinal pigment epithelial cells are immunoreactive for vascular endothelial growth factor in surgically excised age-related macular degeneration-related choroidal neovascular membranes. Invest Ophthalmol Vis Sci. 1996;37(5):855-68.
94. Wada M, Ogata N, Otsuji T, Uyama M. Expression of vascular endothelial growth factor and its receptor (KDR/flk-1) mRNA in experimental choroidal neovascularization. Curr Eye Res. 1999;18(3):203-13.
95. Otani A, Takagi H, Oh H, Koyama S, Ogura Y, Matumura M, et al. Vascular endothelial growth factor family and receptor expression in human choroidal neovascular membranes. Microvasc Res. 2002;64(1):162-9.
96. Ferrara N, Gerber HP, LeCouter J. The biology of VEGF and its receptors. Nat Med. 2003;9(6):669-76.

97. Wise LM, Inder MK, Real NC, Stuart GS, Fleming SB, Mercer AA. The vascular endothelial growth factor (VEGF)-E encoded by orf virus regulates keratinocyte proliferation and migration and promotes epidermal regeneration. Cell Microbiol. 2012;14(9):1376-90.
98. Ferrara N. Vascular endothelial growth factor: basic science and clinical progress. Endocr Rev. 2004;25(4):581-611.
99. Ferrara N, Davis-Smyth T. The biology of vascular endothelial growth factor. Endocr Rev. 1997;18(1):4-25.
100. Park JE, Keller GA, Ferrara N. The vascular endothelial growth factor (VEGF) isoforms: differential deposition into the subepithelial extracellular matrix and bioactivity of extracellular matrix-bound VEGF. Mol Biol Cell. 1993;4(12):1317-26.
101. Shibuya M, Yamaguchi S, Yamane A, Ikeda T, Tojo A, Matsushime H, et al. Nucleotide sequence and expression of a novel human receptor-type tyrosine kinase gene (flt) closely related to the fms family. Oncogene. 1990;5(4):519-24.
102. Matthews W, Jordan CT, Gavin M, Jenkins NA, Copeland NG, Lemischka IR. A receptor tyrosine kinase cDNA isolated from a population of enriched primitive hematopoietic cells and exhibiting close genetic linkage to c-kit. Proc Natl Acad Sci U S A. 1991;88(20):9026-30.
103. Terman BI, Carrion ME, Kovacs E, Rasmussen BA, Eddy RL, Shows TB. Identification of a new endothelial cell growth factor receptor tyrosine kinase. Oncogene. 1991;6(9):1677-83.
104. Rosenfeld PJ, Brown DM, Heier JS, Boyer DS, Kaiser PK, Chung CY, et al. Ranibizumab for neovascular age-related macular degeneration. N Engl J Med. 2006;355(14):1419-31.
105. Rezende FA, Lapalme E, Qian CX, Smith LE, SanGiovanni JP, Sapieha P. Omega-3 supplementation combined with anti-vascular endothelial growth factor lowers vitreal levels of vascular endothelial growth factor in wet age-related macular degeneration. Am J Ophthalmol. 2014;158(5):1071-78.
106. Ghasemi Falavarjani K, Nguyen QD. Adverse events and complications associated with intravitreal injection of anti-VEGF agents: a review of literature. Eye. 2013;27(7):787-94.
107. Velez-Montoya R, Oliver SC, Olson JL, Fine SL, Mandava N, Quiroz-Mercado H. Current knowledge and trends in age-related macular degeneration: today's and future treatments. Retina. 2013;33(8):1487-502.
108. Hernandez-Zimbron LF, Zamora-Alvarado R, Ochoa-De la Paz L, Velez-Montoya R, Zenteno E, Gulias-Canizo R, et al. Age-Related Macular Degeneration: New Paradigms for Treatment and Management of AMD. Oxid Med Cell Longev. 2018;2018:8374647.
109. de Oliveira Dias JR, de Andrade GC, Novais EA, Farah ME, Rodrigues EB. Fusion proteins for treatment of retinal diseases: aflibercept, ziv-aflibercept, and conbercept. Int J Retina Vitreous. 2016;2:3.
110. Liu K, Song Y, Xu G, Ye J, Wu Z, Liu X, et al. Conbercept for Treatment of Neovascular Age-related Macular Degeneration: Results of the Randomized Phase 3 PHOENIX Study. Am J Ophthalmol. 2019;197:156-67.
111. Cabral T, Mello LGM, Lima LH, Polido J, Regatieri CV, Belfort R, et al. Retinal and choroidal angiogenesis: a review of new targets. International Journal of Retina and Vitreous. 2017;3(1):31.
112. Yang S, Zhao J, Sun X. Resistance to anti-VEGF therapy in neovascular age-related macular degeneration: a comprehensive review. Drug Des Devel Ther. 2016;10:1857-67.
113. Al-Zamil WM, Yassin SA. Recent developments in age-related macular degeneration: a review. Clin Interv Aging. 2017;12:1313-30.
114. Holz FG, Schmitz-Valckenberg S, Fleckenstein M. Recent developments in the treatment of age-related macular degeneration. J Clin Invest. 2014;124(4):1430-8.
115. Grossniklaus HE, Kang SJ, Berglin L. Animal models of choroidal and retinal neovascularization. Prog Retin Eye Res. 2010;29(6):500-19.

116. Pennesi ME, Neuringer M, Courtney RJ. Animal models of age related macular degeneration. Mol Aspects Med. 2012;33(4):487-509.
117. Xiao TS. Innate immunity and inflammation. Cell Mol Immunol. 2017;14(1):1-3.
118. Newton K, Dixit VM. Signaling in innate immunity and inflammation. Cold Spring Harb Perspect Biol. 2012;4(3).
119. Rose-John S. IL-6 trans-signaling via the soluble IL-6 receptor: importance for the pro-inflammatory activities of IL-6. International journal of biological sciences. 2012;8(9):1237-47.
120. Rose-John S. Interleukin-6 signalling in health and disease. F1000Research. 2020;9.
121. Tanaka T, Narazaki M, Kishimoto T. IL-6 in inflammation, immunity, and disease. Cold Spring Harb Perspect Biol. 2014;6(10):a016295.
122. Waage A, Brandtzaeg P, Halstensen A, Kierulf P, Espevik T. The complex pattern of cytokines in serum from patients with meningococcal septic shock. Association between interleukin 6, interleukin 1, and fatal outcome. J Exp Med. 1989;169(1):333-8.
123. Kishimoto T. Interleukin-6: from basic science to medicine--40 years in immunology. Annual review of immunology. 2005;23:1-21.
124. Rose-John S. The biology of interleukin-6 in the 21st century. Semin Immunol. 2014;26(1):1.
125. Müllberg J, Schooltink H, Stoyan T, Günther M, Graeve L, Buse G, et al. The soluble interleukin-6 receptor is generated by shedding. European journal of immunology. 1993;23(2):473-80.
126. Rose-John S, Heinrich PC. Soluble receptors for cytokines and growth factors: generation and biological function. Biochem J. 1994;300 (Pt 2)(Pt 2):281-90.
127. Wallenius V, Wallenius K, Ahrén B, Rudling M, Carlsten H, Dickson SL, et al. Interleukin-6-deficient mice develop mature-onset obesity. Nat Med. 2002;8(1):75-9.
128. Cressman DE, Greenbaum LE, DeAngelis RA, Ciliberto G, Furth EE, Poli V, et al. Liver failure and defective hepatocyte regeneration in interleukin-6-deficient mice. Science. 1996;274(5291):1379-83.
129. Poli V, Balena R, Fattori E, Markatos A, Yamamoto M, Tanaka H, et al. Interleukin-6 deficient mice are protected from bone loss caused by estrogen depletion. Embo j. 1994;13(5):1189-96.
130. Alonzi T, Fattori E, Lazzaro D, Costa P, Probert L, Kollias G, et al. Interleukin 6 is required for the development of collagen-induced arthritis. J Exp Med. 1998;187(4):461-8.
131. Okuda Y, Sakoda S, Bernard CC, Fujimura H, Saeki Y, Kishimoto T, et al. IL-6-deficient mice are resistant to the induction of experimental autoimmune encephalomyelitis provoked by myelin oligodendrocyte glycoprotein. International immunology. 1998;10(5):703-8.
132. Lesina M, Kurkowski MU, Ludes K, Rose-John S, Treiber M, Klöppel G, et al. Stat3/Socs3 activation by IL-6 transsignaling promotes progression of pancreatic intraepithelial neoplasia and development of pancreatic cancer. Cancer Cell. 2011;19(4):456-69.
133. Piotrowski I, Kulcenty K, Suchorska W. Interplay between inflammation and cancer. Reports of practical oncology and radiotherapy : journal of Greatpoland Cancer Center in Poznan and Polish Society of Radiation Oncology. 2020;25(3):422-7.
134. Hartman J, Frishman WH. Inflammation and atherosclerosis: a review of the role of interleukin-6 in the development of atherosclerosis and the potential for targeted drug therapy. Cardiology in review. 2014;22(3):147-51.
135. Zhang JC, Yao W, Dong C, Yang C, Ren Q, Ma M, et al. Blockade of interleukin-6 receptor in the periphery promotes rapid and sustained antidepressant actions: a possible role of gut-microbiota-brain axis. Translational psychiatry. 2017;7(5):e1138.
136. Blum-Degen D, Müller T, Kuhn W, Gerlach M, Przuntek H, Riederer P. Interleukin-1 beta and interleukin-6 are elevated in the cerebrospinal fluid of Alzheimer's and de novo Parkinson's disease patients. Neurosci Lett. 1995;202(1-2):17-20.
137. Franceschi C, Campisi J. Chronic inflammation (inflammaging) and its potential contribution to age-associated diseases. J Gerontol A Biol Sci Med Sci. 2014;69 Suppl 1:S4-9.

138. Spalding KL, Bhardwaj RD, Buchholz BA, Druid H, Frisen J. Retrospective birth dating of cells in humans. Cell. 2005;122(1):133-43.
139. Bowen RL, Atwood CS. Living and dying for sex. A theory of aging based on the modulation of cell cycle signaling by reproductive hormones. Gerontology. 2004;50(5):265-90.
140. Lopez-Otin C, Blasco MA, Partridge L, Serrano M, Kroemer G. The hallmarks of aging. Cell. 2013;153(6):1194-217.
141. Franceschi C, Garagnani P, Parini P, Giuliani C, Santoro A. Inflammaging: a new immune-metabolic viewpoint for age-related diseases. Nat Rev Endocrinol. 2018;14(10):576-90.
142. Franceschi C, Capri M, Monti D, Giunta S, Olivieri F, Sevini F, et al. Inflammaging and anti-inflammaging: a systemic perspective on aging and longevity emerged from studies in humans. Mech Ageing Dev. 2007;128(1):92-105.
143. Anderson DH, Mullins RF, Hageman GS, Johnson LV. A role for local inflammation in the formation of drusen in the aging eye. Am J Ophthalmol. 2002;134(3):411-31.
144. Penfold PL, Killingsworth MC, Sarks SH. Senile macular degeneration: the involvement of immunocompetent cells. Graefes Arch Clin Exp Ophthalmol. 1985;223(2):69-76.
145. Penfold PL, Liew SC, Madigan MC, Provis JM. Modulation of major histocompatibility complex class II expression in retinas with age-related macular degeneration. Invest Ophthalmol Vis Sci. 1997;38(10):2125-33.
146. Tuo J, Grob S, Zhang K, Chan CC. Genetics of immunological and inflammatory components in age-related macular degeneration. Ocul Immunol Inflamm. 2012;20(1):27-36.
147. Perez VL, Caspi RR. Immune mechanisms in inflammatory and degenerative eye disease. Trends Immunol. 2015;36(6):354-63.
148. Taylor AW. Ocular immune privilege. Eye (Lond). 2009;23(10):1885-9.
149. Knickelbein JE, Chan CC, Sen HN, Ferris FL, Nussenblatt RB. Inflammatory Mechanisms of Age-related Macular Degeneration. Int Ophthalmol Clin. 2015;55(3):63-78.
150. Limatola C, Ransohoff RM. Modulating neurotoxicity through CX3CL1/CX3CR1 signaling. Front Cell Neurosci. 2014;8:229.
151. Hu SJ, Calippe B, Lavalette S, Roubeix C, Montassar F, Housset M, et al. Upregulation of P2RX7 in Cx3cr1-Deficient Mononuclear Phagocytes Leads to Increased Interleukin-1β Secretion and Photoreceptor Neurodegeneration. J Neurosci. 2015;35(18):6987-96.
152. Fenn AM, Smith KM, Lovett-Racke AE, Guerau-de-Arellano M, Whitacre CC, Godbout JP. Increased micro-RNA 29b in the aged brain correlates with the reduction of insulin-like growth factor-1 and fractalkine ligand. Neurobiol Aging. 2013;34(12):2748-58.
153. Anastasopoulos E, Kakoulidou A, Coleman AL, Sinsheimer JS, Wilson MR, Yu F, et al. Association of sequence variation in the CX3CR1 gene with geographic atrophy age-related macular degeneration in a Greek population. Curr Eye Res. 2012;37(12):1148-55.
154. Combadière C, Feumi C, Raoul W, Keller N, Rodéro M, Pézard A, et al. CX3CR1-dependent subretinal microglia cell accumulation is associated with cardinal features of age-related macular degeneration. Journal of Clinical Investigation. 2007;117(10):2920-8.
155. Schaumberg DA, Rose L, DeAngelis MM, Semba RD, Hageman GS, Chasman DI. Prospective study of common variants in CX3CR1 and risk of macular degeneration: pooled analysis from 5 long-term studies. JAMA Ophthalmol. 2014;132(1):84-95.
156. Tuo J, Smith BC, Bojanowski CM, Meleth AD, Gery I, Csaky KG, et al. The involvement of sequence variation and expression of CX3CR1 in the pathogenesis of age-related macular degeneration. Faseb j. 2004;18(11):1297-9.
157. Zhang R, Wang LY, Wang YF, Wu CR, Lei CL, Wang MX, et al. Associations Between the T280M and V249I SNPs in CX3CR1 and the Risk of Age-Related Macular Degeneration. Invest Ophthalmol Vis Sci. 2015;56(9):5590-8.

158. Nagata S. Apoptosis by death factor. Cell. 1997;88(3):355-65.
159. Matsumoto H, Murakami Y, Kataoka K, Notomi S, Mantopoulos D, Trichonas G, et al. Membrane-bound and soluble Fas ligands have opposite functions in photoreceptor cell death following separation from the retinal pigment epithelium. Cell Death Dis. 2015;6(11):e1986.
160. Zacks DN, Zheng QD, Han Y, Bakhru R, Miller JW. FAS-mediated apoptosis and its relation to intrinsic pathway activation in an experimental model of retinal detachment. Invest Ophthalmol Vis Sci. 2004;45(12):4563-9.
161. Zacks DN, Boehlke C, Richards AL, Zheng QD. Role of the Fas-signaling pathway in photoreceptor neuroprotection. Arch Ophthalmol. 2007;125(10):1389-95.
162. Besirli CG, Chinskey ND, Zheng QD, Zacks DN. Inhibition of retinal detachment-induced apoptosis in photoreceptors by a small peptide inhibitor of the fas receptor. Invest Ophthalmol Vis Sci. 2010;51(4):2177-84.
163. Levy O, Calippe B, Lavalette S, Hu SJ, Raoul W, Dominguez E, et al. Apolipoprotein E promotes subretinal mononuclear phagocyte survival and chronic inflammation in age-related macular degeneration. EMBO molecular medicine. 2015;7(2):211-26.
164. Medzhitov R. Origin and physiological roles of inflammation. Nature. 2008;454(7203):428-35.
165. Gordon S, Plüddemann A, Firestein GS, Gabriel SE, McInnes IB, O'Dell JR. Chapter 10 - Mononuclear Phagocytes. Kelley and Firestein's textbook of rheumatology. Tenth edition. ed. Philadelphia, PA: Elsevier; 2017. p. 145-68.
166. Ginhoux F, Jung S. Monocytes and macrophages: developmental pathways and tissue homeostasis. Nat Rev Immunol. 2014;14(6):392-404.
167. Sunderkotter C, Steinbrink K, Goebeler M, Bhardwaj R, Sorg C. Macrophages and angiogenesis. J Leukoc Biol. 1994;55(3):410-22.
168. Corliss BA, Azimi MS, Munson JM, Peirce SM, Murfee WL. Macrophages: An Inflammatory Link Between Angiogenesis and Lymphangiogenesis. Microcirculation. 2016;23(2):95-121.
169. Italiani P, Boraschi D. From Monocytes to M1/M2 Macrophages: Phenotypical vs. Functional Differentiation. Frontiers in immunology. 2014;5:514.
170. Mosser DM, Edwards JP. Exploring the full spectrum of macrophage activation. Nat Rev Immunol. 2008;8(12):958-69.
171. Murray PJ. Macrophage Polarization. Annu Rev Physiol. 2017;79:541-66.
172. Martinez FO, Gordon S. The M1 and M2 paradigm of macrophage activation: time for reassessment. F1000Prime Rep. 2014;6:13.
173. Apte RS. Regulation of angiogenesis by macrophages. Adv Exp Med Biol. 2010;664:15-9.
174. Owen JL, Mohamadzadeh M. Macrophages and chemokines as mediators of angiogenesis. Front Physiol. 2013;4:159.
175. Spiller KL, Anfang RR, Spiller KJ, Ng J, Nakazawa KR, Daulton JW, et al. The role of macrophage phenotype in vascularization of tissue engineering scaffolds. Biomaterials. 2014;35(15):4477-88.
176. Bertani FR, Mozetic P, Fioramonti M, Iuliani M, Ribelli G, Pantano F, et al. Classification of M1/M2-polarized human macrophages by label-free hyperspectral reflectance confocal microscopy and multivariate analysis. Sci Rep. 2017;7(1):8965.
177. Heinrich F, Lehmbecker A, Raddatz BB, Kegler K, Tipold A, Stein VM, et al. Morphologic, phenotypic, and transcriptomic characterization of classically and alternatively activated canine blood-derived macrophages in vitro. PLoS One. 2017;12(8):e0183572.
178. Barros MH, Hauck F, Dreyer JH, Kempkes B, Niedobitek G. Macrophage polarisation: an immunohistochemical approach for identifying M1 and M2 macrophages. PLoS One. 2013;8(11):e80908.
179. Misharin AV, Morales-Nebreda L, Mutlu GM, Budinger GR, Perlman H. Flow cytometric analysis of macrophages and dendritic cell subsets in the mouse lung. American journal of respiratory cell and molecular biology. 2013;49(4):503-10.

180. Stöger JL, Gijbels MJ, van der Velden S, Manca M, van der Loos CM, Biessen EA, et al. Distribution of macrophage polarization markers in human atherosclerosis. Atherosclerosis. 2012;225(2):461-8.
181. Atri C, Guerfali FZ, Laouini D. Role of Human Macrophage Polarization in Inflammation during Infectious Diseases. Int J Mol Sci. 2018;19(6).
182. Vogel DY, Glim JE, Stavenuiter AW, Breur M, Heijnen P, Amor S, et al. Human macrophage polarization in vitro: maturation and activation methods compared. Immunobiology. 2014;219(9):695-703.
183. Tarique AA, Logan J, Thomas E, Holt PG, Sly PD, Fantino E. Phenotypic, functional, and plasticity features of classical and alternatively activated human macrophages. American journal of respiratory cell and molecular biology. 2015;53(5):676-88.
184. Martinez FO, Gordon S, Locati M, Mantovani A. Transcriptional profiling of the human monocyte-to-macrophage differentiation and polarization: new molecules and patterns of gene expression. J Immunol. 2006;177(10):7303-11.
185. Derlindati E, Dei Cas A, Montanini B, Spigoni V, Curella V, Aldigeri R, et al. Transcriptomic analysis of human polarized macrophages: more than one role of alternative activation? PLoS One. 2015;10(3):e0119751.
186. Beyer M, Mallmann MR, Xue J, Staratschek-Jox A, Vorholt D, Krebs W, et al. High-resolution transcriptome of human macrophages. PLoS One. 2012;7(9):e45466.
187. Biswas SK, Chittezhath M, Shalova IN, Lim J-Y. Macrophage polarization and plasticity in health and disease. Immunologic Research. 2012;53(1):11-24.
188. Tugal D, Liao X, Jain MK. Transcriptional control of macrophage polarization. Arterioscler Thromb Vasc Biol. 2013;33(6):1135-44.
189. Kumar A, Zhao L, Fariss RN, McMenamin PG, Wong WT. Vascular associations and dynamic process motility in perivascular myeloid cells of the mouse choroid: implications for function and senescent change. Invest Ophthalmol Vis Sci. 2014;55(3):1787-96.
190. Chow A, Brown BD, Merad M. Studying the mononuclear phagocyte system in the molecular age. Nat Rev Immunol. 2011;11(11):788-98.
191. Madeira MH, Boia R, Santos PF, Ambrosio AF, Santiago AR. Contribution of microglia-mediated neuroinflammation to retinal degenerative diseases. Mediators Inflamm. 2015;2015:673090.
192. Ginhoux F, Prinz M. Origin of microglia: current concepts and past controversies. Cold Spring Harb Perspect Biol. 2015;7(8):a020537.
193. Wang X, Zhao L, Zhang J, Fariss RN, Ma W, Kretschmer F, et al. Requirement for Microglia for the Maintenance of Synaptic Function and Integrity in the Mature Retina. J Neurosci. 2016;36(9):2827-42.
194. Ajami B, Bennett JL, Krieger C, Tetzlaff W, Rossi FM. Local self-renewal can sustain CNS microglia maintenance and function throughout adult life. Nat Neurosci. 2007;10(12):1538-43.
195. Mildner A, Schmidt H, Nitsche M, Merkler D, Hanisch UK, Mack M, et al. Microglia in the adult brain arise from Ly-6ChiCCR2+ monocytes only under defined host conditions. Nat Neurosci. 2007;10(12):1544-53.
196. Reu P, Khosravi A, Bernard S, Mold JE, Salehpour M, Alkass K, et al. The Lifespan and Turnover of Microglia in the Human Brain. Cell Rep. 2017;20(4):779-84.
197. Karlstetter M, Scholz R, Rutar M, Wong WT, Provis JM, Langmann T. Retinal microglia: just bystander or target for therapy? Prog Retin Eye Res. 2015;45:30-57.
198. Hume DA, Perry VH, Gordon S. Immunohistochemical localization of a macrophage-specific antigen in developing mouse retina: phagocytosis of dying neurons and differentiation of microglial cells to form a regular array in the plexiform layers. J Cell Biol. 1983;97(1):253-7.
199. Sennlaub F, Auvynet C, Calippe B, Lavalette S, Poupel L, Hu SJ, et al. CCR2(+) monocytes infiltrate atrophic lesions in age-related macular disease and mediate photoreceptor degeneration in

experimental subretinal inflammation in Cx3cr1 deficient mice. EMBO molecular medicine. 2013;5(11):1775-93.
200. Matcovitch-Natan O, Winter DR, Giladi A, Vargas Aguilar S, Spinrad A, Sarrazin S, et al. Microglia development follows a stepwise program to regulate brain homeostasis. Science. 2016;353(6301):aad8670.
201. Akhtar-Schafer I, Wang L, Krohne TU, Xu H, Langmann T. Modulation of three key innate immune pathways for the most common retinal degenerative diseases. EMBO molecular medicine. 2018;10(10).
202. Copland DA, Theodoropoulou S, Liu J, Dick AD. A Perspective of AMD Through the Eyes of Immunology. Invest Ophthalmol Vis Sci. 2018;59(4):AMD83-AMD92.
203. Ferrer-Martin RM, Martin-Oliva D, Sierra-Martin A, Carrasco MC, Martin-Estebane M, Calvente R, et al. Microglial Activation Promotes Cell Survival in Organotypic Cultures of Postnatal Mouse Retinal Explants. PLoS One. 2015;10(8):e0135238.
204. Kohno H, Maeda T, Perusek L, Pearlman E, Maeda A. CCL3 production by microglial cells modulates disease severity in murine models of retinal degeneration. J Immunol. 2014;192(8):3816-27.
205. Gautier EL, Ivanov S, Lesnik P, Randolph GJ. Local apoptosis mediates clearance of macrophages from resolving inflammation in mice. Blood. 2013;122(15):2714-22.
206. Harada T, Harada C, Kohsaka S, Wada E, Yoshida K, Ohno S, et al. Microglia-Muller glia cell interactions control neurotrophic factor production during light-induced retinal degeneration. J Neurosci. 2002;22(21):9228-36.
207. Langmann T. Microglia activation in retinal degeneration. J Leukoc Biol. 2007;81(6):1345-51.
208. Wolf Y, Yona S, Kim KW, Jung S. Microglia, seen from the CX3CR1 angle. Front Cell Neurosci. 2013;7:26.
209. Yu C, Roubeix C, Sennlaub F, Saban DR. Microglia versus Monocytes: Distinct Roles in Degenerative Diseases of the Retina. Trends Neurosci. 2020;43(6):433-49.
210. Zhong Z, Zhang H, Hong M, Sun C, Xu Y, Chen X, et al. FNDC3B promotes epithelial-mesenchymal transition in tongue squamous cell carcinoma cells in a hypoxic microenvironment. Oncol Rep. 2018;39(4):1853-9.
211. Gupta N, Brown KE, Milam AH. Activated microglia in human retinitis pigmentosa, late-onset retinal degeneration, and age-related macular degeneration. Exp Eye Res. 2003;76(4):463-71.
212. Omri S, Behar-Cohen F, de Kozak Y, Sennlaub F, Verissimo LM, Jonet L, et al. Microglia/macrophages migrate through retinal epithelium barrier by a transcellular route in diabetic retinopathy: role of PKCzeta in the Goto Kakizaki rat model. Am J Pathol. 2011;179(2):942-53.
213. Andriessen EM, Wilson AM, Mawambo G, Dejda A, Miloudi K, Sennlaub F, et al. Gut microbiota influences pathological angiogenesis in obesity-driven choroidal neovascularization. EMBO molecular medicine. 2016;8(12):1366-79.
214. Donoso LA, Kim D, Frost A, Callahan A, Hageman G. The role of inflammation in the pathogenesis of age-related macular degeneration. Surv Ophthalmol. 2006;51(2):137-52.
215. Liu J, Copland DA, Horie S, Wu WK, Chen M, Xu Y, et al. Myeloid cells expressing VEGF and arginase-1 following uptake of damaged retinal pigment epithelium suggests potential mechanism that drives the onset of choroidal angiogenesis in mice. PLoS One. 2013;8(8):e72935.
216. Sato T, Takeuchi M, Karasawa Y, Enoki T, Ito M. Intraocular inflammatory cytokines in patients with neovascular age-related macular degeneration before and after initiation of intravitreal injection of anti-VEGF inhibitor. Sci Rep. 2018;8(1):1098.
217. Scholz R, Caramoy A, Bhuckory MB, Rashid K, Chen M, Xu H, et al. Targeting translocator protein (18 kDa) (TSPO) dampens pro-inflammatory microglia reactivity in the retina and protects from degeneration. J Neuroinflammation. 2015;12:201.

218. Madeira MH, Rashid K, Ambrosio AF, Santiago AR, Langmann T. Blockade of microglial adenosine A2A receptor impacts inflammatory mechanisms, reduces ARPE-19 cell dysfunction and prevents photoreceptor loss in vitro. Sci Rep. 2018;8(1):2272.
219. Brown GC, Neher JJ. Eaten alive! Cell death by primary phagocytosis: 'phagoptosis'. Trends Biochem Sci. 2012;37(8):325-32.
220. Brown GC, Neher JJ. Microglial phagocytosis of live neurons. Nat Rev Neurosci. 2014;15(4):209-16.
221. Allan SM, Tyrrell PJ, Rothwell NJ. Interleukin-1 and neuronal injury. Nat Rev Immunol. 2005;5(8):629-40.
222. Schweighofer B, Testori J, Sturtzel C, Sattler S, Mayer H, Wagner O, et al. The VEGF-induced transcriptional response comprises gene clusters at the crossroad of angiogenesis and inflammation. Thrombosis and haemostasis. 2009;102(3):544-54.
223. Olson JL, Courtney RJ, Rouhani B, Mandava N, Dinarello CA. Intravitreal anakinra inhibits choroidal neovascular membrane growth in a rat model. Ocul Immunol Inflamm. 2009;17(3):195-200.
224. Lavalette S, Raoul W, Houssier M, Camelo S, Levy O, Calippe B, et al. Interleukin-1β inhibition prevents choroidal neovascularization and does not exacerbate photoreceptor degeneration. Am J Pathol. 2011;178(5):2416-23.
225. Simi A, Tsakiri N, Wang P, Rothwell NJ. Interleukin-1 and inflammatory neurodegeneration. Biochem Soc Trans. 2007;35(Pt 5):1122-6.
226. Simi A, Lerouet D, Pinteaux E, Brough D. Mechanisms of regulation for interleukin-1beta in neurodegenerative disease. Neuropharmacology. 2007;52(8):1563-9.
227. Eandi CM, Charles Messance H, Augustin S, Dominguez E, Lavalette S, Forster V, et al. Subretinal mononuclear phagocytes induce cone segment loss via IL-1β. Elife. 2016;5.
228. Lichtlen P, Lam TT, Nork TM, Streit T, Urech DM. Relative contribution of VEGF and TNF-alpha in the cynomolgus laser-induced CNV model: comparing the efficacy of bevacizumab, adalimumab, and ESBA105. Invest Ophthalmol Vis Sci. 2010;51(9):4738-45.
229. Shi X, Semkova I, Müther PS, Dell S, Kociok N, Joussen AM. Inhibition of TNF-alpha reduces laser-induced choroidal neovascularization. Exp Eye Res. 2006;83(6):1325-34.
230. Cousins SW, Espinosa-Heidmann DG, Csaky KG. Monocyte activation in patients with age-related macular degeneration: a biomarker of risk for choroidal neovascularization? Arch Ophthalmol. 2004;122(7):1013-8.
231. Lad EM, Cousins SW, Van Arnam JS, Proia AD. Abundance of infiltrating CD163+ cells in the retina of postmortem eyes with dry and neovascular age-related macular degeneration. Graefes Arch Clin Exp Ophthalmol. 2015;253(11):1941-5.
232. Mathis T, Housset M, Eandi C, Beguier F, Touhami S, Reichman S, et al. Activated monocytes resist elimination by retinal pigment epithelium and downregulate their OTX2 expression via TNF-α. Aging Cell. 2017;16(1):173-82.
233. Izumi-Nagai K, Nagai N, Ozawa Y, Mihara M, Ohsugi Y, Kurihara T, et al. Interleukin-6 receptor-mediated activation of signal transducer and activator of transcription-3 (STAT3) promotes choroidal neovascularization. Am J Pathol. 2007;170(6):2149-58.
234. Thomas SJ, Snowden JA, Zeidler MP, Danson SJ. The role of JAK/STAT signalling in the pathogenesis, prognosis and treatment of solid tumours. Br J Cancer. 2015;113(3):365-71.
235. Miao H, Tao Y, Li XX. Inflammatory cytokines in aqueous humor of patients with choroidal neovascularization. Mol Vis. 2012;18:574-80.
236. Chalam KV, Grover S, Sambhav K, Balaiya S, Murthy RK. Aqueous interleukin-6 levels are superior to vascular endothelial growth factor in predicting therapeutic response to bevacizumab in age-related macular degeneration. J Ophthalmol. 2014;2014:502174.

237. Bluher M. Obesity: global epidemiology and pathogenesis. Nat Rev Endocrinol. 2019;15(5):288-98.
238. Hruby A, Hu FB. The Epidemiology of Obesity: A Big Picture. Pharmacoeconomics. 2015;33(7):673-89.
239. World-Health-Organization. Obesity and Overweight [Available from: https://www.who.int/blindness/causes/priority/en/index7.html.
240. Schwartz MW, Seeley RJ, Zeltser LM, Drewnowski A, Ravussin E, Redman LM, et al. Obesity Pathogenesis: An Endocrine Society Scientific Statement. Endocr Rev. 2017;38(4):267-96.
241. Centers-for-Disease-Control-and-Prevention. Defining adult overweight and obesity [Available from: www.cdc.gov/obesity/adult/defining.html.
242. Kim DD, Basu A. Estimating the Medical Care Costs of Obesity in the United States: Systematic Review, Meta-Analysis, and Empirical Analysis. Value Health. 2016;19(5):602-13.
243. Hotamisligil GS. Inflammation, metaflammation and immunometabolic disorders. Nature. 2017;542(7640):177-85.
244. Hotamisligil GS. Inflammation and metabolic disorders. Nature. 2006;444(7121):860-7.
245. Lumeng CN, Saltiel AR. Inflammatory links between obesity and metabolic disease. J Clin Invest. 2011;121(6):2111-7.
246. Lackey DE, Olefsky JM. Regulation of metabolism by the innate immune system. Nat Rev Endocrinol. 2016;12(1):15-28.
247. Saltiel AR, Olefsky JM. Inflammatory mechanisms linking obesity and metabolic disease. J Clin Invest. 2017;127(1):1-4.
248. Singer K, Lumeng CN. The initiation of metabolic inflammation in childhood obesity. J Clin Invest. 2017;127(1):65-73.
249. Zhou H, Urso CJ, Jadeja V. Saturated Fatty Acids in Obesity-Associated Inflammation. J Inflamm Res. 2020;13:1-14.
250. Rogero MM, Calder PC. Obesity, Inflammation, Toll-Like Receptor 4 and Fatty Acids. Nutrients. 2018;10(4).
251. Shi H, Kokoeva MV, Inouye K, Tzameli I, Yin H, Flier JS. TLR4 links innate immunity and fatty acid-induced insulin resistance. J Clin Invest. 2006;116(11):3015-25.
252. Lee YS, Kim JW, Osborne O, Oh DY, Sasik R, Schenk S, et al. Increased adipocyte O2 consumption triggers HIF-1alpha, causing inflammation and insulin resistance in obesity. Cell. 2014;157(6):1339-52.
253. He Q, Gao Z, Yin J, Zhang J, Yun Z, Ye J. Regulation of HIF-1{alpha} activity in adipose tissue by obesity-associated factors: adipogenesis, insulin, and hypoxia. Am J Physiol Endocrinol Metab. 2011;300(5):E877-85.
254. Sun K, Kusminski CM, Scherer PE. Adipose tissue remodeling and obesity. J Clin Invest. 2011;121(6):2094-101.
255. Cani PD, Possemiers S, Van de Wiele T, Guiot Y, Everard A, Rottier O, et al. Changes in gut microbiota control inflammation in obese mice through a mechanism involving GLP-2-driven improvement of gut permeability. Gut. 2009;58(8):1091-103.
256. Amar J, Chabo C, Waget A, Klopp P, Vachoux C, Bermudez-Humaran LG, et al. Intestinal mucosal adherence and translocation of commensal bacteria at the early onset of type 2 diabetes: molecular mechanisms and probiotic treatment. EMBO molecular medicine. 2011;3(9):559-72.
257. Tada H, Takeuchi S, Takagi M, Isogai S. The effect of glycemic control on plasma soluble fibrin monomer complexes and fibronectin in diabetic patients. Tohoku J Exp Med. 1987;153(2):145-50.
258. Delcourt C, Michel F, Colvez A, Lacroux A, Delage M, Vernet MH. Associations of cardiovascular disease and its risk factors with age-related macular degeneration: the POLA study. Ophthalmic epidemiology. 2001;8(4):237-49.

259. Paunksnis A, Cimbalas A, Cerniauskiene LR, Luksiene DI, Margeviciene L, Domarkiene S, et al. Early age-related maculopathy and risk factors of cardiovascular disease in middle-aged Lithuanian urban population. European journal of ophthalmology. 2005;15(2):255-62.
260. Klein R, Klein BE, Jensen SC. The relation of cardiovascular disease and its risk factors to the 5-year incidence of age-related maculopathy: the Beaver Dam Eye Study. Ophthalmology. 1997;104(11):1804-12.
261. Klein R, Klein BE, Tomany SC, Cruickshanks KJ. The association of cardiovascular disease with the long-term incidence of age-related maculopathy: the Beaver Dam Eye Study. Ophthalmology. 2003;110(6):1273-80.
262. Schaumberg DA, Christen WG, Hankinson SE, Glynn RJ. Body mass index and the incidence of visually significant age-related maculopathy in men. Arch Ophthalmol. 2001;119(9):1259-65.
263. Clemons TE, Milton RC, Klein R, Seddon JM, Ferris FL, 3rd. Risk factors for the incidence of Advanced Age-Related Macular Degeneration in the Age-Related Eye Disease Study (AREDS) AREDS report no. 19. Ophthalmology. 2005;112(4):533-9.
264. Peeters A, Magliano DJ, Stevens J, Duncan BB, Klein R, Wong TY. Changes in abdominal obesity and age-related macular degeneration: the Atherosclerosis Risk in Communities Study. Arch Ophthalmol. 2008;126(11):1554-60.
265. Smith W, Mitchell P, Leeder SR, Wang JJ. Plasma fibrinogen levels, other cardiovascular risk factors, and age-related maculopathy: the Blue Mountains Eye Study. Arch Ophthalmol. 1998;116(5):583-7.
266. Seddon JM, Cote J, Davis N, Rosner B. Progression of age-related macular degeneration: association with body mass index, waist circumference, and waist-hip ratio. Arch Ophthalmol. 2003;121(6):785-92.
267. Hirvelä H, Luukinen H, Läärä E, Sc L, Laatikainen L. Risk factors of age-related maculopathy in a population 70 years of age or older. Ophthalmology. 1996;103(6):871-7.
268. Klein BE, Klein R, Lee KE, Jensen SC. Measures of obesity and age-related eye diseases. Ophthalmic epidemiology. 2001;8(4):251-62.
269. Klein R, Deng Y, Klein BE, Hyman L, Seddon J, Frank RN, et al. Cardiovascular disease, its risk factors and treatment, and age-related macular degeneration: Women's Health Initiative Sight Exam ancillary study. Am J Ophthalmol. 2007;143(3):473-83.
270. Zhang QY, Tie LJ, Wu SS, Lv PL, Huang HW, Wang WQ, et al. Overweight, Obesity, and Risk of Age-Related Macular Degeneration. Invest Ophthalmol Vis Sci. 2016;57(3):1276-83.
271. Miyazaki M, Nakamura H, Kubo M, Kiyohara Y, Oshima Y, Ishibashi T, et al. Risk factors for age related maculopathy in a Japanese population: the Hisayama study. Br J Ophthalmol. 2003;87(4):469-72.
272. Tan JS, Mitchell P, Smith W, Wang JJ. Cardiovascular risk factors and the long-term incidence of age-related macular degeneration: the Blue Mountains Eye Study. Ophthalmology. 2007;114(6):1143-50.
273. Tomany SC, Wang JJ, Van Leeuwen R, Klein R, Mitchell P, Vingerling JR, et al. Risk factors for incident age-related macular degeneration: pooled findings from 3 continents. Ophthalmology. 2004;111(7):1280-7.
274. Moeini HA, Masoudpour H, Ghanbari H. A study of the relation between body mass index and the incidence of age related macular degeneration. Br J Ophthalmol. 2005;89(8):964-6.
275. Garn SM, Leonard WR, Hawthorne VM. Three limitations of the body mass index. Am J Clin Nutr. 1986;44(6):996-7.
276. Scaldaferri F, Pizzoferrato M, Gerardi V, Lopetuso L, Gasbarrini A. The gut barrier: new acquisitions and therapeutic approaches. J Clin Gastroenterol. 2012;46 Suppl:S12-7.

277. Graziani C, Talocco C, De Sire R, Petito V, Lopetuso LR, Gervasoni J, et al. Intestinal permeability in physiological and pathological conditions: major determinants and assessment modalities. Eur Rev Med Pharmacol Sci. 2019;23(2):795-810.
278. Tsukita S, Furuse M, Itoh M. Multifunctional strands in tight junctions. Nat Rev Mol Cell Biol. 2001;2(4):285-93.
279. Arrieta MC, Bistritz L, Meddings JB. Alterations in intestinal permeability. Gut. 2006;55(10):1512-20.
280. Anderson JM. Molecular structure of tight junctions and their role in epithelial transport. News in physiological sciences : an international journal of physiology produced jointly by the International Union of Physiological Sciences and the American Physiological Society. 2001;16:126-30.
281. Tsukita S, Furuse M. The structure and function of claudins, cell adhesion molecules at tight junctions. Ann N Y Acad Sci. 2000;915:129-35.
282. Holmes JL, Van Itallie CM, Rasmussen JE, Anderson JM. Claudin profiling in the mouse during postnatal intestinal development and along the gastrointestinal tract reveals complex expression patterns. Gene expression patterns : GEP. 2006;6(6):581-8.
283. Mitic LL, Van Itallie CM, Anderson JM. Molecular physiology and pathophysiology of tight junctions I. Tight junction structure and function: lessons from mutant animals and proteins. Am J Physiol Gastrointest Liver Physiol. 2000;279(2):G250-4.
284. Bruewer M, Luegering A, Kucharzik T, Parkos CA, Madara JL, Hopkins AM, et al. Proinflammatory cytokines disrupt epithelial barrier function by apoptosis-independent mechanisms. J Immunol. 2003;171(11):6164-72.
285. Nusrat A, Turner JR, Madara JL. Molecular physiology and pathophysiology of tight junctions. IV. Regulation of tight junctions by extracellular stimuli: nutrients, cytokines, and immune cells. Am J Physiol Gastrointest Liver Physiol. 2000;279(5):G851-7.
286. Collins SM. Stress and the Gastrointestinal Tract IV. Modulation of intestinal inflammation by stress: basic mechanisms and clinical relevance. Am J Physiol Gastrointest Liver Physiol. 2001;280(3):G315-8.
287. Santos J, Yang PC, Söderholm JD, Benjamin M, Perdue MH. Role of mast cells in chronic stress induced colonic epithelial barrier dysfunction in the rat. Gut. 2001;48(5):630-6.
288. Sonoda N, Furuse M, Sasaki H, Yonemura S, Katahira J, Horiguchi Y, et al. Clostridium perfringens enterotoxin fragment removes specific claudins from tight junction strands: Evidence for direct involvement of claudins in tight junction barrier. J Cell Biol. 1999;147(1):195-204.
289. Fasano A, Nataro JP. Intestinal epithelial tight junctions as targets for enteric bacteria-derived toxins. Advanced drug delivery reviews. 2004;56(6):795-807.
290. Floyd JL, Grant MB. The Gut-Eye Axis: Lessons Learned from Murine Models. Ophthalmology and therapy. 2020;9(3):499-513.
291. Cani PD. Human gut microbiome: hopes, threats and promises. Gut. 2018;67(9):1716-25.
292. Natividad JM, Verdu EF. Modulation of intestinal barrier by intestinal microbiota: pathological and therapeutic implications. Pharmacol Res. 2013;69(1):42-51.
293. Camilleri M, Lyle BJ, Madsen KL, Sonnenburg J, Verbeke K, Wu GD. Role for diet in normal gut barrier function: developing guidance within the framework of food-labeling regulations. Am J Physiol Gastrointest Liver Physiol. 2019;317(1):G17-g39.
294. David L, Maurice C, Carmody R, Gootenberg D, Button J, Wolfe B, et al. Diet rapidly and reproducibly alters the human gut microbiome. Nature. 2014;505(7484):559-63.
295. Wu GD, Chen J, Hoffmann C, Bittinger K, Chen YY, Keilbaugh SA, et al. Linking long-term dietary patterns with gut microbial enterotypes. Science. 2011;334(6052):105-8.
296. Bischoff SC, Barbara G, Buurman W, Ockhuizen T, Schulzke JD, Serino M, et al. Intestinal permeability--a new target for disease prevention and therapy. BMC Gastroenterol. 2014;14:189.

297. Fiorucci S, Mencarelli A, Palladino G, Cipriani S. Bile-acid-activated receptors: targeting TGR5 and farnesoid-X-receptor in lipid and glucose disorders. Trends Pharmacol Sci. 2009;30(11):570-80.
298. Cohen ME, Hathway JM, Salmasian H, Liu J, Terry M, Abrams JA, et al. Prophylaxis for Stress Ulcers With Proton Pump Inhibitors Is Not Associated With Increased Risk of Bloodstream Infections in the Intensive Care Unit. Clinical gastroenterology and hepatology : the official clinical practice journal of the American Gastroenterological Association. 2017;15(7):1030-6.e1.
299. Araki Y, Fujiyama Y, Andoh A, Nakamura F, Shimada M, Takaya H, et al. Hydrophilic and hydrophobic bile acids exhibit different cytotoxicities through cytolysis, interleukin-8 synthesis and apoptosis in the intestinal epithelial cell lines. IEC-6 and Caco-2 cells. Scandinavian journal of gastroenterology. 2001;36(5):533-9.
300. Raimondi F, Santoro P, Barone MV, Pappacoda S, Barretta ML, Nanayakkara M, et al. Bile acids modulate tight junction structure and barrier function of Caco-2 monolayers via EGFR activation. Am J Physiol Gastrointest Liver Physiol. 2008;294(4):G906-13.
301. Fujiyama Y, Hokari R, Miura S, Watanabe C, Komoto S, Oyama T, et al. Butter feeding enhances TNF-alpha production from macrophages and lymphocyte adherence in murine small intestinal microvessels. Journal of gastroenterology and hepatology. 2007;22(11):1838-45.
302. Kawano Y, Nakae J, Watanabe N, Kikuchi T, Tateya S, Tamori Y, et al. Colonic Pro-inflammatory Macrophages Cause Insulin Resistance in an Intestinal Ccl2/Ccr2-Dependent Manner. Cell Metab. 2016;24(2):295-310.
303. Yoshida H, Miura S, Kishikawa H, Hirokawa M, Nakamizo H, Nakatsumi RC, et al. Fatty acids enhance GRO/CINC-1 and interleukin-6 production in rat intestinal epithelial cells. J Nutr. 2001;131(11):2943-50.
304. Luck H, Tsai S, Chung J, Clemente-Casares X, Ghazarian M, Revelo XS, et al. Regulation of obesity-related insulin resistance with gut anti-inflammatory agents. Cell Metab. 2015;21(4):527-42.
305. Hamilton MK, Boudry G, Lemay DG, Raybould HE. Changes in intestinal barrier function and gut microbiota in high-fat diet-fed rats are dynamic and region dependent. Am J Physiol Gastrointest Liver Physiol. 2015;308(10):G840-51.
306. Peluso I, Raguzzini A, Villano DV, Cesqui E, Toti E, Catasta G, et al. High fat meal increase of IL-17 is prevented by ingestion of fruit juice drink in healthy overweight subjects. Current pharmaceutical design. 2012;18(1):85-90.
307. Zou J, Chassaing B, Singh V, Pellizzon M, Ricci M, Fythe MD, et al. Fiber-Mediated Nourishment of Gut Microbiota Protects against Diet-Induced Obesity by Restoring IL-22-Mediated Colonic Health. Cell Host Microbe. 2018;23(1):41-53.e4.
308. Rohr MW, Narasimhulu CA, Rudeski-Rohr TA, Parthasarathy S. Negative Effects of a High-Fat Diet on Intestinal Permeability: A Review. Adv Nutr. 2020;11(1):77-91.
309. de La Serre CB, Ellis CL, Lee J, Hartman AL, Rutledge JC, Raybould HE. Propensity to high-fat diet-induced obesity in rats is associated with changes in the gut microbiota and gut inflammation. Am J Physiol Gastrointest Liver Physiol. 2010;299(2):G440-8.
310. Murphy EA, Velazquez KT, Herbert KM. Influence of high-fat diet on gut microbiota: a driving force for chronic disease risk. Curr Opin Clin Nutr Metab Care. 2015;18(5):515-20.
311. Brody H. The gut microbiome. Nature. 2020;577(7792):S5.
312. LEDERBERG J, and ALEXA T. MCCRAY. . "`Ome Sweet `Omics--A Genealogical Treasury of Words.". The Scientist. 2 Apr. 2001;vol. 15, no. 7:8.
313. Blum HE. The human microbiome. Advances in medical sciences. 2017;62(2):414-20.
314. Bäckhed F, Ley RE, Sonnenburg JL, Peterson DA, Gordon JI. Host-bacterial mutualism in the human intestine. Science. 2005;307(5717):1915-20.
315. Whitman WB, Coleman DC, Wiebe WJ. Prokaryotes: the unseen majority. Proc Natl Acad Sci U S A. 1998;95(12):6578-83.

316. Costello EK, Stagaman K, Dethlefsen L, Bohannan BJ, Relman DA. The application of ecological theory toward an understanding of the human microbiome. Science. 2012;336(6086):1255-62.
317. Sender R, Fuchs S, Milo R. Revised Estimates for the Number of Human and Bacteria Cells in the Body. PLoS Biol. 2016;14(8):e1002533.
318. Carding S, Verbeke K, Vipond DT, Corfe BM, Owen LJ. Dysbiosis of the gut microbiota in disease. Microb Ecol Health Dis. 2015;26:26191.
319. Hooper LV, Gordon JI. Commensal host-bacterial relationships in the gut. Science. 2001;292(5519):1115-8.
320. The gut microbiome. Nature. 2020;577(7792).
321. Dolgin E. Fighting cancer with microbes. Nature. 2020;577(7792):S16-s8.
322. Bender E. Could a bacteria-stuffed pill cure autoimmune diseases? Nature. 2020;577(7792):S12-s3.
323. Svoboda E. Could the gut microbiome be linked to autism? Nature. 2020;577(7792):S14-s5.
324. Savage N. The complex relationship between drugs and the microbiome. Nature. 2020;577(7792):S10-s1.
325. Eisenstein M. The hunt for a healthy microbiome. Nature. 2020;577(7792):S6-s8.
326. Turnbaugh PJ. Diet should be a tool for researchers, not a treatment. Nature. 2020;577(7792):S23.
327. Lin Z, Iqbal Z, Ortiz JF, Khan SA, Jahan N. Fecal Microbiota Transplantation in Recurrent Clostridium Difficile Infection: Is it Superior to Other Conventional Methods? Cureus. 2020;12(8):e9653.
328. O'Hara AM, Shanahan F. The gut flora as a forgotten organ. EMBO reports. 2006;7(7):688-93.
329. Aagaard K, Ma J, Antony KM, Ganu R, Petrosino J, Versalovic J. The placenta harbors a unique microbiome. Sci Transl Med. 2014;6(237):237ra65.
330. Putignani L, Carsetti R, Signore F, Manco M. Additional maternal and nonmaternal factors contribute to microbiota shaping in newborns. Proc Natl Acad Sci U S A. 2010;107(42):E159; author reply E60.
331. Jakobsson HE, Abrahamsson TR, Jenmalm MC, Harris K, Quince C, Jernberg C, et al. Decreased gut microbiota diversity, delayed Bacteroidetes colonisation and reduced Th1 responses in infants delivered by caesarean section. Gut. 2014;63(4):559-66.
332. Salminen S, Gibson GR, McCartney AL, Isolauri E. Influence of mode of delivery on gut microbiota composition in seven year old children. Gut. 2004;53(9):1388-9.
333. Dominguez-Bello MG, De Jesus-Laboy KM, Shen N, Cox LM, Amir A, Gonzalez A, et al. Partial restoration of the microbiota of cesarean-born infants via vaginal microbial transfer. Nat Med. 2016;22(3):250-3.
334. Koenig JE, Spor A, Scalfone N, Fricker AD, Stombaugh J, Knight R, et al. Succession of microbial consortia in the developing infant gut microbiome. Proc Natl Acad Sci U S A. 2011;108 Suppl 1:4578-85.
335. Rodriguez JM, Murphy K, Stanton C, Ross RP, Kober OI, Juge N, et al. The composition of the gut microbiota throughout life, with an emphasis on early life. Microb Ecol Health Dis. 2015;26:26050.
336. Thursby E, Juge N. Introduction to the human gut microbiota. Biochem J. 2017;474(11):1823-36.
337. Turnbaugh P, Ridaura V, Faith J, Rey F, Knight R, Gordon J. The effect of diet on the human gut microbiome: a metagenomic analysis in humanized gnotobiotic mice. Science translational medicine. 2009;1(6):6-.
338. Evans C, LePard K, Kwak J, Stancukas M, Laskowski S, Dougherty J, et al. Exercise prevents weight gain and alters the gut microbiota in a mouse model of high fat diet-induced obesity. PLoS One. 2014;9(3):e92193-e.
339. Holmes A, Finger C, Morales-Scheihing D, Lee J, McCullough LD. Gut dysbiosis and age-related neurological diseases; an innovative approach for therapeutic interventions. Translational research : the journal of laboratory and clinical medicine. 2020.

340. Osman MA, Neoh HM, Ab Mutalib NS, Chin SF, Jamal R. 16S rRNA Gene Sequencing for Deciphering the Colorectal Cancer Gut Microbiome: Current Protocols and Workflows. Front Microbiol. 2018;9:767.
341. Woese CR, Olsen GJ. Archaebacterial phylogeny: perspectives on the urkingdoms. Systematic and applied microbiology. 1986;7:161-77.
342. Woese CR, Fox GE. Phylogenetic structure of the prokaryotic domain: the primary kingdoms. Proc Natl Acad Sci U S A. 1977;74(11):5088-90.
343. Stahl DA, Lane DJ, Olsen GJ, Pace NR. Analysis of hydrothermal vent-associated symbionts by ribosomal RNA sequences. Science. 1984;224(4647):409-11.
344. Peterson J, Garges S, Giovanni M, McInnes P, Wang L, Schloss JA, et al. The NIH Human Microbiome Project. Genome research. 2009;19(12):2317-23.
345. Pei Z, Bini EJ, Yang L, Zhou M, Francois F, Blaser MJ. Bacterial biota in the human distal esophagus. Proc Natl Acad Sci U S A. 2004;101(12):4250-5.
346. Verhelst R, Verstraelen H, Claeys G, Verschraegen G, Delanghe J, Van Simaey L, et al. Cloning of 16S rRNA genes amplified from normal and disturbed vaginal microflora suggests a strong association between Atopobium vaginae, Gardnerella vaginalis and bacterial vaginosis. BMC Microbiol. 2004;4:16.
347. Faveri M, Mayer MP, Feres M, de Figueiredo LC, Dewhirst FE, Paster BJ. Microbiological diversity of generalized aggressive periodontitis by 16S rRNA clonal analysis. Oral microbiology and immunology. 2008;23(2):112-8.
348. Hyman RW, Fukushima M, Diamond L, Kumm J, Giudice LC, Davis RW. Microbes on the human vaginal epithelium. Proc Natl Acad Sci U S A. 2005;102(22):7952-7.
349. Virtanen S, Kalliala I, Nieminen P, Salonen A. Comparative analysis of vaginal microbiota sampling using 16S rRNA gene analysis. PLoS One. 2017;12(7):e0181477.
350. Ross AA, Müller KM, Weese JS, Neufeld JD. Comprehensive skin microbiome analysis reveals the uniqueness of human skin and evidence for phylosymbiosis within the class Mammalia. Proc Natl Acad Sci U S A. 2018;115(25):E5786-e95.
351. Mas-Lloret J, Obón-Santacana M, Ibáñez-Sanz G, Guinó E, Pato ML, Rodriguez-Moranta F, et al. Gut microbiome diversity detected by high-coverage 16S and shotgun sequencing of paired stool and colon sample. Scientific data. 2020;7(1):92.
352. Eckburg PB, Bik EM, Bernstein CN, Purdom E, Dethlefsen L, Sargent M, et al. Diversity of the human intestinal microbial flora. Science. 2005;308(5728):1635-8.
353. Ley RE, Backhed F, Turnbaugh P, Lozupone CA, Knight RD, Gordon JI. Obesity alters gut microbial ecology. Proc Natl Acad Sci U S A. 2005;102(31):11070-5.
354. Ley R, Turnbaugh P, Klein S, Gordon J. Microbial ecology: human gut microbes associated with obesity. Nature. 2006;444(7122):1022-3.
355. Turnbaugh PJ, Hamady M, Yatsunenko T, Cantarel BL, Duncan A, Ley RE, et al. A core gut microbiome in obese and lean twins. Nature. 2009;457(7228):480-4.
356. Donaldson GP, Lee SM, Mazmanian SK. Gut biogeography of the bacterial microbiota. Nat Rev Microbiol. 2016;14(1):20-32.
357. De Filippo C, Cavalieri D, Di Paola M, Ramazzotti M, Poullet JB, Massart S, et al. Impact of diet in shaping gut microbiota revealed by a comparative study in children from Europe and rural Africa. Proc Natl Acad Sci U S A. 2010;107(33):14691-6.
358. Burkitt DP. Epidemiology of large bowel disease: the role of fibre. Proc Nutr Soc. 1973;32(3):145-9.
359. Zoetendal EG, Raes J, van den Bogert B, Arumugam M, Booijink CC, Troost FJ, et al. The human small intestinal microbiota is driven by rapid uptake and conversion of simple carbohydrates. ISME J. 2012;6(7):1415-26.

360. Ley RE, Hamady M, Lozupone C, Turnbaugh PJ, Ramey RR, Bircher JS, et al. Evolution of mammals and their gut microbes. Science. 2008;320(5883):1647-51.
361. Yarza P, Yilmaz P, Pruesse E, Glöckner FO, Ludwig W, Schleifer KH, et al. Uniting the classification of cultured and uncultured bacteria and archaea using 16S rRNA gene sequences. Nat Rev Microbiol. 2014;12(9):635-45.
362. Qin J, Li R, Raes J, Arumugam M, Burgdorf KS, Manichanh C, et al. A human gut microbial gene catalogue established by metagenomic sequencing. Nature. 2010;464(7285):59-65.
363. Rajilić-Stojanović M, Smidt H, de Vos WM. Diversity of the human gastrointestinal tract microbiota revisited. Environ Microbiol. 2007;9(9):2125-36.
364. Zoetendal EG, Rajilic-Stojanovic M, de Vos WM. High-throughput diversity and functionality analysis of the gastrointestinal tract microbiota. Gut. 2008;57(11):1605-15.
365. Cani P, Bibiloni R, Knauf C, Waget A, Neyrinck A, Delzenne N, et al. Changes in gut microbiota control metabolic endotoxemia-induced inflammation in high-fat diet-induced obesity and diabetes in mice. Diabetes. 2008;57(6):1470-81.
366. Gkouskou KK, Deligianni C, Tsatsanis C, Eliopoulos AG. The gut microbiota in mouse models of inflammatory bowel disease. Front Cell Infect Microbiol. 2014;4:28.
367. Liu X, Zeng B, Zhang J, Li W, Mou F, Wang H, et al. Role of the Gut Microbiome in Modulating Arthritis Progression in Mice. Sci Rep. 2016;6:30594.
368. Schwarz Q, Ruhrberg C. Neuropilin, you gotta let me know: should I stay or should I go? Cell Adh Migr. 2010;4(1):61-6.
369. Raimondi C, Brash JT, Fantin A, Ruhrberg C. NRP1 function and targeting in neurovascular development and eye disease. Prog Retin Eye Res. 2016;52:64-83.
370. Roy S, Bag AK, Singh RK, Talmadge JE, Batra SK, Datta K. Multifaceted Role of Neuropilins in the Immune System: Potential Targets for Immunotherapy. Front Immunol. 2017;8:1228.
371. Takagi S, Tsuji T, Amagai T, Takamatsu T, Fujisawa H. Specific cell surface labels in the visual centers of Xenopus laevis tadpole identified using monoclonal antibodies. Dev Biol. 1987;122(1):90-100.
372. Kolodkin AL, Levengood DV, Rowe EG, Tai YT, Giger RJ, Ginty DD. Neuropilin is a semaphorin III receptor. Cell. 1997;90(4):753-62.
373. He Z, Tessier-Lavigne M. Neuropilin is a receptor for the axonal chemorepellent Semaphorin III. Cell. 1997;90(4):739-51.
374. Soker S, Takashima S, Miao HQ, Neufeld G, Klagsbrun M. Neuropilin-1 is expressed by endothelial and tumor cells as an isoform-specific receptor for vascular endothelial growth factor. Cell. 1998;92(6):735-45.
375. Oussa NA, Dahmani A, Gomis M, Richaud M, Andreev E, Navab-Daneshmand AR, et al. VEGF Requires the Receptor NRP-1 To Inhibit Lipopolysaccharide-Dependent Dendritic Cell Maturation. J Immunol. 2016;197(10):3927-35.
376. Yadav M, Louvet C, Davini D, Gardner JM, Martinez-Llordella M, Bailey-Bucktrout S, et al. Neuropilin-1 distinguishes natural and inducible regulatory T cells among regulatory T cell subsets in vivo. J Exp Med. 2012;209(10):1713-22, S1-19.
377. Renand A, Milpied P, Rossignol J, Bruneau J, Lemonnier F, Dussiot M, et al. Neuropilin-1 expression characterizes T follicular helper (Tfh) cells activated during B cell differentiation in human secondary lymphoid organs. PLoS One. 2013;8(12):e85589.
378. Casazza A, Laoui D, Wenes M, Rizzolio S, Bassani N, Mambretti M, et al. Impeding macrophage entry into hypoxic tumor areas by Sema3A/Nrp1 signaling blockade inhibits angiogenesis and restores antitumor immunity. Cancer Cell. 2013;24(6):695-709.
379. Wilson AM, Shao Z, Grenier V, Mawambo G, Daudelin JF, Dejda A, et al. Neuropilin-1 expression in adipose tissue macrophages protects against obesity and metabolic syndrome. Sci Immunol. 2018;3(21).

380. Lee P, Goishi K, Davidson AJ, Mannix R, Zon L, Klagsbrun M. Neuropilin-1 is required for vascular development and is a mediator of VEGF-dependent angiogenesis in zebrafish. Proc Natl Acad Sci U S A. 2002;99(16):10470-5.
381. Gluzman-Poltorak Z, Cohen T, Shibuya M, Neufeld G. Vascular endothelial growth factor receptor-1 and neuropilin-2 form complexes. J Biol Chem. 2001;276(22):18688-94.
382. Mamluk R, Gechtman Z, Kutcher ME, Gasiunas N, Gallagher J, Klagsbrun M. Neuropilin-1 binds vascular endothelial growth factor 165, placenta growth factor-2, and heparin via its b1b2 domain. J Biol Chem. 2002;277(27):24818-25.
383. Pruszak J. Neural surface antigens : from basic biology towards biomedical applications. London, UK ; San Diego, CA, USA: Elsevier/AP, Academic Press is an imprint of Elsevier; 2015. xvi, 235 pages p.
384. Soker S, Fidder H, Neufeld G, Klagsbrun M. Characterization of novel vascular endothelial growth factor (VEGF) receptors on tumor cells that bind VEGF165 via its exon 7-encoded domain. J Biol Chem. 1996;271(10):5761-7.
385. Glinka Y, Prud'homme GJ. Neuropilin-1 is a receptor for transforming growth factor beta-1, activates its latent form, and promotes regulatory T cell activity. J Leukoc Biol. 2008;84(1):302-10.
386. Ball SG, Bayley C, Shuttleworth CA, Kielty CM. Neuropilin-1 regulates platelet-derived growth factor receptor signalling in mesenchymal stem cells. Biochem J. 2010;427(1):29-40.
387. Muhl L, Folestad EB, Gladh H, Wang Y, Moessinger C, Jakobsson L, et al. Neuropilin 1 binds PDGF-D and is a co-receptor in PDGF-D-PDGFRbeta signaling. J Cell Sci. 2017;130(8):1365-78.
388. Ellis LM. The role of neuropilins in cancer. Mol Cancer Ther. 2006;5(5):1099-107.
389. Yazdani U, Terman JR. The semaphorins. Genome Biol. 2006;7(3):211.
390. Alto LT, Terman JR. Semaphorins and their Signaling Mechanisms. Methods Mol Biol. 2017;1493:1-25.
391. Tamagnone L, Artigiani S, Chen H, He Z, Ming GI, Song H, et al. Plexins are a large family of receptors for transmembrane, secreted, and GPI-anchored semaphorins in vertebrates. Cell. 1999;99(1):71-80.
392. Soker S, Miao HQ, Nomi M, Takashima S, Klagsbrun M. VEGF165 mediates formation of complexes containing VEGFR-2 and neuropilin-1 that enhance VEGF165-receptor binding. J Cell Biochem. 2002;85(2):357-68.
393. Gagnon ML, Bielenberg DR, Gechtman Z, Miao HQ, Takashima S, Soker S, et al. Identification of a natural soluble neuropilin-1 that binds vascular endothelial growth factor: In vivo expression and antitumor activity. Proc Natl Acad Sci U S A. 2000;97(6):2573-8.
394. Rossignol M, Gagnon ML, Klagsbrun M. Genomic organization of human neuropilin-1 and neuropilin-2 genes: identification and distribution of splice variants and soluble isoforms. Genomics. 2000;70(2):211-22.
395. Cackowski FC, Xu L, Hu B, Cheng SY. Identification of two novel alternatively spliced Neuropilin-1 isoforms. Genomics. 2004;84(1):82-94.
396. Chen H, Chedotal A, He Z, Goodman CS, Tessier-Lavigne M. Neuropilin-2, a novel member of the neuropilin family, is a high affinity receptor for the semaphorins Sema E and Sema IV but not Sema III. Neuron. 1997;19(3):547-59.
397. Gluzman-Poltorak Z, Cohen T, Herzog Y, Neufeld G. Neuropilin-2 is a receptor for the vascular endothelial growth factor (VEGF) forms VEGF-145 and VEGF-165 [corrected]. J Biol Chem. 2000;275(24):18040-5.
398. The Human Protein Atlas.
399. Kawasaki T, Kitsukawa T, Bekku Y, Matsuda Y, Sanbo M, Yagi T, et al. A requirement for neuropilin-1 in embryonic vessel formation. Development. 1999;126(21):4895-902.

400. Kitsukawa T, Shimizu M, Sanbo M, Hirata T, Taniguchi M, Bekku Y, et al. Neuropilin-semaphorin III/D-mediated chemorepulsive signals play a crucial role in peripheral nerve projection in mice. Neuron. 1997;19(5):995-1005.
401. Lampropoulou A, Ruhrberg C. Neuropilin regulation of angiogenesis. Biochem Soc Trans. 2014;42(6):1623-8.
402. Graziani G, Lacal PM. Neuropilin-1 as Therapeutic Target for Malignant Melanoma. Front Oncol. 2015;5:125.
403. Latil A, Bieche I, Pesche S, Valeri A, Fournier G, Cussenot O, et al. VEGF overexpression in clinically localized prostate tumors and neuropilin-1 overexpression in metastatic forms. Int J Cancer. 2000;89(2):167-71.
404. Lantuejoul S, Constantin B, Drabkin H, Brambilla C, Roche J, Brambilla E. Expression of VEGF, semaphorin SEMA3F, and their common receptors neuropilins NP1 and NP2 in preinvasive bronchial lesions, lung tumours, and cell lines. J Pathol. 2003;200(3):336-47.
405. Parikh AA, Fan F, Liu WB, Ahmad SA, Stoeltzing O, Reinmuth N, et al. Neuropilin-1 in human colon cancer: expression, regulation, and role in induction of angiogenesis. Am J Pathol. 2004;164(6):2139-51.
406. Stephenson JM, Banerjee S, Saxena NK, Cherian R, Banerjee SK. Neuropilin-1 is differentially expressed in myoepithelial cells and vascular smooth muscle cells in preneoplastic and neoplastic human breast: a possible marker for the progression of breast cancer. Int J Cancer. 2002;101(5):409-14.
407. Broholm H, Laursen H. Vascular endothelial growth factor (VEGF) receptor neuropilin-1's distribution in astrocytic tumors. APMIS. 2004;112(4-5):257-63.
408. Caponegro MD, Moffitt RA, Tsirka SE. Expression of neuropilin-1 is linked to glioma associated microglia and macrophages and correlates with unfavorable prognosis in high grade gliomas. Oncotarget. 2018;9(86):35655-65.
409. Rizzolio S, Tamagnone L. Multifaceted role of neuropilins in cancer. Curr Med Chem. 2011;18(23):3563-75.
410. Guttmann-Raviv N, Kessler O, Shraga-Heled N, Lange T, Herzog Y, Neufeld G. The neuropilins and their role in tumorigenesis and tumor progression. Cancer Lett. 2006;231(1):1-11.
411. Bachelder RE, Crago A, Chung J, Wendt MA, Shaw LM, Robinson G, et al. Vascular endothelial growth factor is an autocrine survival factor for neuropilin-expressing breast carcinoma cells. Cancer Res. 2001;61(15):5736-40.
412. Nasarre P, Kusy S, Constantin B, Castellani V, Drabkin HA, Bagnard D, et al. Semaphorin SEMA3F has a repulsing activity on breast cancer cells and inhibits E-cadherin-mediated cell adhesion. Neoplasia. 2005;7(2):180-9.
413. Li M, Yang H, Chai H, Fisher WE, Wang X, Brunicardi FC, et al. Pancreatic carcinoma cells express neuropilins and vascular endothelial growth factor, but not vascular endothelial growth factor receptors. Cancer. 2004;101(10):2341-50.
414. Miao HQ, Lee P, Lin H, Soker S, Klagsbrun M. Neuropilin-1 expression by tumor cells promotes tumor angiogenesis and progression. FASEB J. 2000;14(15):2532-9.
415. Takahashi T, Fournier A, Nakamura F, Wang LH, Murakami Y, Kalb RG, et al. Plexin-neuropilin-1 complexes form functional semaphorin-3A receptors. Cell. 1999;99(1):59-69.
416. Djordjevic S, Driscoll PC. Targeting VEGF signalling via the neuropilin co-receptor. Drug Discov Today. 2013;18(9-10):447-55.
417. Glinka Y, Stoilova S, Mohammed N, Prud'homme GJ. Neuropilin-1 exerts co-receptor function for TGF-beta-1 on the membrane of cancer cells and enhances responses to both latent and active TGF-beta. Carcinogenesis. 2011;32(4):613-21.
418. Rizzolio S, Rabinowicz N, Rainero E, Lanzetti L, Serini G, Norman J, et al. Neuropilin-1-dependent regulation of EGF-receptor signaling. Cancer Res. 2012;72(22):5801-11.

419. Rizzolio S TL. Neuropilins as signaling hubs, controlling tyrosine kinases and other cell surface receptors. In: Neufeld G, editor. The neuropilins: role and function in health and disease. New York: Springer International Publishing; 2017. p. 23-39.
420. Prud'homme GJ, Glinka Y. Neuropilins are multifunctional coreceptors involved in tumor initiation, growth, metastasis and immunity. Oncotarget. 2012;3(9):921-39.
421. Ruhrberg C, Gerhardt H, Golding M, Watson R, Ioannidou S, Fujisawa H, et al. Spatially restricted patterning cues provided by heparin-binding VEGF-A control blood vessel branching morphogenesis. Genes Dev. 2002;16(20):2684-98.
422. Gerhardt H, Golding M, Fruttiger M, Ruhrberg C, Lundkvist A, Abramsson A, et al. VEGF guides angiogenic sprouting utilizing endothelial tip cell filopodia. J Cell Biol. 2003;161(6):1163-77.
423. Blanco R, Gerhardt H. VEGF and Notch in tip and stalk cell selection. Cold Spring Harb Perspect Med. 2013;3(1):a006569.
424. Tordjman R, Lepelletier Y, Lemarchandel V, Cambot M, Gaulard P, Hermine O, et al. A neuronal receptor, neuropilin-1, is essential for the initiation of the primary immune response. Nat Immunol. 2002;3(5):477-82.
425. Delgoffe GM, Woo SR, Turnis ME, Gravano DM, Guy C, Overacre AE, et al. Stability and function of regulatory T cells is maintained by a neuropilin-1-semaphorin-4a axis. Nature. 2013;501(7466):252-6.
426. Sarris M, Andersen KG, Randow F, Mayr L, Betz AG. Neuropilin-1 expression on regulatory T cells enhances their interactions with dendritic cells during antigen recognition. Immunity. 2008;28(3):402-13.
427. Takamatsu H, Takegahara N, Nakagawa Y, Tomura M, Taniguchi M, Friedel RH, et al. Semaphorins guide the entry of dendritic cells into the lymphatics by activating myosin II. Nat Immunol. 2010;11(7):594-600.
428. Daly JL, Simonetti B, Klein K, Chen K-E, Williamson MK, Antón-Plágaro C, et al. Neuropilin-1 is a host factor for SARS-CoV-2 infection. Science. 2020;370(6518):861-5.
429. Alais S, Mahieux R, Dutartre H. Viral Source-Independent High Susceptibility of Dendritic Cells to Human T-Cell Leukemia Virus Type 1 Infection Compared to That of T Lymphocytes. J Virol. 2015;89(20):10580-90.
430. Lambert S, Bouttier M, Vassy R, Seigneuret M, Petrow-Sadowski C, Janvier S, et al. HTLV-1 uses HSPG and neuropilin-1 for entry by molecular mimicry of VEGF165. Blood. 2009;113(21):5176-85.
431. Lanahan A, Zhang X, Fantin A, Zhuang Z, Rivera-Molina F, Speichinger K, et al. The neuropilin 1 cytoplasmic domain is required for VEGF-A-dependent arteriogenesis. Dev Cell. 2013;25(2):156-68.
432. Fantin A, Vieira JM, Plein A, Denti L, Fruttiger M, Pollard JW, et al. NRP1 acts cell autonomously in endothelium to promote tip cell function during sprouting angiogenesis. Blood. 2013;121(12):2352-62.
433. Fantin A, Vieira JM, Gestri G, Denti L, Schwarz Q, Prykhozhij S, et al. Tissue macrophages act as cellular chaperones for vascular anastomosis downstream of VEGF-mediated endothelial tip cell induction. Blood. 2010;116(5):829-40.
434. Lewis CE, Pollard JW. Distinct role of macrophages in different tumor microenvironments. Cancer Res. 2006;66(2):605-12.
435. Noy R, Pollard JW. Tumor-associated macrophages: from mechanisms to therapy. Immunity. 2014;41(1):49-61.
436. Qian BZ, Pollard JW. Macrophage diversity enhances tumor progression and metastasis. Cell. 2010;141(1):39-51.
437. Rivera LB, Bergers G. Location, location, location: macrophage positioning within tumors determines pro- or antitumor activity. Cancer Cell. 2013;24(6):687-9.

438. Mantovani A, Sozzani S, Locati M, Allavena P, Sica A. Macrophage polarization: tumor-associated macrophages as a paradigm for polarized M2 mononuclear phagocytes. Trends Immunol. 2002;23(11):549-55.
439. Wilson AM, Shao Z, Grenier V, Mawambo G, Daudelin J-F, Dejda A, et al. Neuropilin-1 expression in adipose tissue macrophages protects against obesity and metabolic syndrome. Science Immunology. 2018;3(21):eaan4626.
440. Nissen JC, Selwood DL, Tsirka SE. Tuftsin signals through its receptor neuropilin-1 via the transforming growth factor beta pathway. J Neurochem. 2013;127(3):394-402.
441. Nissen JC, Tsirka SE. Tuftsin-driven experimental autoimmune encephalomyelitis recovery requires neuropilin-1. Glia. 2016;64(6):923-36.
442. Resnikoff S, Pascolini D, Etya'ale D, Kocur I, Pararajasegaram R, Pokharel GP, et al. Global data on visual impairment in the year 2002. Bull World Health Organ. 2004;82(11):844-51.
443. Maralani HG, Tai BC, Wong TY, Tai ES, Li J, Wang JJ, et al. Metabolic syndrome and risk of age-related macular degeneration. Retina. 2015;35(3):459-66.
444. Cani P, Osto M, Geurts L, Everard A. Involvement of gut microbiota in the development of low-grade inflammation and type 2 diabetes associated with obesity. Gut microbes. 2012;3(4):279-88.
445. Krebs I, Glittenberg C, Ansari-Shahrezaei S, Hagen S, Steiner I, Binder S. Non-responders to treatment with antagonists of vascular endothelial growth factor in age-related macular degeneration. Br J Ophthalmol. 2013;97(11):1443-6.
446. Takamatsu H, Kumanogoh A. Diverse roles for semaphorin-plexin signaling in the immune system. Trends Immunol. 2012;33(3):127-35.
447. Fletcher EL, Jobling AI, Greferath U, Mills SA, Waugh M, Ho T, et al. Studying age-related macular degeneration using animal models. Optom Vis Sci. 2014;91(8):878-86.
448. Malek G, Johnson LV, Mace BE, Saloupis P, Schmechel DE, Rickman DW, et al. Apolipoprotein E allele-dependent pathogenesis: a model for age-related retinal degeneration. Proc Natl Acad Sci U S A. 2005;102(33):11900-5.
449. Ambati J, Anand A, Fernandez S, Sakurai E, Lynn BC, Kuziel WA, et al. An animal model of age-related macular degeneration in senescent Ccl-2- or Ccr-2-deficient mice. Nat Med. 2003;9(11):1390-7.
450. Vojdani A. For the assessment of intestinal permeability, size matters. Alternative therapies in health and medicine. 2013;19(1):12-24.
451. Weaver LT, Coombs RR. Does 'sugar' permeability reflect macromolecular absorption? A comparison of the gastro-intestinal uptake of lactulose and beta-lactoglobulin in the neonatal guinea pig. International archives of allergy and applied immunology. 1988;85(1):133-5.
452. Peeters M, Hiele M, Ghoos Y, Huysmans V, Geboes K, Vantrappen G, et al. Test conditions greatly influence permeation of water soluble molecules through the intestinal mucosa: need for standardisation. Gut. 1994;35(10):1404-8.
453. Ménard S, Cerf-Bensussan N, Heyman M. Multiple facets of intestinal permeability and epithelial handling of dietary antigens. Mucosal immunology. 2010;3(3):247-59.
454. Oman H, Akerblom E, Richter W, Johansson SG. Chemical and physiological properties of polysucrose, a new marker of intestinal permeability to macromolecules. International archives of allergy and immunology. 1992;98(3):220-6.
455. Oman H, Blomquist L, Henriksson AE, Johansson SG. Comparison of polysucrose 15000, 51Cr-labelled ethylenediaminetetraacetic acid, and 14C-mannitol as markers of intestinal permeability in man. Scandinavian journal of gastroenterology. 1995;30(12):1172-7.
456. Farzi A, Fröhlich EE, Holzer P. Gut Microbiota and the Neuroendocrine System. Neurotherapeutics : the journal of the American Society for Experimental NeuroTherapeutics. 2018;15(1):5-22.

457. Kowalski K, Mulak A. Brain-Gut-Microbiota Axis in Alzheimer's Disease. Journal of neurogastroenterology and motility. 2019;25(1):48-60.
458. Beli E, Yan Y, Moldovan L, Vieira CP, Gao R, Duan Y, et al. Restructuring of the Gut Microbiome by Intermittent Fasting Prevents Retinopathy and Prolongs Survival in db/db Mice. Diabetes. 2018;67(9):1867-79.
459. Nakamura YK, Metea C, Karstens L, Asquith M, Gruner H, Moscibrocki C, et al. Gut Microbial Alterations Associated With Protection From Autoimmune Uveitis. Invest Ophthalmol Vis Sci. 2016;57(8):3747-58.
460. Statovci D, Aguilera M, MacSharry J, Melgar S. The Impact of Western Diet and Nutrients on the Microbiota and Immune Response at Mucosal Interfaces. Front Immunol. 2017;8:838.
461. Collaborators GBDO, Afshin A, Forouzanfar MH, Reitsma MB, Sur P, Estep K, et al. Health Effects of Overweight and Obesity in 195 Countries over 25 Years. N Engl J Med. 2017;377(1):13-27.
462. Hill JO, Peters JC. Environmental contributions to the obesity epidemic. Science. 1998;280(5368):1371-4.
463. Zhang Y, Proenca R, Maffei M, Barone M, Leopold L, Friedman JM. Positional cloning of the mouse obese gene and its human homologue. Nature. 1994;372(6505):425-32.
464. Buettner R, Scholmerich J, Bollheimer LC. High-fat diets: modeling the metabolic disorders of human obesity in rodents. Obesity (Silver Spring). 2007;15(4):798-808.
465. Coelho DF, Pereira-Lancha LO, Chaves DS, Diwan D, Ferraz R, Campos-Ferraz PL, et al. Effect of high-fat diets on body composition, lipid metabolism and insulin sensitivity, and the role of exercise on these parameters. Braz J Med Biol Res. 2011;44(10):966-72.
466. Ikemoto S, Takahashi M, Tsunoda N, Maruyama K, Itakura H, Ezaki O. High-fat diet-induced hyperglycemia and obesity in mice: differential effects of dietary oils. Metabolism. 1996;45(12):1539-46.
467. Storlien LH, Kraegen EW, Chisholm DJ, Ford GL, Bruce DG, Pascoe WS. Fish oil prevents insulin resistance induced by high-fat feeding in rats. Science. 1987;237(4817):885-8.
468. Storlien LH, James DE, Burleigh KM, Chisholm DJ, Kraegen EW. Fat feeding causes widespread in vivo insulin resistance, decreased energy expenditure, and obesity in rats. Am J Physiol. 1986;251(5 Pt 1):E576-83.
469. Wang H, Storlien LH, Huang XF. Effects of dietary fat types on body fatness, leptin, and ARC leptin receptor, NPY, and AgRP mRNA expression. Am J Physiol Endocrinol Metab. 2002;282(6):E1352-9.
470. Hancock CR, Han DH, Chen M, Terada S, Yasuda T, Wright DC, et al. High-fat diets cause insulin resistance despite an increase in muscle mitochondria. Proc Natl Acad Sci U S A. 2008;105(22):7815-20.
471. Cheung N, Wong TY. Obesity and eye diseases. Surv Ophthalmol. 2007;52(2):180-95.
472. Rowan S, Jiang S, Korem T, Szymanski J, Chang ML, Szelog J, et al. Involvement of a gut-retina axis in protection against dietary glycemia-induced age-related macular degeneration. Proc Natl Acad Sci U S A. 2017;114(22):E4472-e81.
473. Lee S, Sung J, Lee J, Ko G. Comparison of the gut microbiotas of healthy adult twins living in South Korea and the United States. Appl Environ Microbiol. 2011;77(20):7433-7.
474. Yatsunenko T, Rey FE, Manary MJ, Trehan I, Dominguez-Bello MG, Contreras M, et al. Human gut microbiome viewed across age and geography. Nature. 2012;486(7402):222-7.
475. Song SJ, Lauber C, Costello EK, Lozupone CA, Humphrey G, Berg-Lyons D, et al. Cohabiting family members share microbiota with one another and with their dogs. Elife. 2013;2:e00458.
476. Kurilshikov A, Wijmenga C, Fu J, Zhernakova A. Host Genetics and Gut Microbiome: Challenges and Perspectives. Trends Immunol. 2017;38(9):633-47.
477. Goodrich JK, Waters JL, Poole AC, Sutter JL, Koren O, Blekhman R, et al. Human genetics shape the gut microbiome. Cell. 2014;159(4):789-99.
478. Turpin W, Espin-Garcia O, Xu W, Silverberg MS, Kevans D, Smith MI, et al. Association of host genome with intestinal microbial composition in a large healthy cohort. Nat Genet. 2016;48(11):1413-7.

479. Goodrich JK, Davenport ER, Clark AG, Ley RE. The Relationship Between the Human Genome and Microbiome Comes into View. Annu Rev Genet. 2017;51:413-33.
480. Goodrich JK, Davenport ER, Beaumont M, Jackson MA, Knight R, Ober C, et al. Genetic Determinants of the Gut Microbiome in UK Twins. Cell Host Microbe. 2016;19(5):731-43.
481. Rothschild D, Weissbrod O, Barkan E, Kurilshikov A, Korem T, Zeevi D, et al. Environment dominates over host genetics in shaping human gut microbiota. Nature. 2018;555(7695):210-5.
482. Hansen EE, Lozupone CA, Rey FE, Wu M, Guruge JL, Narra A, et al. Pan-genome of the dominant human gut-associated archaeon, Methanobrevibacter smithii, studied in twins. Proc Natl Acad Sci U S A. 2011;108 Suppl 1:4599-606.
483. Rausch P, Rehman A, Kunzel S, Hasler R, Ott SJ, Schreiber S, et al. Colonic mucosa-associated microbiota is influenced by an interaction of Crohn disease and FUT2 (Secretor) genotype. Proc Natl Acad Sci U S A. 2011;108(47):19030-5.
484. Rehman A, Sina C, Gavrilova O, Hasler R, Ott S, Baines JF, et al. Nod2 is essential for temporal development of intestinal microbial communities. Gut. 2011;60(10):1354-62.
485. Wacklin P, Makivuokko H, Alakulppi N, Nikkila J, Tenkanen H, Rabina J, et al. Secretor genotype (FUT2 gene) is strongly associated with the composition of Bifidobacteria in the human intestine. PLoS One. 2011;6(5):e20113.
486. Malla MA, Dubey A, Kumar A, Yadav S, Hashem A, Abd Allah EF. Exploring the Human Microbiome: The Potential Future Role of Next-Generation Sequencing in Disease Diagnosis and Treatment. Front Immunol. 2018;9:2868.
487. Ursell LK, Clemente JC, Rideout JR, Gevers D, Caporaso JG, Knight R. The interpersonal and intrapersonal diversity of human-associated microbiota in key body sites. J Allergy Clin Immunol. 2012;129(5):1204-8.
488. Church GM, Kieffer-Higgins S. Multiplex DNA sequencing. Science. 1988;240(4849):185-8.
489. Huber JA, Mark Welch DB, Morrison HG, Huse SM, Neal PR, Butterfield DA, et al. Microbial population structures in the deep marine biosphere. Science. 2007;318(5847):97-100.
490. Hamady M, Walker JJ, Harris JK, Gold NJ, Knight R. Error-correcting barcoded primers for pyrosequencing hundreds of samples in multiplex. Nat Methods. 2008;5(3):235-7.
491. Caporaso JG, Lauber CL, Walters WA, Berg-Lyons D, Lozupone CA, Turnbaugh PJ, et al. Global patterns of 16S rRNA diversity at a depth of millions of sequences per sample. Proc Natl Acad Sci U S A. 2011;108 Suppl 1(Suppl 1):4516-22.
492. Metzker ML. Sequencing technologies - the next generation. Nature reviews Genetics. 2010;11(1):31-46.
493. DeSantis TZ, Hugenholtz P, Larsen N, Rojas M, Brodie EL, Keller K, et al. Greengenes, a chimera-checked 16S rRNA gene database and workbench compatible with ARB. Appl Environ Microbiol. 2006;72(7):5069-72.
494. Cole JR, Wang Q, Cardenas E, Fish J, Chai B, Farris RJ, et al. The Ribosomal Database Project: improved alignments and new tools for rRNA analysis. Nucleic Acids Res. 2009;37(Database issue):D141-5.
495. Pruesse E, Quast C, Knittel K, Fuchs BM, Ludwig W, Peplies J, et al. SILVA: a comprehensive online resource for quality checked and aligned ribosomal RNA sequence data compatible with ARB. Nucleic Acids Res. 2007;35(21):7188-96.
496. Caporaso JG, Kuczynski J, Stombaugh J, Bittinger K, Bushman FD, Costello EK, et al. QIIME allows analysis of high-throughput community sequencing data. Nat Methods. 2010;7(5):335-6.
497. Glass EM, Wilkening J, Wilke A, Antonopoulos D, Meyer F. Using the metagenomics RAST server (MG-RAST) for analyzing shotgun metagenomes. Cold Spring Harbor protocols. 2010;2010(1):pdb.prot5368.

498. Edgar RC. Accuracy of taxonomy prediction for 16S rRNA and fungal ITS sequences. PeerJ. 2018;6:e4652.
499. Grice EA, Kong HH, Renaud G, Young AC, Bouffard GG, Blakesley RW, et al. A diversity profile of the human skin microbiota. Genome research. 2008;18(7):1043-50.
500. Grice EA, Kong HH, Conlan S, Deming CB, Davis J, Young AC, et al. Topographical and temporal diversity of the human skin microbiome. Science. 2009;324(5931):1190-2.
501. Costello EK, Lauber CL, Hamady M, Fierer N, Gordon JI, Knight R. Bacterial community variation in human body habitats across space and time. Science. 2009;326(5960):1694-7.
502. Konstantinidis KT, Tiedje JM. Prokaryotic taxonomy and phylogeny in the genomic era: advancements and challenges ahead. Curr Opin Microbiol. 2007;10(5):504-9.
503. Boers SA, Jansen R, Hays JP. Understanding and overcoming the pitfalls and biases of next-generation sequencing (NGS) methods for use in the routine clinical microbiological diagnostic laboratory. European journal of clinical microbiology & infectious diseases : official publication of the European Society of Clinical Microbiology. 2019;38(6):1059-70.
504. Brandt LJ, Aroniadis OC. An overview of fecal microbiota transplantation: techniques, indications, and outcomes. Gastrointest Endosc. 2013;78(2):240-9.
505. Bakken JS, Borody T, Brandt LJ, Brill JV, Demarco DC, Franzos MA, et al. Treating Clostridium difficile infection with fecal microbiota transplantation. Clinical gastroenterology and hepatology : the official clinical practice journal of the American Gastroenterological Association. 2011;9(12):1044-9.
506. Kelly CR, Khoruts A, Staley C, Sadowsky MJ, Abd M, Alani M, et al. Effect of Fecal Microbiota Transplantation on Recurrence in Multiply Recurrent Clostridium difficile Infection: A Randomized Trial. Ann Intern Med. 2016;165(9):609-16.
507. van Nood E, Vrieze A, Nieuwdorp M, Fuentes S, Zoetendal EG, de Vos WM, et al. Duodenal infusion of donor feces for recurrent Clostridium difficile. N Engl J Med. 2013;368(5):407-15.
508. Kim KO, Gluck M. Fecal Microbiota Transplantation: An Update on Clinical Practice. Clinical endoscopy. 2019;52(2):137-43.
509. Zhang SL, Wang SN, Miao CY. Influence of Microbiota on Intestinal Immune System in Ulcerative Colitis and Its Intervention. Front Immunol. 2017;8:1674.
510. Costello SP, Soo W, Bryant RV, Jairath V, Hart AL, Andrews JM. Systematic review with meta-analysis: faecal microbiota transplantation for the induction of remission for active ulcerative colitis. Aliment Pharmacol Ther. 2017;46(3):213-24.
511. Choi HH, Cho YS. Fecal Microbiota Transplantation: Current Applications, Effectiveness, and Future Perspectives. Clinical endoscopy. 2016;49(3):257-65.
512. Tun HM, Konya T, Takaro TK, Brook JR, Chari R, Field CJ, et al. Exposure to household furry pets influences the gut microbiota of infant at 3-4 months following various birth scenarios. Microbiome. 2017;5(1):40.
513. Blander JM, Longman RS, Iliev ID, Sonnenberg GF, Artis D. Regulation of inflammation by microbiota interactions with the host. Nat Immunol. 2017;18(8):851-60.
514. Myhrstad MCW, Tunsjø H, Charnock C, Telle-Hansen VH. Dietary Fiber, Gut Microbiota, and Metabolic Regulation-Current Status in Human Randomized Trials. Nutrients. 2020;12(3).
515. Mosmann TR, Cherwinski H, Bond MW, Giedlin MA, Coffman RL. Two types of murine helper T cell clone. I. Definition according to profiles of lymphokine activities and secreted proteins. J Immunol. 1986;136(7):2348-57.
516. Roszer T. Understanding the Mysterious M2 Macrophage through Activation Markers and Effector Mechanisms. Mediators Inflamm. 2015;2015:816460.
517. Cunningham C. Microglia and neurodegeneration: the role of systemic inflammation. Glia. 2013;61(1):71-90.

518. Biswas SK, Mantovani A. Macrophage plasticity and interaction with lymphocyte subsets: cancer as a paradigm. Nat Immunol. 2010;11(10):889-96.
519. Hao NB, Lu MH, Fan YH, Cao YL, Zhang ZR, Yang SM. Macrophages in tumor microenvironments and the progression of tumors. Clin Dev Immunol. 2012;2012:948098.
520. Liu J, Copland D, Horie S, Wu W-K, Chen M, Xu Y, et al. Myeloid cells expressing VEGF and arginase-1 following uptake of damaged retinal pigment epithelium suggests potential mechanism that drives the onset of choroidal angiogenesis in mice. PLoS One. 2013;8(8):e72935-e.
521. Risau W. Mechanisms of angiogenesis. Nature. 1997;386(6626):671-4.
522. Lu J, Pompili VJ, Das H. Neovascularization and hematopoietic stem cells. Cell Biochem Biophys. 2013;67(2):235-45.
523. Motz GT, Coukos G. The parallel lives of angiogenesis and immunosuppression: cancer and other tales. Nat Rev Immunol. 2011;11(10):702-11.
524. Hobson B, Denekamp J. Endothelial proliferation in tumours and normal tissues: continuous labelling studies. Br J Cancer. 1984;49(4):405-13.
525. Kiefer F, Siekmann AF. The role of chemokines and their receptors in angiogenesis. Cell Mol Life Sci. 2011;68(17):2811-30.
526. Lahmar Q, Keirsse J, Laoui D, Movahedi K, Van Overmeire E, Van Ginderachter JA. Tissue-resident versus monocyte-derived macrophages in the tumor microenvironment. Biochim Biophys Acta. 2016;1865(1):23-34.
527. De Palma M, Biziato D, Petrova TV. Microenvironmental regulation of tumour angiogenesis. Nat Rev Cancer. 2017;17(8):457-74.
528. Baer C, Squadrito ML, Iruela-Arispe ML, De Palma M. Reciprocal interactions between endothelial cells and macrophages in angiogenic vascular niches. Exp Cell Res. 2013;319(11):1626-34.
529. Murdoch C, Muthana M, Coffelt SB, Lewis CE. The role of myeloid cells in the promotion of tumour angiogenesis. Nat Rev Cancer. 2008;8(8):618-31.
530. Miyauchi JT, Caponegro MD, Chen D, Choi MK, Li M, Tsirka SE. Deletion of Neuropilin 1 from Microglia or Bone Marrow-Derived Macrophages Slows Glioma Progression. Cancer Res. 2018;78(3):685-94.
531. Chen XJ, Wu S, Yan RM, Fan LS, Yu L, Zhang YM, et al. The role of the hypoxia-Nrp-1 axis in the activation of M2-like tumor-associated macrophages in the tumor microenvironment of cervical cancer. Mol Carcinog. 2019;58(3):388-97.
532. Dai X, Okon I, Liu Z, Wu Y, Zhu H, Song P, et al. A novel role for myeloid cell-specific neuropilin 1 in mitigating sepsis. FASEB J. 2017;31(7):2881-92.
533. Carrer A, Moimas S, Zacchigna S, Pattarini L, Zentilin L, Ruozi G, et al. Neuropilin-1 identifies a subset of bone marrow Gr1- monocytes that can induce tumor vessel normalization and inhibit tumor growth. Cancer Res. 2012;72(24):6371-81.
534. Dejda A, Mawambo G, Cerani A, Miloudi K, Shao Z, Daudelin JF, et al. Neuropilin-1 mediates myeloid cell chemoattraction and influences retinal neuroimmune crosstalk. J Clin Invest. 2014;124(11):4807-22.
535. Joyal JS, Sitaras N, Binet F, Rivera JC, Stahl A, Zaniolo K, et al. Ischemic neurons prevent vascular regeneration of neural tissue by secreting semaphorin 3A. Blood. 2011;117(22):6024-35.
536. Sapieha P. Eyeing central neurons in vascular growth and reparative angiogenesis. Blood. 2012;120(11):2182-94.
537. Campochiaro PA. Molecular pathogenesis of retinal and choroidal vascular diseases. Prog Retin Eye Res. 2015;49:67-81.
538. Lores-Motta L, van Asten F, Muether PS, Smailhodzic D, Groenewoud JM, Omar A, et al. A genetic variant in NRP1 is associated with worse response to ranibizumab treatment in neovascular age-related macular degeneration. Pharmacogenet Genomics. 2016;26(1):20-7.

539. Lores-Motta L, Riaz M, Grunin M, Corominas J, van Asten F, Pauper M, et al. Association of Genetic Variants With Response to Anti-Vascular Endothelial Growth Factor Therapy in Age-Related Macular Degeneration. JAMA Ophthalmol. 2018;136(8):875-84.
540. Pan Q, Chanthery Y, Liang WC, Stawicki S, Mak J, Rathore N, et al. Blocking neuropilin-1 function has an additive effect with anti-VEGF to inhibit tumor growth. Cancer Cell. 2007;11(1):53-67.
541. Nagineni CN, Samuel W, Nagineni S, Pardhasaradhi K, Wiggert B, Detrick B, et al. Transforming growth factor-beta induces expression of vascular endothelial growth factor in human retinal pigment epithelial cells: involvement of mitogen-activated protein kinases. J Cell Physiol. 2003;197(3):453-62.
542. Bian ZM, Elner SG, Elner VM. Regulation of VEGF mRNA expression and protein secretion by TGF-beta2 in human retinal pigment epithelial cells. Exp Eye Res. 2007;84(5):812-22.
543. Iwanishi H, Fujita N, Tomoyose K, Okada Y, Yamanaka O, Flanders KC, et al. Inhibition of development of laser-induced choroidal neovascularization with suppression of infiltration of macrophages in Smad3-null mice. Lab Invest. 2016;96(6):641-51.
544. Wang X, Abraham S, McKenzie JAG, Jeffs N, Swire M, Tripathi VB, et al. LRG1 promotes angiogenesis by modulating endothelial TGF-β signalling. Nature. 2013;499(7458):306-11.
545. Aspalter IM, Gordon E, Dubrac A, Ragab A, Narloch J, Vizán P, et al. Alk1 and Alk5 inhibition by Nrp1 controls vascular sprouting downstream of Notch. Nature Communications. 2015;6(1):7264.
546. Loomans HA, Andl CD. Activin receptor-like kinases: a diverse family playing an important role in cancer. Am J Cancer Res. 2016;6(11):2431-47.
547. Cunha SI, Pietras K. ALK1 as an emerging target for antiangiogenic therapy of cancer. Blood. 2011;117(26):6999-7006.
548. Pardali E, Goumans MJ, ten Dijke P. Signaling by members of the TGF-beta family in vascular morphogenesis and disease. Trends Cell Biol. 2010;20(9):556-67.
549. Goumans MJ, Mummery C. Functional analysis of the TGFbeta receptor/Smad pathway through gene ablation in mice. Int J Dev Biol. 2000;44(3):253-65.
550. Goumans MJ, Liu Z, ten Dijke P. TGF-beta signaling in vascular biology and dysfunction. Cell Res. 2009;19(1):116-27.
551. Goumans MJ, Ten Dijke P. TGF-β Signaling in Control of Cardiovascular Function. Cold Spring Harb Perspect Biol. 2018;10(2).
552. Baeyens N, Larrivée B, Ola R, Hayward-Piatkowskyi B, Dubrac A, Huang B, et al. Defective fluid shear stress mechanotransduction mediates hereditary hemorrhagic telangiectasia. J Cell Biol. 2016;214(7):807-16.
553. Ola R, Dubrac A, Han J, Zhang F, Fang JS, Larrivée B, et al. PI3 kinase inhibition improves vascular malformations in mouse models of hereditary haemorrhagic telangiectasia. Nat Commun. 2016;7:13650.
554. van Meeteren LA, Thorikay M, Bergqvist S, Pardali E, Stampino CG, Hu-Lowe D, et al. Anti-human activin receptor-like kinase 1 (ALK1) antibody attenuates bone morphogenetic protein 9 (BMP9)-induced ALK1 signaling and interferes with endothelial cell sprouting. J Biol Chem. 2012;287(22):18551-61.
555. Moya IM, Umans L, Maas E, Pereira PN, Beets K, Francis A, et al. Stalk cell phenotype depends on integration of Notch and Smad1/5 signaling cascades. Dev Cell. 2012;22(3):501-14.
556. Larrivée B, Prahst C, Gordon E, del Toro R, Mathivet T, Duarte A, et al. ALK1 signaling inhibits angiogenesis by cooperating with the Notch pathway. Dev Cell. 2012;22(3):489-500.
557. Potente M, Gerhardt H, Carmeliet P. Basic and therapeutic aspects of angiogenesis. Cell. 2011;146(6):873-87.
558. Prud'homme GJ. Pathobiology of transforming growth factor beta in cancer, fibrosis and immunologic disease, and therapeutic considerations. Lab Invest. 2007;87(11):1077-91.
559. Ihara S, Hirata Y, Koike K. TGF-β in inflammatory bowel disease: a key regulator of immune cells, epithelium, and the intestinal microbiota. J Gastroenterol. 2017;52(7):777-87.

560. Abraham C, Cho JH. Inflammatory bowel disease. N Engl J Med. 2009;361(21):2066-78.
561. Xavier RJ, Podolsky DK. Unravelling the pathogenesis of inflammatory bowel disease. Nature. 2007;448(7152):427-34.
562. Jostins L, Ripke S, Weersma RK, Duerr RH, McGovern DP, Hui KY, et al. Host-microbe interactions have shaped the genetic architecture of inflammatory bowel disease. Nature. 2012;491(7422):119-24.
563. Di Sabatino A, Pickard KM, Rampton D, Kruidenier L, Rovedatti L, Leakey NA, et al. Blockade of transforming growth factor beta upregulates T-box transcription factor T-bet, and increases T helper cell type 1 cytokine and matrix metalloproteinase-3 production in the human gut mucosa. Gut. 2008;57(5):605-12.
564. Monteleone G, Kumberova A, Croft NM, McKenzie C, Steer HW, MacDonald TT. Blocking Smad7 restores TGF-beta1 signaling in chronic inflammatory bowel disease. J Clin Invest. 2001;108(4):601-9.
565. Bauché D, Marie JC. Transforming growth factor β: a master regulator of the gut microbiota and immune cell interactions. Clin Transl Immunology. 2017;6(4):e136.
566. Lees CW, Barrett JC, Parkes M, Satsangi J. New IBD genetics: common pathways with other diseases. Gut. 2011;60(12):1739-53.
567. Hong SH, Kang M, Lee KS, Yu K. High fat diet-induced TGF-β/Gbb signaling provokes insulin resistance through the tribbles expression. Sci Rep. 2016;6:30265.
568. Biasi F, Mascia C, Poli G. The contribution of animal fat oxidation products to colon carcinogenesis, through modulation of TGF-beta1 signaling. Carcinogenesis. 2008;29(5):890-4.
569. Nakamura R, Sene A, Santeford A, Gdoura A, Kubota S, Zapata N, et al. IL10-driven STAT3 signalling in senescent macrophages promotes pathological eye angiogenesis. Nat Commun. 2015;6:7847.
570. Zandi S, Nakao S, Chun KH, Fiorina P, Sun D, Arita R, et al. ROCK-isoform-specific polarization of macrophages associated with age-related macular degeneration. Cell Rep. 2015;10(7):1173-86.